The Pennsylvania State University

The Graduate School

College of Medicine

EVALUATION OF BAC-BASED REPORTERS FOR THE STUDY OF HUMAN TELOMERASE

A Thesis in

Cell and Molecular Biology

by

Melanie A. Leiby

Submitted in Partial Fulfillment
of the Requirements
for the Degree of

Doctor of Philosophy

May 2007

The thesis of Melanie A. Leiby was reviewed and approved* by the following:

Henry J. Donahue
Professor of Cellular and Molecular Physiology
Chair of Committee
Head of the Cell and Molecular Biology Graduate Program

Sarah K. Bronson
Assistant Professor of Cellular and Molecular Physiology

Kristin A. Eckert
Associate Professor of Pathology and Biochemistry and Molecular Biology

M. Judith Tevethia
Professor of Microbiology and Immunology

*Signatures are on file in the Graduate School.

ABSTRACT

The ongoing efforts to sequence eukaryotic genomes have revealed that contrary to initial predictions, more complex organisms do not necessarily have more complex genomes or more genes. Instead, it has been shown that higher eukaryotes have more complex gene regulatory mechanisms, leading to increased organismal complexity. Understanding the ways in which genes are regulated is critical to understanding how organisms function in normal and diseased states. Many techniques and model systems have been used to study gene regulation, including transgenic mice and cell lines and promoter analysis via reporter genes. Some of the biggest problems when studying gene regulation are the susceptibility of transgenes to position effect variegation (PEV) and copy number dependence. To alleviate these problems, techniques have been developed to introduce transgenes in a single copy at predetermined genomic loci. Another concern when using standard transgenes to study gene regulation is that they do not always mimic the expression patterns of the endogenous locus, either because they do not contain all appropriate regulatory elements and/or are unable to re-form the native chromatin environment. The use of yeast, bacterial, and P1 artificial chromosomes (YACs, BACs, and PACs, respectively) as transgenes has been shown to increase the likelihood that a transgene will be expressed in an endogenous manner due to the increased amount of genomic sequence they harbor. Therefore, transgenics created using artificial chromosomes targeted in a single copy to a predetermined genomic locus should be very beneficial to the study of gene regulation.

One gene that would benefit from such a system is human telomerase reverse transcriptase (*TERT*). *TERT* encodes a reverse transcriptase specific for telomeres, the tandemly repeated sequence located at the ends of all eukaryotic chromosomes that, in addition to their associated proteins, serve as caps to prevent critical genetic information from being lost due to the end replication problem and protect chromosomes from end-to-end fusions. In humans, *TERT* is expressed at high levels during embryogenesis, but in adult somatic cells, *TERT* is silenced; however, in 85-90% of all human tumors, telomerase is reactivated. The correlation between a lack of telomerase activity and hTERT mRNA seems to suggest telomerase expression is regulated predominantly at the

level of transcription; however, despite almost 25 years of study, the mechanisms of hTERT regulation have remained elusive. One of the main reasons for this is the lack of a powerful model system. Mice, which are often used to study human genes, are not good models for studying h*TERT* because m*TERT* expression is much more promiscuous than that of h*TERT* and their overall telomere length is much longer. Additionally, transiently expressed, h*TERT* promoter-based reporters do not always mimic the endogenous telomerase activity of the cells into which they are introduced.

We hypothesized that an h*TERT* reporter created from a BAC introduced in a single copy to a preexisting acceptor locus via recombinase-mediated cassette exchange (RMCE) would be able to mimic the endogenous telomerase expression patterns of genetically related telomerase positive (TERT(+)) and telomerase negative (TERT(-)) cells. To test this hypothesis, an acceptor locus containing a tkNeo fusion gene and Cre recombinase fused to the estrogen receptor under control of the cytomegalovirus immediate early promoter and the Cre recombinase recognition sites *loxP* and *lox511* surrounded by single copies of the chicken β-globin insulator, cHS4, was created and introduced into genetically related TERT(+) and (-) cells via retroviral integration. (These TERT(+) and (-) cells were immortal clones that arose after IMR-90 human fibroblasts stably expressing SV40 large T and small t antigens survived crisis.) Overall, five TERT(+) and three TERT(-) cell lines containing the acceptor locus at a single site were identified. Several BAC reporters were constructed by inserting the firefly, *Renilla*, and h*Renilla* luciferase open reading frames into the start codons of *CRR9* and *TERT*, as well as the puromycin resistance gene (*puro*) into the vector backbone, of the h*TERT*-containing BAC RP11-117B23 using a two-step homologous recombination technique in bacteria termed recombineering. Smaller RMCE-competent plasmids were also created using recombineering by introducing *puro* into the base BAC vectors.

The ability of the acceptor locus-containing TERT(+) and TERT(-) cells to undergo RMCE was verified using the plasmid-based BAC vectors. Attempts to target both circular and linear h*TERT*-containing BAC reporters to the acceptor locus were unsuccessful in both TERT(+) and (-) cells. Random integration of linearized BAC reporters to the genome of acceptor locus-containing TERT(+) and (-) cells resulted in a total of 186 stable integrants. Analysis of these clones by luciferase assay, Southern

hybridization, and PCR amplification revealed that only 12 of these 186 clones (6.45%) appeared to be intact after integration and were therefore useful for addressing the modified hypothesis that BAC-based h*TERT* reporters would be able to mimic endogenous telomerase expression upon their introduction to genetically related TERT(+) and (-) cells. All 12 of these clones (seven TERT(+) and five TERT(-)) expressed high-level *CRR9* expression, as read out by firefly luciferase activity, and low-level *TERT* expression, as read out by *Renilla* luciferase activity. Therefore, BAC-based h*TERT* reporters do not appear to mimic endogenous telomerase expression patterns in genetically related, crisis-derived TERT(+) and (-) human fibroblasts.

TABLE OF CONTENTS

List of Tables

List of Figures

List of Abbreviations

166a	TERT(-) 3C-166a cells derived from IMR-90 cells
167b	TERT(+) 3C-167b cells derived from IMR-90 cells
293T	HEKs transformed with SV40 large T antigen
4HT	4-hydroxytamoxifen
5' HS4	DNaseI hypersensitivity site; chicken β-globin insulator
α–^{32}P-dCTP	deoxycytosine triphosphate labeled with ^{32}P
ψ	retroviral packaging signal
A	adenine
A260/A280	absorbance at a wavelength of 260 or 280 nm
alt	alternative lengthening of telomeres
APAP	alkaline phosphatase
ATP	adenosine triphosphate
BAC	bacterial artificial chromosome
β-gal	β-galactosidase
BLAST	basic local alignment search tool
bp	base pair
BSA	bovine serum albumin
C	cytosine
C.elegans	*Caenorhabditis elegans*
ChIP	chromatin immunoprecipitation
cHS4	chicken β-globin insulator
CIP	calf intestinal phosphatase
CMV	cytomegalovirus
CMV_{IEP}	CMV immediate early promoter
cmr	chloramphenicol resistance gene
CV1 cells	African green monkey kidney cells
DMEM	Dulbecco's modified Eagle medium
DMSO	dimethylsulfoxide
DNA	deoxyribonucleic acid

DNMT	DNA methyltransferase
dNTP	deoxynucleotide triphosphate
DPE	downstream promoter element
EDTA	ethylenediaminetetraacetic acid
EMEM	enhanced minimal essential media
EMSA	electrophoretic mobility shift assay
ES cell	embryonic stem cell
E.coli	*Escherichia coli*
EST	expressed sequence tag
Est2	ever-shortening telomeres
FBS	fetal bovine serum
FIAU	fialuridine
FL	firefly luciferase
G	guanine
G418	G418 sulfate
GCV	gancyclovir
gDNA	genomic DNA
GFP	green fluorescent protein
GMP	guanosine monophosphate
HAT	histone acetyltransferase
HDAC	histone deactelyase
HEK	human embryonic kidney cell
HeLa	human cervical cancer cells
HL60	human promyelocytic leukemia cells
HPRT	hypoxanthine-guanine phosphororibosyltransferase
HSV	herpes simplex virus
hTERC	human telomerase RNA component
hTERT	human telomerase ribonucleoprotein
IMR-90	primary human lung fibroblasts
Inr	initiator
IRES	internal ribosomal entry site

kana	neomycin phosphotransferase (prokaryotic selection)
kana/rpsL$^+$	cassette containing *kana* and *rpsL*$^+$
kb	kilobases
kD	kilodalton
LARII	luciferase assay buffer II
LCR	locus control region
LTR	long terminal repeat
M1	Mortality 1
M2	Mortality 2; crisis
MAPK	mitogen-activated protein kinase
Mb	megabase
MCF-7	human breast cancer cell line
MEF	mouse embryonic fibroblast
mPGK	mouse phosphoglycerate kinase
mRNA	messenger ribonucleic acid
mTERT	mouse telomere ribonucleoprotein
neo	neomycin phosphotransferase (eukaryotic selection)
neo^R	G418-resistant
nt	nucleotide
OD	optical density
oligo	oligonucleotide
ORF	open reading frame
PAC	P1 artificial chromosome
PBS	phosphate-buffered saline
PCR	polymerase chain reaction
pen/strep/gln	penicillin/streptomycin/L-glutamine
PEV	position effect variegation
PFGE	pulsed field gel electrophoresis
PLB	passive lysis buffer
PolII	RNA Polymerase II
POT1	protection of telomeres 1

pSK$^+$	pBluescriptSK$^+$ cloning vector
puro	puromcyin N-acetyltransferase
puroRL	fusion of *puro* and *Renilla* luciferase ORF
RL	*Renilla* luciferase
RLU/s	relative light units per second
RMCE	recombinase-mediated cassette exchange
RNA	ribonucleic acid
rpsL$^+$	gene providing streptomycin sensitivity to *E.coli*
RT	reverse transcriptase
S&G	stop & glo solution
S. cerevisiae	*Saccharomyces cerevisiae*
SDS	sodium dodecyl sulfate
SIN	self-inactivating
siRNA	small-interfering RNA
SSC	sodium chloride/sodium citrate buffer
ssDNA	single-stranded DNA
STAGA	SPT3-TAF-GCN5 acetylase
SV40	simian virus strain 40
T	thymine
TAF	transcription-associated factor
TBE	Tris/borate/EDTA electrophoresis buffer
TE	Tris-EDTA buffer
TERC	telomerase RNA component
TERT	telomerase reverse transcriptase
TERT(+)	cells displaying telomerase activity
TERT(-)	cells that do not display telomerase activity
TF	transcription factor
TIN2	TRF1-interacting nuclear factor 2
tk	thymidine kinase
TPP1	POT1 and TIN2 organizing protein
TRAP	telomeric repeat amplification protocol

TRF1/2	telomeric repeat binding factor 1/2
TRRAP	transformation-transactivation domain associated protein
TSA	trichostatin A
USF1/2	upstream stimulatory factor 1/2
UV	ultraviolet
VNTR	variable number of tandem repeats
WT1	Wilms' tumor 1 protein
YAC	yeast artificial chromosome

Acknowledgments

First and foremost, I would like to acknowledge Dr. Patrick G. Quinn, who was an integral member of my thesis committee up until his passing after a long battle with cancer. Even during his sickness, he made it a point to not only attend my committee meetings, but contribute scientifically and provide encouragement. Without his efforts on my behalf, I would have been unable to complete this thesis. I would also like to thank all of the many individuals who worked so hard to help me complete the requirements necessary to receive my doctorate, especially Drs. Sarah K. Bronson, Henry J. Donahue, Kristin A. Eckert, Leonard S. Jefferson, Jr., M. Judith Tevethia, and Michael F. Verderame. Drs. Donahue and Jefferson deserve special thanks for providing me with monetary support through the Cell and Molecular Biology Graduate Program and the Department of Cellular and Molecular Physiology, respectively. While Dr. Bronson may not have been my "official" mentor, I don't think I would have even made it past my first year without her support, especially in the last fifteen months when she provided me with a place to learn to love science again.

While so many other individuals helped me through the years, a few deserve extra recognition. I want to thank Dr. Steven Rannels for always providing an ear when I needed it, but more importantly, for showing me what courage, never giving up, and a strong will to live can give you. I also want to thank Dr. Diane McCloskey, who has been an amazing friend who helped me more than she can know in surviving the graduate school experience. I also wish to acknowledge the former and present members of the Bronson and Zhu labs and the staffs of the Cell and Molecular Biology Graduate Program, the Cellular and Molecular Physiology Department office, and the Graduate Student Affairs Office.

Last, but certainly not least, I want to thank my family for their never-ending support during this long journey. I really can't express what your love and unconditional support has meant to me not only during graduate school, but throughout my whole life. Mom, Dad, and Stacey, I love you from the bottom of my heart, and I thank you so much for helping me become who I am today.

Chapter 1
Introduction

1.1 Control of Eukaryotic Gene Expression

The manner in which organisms, from the simplest prokaryotes to the most complex eukaryotes, express their genes has long been understood to be critical for their identity, structure, and function. Initially, it was thought that more complex organisms would have more complex genomes, including more genes. While eukaryotic genomes are certainly more complex than those of prokaryotes, genome sequencing projects have revealed that increased organismal complexity does not necessarily correlate with an increase in overall gene number. For example, the relatively simple eukaryote *Caenorhabditis elegans* (*C.elegans*) has ~20,000 genes (1) while the more complex eukaryote *Drosophila melanogaster* has less than 14,000 (2). Furthermore, the human genome contains only twice the number of genes (~30,000) (3) as *Drosophila* but is obviously more than two times as complex. Genome sequencing thus underscores the importance of gene regulation in controlling organismal complexity. Appropriate gene regulation is also critical for normal organismal function, and is underscored by the numerous diseases caused by aberrant gene expression. As expected for such an important process, eukaryotes have developed numerous mechanisms for controlling gene expression at all levels, including DNA, chromatin, RNA, and protein. As many genes are thought to be controlled at the levels of transcription and RNA processing, a discussion of the salient points concerning gene control at the DNA, chromatin, and RNA levels is included here.

1.1.1 Control of Gene Expression at the DNA Level

The most basic level of gene regulation is encoded at the DNA level in the form of gene-specific promoters, enhancers, and silencers. The core promoter of a gene is the minimal DNA sequence able to coordinate transcriptional initiation by RNA polymerase

II (PolII) and its associated factors. The core promoter is a compact region of DNA ~40 nucleotides (nt) long that includes the transcription start site. Because the core promoter contains the transcription start site, it is therefore important in recruiting the basal transcription machinery, which consists of transcription factors (TF) IIA, TFIIB, TFIID, TFIIE, TFIIF, TFIIH, and PolII (reviewed in (4)). In order to recruit the basal transcription machinery, core promoters rely on various DNA binding elements. One such element is the TATA box, a region of DNA composed mostly of adenine and thymidine nucleotides located ~30 base pairs (bp) upstream of the transcriptional start site. The TATA box binds the TATA-binding protein (TBP), a component of TFIID (5). The TFIIB recognition element (BRE) is located immediately upstream of some TATA-containing promoters and functions to increase the affinity of TFIIB for the core promoter (6). Given that only 32% of human genes were found to contain a TATA box (7), there is an obvious requirement for alternative core promoter elements capable of recruiting the basal transcription machinery. Downstream promoter elements (DPEs) are found in core promoters that lack TATA boxes, are located ~30 bp downstream of the transcription start site, and are able to initiate transcription via binding of TBP-associated factors (TAFs) of the TFIID transcription initiation complex (8;9). Transcriptional initiation mediated by DPEs requires the initiator (Inr), a conserved sequence element covering the transcription start site. Inrs are able to initiate transcription either by themselves or along with TATA boxes and DPEs by binding TAFs of TFIID and/or PolII (10).

Immediately surrounding the core promoter is the proximal promoter, a region of DNA capable of binding transcription activators and repressors, as well as proteins that serve to recruit distal enhancers to the core promoter (11). While the core promoter binds transcription factors common to most genes, the proximal promoter binds factors that are gene- and/or tissue-specific, adding a finer level of control to gene expression. (A summary of some common transcription factors is found in Table 1.1.) In addition to transcription factor binding sites, proximal promoters also contain hormone response elements, which further control gene expression (12;13). Enhancers are DNA sequence elements that range in size from 50 bp to 1.5 kilobases (kb) and also bind transcription factors. In contrast to promoters, enhancers can be located anywhere within ~100 kb of a

gene and function in an orientation-independent manner (14;15). Genes typically rely on more than one enhancer to aid in their regulation such that each individual enhancer is responsible for directing expression at a specific developmental stage or in a specific tissue (15). In conjunction with enhancers, many genes also contain silencers, DNA elements that function in a location- and orientation-independent manner to repress gene expression (16).

A final sequence element involved in regulating select genes is the insulator, an element that marks gene boundaries by stopping the spread of condensed chromatin and preventing distant enhancers and silencers from influencing expression of the wrong gene (17;18). While insulators have been well-characterized in lower eukaryotes such as *Drosophila* and yeast (19), they remain relatively uncharacterized in higher eukaryotes. The exception is the chicken β-globin insulator 5' DNaseI hypersensitive site (5'HS4), which marks the boundary between the open chromatin conformation of the β-globin locus from the closed chromatin conformation of the upstream region (18). Fine analysis of 5'HS4 revealed the enhancer blocking function to be provided by its binding of the highly conserved regulatory protein CTCF (20). The chromatin barrier function, which is CTCF-independent (21), relies on the ability of the highly acetylated histones of chromatin at the insulator to prevent both DNA and histone methylation (22).

In order to coordinate the activities of the core and proximal promoters with those of distant enhancers, silencers, and insulators, cells rely on transcriptional cofactors, adaptor proteins involved in transcriptional activation and repression. Transcriptional cofactors do not bind directly to the DNA (23;24); instead, they associate with factors already bound to the DNA. In combination with processes such as DNA looping, cofactors bring distal elements into the proximity of promoters, allowing them to coordinately regulate gene expression. Similar to transcription factors, cofactors can be tissue-, lineage-, or cell-dependent and are conserved in higher eukaryotes. Examples of co-activators are the TAFs of the TFIID complex (25), CBP (26) and its homologue p300 (27), and TAZ (28); co-repressors include groucho (29), CtBP (30), N-CoR (31), and TGIF (32).

Methylation of cytosine residues by DNA methyltransferases (DNMTs) is another mechanism by which eukaryotes regulate gene expression at the DNA level, specifically

by repressing transcription. DNA methylation inhibits gene expression in one of two ways: by preventing DNA-binding factors from binding to their recognition sites (33;34) or by binding methyl-CpG-binding proteins (MBPs) that recruit transcriptional co-repressors and/or chromatin remodeling factors (35;36). DNA methylation is especially important for maintaining the appropriate expression of imprinted genes, which are those genes expressed preferentially from either the paternal or maternal locus (reviewed in (37)). While it is known that global demethylation and remethylation occur during embryogenesis and development, the exact mechanisms by which these processes occur are not clear (reviewed in (38) and (39)). It is known that DNMT3a and DNMT3b are *de novo* methylases that methylate previously unmethylated cytosines and that DNMT1 is a maintenance methylase that copies the methylation marks of the parental DNA strand onto the newly replicated one. Regardless of the exact mechanism, the necessity of DNA methylation and its appropriate recognition by MBPs is underscored by the embryonic lethality of *Dnmt3b* and *Mbd3* knockout mice (40;41) and the failure of *Mbd2* knockout mice to nurture their offspring (41). Human manifestations of aberrant methylation and methylation recognition include ICF syndrome, an autosomal recessive disease characterized by immunodeficiency and caused by mutations in *DNMT3b* (42), Rett syndrome, a neurological disease affecting females caused by mutations in the *MECP2* gene (43), and Prader-Willi and Angelman syndromes, diseases associated with obesity and metal retardation caused by a failure of imprinting (44;45).

1.1.2 Control of Gene Expression at the Chromatin Level

In order to fit the billions of DNA nucleotides into the nucleus, they must be compacted. The condensed form of DNA and its associated proteins is known as chromatin. Nucleosomes, the basic unit of chromatin, consist of ~150 bp of DNA wrapped around a histone octamer composed of the core histones H2A, H2B, H3, and H4 (reviewed in (46)). Chromosomes consist of one long association of adjacent nucleosomes, separated by ~30-40 bp of linker DNA, that are folded in a dynamic manner. The organization of DNA into chromatin also plays an important role in controlling gene expression. Traditionally, only two chromatin states were assigned:

regions of active gene transcription were associated with a more open chromatin state, referred to as euchromatin, while regions of silenced genes were associated with a closed chromatin state, referred to as heterochromatin. It is now known that chromatin exists in many different structural and functional conformations and that changes in the state of chromatin are tightly linked with changes in gene activity.

The chromatin status is regulated through covalent modifications of the core histones and ATP-dependent chromatin remodeling complexes. Core histones contain N-terminal tails subject to post-translational modifications including acetylation, methylation, phosphorylation, and ubiquitination. As proposed by Allis, these modifications serve as a "histone code" that aids in determining the fate of a particular region of chromatin (47-49). Although histone modifications signal in a combinatorial manner to aid in the control of gene expression, correlations between acetylation, methylation, and gene transcription are well established. In general, hyperacetylated histones are associated with open chromatin and active gene transcription while deacetylated histones are associated with closed chromatin and transcriptional suppression (50). Histone acetylation is a rapidly reversible process mediated by histone acetyltransferases (HATs) and histone deacetylases (HDACs) and occurs at lysine residues of histones H3 (K9, K14, K18, and K23) and H4 (K5, K8, K12, and K16) (51;52). Along with histone acetylation, phosphorylation of serine residue 10 of histone H3 (H3S10) is associated with active transcription (53). Histone modifications are closely linked to the general transcriptional machinery through the recruitment of HATs and HDACs by transcription factors and cofactors; in fact, HATs and HDACs themselves can function as cofactors themselves. One example of this phenomenon is the recruitment of the HAT p300/CBP to promoters by the transcription factor CREB (26) and its ability to facilitate transcription by binding TFIIB (54). The importance of appropriate histone acetylation is revealed by the linking of aberrant histone acetylation with leukemia (55;56).

As opposed to histone acetylation, histone methylation is associated with both heterochromatin (methylation of histone H3 at K9, K27, and K35 and histone H4 at K20) and euchromatin (methylation of histone H3 at K4, K36, and K79) (46;57). The most important methylated lysine residue associated with transcriptional repression is H3K9;

methylation of this residue by the histone methyltransferase SUV39H1 creates a binding site for the heterochromatin-associated protein HP1 and thus results in gene repression (58;59). Histone and DNA methylation are closely related processes that seem to perpetuate each other in the formation of epigenetic heterochromatin (60;61). The methylation of H3K9 by SUV39H1 is inhibited if H3K4 is already methylated by its methylase, Set9 (62); a lack of H3K9 methylation prevents the binding of HP1 and the subsequent formation of heterochromatin, thus providing a mechanism by which H3K4 methylation promotes active transcription. Until recently, histone methylation was thought to be a permanent modification as no histone demethylases were known; however, the discovery of LSD1, a protein that specifically demethylates H3K4 and therefore serves as a transcriptional co-repressor (63), has changed this view. Since the discovery of LSD1, other histone demethylases have been uncovered, including JHDM1, which represses gene expression by demethylating dimethylated H3K36 (64), and JHDM2, which activates gene expression by demethylating H3K9 (65).

A second means of modifying chromatin is via the ATP-dependent chromatin-remodeling complexes (reviewed in (66)). As expected, genes within open chromatin, or nucleosome-free regions, are more easily transcribed than those within closed chromatin, or those that are nucleosome-rich. To move the nucleosomes, ATP-dependent chromatin-remodeling complexes move the nucleosomes within the DNA via ATP hydrolysis, leading to the exposure of some regions of DNA while concurrently hiding others. As expected, ATP-dependent remodeling complexes have been shown to work in close association with HATs and HDACs to mediate the overall effect of the chromatin status on gene expression. For example, chromatin immunoprecipitation (ChIP) analysis following treatment of MCF-7 breast cancer cells with estrogen revealed that both the ATP-dependent chromatin-remodeling complex BRG1 and the HAT p300/CBP were recruited to promoters containing estrogen response elements (67). A second example of the interplay between ATP-dependent chromatin remodeling and the histone code is the ability of methylated H3K4 to prevent the association of HDACs and the ATP-dependent remodeller NuRD, thus preventing chromatin condensation and promoting gene expression (68). As is the case with HATs and HDACs, ATP-dependent complexes are associated with transcription factors, including SWI/SNF with HSF1 (69). Taken

together, transcription factor binding to promoters, enhancers, and silencers and the chromatin remodeling complexes can be thought of as forming a giant holoenzyme complex that mediates transcription ((70); reviewed in (71;72)).

1.1.3 Control of Gene Expression at the mRNA Level

The next level in gene expression is the formation of RNA transcripts from the DNA template. These transcripts will eventually be transported to the cytoplasm for protein synthesis; however, before protein synthesis can be initiated, the RNA must be processed. The raw transcript of DNA produced by RNA polymerase is known as pre-messenger RNA (pre-mRNA) and contains both the coding sequence (exons) and non-coding sequence (introns) of the gene. Following the synthesis of the pre-mRNA, an N^7-methyl GMP cap is added to the 5' end of the transcript, the introns are removed in a process known as splicing, and a polyA tail of ~200 adenosines is added to the 3' end of the transcript. The result of pre-mRNA processing is the formation of the mRNA proper, which, after export to the cytoplasm, serves as the template for protein synthesis via translation. (Further details can be found in a review by Soller (73).) The importance of alternative pre-mRNA processing in gene expression is evidenced by the fact that ~60% of human genes have multiple splice variants (74) and ~30% of human genes have alternate polyA sites (75). Splicing is mediated by the spliceosome complex, which consists of five small ribonucleoprotein particles (snRNPs; U1, U2, U4, U5, and U6) that bind to four sequence elements: the 5' splice site, the branchpoint, a polypyrimidine tract, and the 3' splice site (76;77). The choice of the splice site is dependent on the binding of RNA binding proteins to exonic and intronic splicing enhancers and suppressors. Many of these RNA binding proteins are tissue-specific factors, leading to the expression of certain splice variants in one tissue type and other variants in a different tissue (78) or different splice variants at different developmental timepoints (79). Aberrant splicing has been implicated in many diseases, including the tumor-susceptibility syndrome neurofibromatosis (80), spinal muscular atrophy (81), ataxia-telangiectasia (82), and cancer (reviewed in (83-85)). Although it was originally thought that pre-mRNA processing was separate from transcription, recent evidence has revealed that these

processes are actually coupled. For example, the splicing factor CPSF was found to associate with the general transcription factor TFIID (86). The association of proteins involved in mRNA processing with those of transcription, and the association of transcription factors with those involved in chromatin modification, further underscores the interrelated nature of gene control.

1.2 Telomeres

1.2.1 Discovery and Definition of Telomeres

Telomeres are the sequence found at the ends of all eukaryotic chromosomes and function as caps that protect essential genetic information from being lost during replication. The pioneering work that revealed the importance and necessity of telomeres was performed by Hermann Müller in his studies of X-ray-induced mutations of *Drosophila melanogaster* chromosomes in the 1920s and 30s (summarized in (87)). Further underscoring the importance of telomeres was Barbara McClintock's seminal paper on recombination in maize, published in the journal *Genetics* in 1941 (88). Both Müller and McClintock showed that while normal, undamaged linear chromosomes did not fuse to one another, the pieces of chromosomes produced by chemical and physical stress were able to fuse to one another, leading to bridge-fusion-breakage cycles and subsequent aneuploidy. These observations led them to conclude there must be some specialized sequence and/or structure located at the ends of chromosomes that prevents their fusion to one another.

1.2.2 Conservation of Telomere Structure and Function

As demonstrated by the work of Müller and McClintock, telomeres are present in such disparate organisms as insects and plants. Subsequent work has shown, as predicted by Müller and McClintock, that all eukaryotic chromosomes harbor telomeric sequence at their ends to protect themselves from end-to-end fusion and exonucleolytic activity. In 1978, the first telomere sequence was published by Blackburn and Gall (89). Taking advantage of the extrachromosomal, high-copy number ribosomal RNA genes (rDNA) found in the protozoan *Tetrahymena thermophila* macronucleus to isolate enough DNA to sequence the terminal ends. This sequencing revealed that all of the rDNA molecules shared the same hexanucleotide sequence, 5'-TTGGGG-3', repeated tandemly at their ends. In the next decade, the telomere sequences of additional eukaryotes were

determined, including those of yeast (*Saccharomyces cerevisiae* (90)), plants (*Arabidopsis thaliana* (91)), and humans (92). Even though there is no single telomere sequence found in all eukaryotes, all telomeres share similar characteristics with few exceptions. (For an overview of telomeres of different species, see Table 1.2.) Telomeres are comprised of tandem copies of simple repeats rich in thymine (T) and guanine (G) nucleotides on the 5'-3' strand, where 5' refers to the centromere. The number of these repeats varies between species, and even within chromosomes of the same species in the same cell (93-95). Additionally, the 5'-3' strand of the telomere, referred to as the G-strand, overhangs the 3'-5' strand, or C-strand, by a number of repeats as small as 12-16 bases in ciliated protozoans (96) and as large as 130-210 bases in mammals (97). To protect themselves from degradation, G-strand overhangs invade the duplex telomere sequence to form what is known as a t-loop (98-101). The conserved nature of telomeres is revealed by studies that showed ciliate telomeric repeats were able to be elongated when introduced as linear plasmids in yeast even though the two species have different telomere repeats (90;102).

1.2.3 Telomere/Protein Complex

While the tandemly repeated copies of DNA that comprise the telomere are critical to the protection of linear chromosome ends, the DNA sequence itself does not function as a cap without its host of associated proteins. All eukaryotic telomeres are associated with some form of protein complex, although the composition varies somewhat between species. The six proteins associated with telomeres throughout the cell cycle in vertebrates form a complex referred to as shelterin (Figure 1.1) (103). The six shelterin proteins are telomeric repeat binding factor 1 (TRF1), telomeric repeat binding factor 2 (TRF2), TRF1 interacting nuclear factor 2 (TIN2), telomeric repeat binding factor similar to *S.cerevisae* Rap1 (RAP1), POT1 and TIN2 organizing protein (TPP1), and protection of telomeres 1 (POT1); briefly, they function as follows. Through Myb-type DNA-binding domains, TRF1 and TRF2 bind the sequence 5'-YTAGGGTTR-3' and serve as scaffolds for the binding of the remaining shelterin subunits (104;105). Through their ability to form homodimers and higher order oligomers, TRF1 and TRF2

allow for the accumulation of multiple shelterin complexes at the telomere. RAP1, identified by a yeast 2-hybrid assay, associates with TRF2 and functions as a regulator of telomere length (106). Although originally identified through a yeast 2-hybrid experiment using TRF1 as bait (107), TIN2 has since been shown to bind both TRF1 and TRF2, forming a bridge connecting the functions of both protein complexes (108). POT1 was identified due its sequence homology with known telomere binding proteins in other eukaryotes (109); through its ability to recognize the sequence 5'-(T)TAGGGTTAG-3', POT1 binds the G-strand overhang to maintain and regulate its length (110). TPP1, more commonly known as TINT1, PTOP, or PIP1, binds both TIN2 and POT1, thus tethering POT1 to the remainder of the shelterin complex (111).

The protection of linear chromosomes is mediated by shelterin's modulation of the structure of the telomere and its prevention of the DNA damage response. The structural effects of shelterin on the telomere include the formation of t-loops, regulation of the length of the G-strand overhang, and overall telomere length maintenance. As mentioned above, the t-loop is critical to maintaining the integrity of the telomere, and, therefore, the entire chromosome. While not yet verified by *in vivo* studies, purified TRF2 has been shown to be sufficient for t-loop formation of synthetic telomere substrates *in vitro* (98). Additionally, TRF1 has been shown, *in vitro*, to modulate the looping, bending, and pairing of synthetic telomere substrates (104). The importance of shelterin in maintaining the single-stranded G-strand of the telomere has been demonstrated by studies showing that inhibiting either TRF2 (112) or POT1 (110) results in the shortening of the G-strand by up to 50%. From the standpoint of human disease, a recently published report suggests that aberrant expression of TRF1, TRF2, and TIN2 is implicated in the etiology of adult T-cell leukemia (113).

As is well established, the DNA damage response is critical to cell survival, faithful DNA replication, and normal cellular function. Intuitively, shelterin must be involved in preventing telomeres from undergoing unnecessary repair events usually initiated by single-stranded DNA (ssDNA) or double-stranded breaks but allowing repair when telomeres are truly damaged or critically shortened. The prevention of unnecessary repair by such processes as nonhomologous end-joining (NHEJ) and homologous recombination is thought to be mediated by t-loop formation and the subsequent

nucleosomal changes in the DNA (reviewed in (103)). One way in which telomeres signal DNA damage is via the loss of shelterin components; the loss of shelterin components results in the telomeres becoming unprotected, leading to ATM kinase activation, p53 upregulation, and p21-mediated G1/S cell cycle arrest (114). Besides the shelterin proteins, many additional proteins play a role in regulating appropriate DNA repair at the telomere, including endonucleases (ERCC1/XPF (115)), helicases (WRN and BLM (116)), and the MRE11/RAD50/NBS1 recombination repair complex (117). These proteins are not considered to be members of shelterin because they are not constitutively associated with the telomere and they function elsewhere in the DNA; nevertheless, they are critical to the protection of eukaryotic chromosomes. Overall, telomeres rely on the action of many proteins, including those of the shelterin complex, for proper function. This is evidenced by the critically shortened telomeres found in cells of individuals with various genomic instability syndromes, including ataxia telangiectasia (mutated *ATM*; (118)), Werner syndrome (mutated *WRN*; (119)), and Bloom syndrome (mutated *BLM*; (120)).

1.3 Telomerase

1.3.1 The End Replication Problem and the Need For a Reverse Transcriptase

As was clearly demonstrated in the seminal study by Matthew Meselson and Frank Stahl in 1958, DNA is replicated in a semi-conservative fashion (121). (While both prokaryotes and eukaryotes undergo semi-conservative replication, the mechanisms are slightly different due to the circularity of prokaryotic chromosomes and the linearity of eukaryotic chromosomes; the eukaryotic method of replication is discussed here.) The first step in DNA replication is the formation of an origin of replication, an area of localized DNA melting that results in the separation of the two strands of the double helix. Once the DNA is melted, helicases bind to the DNA and unwind the double helix; the unwound helix is now accessible to the polymerases necessary to synthesize the two new strands of DNA. As DNA polymerase is unable to synthesize DNA *de novo*, short RNA primers are laid down by primase and then elongated by DNA polymerase. In addition, DNA polymerase is only able to synthesize DNA in the 5'-3' direction. Therefore, while one strand of DNA, the leading strand, requires only one RNA primer, the other, the lagging strand, requires multiple priming events, leading to the formation of short stretches of newly synthesized DNA referred to as Okazaki fragments. These RNA primers are eventually removed by FEN1 and/or the exonuclease activity of DNA polymerase, and the Okazaki fragments of the lagging strand are joined by DNA ligase. However, because of DNA polymerase's inability to self-prime or synthesize DNA in the 3'-5' direction, the ends of the chromosome are unable to be replicated. Without another mechanism to replicate chromosomal ends, terminal DNA sequence (telomeres) would be lost with every round of replication. In fact, eukaryotic cells do possess the ability to lengthen and maintain telomeres via the ribonucleoprotein complex telomerase.

The existence of a telomere terminal transferase was hypothesized by Shampay et al. in 1984 to explain the ability of *S.cerevisae* to maintain and elongate telomeres, both native and trans-species (90). Elegant experiments performed by Greider and Blackburn using *Tetrahymena* cell-free extracts and both native *Tetrahymena* telomeres and yeast telomeres introduced as oligomers verified the existence of a telomere transferase (122).

Two years later, in 1987, Greider and Blackburn used a series of different chromatography columns to purify a ribonucleoprotein complex from *Tetrahymena* S100 extracts that possessed the telomere terminal transferase activity; they named this complex telomerase (123). Their experiments with purified telomerase demonstrated that telomere elongation occurs only when there is a 5'-3' sequence overhang and when this overhang sequence is rich in thymine and guanine nucleotides, indicating that telomerase has both structural and sequence specificity. The hypothesized existence of a telomere terminal transferase in all eukaryotes was bolstered by the isolation of a protein complex from cells of the HeLa human cervical cancer cell line that possessed the same characteristics as the telomerase ribonucleoprotein of *Tetrahymena* (124).

1.3.2 TERC: The Telomerase RNA Component

The consistent co-purification of a 159 nt RNA molecule with the protein complex that permitted *in vitro* extension of telomeres led Greider and Blackburn to the conclusion that this RNA component was essential for elongating telomeres, implying that telomerase was a ribonucleoprotein complex (123). They further hypothesized that this RNA component might serve as the template for telomerase activity since telomere elongation by this same purified complex did not require the addition of exogenous template. The role of RNA molecules in substrate recognition was already established for many ribonucleoproteins, including those involved in mRNA splicing (125;126). The subsequent cloning of the *Tetrahymena* gene for the 159 nt RNA molecule revealed the presence of the sequence 5'-CAACCCCAA-3' in its coding region, supporting the claim that the RNA component did indeed serve as the template for telomerase activity (127); later studies verified the essential nature of the telomerase RNA component (TERC) for all eukaryotes (128-130).

The human *TERC* (h*TERC*) gene is located on chromosome 3, arm q, band 26 (3q26) (131) and is also known as h*TR* and h*TRC3*. While all eukaryotes require TERC for appropriate telomere elongation, the TERC molecule itself varies greatly between species; *Tetrahymena* TERC is 159 nt, that of budding yeast around 1,000 nt, and that of vertebrates about 450 nt (reviewed in (132)). All TERC molecules share conserved

structural domains directly related to their function, including a 5' template boundary element, a large loop containing the template proper, a pseudoknot region, and a loop-closing helical region; these domains function in TERC binding to TERT, TERC association with the telomere, and, potentially, TERC dimerization. (For a review, please see (132).) Studies in transgenic mouse models of multi-step tumorigenesis revealed that while m*TERC* was upregulated during tumorigenesis, its expression did not necessarily correlate with increased telomerase activity (133). A similar finding was found in studies on human cells that showed h*TERC* was expressed in all somatic cells, and even though it was upregulated in some cancers, its expression did not directly correlate with telomerase activity (134). Mutations in h*TERC* cause autosomal dominant inheritance of dyskeratosis congenita (AD-DC), a disease characterized by cutaneous abnormalities, bone marrow failure, and a predisposition to cancer (135). The severity of AD-DC is closely tied to overall telomere length as successive generations of eight different families with AD-DC showed increased disease anticipation correlated with shorter telomeres (136).

1.3.3 TERT: The Telomerase Protein Component

The protein component of the telomerase ribonucleoprotein (TERT) is a reverse transcriptase that uses TERC as its RNA template to synthesize telomeric DNA repeats. The first telomerase reverse transcriptases to be identified and cloned were those of *Euplotes aediculatus* (p123 and p43 (137)) and *S. cerevisiae* (Est2 (138)). Utilizing BLAST searches of the human EST database with the known sequences of p123 and Est2, several groups identified and cloned the human telomerase reverse transcriptase (139-141). Examination of the protein sequence of the telomerase proteins revealed motifs common to known retroviral reverse transcriptases, further solidifying telomerase's role as a reverse transcriptase (138). Using a telomerase-specific motif (motif T (141)) to search newly sequenced genomes, putative telomerase genes have been identified in *Mus musculus* (mouse; GeneID 21752), *Bos taurus* (cow; GeneID 518884), *Canis familiaris* (dog; GeneID 403412), *Pan troglodytes* (chimpanzee; GeneID 461695), and *Arabidopsis thaliana* (plant; GeneID 831548), among others.

1.3.4 Differential Telomerase Expression Among Species and Its Implications

While all eukaryotes express some form of telomerase, the levels and time of expression vary among species. In unicellular species, including the ciliates *Tetrahymena* and *Euplotes* and the yeasts *Saccharomyces cerevisiae* and *Schizosaccharomyces pombe*, telomerase is expressed throughout the organisms' lifespan, and therefore, telomere length is relatively stable. The necessity of telomerase activity in these organisms is evidenced by the aberrant growth and eventual senescence of yeast cells that lack *EST2* (138;141). Mice display high levels of telomerase (m*TERT*) expression throughout embryonic development (142). In adult animals, virtually all cells express mTERT mRNA, although the level varies from very high in cells that display significant levels of mTERT activity, including those of the liver, testis, and thymus, to low in cells that lack detectable telomerase activity, including those of the brain and kidney (142-144). In cultured mouse embryonic fibroblasts (MEFs), mTERT mRNA is expressed at a constant level throughout culture while telomerase activity fluctuates from detectable at early passage, decreased during continued culture, and high when the cells become immortal (144).

In humans, telomerase activity is more highly regulated. During early embryogenesis and development, telomerase activity is high (145-147), but by the time humans reach adulthood, the only cells that retain telomerase activity are cells of the germline, some hematopoietic precursors, and the stem cells of tissues with a high turnover rate, such as the intestine and skin (145;148-153). As opposed to the mouse, where mTERT mRNA can be found in cells that lack telomerase activity, hTERT mRNA is only expressed in those cells with detectable telomerase activity (154-158). This difference in telomerase expression between mice and humans has been hypothesized to be the cause of various *in vitro* and *in vivo* phenomena noted in the literature. *In vitro*, the less restricted expression of m*TERT* is hypothesized to be the reason for the ability of primary murine cells, but not primary human cells, to spontaneously immortalize during extended culture (159); *in vivo*, the less restricted expression of m*TERT* is thought to be one of the causes of spontaneous tumorigenesis in mice (144) and the lack of a phenotype

in telomerase knockout mice until later generations (130;160;161).

1.3.5 Role of Telomeres and Telomerase in Normal and Diseased States

The lack of telomerase activity in adult human somatic cells implies that with each round of replication, telomeric DNA will be lost from the chromosome ends. Studies in a variety of cell types have revealed that telomere length is heterogeneous and does decrease *in vitro* with each round of replication (162;163) and *in vivo* with aging (164-166). Theoretically, if telomere shortening was due only to the end-replication problem, telomeres would shorten by the length of the terminal RNA primer, or 8-12 bp per cell division. The actual shortening of telomeres by 50-200 bp per cell division indicates that other factors besides the end-replication problem are responsible for the loss of telomere sequence. One possible contributor to telomere shortening is the active degradation necessary to create the G strand overhang following replication (97). Psychological stress, both perceived and chronic, has recently been linked to telomere shortening (167). This effect is thought to be mediated via oxidative stress due to previous studies that showed the increased presence of oxidative damage in cells isolated from individuals with high levels of psychological stress (168-170) and the correlation between increased oxidative stress and accelerated telomere shortening (171-173).

It has been known for decades that primary cells continuously cultured under standard conditions stop proliferating after a reproducible period of time in culture. Hayflick defined this permanent exit from the cell cycle as senescence (174). (The maximum number of population doublings (PD) cells undergo before senescing is referred to as the Hayflick limit in honor of Hayflick's insights.) The inverse correlation between donor cell age and replicative lifespan, as well as the positive correlation between expression of senescence-associated markers and the decreased Hayflick limit of cells isolated from patients with premature aging syndromes, led many to argue that senescence is a model of aging (reviewed in (175)). The telomere hypothesis of aging was established in the late 1990s as an explanation of senescence. The observations that led to the hypothesis that telomeres serve as a "mitotic clock" include the decrease of telomere length during serial culture (162), the decreased length of telomeres isolated

from elderly donors (162), the expression of telomerase in immortal cell lines and cancer (145;151), and the immortalization of human cells by hTERT transfection (176). It has since been shown that it is not telomere length that leads to senescence, but rather the presence of dysfunctional telomeres. Dysfunctional telomeres, which include those that have lost shelterin components and are therefore uncapped and those that have a shortened G-strand overhang (177-179), induce senescence via activation of the DNA damage response through either the phosphorylation of p53 by ATM kinase (114) or, in humans, through the p16/pRb pathway (180). The idea that telomeres alone serve as the mitotic clock and are the cause of aging has fallen out of favor; instead, it is now thought that a combination of factors, including telomere shortening, oxidative damage, DNA cross-links, loss of DNA methylation, and heterochromatin instability are responsible for aging (reviewed in (181-185)). Even though telomere shortening may not be the sole cause of organismal aging, shortened telomeres are associated with various age-related disorders in humans, including vascular dementia (186) and atherosclerosis (187), as well as an overall increase in mortality (188).

While there may not be a clear link between telomere length and human aging, there is an indisputable correlation between telomere length, telomerase activity, and cancer. The link between cancer and telomerase activity was clearly established over twenty years ago in studies that showed cells isolated from cancerous lesions displayed telomerase activity while cells isolated from adjacent non-cancerous tissue did not (145;189). Since these initial studies, telomerase activity has been found in 85-90% of all human tumors (151). Intuitively, one might think cancer cells would have longer telomeres than normal cells due to the activation of telomerase; however, in actuality, the telomeres of cancer cells have been consistently shown to have very short telomeres (reviewed in (190;191)). It is currently understood that these short telomeres are the result of cancer cells being able to bypass normal replicative senescence (Mortality 1, or M1) due to mutations in genes of the DNA damage/DNA checkpoint pathways. Eventually, these cells will reach a second plateau (M2, or crisis) where they have lost the ability to cap their chromosomes due to extensive telomere loss, resulting in bridge-fusion-breakage cycles and genomic instability. The subsequent mass DNA damage results in apoptosis for most cells; however, if cells are able to stabilize their shortened

telomeres, either by TERT activation or through the alternative lengthening of telomeres (alt) pathway, they are able to continue dividing indefinitely, thereby becoming immortal (192). The requirement of telomere maintenance and the presence of TERT activity in a large majority of cancers has made telomerase an attractive biomarker for cancer detection (193) and target for anti-cancer therapy (reviewed in (194;195).

1.3.6 Human Telomerase Regulation

Despite almost 25 years of study, the mechanisms of hTERT regulation have remained elusive; however, the correlation between a lack of telomerase activity and hTERT mRNA seems to suggest telomerase expression is regulated mainly at the level of transcription (196). The human telomerase protein is encoded by the *TERT* gene located on 5p15.33. The gene itself is ~40 kb in length and is comprised of 16 exons that produce an mRNA transcript of ~4 kb (Figure 1.2) (197;198); translation of this transcript yields a protein of 1,132 amino acids with a molecular weight of approximately 125 kilodaltons (kD) (139;141). Characterization of the 5' region of h*TERT* revealed the lack of a TATA or CAAT box, but, as is the case for many TATA-less promoters, this region is rich in GC content (>70% from -900 bp to the second exon, relative to the translation start site) and contains an Inr sequence immediately upstream of the transcription start site (197-199). Studies using luciferase reporters driven by various regions of sequence 5' of the transcriptional start site identified the core promoter as being located in the 181 bp upstream of the start site, or 258 bp upstream of the translational start site (199); these studies also revealed the presence of a repressive element located somewhere between -1,400 bp and -776 bp. Analysis of the sequence located -960 to +360 bp relative to the translation start revealed the presence of binding sites for known transcription factors, including E-box family members, Sp1, AP2, NF1, AP4, MyoD, and Myb, and the hormones estrogen and progesterone (197). However, the presence of a binding site does not necessarily guarantee that the transcription factor will bind to it and function in gene regulation. For example, AP2 has not been shown to bind to the h*TERT* core promoter even though its binding sites are present (199). Below is a discussion of the role of transcription factors in regulating h*TERT* transcription.

Even before the initial publication of the h*TERT* sequence and its promoter, there was a report in the literature showing that overexpression of the cellular oncogene c-Myc was able to induce telomerase activity in normal human mammary epithelial cells (HMECs) and normal diploid fibroblasts (IMR-90 and WI-38) (200). Furthermore, this induction of telomerase activity was shown to extend the lifespan of the cells. One year later, Greenberg et al. proved that h*TERT* is a direct target of c-Myc by showing that c-Myc overexpression in telomerase negative (TERT(-)) IMR-90 cells resulted in the induction of hTERT mRNA in the absence of protein synthesis and required the E-box located at -34 bp relative to the translational start site (201). Further probing of the core promoter showed telomerase activation by Myc also required the presence of the Sp1 binding site, suggesting a functional cooperation of these two factors in regulating transcription (202). The functional cooperation of Sp1 and Myc was also found to be necessary for the induction of telomerase by human papilloma virus strain 16 (HPV-16) protein E6 (203). Other members of the Myc/Max network of proteins, including Mad and upstream stimulatory factors 1 and 2 (USF1, USF2), have been shown to function as h*TERT* repressors. Mad was isolated as a repressor of h*TERT* using expression cloning and reporter assays in normal human embryonic kidney cells (HEK) and SV40-transformed kidney cells (293T) (204). This study revealed that Mad's effects were mediated through the E-box and that Myc and Mad competed for binding to the promoter. In a normal cell, Mad is preferentially associated with the promoter, leading to h*TERT* repression, but overexpression of Myc, which is associated with many cancers, results in the replacement of Mad with Myc and transcriptional activation. In another study on HPV-16 protein E6's ability to induce h*TERT* expression, USF1 and USF2 were found to function in the same way as Mad (205). This association of Mad with a lack of hTERT expression and Myc with active expression was confirmed by differentiation studies in human hematopoietic U937 cells (157). U937 cells, in their undifferentiated state, express telomerase, but upon induction of differentiation via the phorbol ester TPA, telomerase expression is lost. Gunes et al. showed that the loss of telomerase expression was due to a loss of h*TERT* transcription and mediated by the upregulation of Mad1. One year later, the same situation was found upon differentiation of the human promyelocytic leukemia line HL60 (206). Together, these studies underscore the point that telomerase

expression is mediated mainly at the level of transcription and is actively repressed in normal, TERT(-) cells.

As indicated above, cooperation between Sp1 and c-Myc seems to be required for activation of h*TERT* expression. Sp1 belongs to the Sp1 zinc finger family of transcription factors, which consists of Sp1, Sp3, and Sp4. Similar to the Myc/Mad family where some members are transcriptional activators and others are transcriptional repressors, Sp1 and Sp4 are known to be a transcriptional activators while Sp3 can either activate or repress transcription (reviewed in (207)). Within the core promoter, there are numerous binding sites for Sp1 family members, and electrophoretic mobility shift assays (EMSA) have shown that Sp1 and Sp3 do indeed bind to the h*TERT* promoter (208;209). The role of Sp1 and Sp3 in h*TERT* transcriptional regulation was verified by siRNA experiments that showed knockdown of Sp1 resulted in decreased h*TERT* reporter activity while knockdown of Sp3 resulted in increased h*TERT* reporter activity (210). Wooten and Ogretmen also showed that Sp1 and Sp3 are localized to endogenous h*TERT* promoters and that it is the relative ratio of Sp1 to Sp3 that determines whether h*TERT* is expressed (210). Binding of Sp1 and Sp3 to a GC-box located -31 to -24 bp relative to the transcription start site of h*TERT* was recently shown to be responsible for the differential expression of mouse and human telomerase (211). Additionally, the tumor suppressors p53 and p73 may inhibit h*TERT* transcription in normal cells by binding to Sp1 and inhibiting its transactivation functions (212-214). The role of Sp1 in h*TERT* activation was revealed in studies that showed the LANA protein of Kaposi's sarcoma-associated herpesvirus required binding to Sp1 to activate telomerase expression (215).

While the Myc/Max and Sp1 families have been the most-studied transcription factors with regards to the control of h*TERT* expression, other transcription factors have also been implicated. AP-1, a heterodimeric transcription factor complex consisting of Jun and Fos proteins, has been shown to associate with the h*TERT* promoter by EMSA and to repress activity of transiently transfected telomerase reporters, dependent on the presence of its binding sites (216). By expression cloning, Oh et al. isolated the Wilms' tumor 1 (WT1) tumor suppressor as a transcriptional repressor of telomerase in kidney cells; they showed WT1 was able to repress the activity of transiently transfected telomerase reporters dependent on the presence of the WT1 binding site, and, by EMSA

and RNase protection assays (RPA), that WT1 does bind to the h*TERT* promoter (217). The tumor suppressor Menin was isolated in a genetic screen for telomerase repressors in HeLa cells (218). Overexpression of Menin was shown to decrease endogenous levels of hTERT mRNA in HeLa, MCF-7, and BJ-hTERT (human foreskin fibroblasts stably expressing hTERT) cells; inhibition of Menin by siRNA in the TERT(-) human osteosarcoma cell line U2OS led to an induction of both hTERT mRNA and telomerase protein expression. Finally, Menin was shown to associate with the h*TERT* promoter by ChIP assays. The transcriptional repressor MZF-2 was also shown to bind to the h*TERT* promoter by EMSA and repress telomerase mRNA and protein expression in the TERT(+) human cervical cancer line C33A (219).

The presence of at least one novel transcriptional repressor, most likely two, of hTERT on chromosome 3p has been well established by studies showing that the introduction of normal 3p is able to induce the loss of hTERT mRNA and protein, as well as telomerase activity (220-222). In the human renal cell carcinoma cell line RCC23, normal human foreskin fibroblasts (NHF), and normal prostate epithelial cells (PrEC), the effect of the repressor is due to binding of a downstream E-box located 22 bp downstream of the transcription start site (223). While Myc, Mad, USF1, and USF2 all bind to E-boxes and are known to be involved in h*TERT* regulation, reporter assays and EMSA clearly showed these proteins were not responsible for the repression mediated by the downstream E-box (223;224). In the study by Horikawa et al., they showed that even though introduction of normal 3p to the breast carcinoma cell line 21NT was previously shown to affect h*TERT* transcription (222), this effect was not mediated through the downstream E-boxes. A later study verified these results by showing that h*TERT* activity was controlled by two different regions of 3p in RCC23 and 21NT cells (3p14.2-p21.1 and 3p21.31, respectively), indicating there are two telomerase repressors located on 3p (225).

There is also evidence for the role of hormones in affecting h*TERT* transcription. The differential regulation of telomerase activity during the normal female menstrual cycle has been shown to be regulated by fluctuating estrogen levels (226;227). In addition, estrogen has been shown to induce telomerase expression in mammary and ovarian epithelial cells (228;229). In MCF-7 cells, estrogen was found to bind to the

estrogen responsive element found in the h*TERT* core promoter and to upregulate telomerase mRNA production; this upregulation of h*TERT* mRNA was also due, in part, to the activation of Myc by estrogen (228). In normal human ovarian surface epithelial cells, telomerase activity was absent until the addition of estrogen, and this effect was enhanced by over-expression of estrogen receptor alpha (ERα) but not ERβ (229). The responsivity of telomerase to estrogen has broad implications for cancer treatment by the estrogen agonist tamoxifen (230). A second sex hormone, progesterone, exhibited biphasic effects on telomerase expression (231). Initially, progesterone worked synergistically with estrogen to activate telomerase, but after extended periods, progesterone antagonized estrogen to downregulate telomerase expression. Increased levels of progesterone were shown to correspond with decrease telomerase expression in normal ovarian tissue, highlighting the opposing effects of estrogen and progesterone in regulating normal human menstruation.

It has become increasingly apparent that chromatin plays an important role in regulating h*TERT* transcription. Many studies have shown that inhibition of HDACs with trichostatin A (TSA) results in an induction of telomerase activity in TERT(-) cells and that this induction is associated with an increase in hTERT transcription (206;208;232-236). Even though TSA is a global inhibitor of histone deacetylation and therefore, its effects could be due to an indirect effect on h*TERT* transcription, co-treatment of TERT(-) cells with TSA and the general protein synthesis inhibitor cycloheximide (CHX) resulted in the same induction of telomerase activity as TSA alone (234). These results indicate that histone deacetylation of the h*TERT* promoter is directly responsible for the observed h*TERT* activation (233;234). The association of hypoacetylated histones H3 and H4 with the h*TERT* promoter in normal human fibroblasts and the association of hyperacetylated histones H3 and H4 in TERT(+) cancer cell lines, as determined by ChIP, verifies the importance of histone acetylation in the *in vivo* regulation of h*TERT* transcription (236). Histone H3 phosphorylation of serine 10 via MAPK has been shown to be important for telomerase activation upon the induction of T-cell proliferation (237). In 2004, Wang and Zhu demonstrated that in normal, TERT(-) fibroblasts and ALT immortal fibroblasts, the h*TERT* gene was resistant to DNaseI digestion, while immortal TERT(+) cells displayed a major DNaseI-

hypersensitivity site located within 100 bp of the transcription start site; this same hypersensitivity site could be induced in TERT(-) cells following treatment with TSA (235), underscoring the importance of the chromatin state in regulating h*TERT* expression. It is thought that Sp1 and Sp3, specifically the ratio between the two factors, may be important for the regulation of the acetylation status of the h*TERT* promoter through their direct binding to HDACs (208;210;233). The ability of Mad to repress h*TERT* transcription was found to be due to histone deacetylation (232), while c-Myc-mediated activation of telomerase relies on the recruitment of TRRAP and the HAT GCN5 by the STAGA coactivator complex (238). Likewise, during differentiation of HL60 cells, the switch from telomerase-activating Myc/Max heterodimers to repressive Mad/Max dimers was associated with a decrease in promoter acetylation (206). Additionally, the novel transcription factor found on chromosome 3p functions to repress telomerase activity in 21INT cells by maintaining a closed chromatin state in a region encompassing h*TERT* intron 2 (239). Additional evidence for the importance of chromatin in regulating h*TERT* expression is the failure of transiently-transfected, hTERT promoter-driven luciferase constructs to recapitulate the endogenous telomerase status of TERT(+) and TERT(-) fibroblasts (224;234;240). The luciferase activity displayed in both TERT(+) and TERT(-) cells with a construct controlled by a 14 kb region of h*TERT* (-7369 bp to +6.5 kb relative to the transcription start site) indicates that the appropriate regulatory conditions cannot be met because a regulatory element is missing and/or because proper telomerase regulation requires the chromatin environment, which is not provided by transiently-transfected reporters.

While transcriptional regulation of h*TERT* is the main means by which cells regulate telomerase, alternative splicing, dimerization, and post-translational modifications may also play a role, especially during development. During the initial characterization of the h*TERT* gene, seven alternatively spliced mRNAs were isolated, three with deletions and four with insertions (198;241). The majority of these splice variants were found to disrupt the reverse transcriptase (RT) motifs of the protein or lead to protein truncation, suggesting they are not functional. The alpha variant of hTERT (hTERTα) is missing the first 36 nt of exon 6 and therefore contains a deletion in RT motif A; the lack of RT A not only causes the production of an inactive protein, but

allows hTERTα to act as a dominant negative inhibitor of the full-length telomerase protein when expressed at high levels (242;243). The beta variant of hTERT (hTERTβ) contains a deletion of exons 7 and 8. As the splicing of exon 6 to exon 9 results in a missense mutation, a truncated protein missing critical RT motifs is produced; even though this mutant is inactive, it does not act as a dominant negative inhibitor of full-length telomerase (243). Quantification of the expression of full length hTERT, hTERTα, hTERTβ, and hTERT with both the α and β deletions (hTERTα+β) revealed that in a variety of TERT(+) cancer cell lines, the expression of the four variants was very similar across all cell types (244). The ability of hTERTα to function as a dominant negative inhibitor of full-length TERT explains the data that showed developmentally compromised human oocytes, day 3 cleaved embryos, and day 5 blastocysts displayed full-length hTERT, hTERTα, and hTERTβ, while developmentally competent mature oocytes and day 3 cleaved embryos expressed only full-length hTERT (245). The apparent importance of alternative splicing of hTERT during human fetal development was revealed by a study showing the differential expression of full-length hTERT, hTERTα, hTERTβ, and hTERTα+β in fetal heart, liver, and kidney from gestational weeks 8-21 (246).

Increasing evidence indicates the human telomerase holoenzyme exists as a dimer in its fully functional form. The functional dimerization of hTERT was suggested by a study that showed the minimal size of a complex supporting *in vitro* telomerase activity was 600 kD, or about the size of two molecules each of hTERC and hTERT (247). Later that same year, Beattie et al. showed that two non-functional hTERT mutants, one with a C-terminal deletion and one with an N-terminal deletion, were able to complement each other in *trans* to restore telomerase activity in both a rabbit reticulocyte cell-free assay and in TERT(-) GM847 human fibroblasts (248). Later studies have shown that this functional multimerization of hTERT requires the pseudoknot motif of hTERC and two RNA interaction domains (RID1 and RID2) found in the N-terminus of hTERT (249;250) and is necessary for high processivity of DNA synthesis by hTERT (251).

Initial evidence indicating protein phosphorylation might be important for telomerase activity came from studies that showed incubation of PP2A with nuclear extracts of the breast cancer cell line PMC42 abolished telomerase activity (252). This

effect was able to be reversed in nuclear extracts by incubation with ATP and in intact cells by addition of the PP2A inhibitor Okadaic acid; the effect of PP2A was also shown in the HL60 cell line (253). Later studies revealed that the protein kinase responsible for phosphorylation of telomerase *in vivo* in PMC42 cells is PKCα (254) and that phosphorylation of telomerase by PKC isoforms α, β, δ, ε, and ζ may be necessary for proper assembly of the telomerase holoenzyme (255). Phosphorylation of hTERT by the protein kinase Akt has also been shown to be important for telomerase activity (256-258). An intriguing correlation between telomerase localization and phosphorylation has recently been noted in a number of cell types. For example, the activation of telomerase activity in $CD4^+$ T-cells upon their stimulation was shown to be dependent on phosphorylation of hTERT protein present prior to stimulation; furthermore, the translocation of hTERT from the cytoplasm to the nucleus was also dependent on hTERT phosphorylation (259). The importance of telomerase protein phosphorylation in nuclear translocation has been shown in the human ovarian cancer cell line Caov-3 in which full-strength, estrogen-mediated activation of telomerase required Akt-dependent phosphorylation of hTERT and its subsequent nuclear translocation (260). Phosphorylation of human telomerase has also been implicated in loss of telomerase activity. In contrast to the activating function of phosphorylation mediated by PKC, the protein kinase c-Abl was shown to associate *in vivo* with hTERT in 293T and HeLa cells, and its phosphorylation of hTERT inhibited telomerase activity (261). Further supporting the role of phosphorylation in controlling nuclear localization, activation of Src kinase by reactive oxygen species in 293 cells resulted in the Src-mediated phosphorylation of human telomerase and its subsequent nuclear export (260). Taken together, the regulation of the human telomerase catalytic subunit is a complex process mediated at many levels.

1.4 Artificial Chromosomes

During the late 1980s to mid 1990s, it became increasingly clear that many genes covered stretches of genomic DNA too large for standard cloning in small plasmids. In addition, genome sequencing projects were getting underway and assembly of ordered sequences was difficult using cosmids, hybrid vectors containing properties of plasmids and λ bacteriophages, because they are limited to inserts of only 45 kb (262). To overcome these limitations, several groups developed artificial chromosomes, vectors able to stably maintain large fragments of genomic DNA for purposes of cloning, sequencing, and transgenesis (263). The three types of artificial chromosomes are yeast artificial chromosomes (YACs), P1 artificial chromosomes (PACs), and bacterial artificial chromosomes (BACs). While all three of these systems were designed for similar purposes, their cloning capacities, level of insert stability, and ease of use are somewhat different.

1.4.1 Types of Artificial Chromosomes

The first artificial chromosome system to be published was the YAC system (264); a diagram of this system can be found in Figure 1.3. YACs are maintained as linear molecules in their host, *Saccharomyces cerevisiae*, and therefore contain all the elements necessary for autonomous replication in yeast: centromeres, telomeres, and autonomous replication sequences (ARSs). Also included in YACs are two selectable markers, *TRP1* and *URA3*, and *SUP4*, a gene whose interruption allows for visual selection of YACs containing genomic inserts. While the ability of YACs to maintain genomic inserts of >1 megabase (Mb) (265) makes them valuable tools for physical mapping and the study of large gene clusters, there are technical considerations that make YACs less ideal to work with. Since YACs are large, linear molecules, they are highly susceptible to shear stress during manipulation and can be difficult to cleanly isolate from endogenous yeast chromosomes. Working with YACs also requires equipment and expertise that may not be available in many laboratories. However, it is the presence of

chimeric clones in virtually all YAC libraries (266;267) and their insert instability (268;269) that makes YACs problematic for genomic studies.

Bacterial artificial chromosomes (BACs) were designed in an effort to overcome the limitations of YACs (270). Previous studies on the *Escherichia coli* (*E.coli*) F-factor revealed that plasmids containing F-factor genes were replicated in a tightly controlled manner, were maintained at only one to two copies per cell, and were capable of maintaining bacterial DNA fragments as large as 1 Mb. It was thought that the tightly controlled regulation of replication and the low copy number would prevent unwanted recombination between insert DNA, leading to less chimerism and increased stability. Furthermore, the maintenance of 1 Mb fragments of bacteria DNA indicated that large pieces of mammalian DNA could be maintained and propagated as F-factor plasmids as well. To test these hypotheses, Shizuya et al. created the BAC vector pBAC108L, which contains the F-factor genes *oriS* and *repE* (responsible for unidirectional replication) and *parA* and *parB* (responsible for low copy number), a chloramphenicol resistance marker and a cloning segment (see Figure 1.4A). Human DNA fragments as large as 300 kb were stably maintained when ligated to pBAC108L, as evidenced by the stability of the insert DNA over a period of 100 generations. The BAC system provides many advantages over the YAC system; one of these advantages is the resistance to mechanical shearing due to the super-coiled, circular nature of F-factor-based plasmids. Other advantages include the well-established techniques of isolating and preparing plasmid DNA from *E.coli*, and, most importantly, the stability and lack of chimerism of the insert DNA. Since the initial publication of pBAC108L, additional BAC vectors have been developed, including pBACe3.6 (271) (Figure 1.4B) and pTARBAC1 (272) (Figure 1.4C). These later-generation vectors contain additional features that make them more amenable to manipulation.

A third type of artificial chromosome is the P1 artificial chromosome, or PAC (273). This system combines features of the bacteriophage P1 cloning system (274) with those of the F-factor system. The bacteriophage P1 cloning system (Figure 1.5) relies on the ligation of genomic DNA fragments to P1 vectors, which contain two *loxP* sites, and their subsequent packaging by incubation with P1 phage heads and tails. Fully assembled particles are then used to infect a Cre recombinase-expressing bacteria host, resulting in

the circularization of the DNA by Cre-mediated recombination between the two *lox*P sites. This circularized DNA is able to be propagated as a single-copy plasmid, or, in the presence of IPTG, in multiple copies per cell, which is ideal for DNA isolation. While the P1 phage system is very efficient at creating plasmids with stable genomic inserts, the phage head is only capable of holding a maximum of 110 kb of DNA; as the vectors are ~5 kb in length, this limits the size of the genomic inserts to ~100 kb. PAC vectors (Figure 1.6) combine the positive selection markers and multi-copy replicon of the P1 phage system with the F-factor of BACs, allowing them to be electroporated as circular molecules. The elimination of phage packaging gives PACs the same cloning capacity as BACs (up to ~300 kb), while the inducible *lac* operator allows for multi-copy replication, resulting in greater DNA yield than BACs.

1.4.2 Artificial Chromosomes as Transgenes

The creation and study of transgenic animals, particularly transgenic mice, has been instrumental in elucidating gene function during development and disease, as well as being critical to the creation of animal models of human disease. While transgenic animals are valuable tools, the system is not perfect due to problems with transgene expression. Most transgenes are introduced to the host genome by random integration, and therefore, the site of integration and number of transgene copies integrated is uncontrollable, leading to chromosomal position effects and copy number dependence. Chromosomal position effects refer to the ability of the surrounding host DNA to affect expression of the transgene; thus, expression of the transgene may mimic the expression of surrounding genes, as opposed to being expressed as it would be at its native locus. Such position effects have an obvious detrimental effect on interpreting data obtained from transgenic animals. Another difficulty when interpreting data from transgenic animals is the effect of copy number. Oftentimes, more than one transgene will integrate at a given site, typically in a head-to-tail fashion, but the number integrated varies between sites. In most cases, the level of transgene expression correlates with the overall copy number, implying that an animal with five copies of the transgene would display more transgene activity than one with two copies. The difficulties associated with

chromosomal position effects and copy number dependence require the careful analysis of numerous founder animals before performing experiments addressing a specific hypothesis.

To circumvent chromosomal position effects, artificial chromosomes can be used to construct transgenic animals. Due to the large insert size of artificial chromosomes, it is expected that they will contain all the regions necessary to ensure appropriate gene expression, regardless of the site of integration. Thus, by using artificial chromosomes as transgenes, chromosomal position effects can be eliminated, although transgene expression remains copy number dependant. This position independence implies that fewer founder animals need to be analyzed because all animals, regardless of the site of integration, should display the same transgene activity per copy.

The first transgenic mice to be constructed using artificial chromosomes as the transgene were created from YACs harboring the genes for mouse α_1 (I) collagen (275), human hypoxanthine phosphoribosyltransferase (*HPRT*) (276), and mouse tyrosinase (277). In all three cases, transgene expression was found to be position-independent, as expected, and the transgenes were able to be transmitted through the germ-line. The two murine transgenes displayed activity that was copy number-dependent; importantly, per copy, the level of activity of the transgene was similar to that of the endogenous gene. In the case of the tyrosinase gene, the YAC transgene was able to completely restore pigmentation to albino mice, whereas previous studies using tyrosinase minigenes showed variable levels of pigment restoration due to position dependence (278;279). Taken together, these initial results confirmed the hypothesis that large transgenes in the form of artificial chromosomes are able to confer chromosome position-independent, copy number-dependent gene expression.

Since the initial publication of the aforementioned YAC transgenic mice, the superiority of using artificial chromosomes as transgenes has become increasingly clear. Transgenic mice created using artificial chromosomes have been used to model several human diseases, including Alzheimer's (280;281), Down syndrome (282;283), cystic fibrosis (284;285), and Huntington disease (286;287), to study X-chromosome inactivation (288), and to determine gene regulatory sequences (289;290). Artificial chromosomes have also been used to make transgenic animals other than mice, including

rabbits (291), rats (292), and zebrafish (293). In addition, various BAC-based reporters have been reported in the literature, including an EGFP reporter for the β-globin locus (294), an EGFP reporter for *FRDA* (295), a GFP reporter for *Nkx2-5* (296), a *lacZ* reporter for *Gdf6* (297), a GFP reporter for *Chx10* (298), and an EGFP reporter for *Shh* (299). Overall, it is expected that YACs, PACs, and BACs, in the form of transgenes, will continue to contribute to our overall knowledge base of normal and diseased states.

Family	Selected Family Members	Biological Role	References
ETS	Ets-1	NK cell differentiation	(300)
	Ets-2	T-cell development	(301)
TCF	Elk-1	Neuronal differentiation	(302)
	SAP-1	T-cell differentiation	(303)
Hox	Hoxa-Hoxd loci	Setting anterior-posterior body axis; vertebral development; organogenesis; limb bud development	(304)
POU	Pit-1	Anterior pituitary development	(305)
	Oct-4	Inner cell mass development	(306)
bHLH	MyoD	Skeletal muscle development	(307)
	c-Myc	Cell cycle progression and apoptosis	(308)
	Mad1	Granulocyte differentiation	(309)
bZip	C/EBPα	Energy homeostasis	(310)
		Neutrophil differentiation	(311)
	API	Cellular proliferation, differentiation, and apoptosis	(312)
Hormone Receptors	ERα	Male and female fertility and sexual behavior, cardiovascular function, and normal skeletogenesis, among others	(313)
	RAR	Embryonic patterning, organogenesis, and skeletogenesis	(314)
Sry-Sox	Sry	Testis development	(315)
	Sox2	Retinal precursor cell differentiation	(316)
Sp1	Sp3	Respiratory function and late tooth development	(317)
		Erythroid and myeloid differentiation	(318)
	Sp4	Post-natal growth, male mating behavior, onset of female puberty	(319)

Table 1.1. Selected Families of Common Transcription Factors. Representative members of each family and their common targets are presented. Note: This is not an exhaustive list.

Species	Telomeric Repeat (5'-3')	Average Telomere Length	References
Tetrahymena thermophila	TTGGGG	120-420 bp	(89)
Euplotes aediculatus	TTTTGGGG	~50 bp	(320)
Saccharomyces cerevisiae	$(TG)_{1-3}TC_{2-3}$	200-400 bp	(90;94)
Schizosaccharomyces pombe	$TTACAG_{1-8}$	200-400 bp	(321)
Arabidopis thaliana	TTTAGGG	2-5 kb	(91)
Mus musculus	TTAGGG	20-150 kb*	(322),(323)
Homo sapiens	TTAGGG**	10-14 kb	(92),(164)

Table 1.2. Cross-species Comparison of Telomeric Repeats. For each species, the telomeric repeat is written in the 5'-3' direction, where 5' refers to the centromere. * Murine telomere length varies between mouse strains. ** All vertebrates share the same TTAGGG telomeric repeat (322).

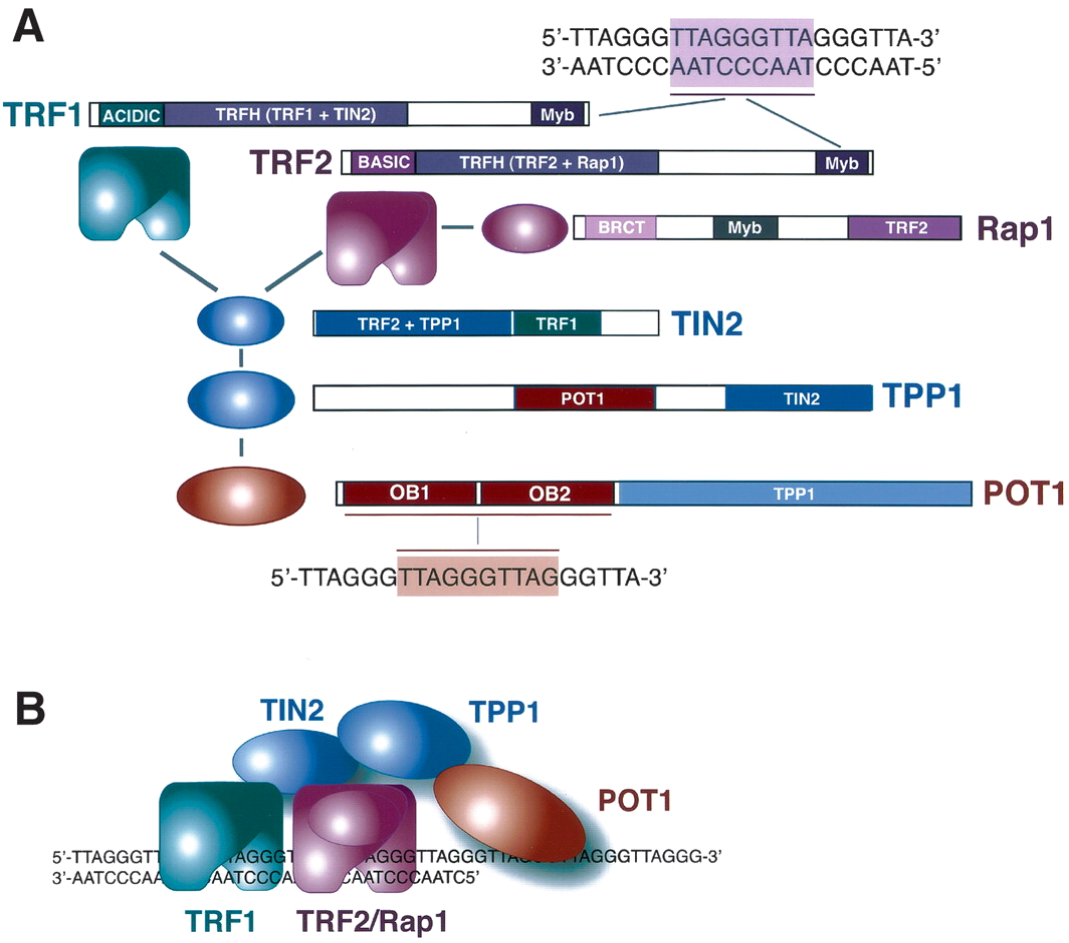

Figure 1.1. Shelterin Complex. In humans, telomeres are constitutively associated with a protein complex referred to as shelterin. The six components of shelterin provide structure and function to telomeres. TRF1 and TRF2 bind directly to double stranded telomeric DNA and serve as a docking point for Rap1 and TIN2. TIN2 binds TPP1 to the complex, which in turn recruits POT1, a protein able to bind single stranded telomeric DNA. The critical protein domains of the individual proteins are shown in **A**. Their association with each other and the telomere is shown in **B**. Note: Figure taken from (103).

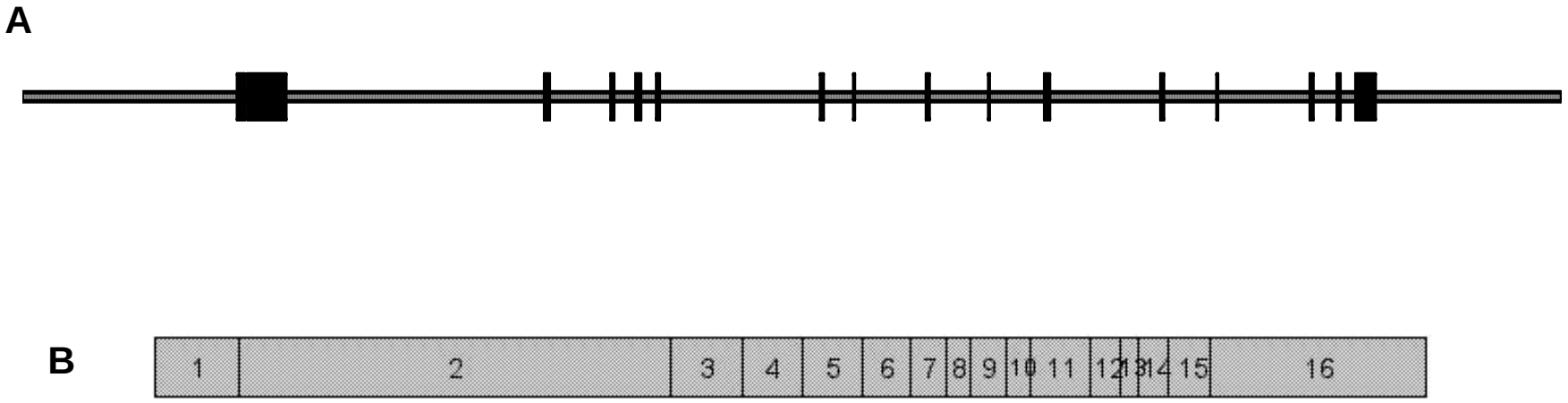

Figure 1.2. h*TERT* Locus. **A.** The genomic locus of the human telomerase gene. The gene is located on 5p15.33 and consists of 16 exons, spanning ~40 kb. **B.** The full-length mRNA of hTERT. The translation start codon is located in exon 1 and the stop codon in exon 16. The exons are the following sizes: 1=210 bp, 2=1,354 bp, 3=196 bp, 4=181 bp, 5=180 bp, 6=156 bp, 7=96 bp, 8=86 bp, 9=114 bp, 10=72 bp, 11=189 bp, 12=127 bp, 13=62 bp, 14=125 bp, 15=138 bp, and 16=664 bp.

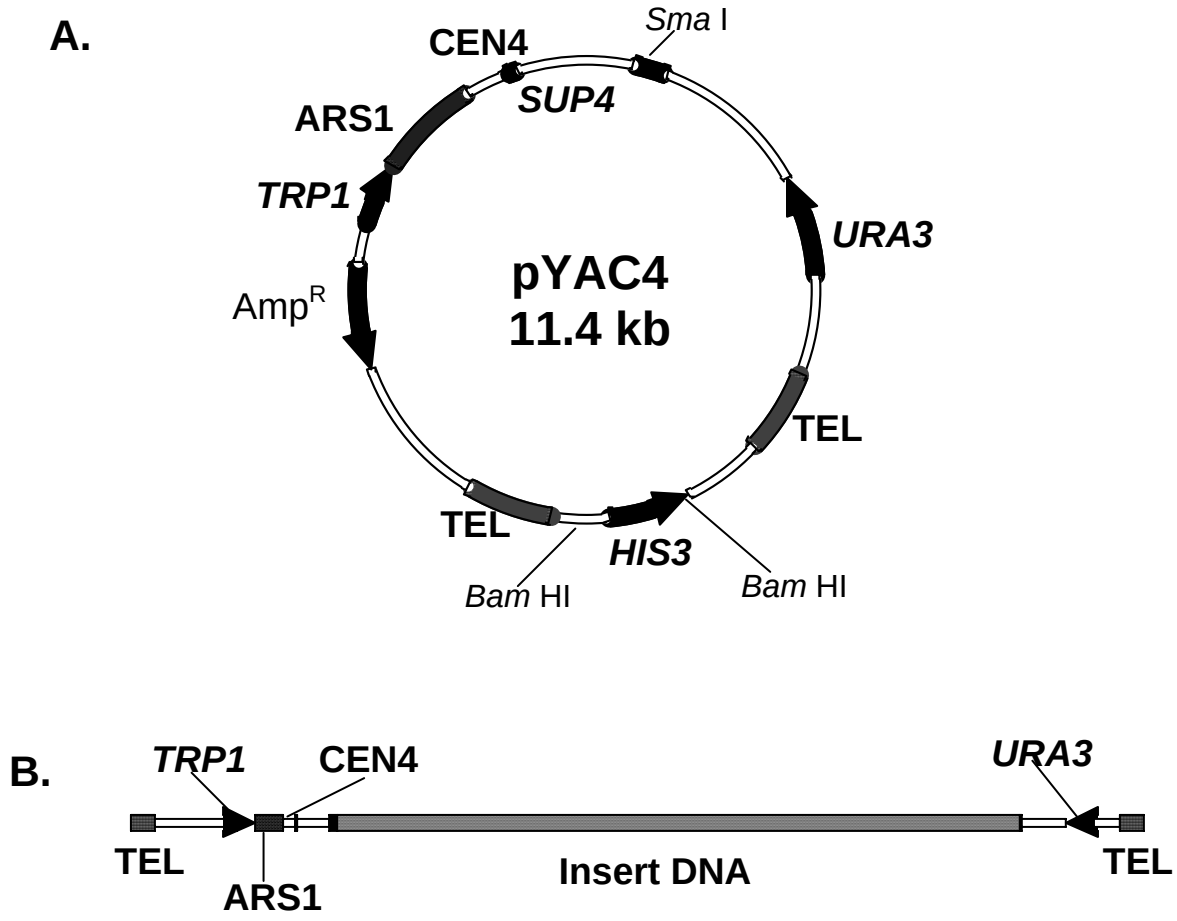

Figure 1.3. Yeast Artificial Chromosomes. **A.** A yeast artificial chromosome vector (YAC) containing telomeric sequence (TEL), an ARS, a centromere (CEN4), the yeast selectable markers *HIS3* and *TRP*, and the ochre suppressor (SUP). pYAC4 is shown here as an example vector. **B.** A generic linearized YAC with insert DNA. To insert genomic DNA, the YAC vector is digested with the restriction endonucleases *Bam* HI and *Sma* I and ligated to blunt-ended DNA of interest. Ligation results in loss of the *HIS3* selectable marker and interruption of the ochre suppressor, allowing for positive selection of YACs containing insert DNA.

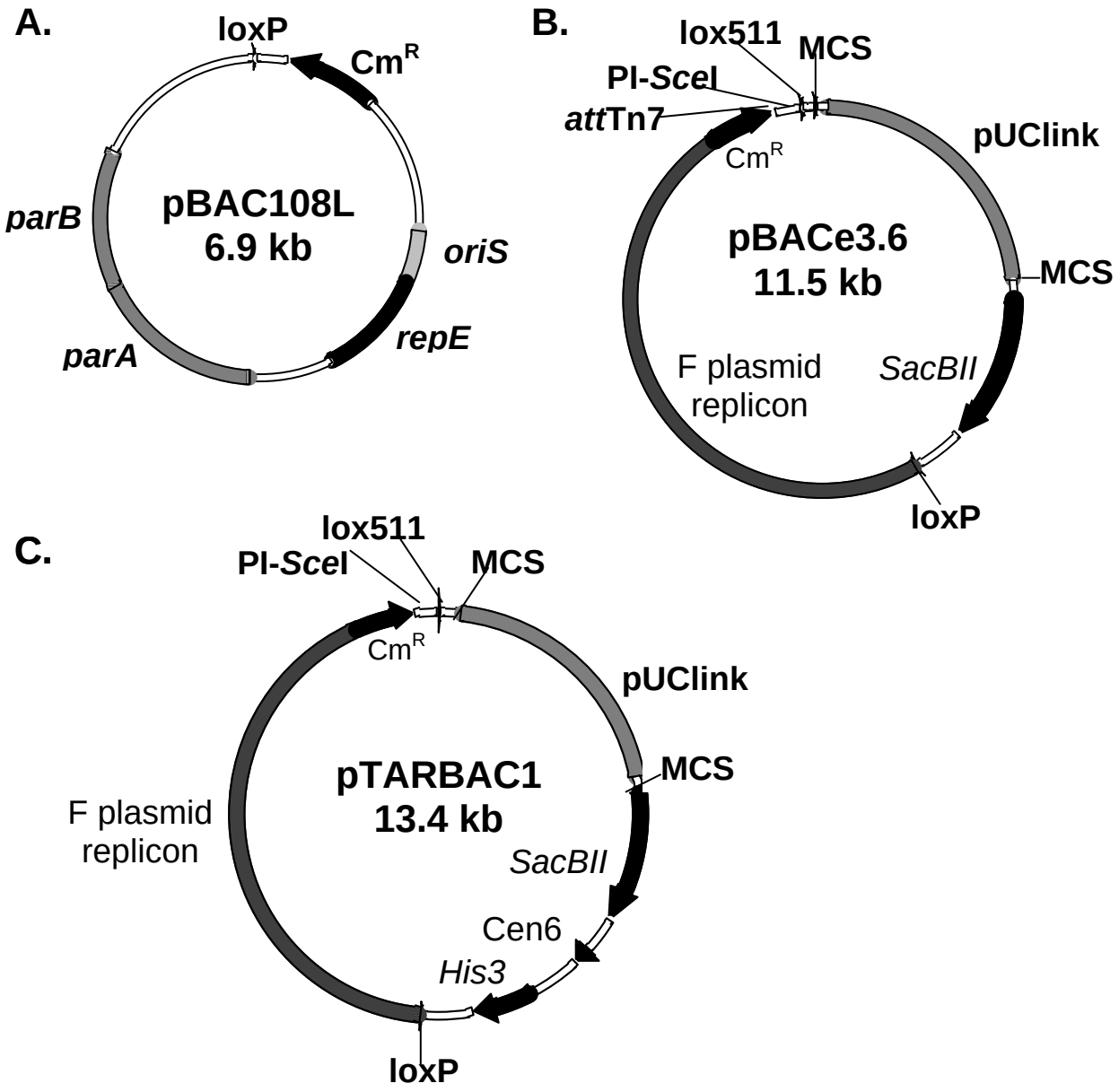

Figure 1.4. Bacterial Artificial Chromosome Vectors. **A.** The original BAC vector pBAC108L, which contains the Cre recombinase recognition site *loxP*, a chloramphenicol resistance marker (Cm^R), and the *oriS*, *repE*, *parA*, and *parB* genes of the F-plasmid replicon. **B.** The BAC vector pBACe3.6 is a modified version of pBAC108L that contains a second Cre recombinase recognition site, *lox511*, the recognition sequence for the homing endonuclease PI-*Sce*I, a recognition sequence for Tn7 transposition, *att*Tn7, the pUClink stuffer fragment surrounded by multiple cloning sites for insertion of genomic DNA, and the selectable marker *SacBII*. The multiple cloning sites include *Not*I, *Bam*HI, *Sac*II, *Eco*RI, *Sac*I, *Mlu*I, and *Nsi*I restriction endonuclease recognition sites. **C.** The BAC vector pTARBAC1 is a modified version of pBACe3.6 that contains the yeast selectable marker *His3* and a yeast centromere sequence, Cen6. These features allow pTARBAC1 to serve as a shuttle between yeast and bacteria hosts.

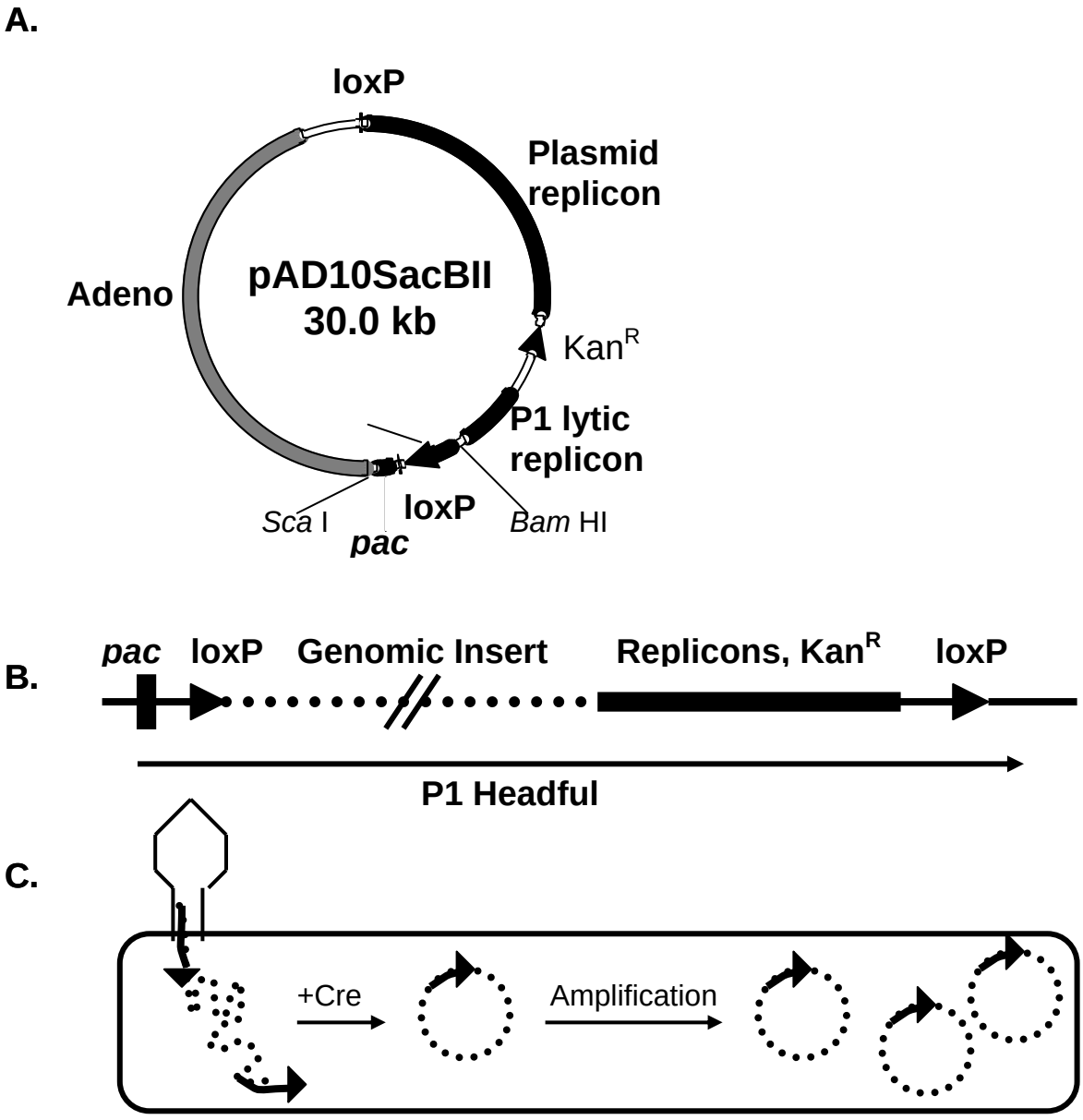

Figure 1.5. P1 Bacteriophage Cloning System. **A.** P1 vector pAD10SacBII, which contains an adenovirus stuffer fragment (Adeno), the *sacBII* and kanamycin resistance genes (Kan^R) for selection, the P1 packaging gene *pac*, two *loxP* sites for Cre recombinase recognition, and the lytic and plasmid replicons. **B.** After restriction endonuclease digestion of pAD10SacBII with *Sca*I and *Bam*HI, genomic DNA is ligated to the arms, creating a P1 headful. **C.** After incubation with P1 phage heads and tails, the DNA is packaged into an infective particle. These particles are used to infect a Cre recombinase-expressing bacteria host, which results in the circularization of the DNA. Activation of the lytic replicon results in the multi-copy amplification of the circular DNA, which can then be isolated by standard alkaline lysis procedures.

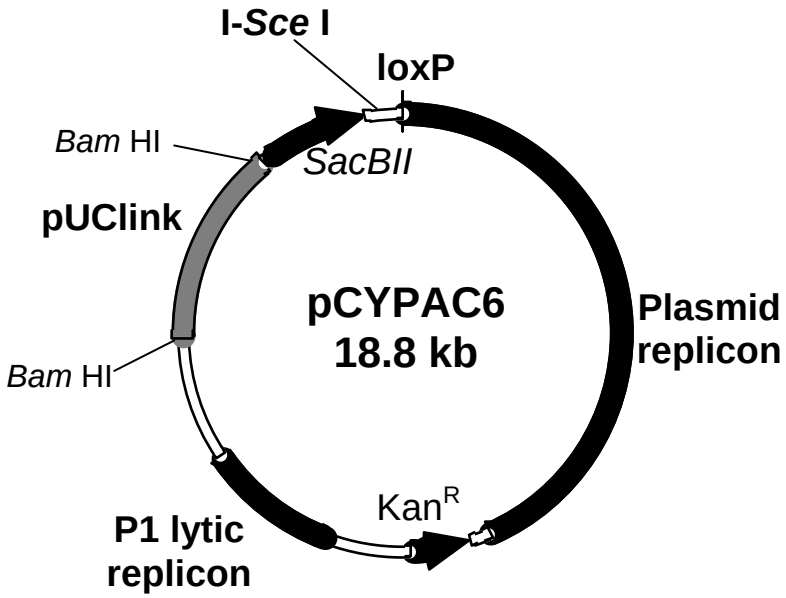

Figure 1.6. P1 Artificial Chromosomes. Shown is one example of a PAC vector, PCYPAC6. PAC vectors contain the P1 lytic replicon of P1 bacteriophage vectors and the pUClink portion of BAC vectors. The maintenance of the lytic replicon allows for high-copy propagation, while features of BAC vectors eliminate the need for a packaging step, resulting in an increase of the maximum insert size from 100 kb to 300 kb.

Chapter 2
CREATION OF A PRE-TARGETED LOCUS

2.1 Introduction

The study of transgenes in cell culture and animal models has been instrumental to furthering the understanding of gene expression and the ways in which gene expression affects development. However, transgenes are not perfect models, and the interpretation of data obtained from transgenic systems must take into consideration the three main problems with associated with transgenes, namely, position-effect variegation, lack of necessary regulatory elements, and copy number dependence. Position-effect variegation (PEV) refers to the phenomenon in which the site of transgene integration affects its expression. PEV was initially described in 1930 by Hermann Müller to explain his studies of X-ray-induced mutations in *Drosophila* (324) and has since been shown to be due to effects of heterochromatin and be epigenetically modulated (reviewed in (325)). Mosaic transgene expression, in which certain mice express the transgene and others do not or in which certain cells express the transgene more robustly than others, was noted in many early transgene studies, including those of the mouse myelin basic protein gene (326), the mouse tyrosinase gene (327), the rat angiotensinogen II gene (328), and mouse *Hprt* (329). In 1995, Robertson et al. performed studies with many lines of transgenic mice expressing the same transgene construct (a β-galactosidase (*lacZ*) gene driven by the ζ-globin promoter and an αHS-40 enhancer) and found that while *lacZ* staining varied greatly between different transgenic lines, within the same line, expression was similar (330). This effect was shown to be due to the site of integration and linked differential transgene expression to the well known position-effect variegation phenomenon of *Drosophila*. Two years later, Boyer et al. noted that while a CD4 minigene was differentially expressed in various lines of transgenic mice, expression was consistent within animals of the same line (331). They also showed that lines with little or no transgene expression had integrated the transgene near centromeric heterochromatin, further supporting the idea that variable transgene silencing is due to

position-effect variegation. PEV is strongly influenced by many proteins involved in heterochromatin and epigenetics, including methylases and HDACs (332;333), HBP1 (334;335), and HP1 (336).

Various techniques have been used to limit PEV in transgenic studies, including the inclusion of locus control regions (LCRs) and insulators, targeting integration to a specific locus, and using YACs, BACs, and PACs as transgenes. LCRs are higher-order chromatin structures functionally defined by their ability to direct tissue-specific, copy number-dependent expression of transgenes at ectopic sites through transcriptional enhancers, scaffold/matrix attachment regions (S/MARs), and boundary elements (reviewed in (337)). LCRs were initially characterized in mice transgenic for the human β-globin locus (338) and have since been associated with other mammalian loci, including the mouse, rat, goat, and rabbit β-globin loci, the human CD4 gene, and the mouse interleukin-2 gene (337). Because of their ability to direct tissue-specific, copy number-dependent transgene expression, LCRs have been attached to transgenic constructs to create mice with improved transgene expression (339-342).

The inability of LCRs to control appropriate expression of non-native genes limits their use in transgenics. Studies of the chicken β-globin locus revealed the presence of a 1.2 kb sequence element located at a specific DNaseI hypersensitivity site (5'HS4 or cHS4) that was able to prevent PEV of a *white* minigene in *Drosophila* (18). Chung et al. determined this element was an insulator and that it functioned in a directional, additive manner to alter chromatin structure (18;343). Insulators function both to prevent PEV and block distant enhancer activation. These two functions have been shown to be separable activities, with enhancer blocking mediated by the binding of the CCCTC-binding factor (CTCF) and PEV inhibition mediated by histone acetylation and prevention of DNA methylation (20-22;333;344;345). The ability of insulators to act on non-native genes has made them invaluable tools for protecting transgenes against PEV (333;346-349).

Another way to protect against PEV is to ensure transgenes are introduced to the same genomic locus in each cell line or mouse. In murine embryonic stem (ES) cells, homologous recombination can be used to insert single-copy transgenes into the *Hprt* housekeeping gene ((350-353), among others). Homologous recombination can also be

used to introduce changes at the endogenous locus, a process known as gene targeting or gene knockin (354;355). The obvious benefit of targeting to the endogenous locus is the ability to study the effect of a specific mutation in a native chromatin context (332;356-358). The efficiency of gene targeting is increased when using artificial chromosomes due to the large amounts of homology they provide (359;360).

While homologous recombination has been used for gene targeting, the ratio of homologous to nonhomologous insertion of introduced DNA is only 1:1,000, making it rather inefficient (354). A more efficient way to target single-copy transgenes to the genome is by Cre/*lox*- or FLP/FRT-mediated recombination. Cre recombinase is the bacteriophage P1 protein responsible for directing both inter- and intramolecular recombination between two *lox* sites (361), while FLP is the recombinase encoded by the *S.cerevisae* 2μ plasmid responsible for directing recombination between two FRT sites (362). The demonstration by Sauer and Henderson that Cre recombinase was functional in mammalian cells engineered to express *lox* sites opened the door for use of Cre/*lox*-mediated recombination in genome targeting (363;364); later studies showed that FLP was also functional in mammalian cells (365).

Numerous methods have been employed to generate transgenics using Cre/*lox* and FLP/FRT recombination systems. Multiple targeted or randomly integrated *lox* or FRT sites can be used to induce large chromosomal rearrangements and deletions, creating a system useful for studying a variety of human diseases and cancers characterized by such genomic alterations (reviewed in (366;367)). Insertion of single recognition sites into the genome, combined with transgenes containing the same recognition site, allows transgenes to be integrated at the same genomic locus in different experiments (368-370). The ability to express transgenes at a specific timepoint and/or in a specific tissue has been facilitated by the use of the Cre/*lox* system and has been extremely valuable in studying the developmental, spatial, and temporal regulation of gene expression (reviewed in (371)). (A database of Cre-transgenic mice is maintained by the Andras Nagy laboratory at the Samuel Lunenfeld Research Institute and is available at www.mshri.on.ca/nagy (372).)

A final way in which Cre/*lox* and FLP/FRT recombination is used to target transgenes is through recombinase-mediated cassette exchange (RMCE) (373;374). In

RMCE, a cassette containing both a positive and negative selectable marker selectable marker flanked by heterospecific and/or inverted recognition sites is integrated into the genome to create an acceptor locus. A second cassette, containing the region of interest and flanked by the same recognition sites, is then introduced to the cells containing the acceptor locus, and in the presence of the appropriate recombinase, the selection cassette is replaced by the cassette of interest (Figure 2.1A). Because heterospecific recognition sites are recognized by the recombinase but do not recombine with each other (375-377), the integrated acceptor locus is unable to excise itself, thus increasing the overall efficiency. Even if the same *lox* sites are used to flank the acceptor locus, as long as they are in opposite orientation with respect to each other, the intervening DNA will be inverted, not lost, upon intramolecular recombination (Figure 2.1B). Another benefit of RMCE is that it does not require the incorporation of undesirable selection markers and/or vector sequence. Since its publication, RMCE has been used to study the LCR of the β-globin gene cluster in murine erythroleukemia (MEL) cells (373), to study the regulation of the MHL-1 locus in murine ES cells (378), to study transcription of immunoglobulin genes in the mouse B hybridoma cell line Sp6 (379), to create a tetracycline-inducible reporter system (380), to study the effect of various mutations of the *Lrp1* gene in mouse ES cells and ES cell-derived animals (381), and to study p53 mutations in mouse ES cells, ES cell-derived animals, and MEFs (382).

A second consideration when interpreting data obtained from transgenic studies is whether or not all appropriate regulatory sequences are present in the transgene. As previously discussed, elements regulating gene expression can be located upwards of 100 kb away from a gene (reviewed in (15;72)) and therefore, are usually absent from small transgenes (383-385). As mentioned above in the discussion of PEV, LCRs are important regulatory regions, and their inclusion in transgenic constructs aids in mediating appropriate transgene expression (339-342). Another way to ensure the presence of appropriate regulatory sequences in transgenes is to use YACs, BACs, and PACs, which cover larger regions of the genome and are therefore more likely to contain all the appropriate regulatory elements and be expressed in a copy number-dependent, position-independent manner (reviewed in (263)). Studies have shown most artificial chromosome-based transgenes to be expressed in this way, but there are documented

reports in which artificial chromosomes fail to prevent PEV (386;387), and in some cases, including the campomelic dysplasia-linked *SOX9* gene, the regulatory regions extend too far to be encompassed in even a YAC (388-390).

A final concern when interpreting the data from transgenics animals is the transgene copy number. In most cases, numerous copies of a transgene will integrate in a head-to-tail manner at a given locus. Due to the variable number of copies integrated, different expression levels can be seen in different animals or cells created with the same transgenic construct. Intuitively, an increase in copy number would yield an increase in gene expression, and in most cases, transgenes are copy number-dependent (reviewed in (263)). However, there are also cases in which too many copies of the transgene lead to aberrant transgene expression (391), disease in the mouse (392), or even transgene silencing (393;394). This effect, termed repeat-induced silencing (RIGS) and first noted in *Drosophila* (395), is attributed to the same process cells use to incorporate endogenous repetitive regions into heterochromatin, thus abrogating their expression (393;394;396). Many of the techniques used to prevent PEV can be used to circumvent problems with multi-copy transgenes as they result in the integration of a single copy of the transgene. These techniques include targeting to the *Hprt* locus (350), gene knockin at the endogenous locus, (354), and RMCE (373;374).

There are many techniques available that can be used to introduce foreign DNA to cells, including electroporation, micro-injection, transfection, and viral infection. Each of these techniques has its own advantages and disadvantages, making certain techniques more useful than others in certain situations. Viral vectors have become invaluable tools to introduce foreign DNA to a host cell in a timely, efficient manner, especially into cells recalcitrant to standard transfection techniques (397;398). The ability to successfully introduce foreign DNA to primary cells has made viral transduction the method of choice in the gene therapy field (399). While many viral vectors, including those based on adenovirus (reviewed in (400)), adeno-associated virus (AAV) (reviewed in (401)), herpes virus (reviewed in (402) and (403)), and vaccinia virus (404), have been used for gene transduction, retroviral vectors are the most commonly employed. Retroviruses are a family of enveloped RNA viruses that use a reverse transcriptase to synthesize double-stranded DNA from single-stranded RNA (Figure 2.2). Retroviruses bind to host cells in

a receptor-mediated manner and insert their RNA into the cytoplasm, where it is reverse transcribed into DNA; this proviral DNA then enters the nucleus and is stably integrated into the host genome. Following transcription, viral transcripts are spliced, exported from the nucleus, and translated into viral proteins that are then assembled and packaged into virion particles that escape the host cell through a process known as budding. (More detailed reviews of the retroviral life cycle can be found in (405) and (406).)

The ability of retroviruses to stably integrate their genome in a highly efficient manner makes them suitable for transgene delivery. The three types of retroviruses most commonly used for gene delivery are the gammaretroviruses, the lentiviruses, and the spumaviruses (reviewed in (406)). To use retroviruses as gene delivery tools, modifications must be made to prevent unwanted infection and pathogenicity. A replication-competent, pathogenic provirus consists of 5' and 3' long terminal repeats (LTRs), the packaging signal psi (ψ), and the *gag*, *pro*, *pol*, and *env* genes (reviewed in (405)). Of these elements, the LTRs contain promoters and enhancers, ψ signals for encapsidation of unspliced viral RNA, *gag* encodes the matrix, capsid, and nucleocapsid proteins, *pro* encodes a protease, *pol* encodes the reverse transcriptase, and *env* encodes the surface and transmembrane glycoproteins. To prevent the formation of replication-competent virus, retroviral vector systems separate the necessary proviral components between at least two vectors. The most common retroviral vector systems used today rely on packaging cells to create replication-defective retroviral particles. The first retroviral packaging cells, ψ-AM, were created by transfecting NIH3T3 mouse embryonic fibroblasts with pMOV-ψ^-, a recombinant retroviral genome consisting of the Moloney murine leukemia virus (MMLV) *gag-pol-pro* genes and the *env* gene of the amphotropic virus 4070A (407). While efficient, first generation systems are dangerous because only one recombination event is required to restore pathogenic function to the virus. Later generations of packaging cells are less likely to produce replication-competent virus due to modifications, including LTR deletions, use of LTRs from different retroviruses, use of non-viral promoters, and separation of the *gag-pol-pro* and *env* genes between two different vectors (408-411).

In this chapter, we report the creation of a single copy acceptor locus in TERT(+) and TERT(-) cells using a retroviral vector. This acceptor locus contains the positive

selectable marker neomycin phosphotransferase, the negative selectable marker thymidine kinase, and an inducible Cre recombinase, all flanked by the *loxP* and *lox511* Cre recombinase recognition sites; in turn, the *lox* sites are flanked by the chicken β-globin insulator cHS4. The function of the *lox* sites in Cre-mediated recombination is verified, as is the inducibility and function of CreER.

2.2 Materials and Methods

Unless otherwise noted, (1) all intermediate plasmid preparations were made using the QiaSpin Mini Kit (Qiagen); (2) all gel purifications were performed using the QiaexII Gel Extraction Kit (Qiagen); (3) all ligations were performed using the Roche Rapid Ligation Kit (Roche Applied Science); (4) all restriction endonucleases were purchased from New England Biolabs (NEB); (5) all primers and oligos were purchased from either Integrated DNA Technologies (IDT) or the Macromolecular Core at The Pennsylvania State University College of Medicine; (6) all genomic DNA (gDNA) was prepared using the Wizard Kit for Genomic DNA Preparation (Promega); (7) all kits were used as recommended by the manufacturer; (8) all microscopy was performed using a Nikon Eclipse TS100 microscope equipped with a Nikon CoolPix 990 digital camera or an Olympus CK2 microscope equipped with a Nikon DXM1200 digital camera. (These points apply to all materials and methods throughout the thesis.)

2.2.1 Construction of Retroviral Acceptor Construct pML2

The acceptor construct pML2 was created using the self-inactivating retroviral vector pQCXIX (BD Clontech™) as a base plasmid. pML2 was preceded in construction by pQCXIX-lox511, pQCXIX-lox, pQloxIns2, and pML1. (Intermediate plasmids can be found in Figures A1 and A2 of Appendix A.) pQCXIX-lox511 and pQCXIX-loxP were constructed to introduce the Cre recombinase recognition sites *lox511* and *loxP* in the same orientation as found in the BAC vector pBACe3.6; both recognition sites were created by linker ligation. (See Figure 2.3 for linkers). To create a vector harboring the *lox511* site, oligonucleotides containing the Cre recognition site and 5' and 3' overhangs to allow for ligation into pQCXIX were pre-annealed by heating to 95˚C in the presence of 1X oligo annealing buffer (10 mM Tris-HCl, pH 8.0, 1 mM EDTA, pH 8.0, 0.1 M NaCl) and slowly cooled to room temperature. Following digestion of pQCXIX with *Bgl*II and *Xba*I, the linkers were ligated by overnight incubation at 4˚C with T4 DNA ligase (NEB) to create pQCXIX-lox511. To introduce the *loxP* site, pQCXIX-lox511 was digested with *Xho*I and *Pvu*II, followed by ligation with pre-annealed oligos (see

above for preparation) to create pQCXIX-lox.

The next step was to introduce the chicken β-globin locus insulator into the 3' LTR. The 1.2 kb insulator fragment was moved from p501 ((412); kind gift of Sergei Grigoryev, The Pennsylvania State University College of Medicine, Hershey, PA) to pUC19M (pUC19 with a mutated *Eco*RI site) by digestion with *Sac*I/*Ssp*I and *Sac*I/*Sma*I, respectively; ligation of these fragments resulted in the creation of pUC19M-cHS4. The insulator was excised from pUC19M-cHS4 with *Sac*I/*Bam*HI, followed by treatment with Klenow to create blunt ends, and then moved into *Nhe*I-digested, Klenow-treated pQCXIX-lox to create pQloxIns2. Following pQloxIns2 construction, a tkNeo fusion gene was placed upstream of the internal ribosomal entry site (IRES). A 2,144 bp fragment containing the tkNeo gene was moved from TNFUS 69 ((413); kind gift of Peter Laird, University of Southern California Norris Comprehensive Cancer Center, Los Angeles, CA) to pBluescriptSK$^+$ (pSK$^+$; Stratagene) by digestion with *Sma*I/*Bam*HI and *Sma*I/*Bgl*II, respectively, to form pSK$^+$tkNeo. The 2.1 kb tkNeo fragment was then moved into pQloxIns2 by digesting both plasmids with *Not*I/*Eco*RI, resulting in the formation of pML1. The final step in creating pML2 was to introduce a CreER fusion gene downstream of the IRES. The CreER gene was initially subcloned into pSK$^+$ by ligating the 2,678 bp *Eco*RI/*Eco*RV fragment of pACYC ((414); kind gift of Frank Buchholz, Max Planck Institute of Molecular and Cellular Biology, Dresden, Germany), to pSK$^+$ digested with *Sma*I/*Eco*RI, forming pSK$^+$CreER. Following digestion of pML1 with *Pml*I/*Xho*I, the 2,315 bp CreER fragment created by digestion of pSK$^+$CreER with *Pml*I/*Sal*I was ligated to form the final retroviral acceptor construct, pML2.

2.2.2 Verification of *lox* Sites

To verify the sequence and orientation of the *loxP* and *lox511* sites, pML2 was sequenced at the Genomics Core Facility, Program in Human Genetics, University of California San Francisco. The *loxP* site was verified by sequencing with primer MAL43 (5'-CCTACAGGTGGGGTCTTTCA-3'), while *lox511* was verified with primer MLVF2' (5'-AATTTTTGCTTTCGGTTTGG-3').

The function of the *lox* sites was verified *in vitro* using the EL350 strain of

bacteria (415). pML2 and a human BAC modified to express a dual kanamycin-streptomycin selection cassette (117B23 cKR) were introduced to 50 µl electrocompetent EL350 bacteria in a 0.10 cm gap cuvette using a BTX-600 electroporator set at 1.75 kV and 186 Ω resistance. After recovery in 1 ml SOC medium (20 g/L bacto-tryptone, 5 g/L bacto-yeast extract, 0.5 g/L NaCl, 2.5 mM KCl, 10 mM $MgCl_2$, 20 mM glucose, pH 7.0) for one hour at 32˚C, the bacteria were plated on LB agar plates (10 g/L bacto-tryptone, 5 g/L bacto-yeast extract, 5 g/L NaCl, 15 g/L agar) containing 12.5 µg/ml chloramphenicol and incubated overnight at 32˚C. Individual chloramphenicol-resistant colonies were streaked on LB agar plates containing 20 µg/ml kanamycin, as well as plates containing 100 µg/ml ampicillin, and again incubated overnight at 32˚C. Colonies resistant to all three antibiotics were assumed to contain both pML2 and 117B23 cKR. One triply resistant colony was seeded in 5 ml LB broth (10 g/L bacto-tryptone, 5 g/L bacto-yeast extract, 5 g/L NaCl) containing 12.5 µg/ml chloramphenicol and incubated at 32˚C with shaking. After overnight growth, a 1:50 dilution of the overnight culture was prepared in 2 ml LB broth without antibiotics (plain LB) and grown for three hours at 32˚C with shaking. Two 1:10 dilutions were prepared in 1 ml plain LB; to one culture, L-arabinose was added at a final concentration of 0.1%. After two hours of growth at 32˚C with shaking, 20 µl of a 10^{-4} dilution of bacteria were plated on two LB agar plates, one containing 12.5 µg/ml chloramphenicol and the second containing 12.5 µg/ml chloramphenicol and 1.0 mg/ml streptomycin. The plates were incubated overnight at 32˚C.

2.2.3 Creation of Retroviral Stocks

Plasmid DNA was prepared for clones 3 and 11 of the retroviral acceptor construct pML2 using the QIAfilter Plasmid Midi Kit (Qiagen) and following the manufacturer's recommended protocol. The DNA purity was verified by the A260/A280 ratio, and DNA integrity was verified by restriction endonuclease digestion with *Hind*III, *Bgl*I, and *Bam*HI/*Eco*RI. Amphotrophic Phoenix retroviral packaging cells (416) were thawed and cultured in Dulbecco's Modified Eagle Medium (DMEM; Invitrogen) supplemented with 10% fetal bovine serum (FBS; HyClone) and 1X

penicillin/streptomycin/L-glutamine (pen/strep/gln; Invitrogen) at 37˚C/5% CO_2. Cells were passaged every three to four days using 0.125% trypsin/EDTA (0.25% trypsin/EDTA (Invitrogen) diluted 1:1 in phosphate-buffered saline without cations (PBS-)) to dislodge the cells. Phoenix cells were plated in 10 cm tissue culture grade plates and transfected 24 hours later with 5.80 μg of pML2 using FuGENE-6 transfection reagent (Roche Applied Science) as per the suggested protocol. Twenty-four hours post-transfection, the cells were shifted to 34˚C/5% CO_2 to allow for retroviral particle production. Twenty-four and 48 hours later, retroviral supernatant was harvested by pulling the media into a syringe using an 18 gauge needle and filtering it through a 0.42 μM filter into six 2 ml screw-cap vials per plate. The supernatant was snap-frozen in liquid nitrogen and stored at -80˚C. Appropriate safety measures for biosafety level 2 were followed when working with the retroviral particles (417). All consumables that came in contact with the retroviral supernatant were soaked in a bleach solution for at least 15 minutes prior to disposal due to the amphotrophic nature of the retrovirus.

2.2.4 Creation of Cell Lines Harboring Acceptor Locus

TERT(+) 3C-167b (167b) and TERT(-) 3C-166a (166a) cells (234) were thawed and cultured in phenol red-free Minimal Essential Media (EMEM; MediaTECH) supplemented with 10% FBS (HyClone), 1X minimal essential amino acid solution (Sigma) and 1X pen/strep/gln (Invitrogen) (EMEM/10% FCS) at 37˚C/5% CO_2. Cells were passaged every three to four days using 0.125% trypsin/EDTA (see section 2.2.3) to dislodge the cells. One day prior to infection, each cell line was plated in a 6-well tissue culture grade plate such that the confluency of each well at the time of infection was approximately 50%. On the day of transfection, one vial each of retroviral supernatants 3 and 11 harvested at 24 hours was thawed slowly in warm water. Once thawed, polybrene was added to a final concentration of 1X. Following removal of the media from each well, approximately 0.5 ml of retroviral supernatant (just enough to cover the well) was added to the cells such that for each cell line, two wells were infected with retroviral stock 3, two wells were infected with retroviral stock 11, and two wells were uninfected (mock); mock-infected wells were incubated with 0.5 ml EMEM/10% FCS. The plates

were rocked every 30 minutes for a total of three and one-half hours. At this point, the cells were washed two times with phosphate-buffered saline supplemented with Ca^{2+} and Mg^{2+} (PBS+) and fed with 2 ml EMEM/10% FCS.

Forty-eight hours post-infection, the cells were approximately 90% confluent, and each well was expanded to three 6 cm plates: (1) 1:2 split; (2) 1:10 split; (3) remainder. The following day, the cells were fed with media containing 400 μg/ml G418 sulfate (G418, CellGro). After 10 days of selection, the mock-infected cells were all dead, indicating selection was complete. From this point forward, the cells were continuously cultured in 400 μg/ml G418. Once the colonies reached a larger size, three colonies from each infection (taken from the 1:10 splits) were cloned into one well of a 24-well tissue culture grade plate using cloning rings. The clones were subsequently expanded to 6-well, 6 cm, and 10 cm tissue culture grade plates. Once they reached confluency in a 10 cm plate, three frozen stocks of each line were prepared in freezing media (normal media supplemented with 5% dimethyl-sulfoxide (DMSO)); the stocks were slowly frozen to prevent crystallization by storing overnight at -80˚C in a pre-chilled cooler and then transferring to liquid nitrogen for long-term storage.

2.2.5 Creation of Cell Lines Harboring Acceptor Locus

Confluent 10 cm plates of cells infected with the retroviral acceptor construct pML2 and non-infected (naïve) cells were harvested by trypsinization with 1 ml 0.125% trypsin/EDTA. Once the cells had lifted off the plate, the total volume was brought up to 5 ml with PBS+. After the cells were pelleted by centrifugation at 1,000 rpm for 5 minutes, they were resuspended in 1 ml of PBS+, transferred to a microcentrifuge tube and re-pelleted by centrifugation at 6,000 rpm for one minute. gDNA was prepared from either freshly isolated cell pellets or cell pellets frozen at -80˚C and thawed at room temperature. The DNA was resuspended in the provided DNA rehydration buffer such that the final concentration was between 0.5 and 1.0 μg/μl. gDNA was stored at 4˚C after sealing the tubes with parafilm in order to prevent evaporation. For Southern analysis, 5 μg of gDNA was digested with 10 U of Taq^{α} I, in a total volume of 20 μl, for five hours at 65˚C, spinning down approximately every 30 minutes. The digested gDNA

was electrophoresed though 0.7% agarose prepared in 0.5X Tris-borate-EDTA buffer (TBE; 0.089 M Tris, 0.089 M boric acid, 0.002 M EDTA) and stained with ethidium bromide to visualize the DNA. The gDNA was denatured by washing the gel twice, 20 minutes each, with 1.5 M NaCl/0.5 N NaOH. Following a brief rinse with sterile water, the gel was neutralized by washing twice, twenty minutes each, with 1.5 M NaCl/0.5 M Tris-HCl. The gDNA was transferred to magnagraph nylon membrane (Osmonics) in 10X sodium chloride-sodium citrate buffer (SSC; 87.65 g/L NaCl, 44.1 g/L sodium citrate, pH 7.0). The DNA was crosslinked to the membrane by exposure to ultraviolet (UV) light using the autolink function of a Stratagene UV crosslinker. The membrane was prehybridized in prewarmed Church buffer (0.5 M sodium phosphate, pH 7.2, 7% SDS, 1 mM EDTA, 1% BSA) for at least one hour at 65˚C in a hybridization oven.

The membrane was probed with a 1.2 kb chicken β-globin insulator fragment. The fragment was isolated from pUC19M-cHS4 by restriction endonuclease digestion with *Spe*I/*Bam*HI and gel-purified. The fragment was labeled with α-^{32}P-dCTP (NEN/Perkin Elmer) using the Ladderman Labeling Kit (Takara) and purified from unincorporated α-^{32}P-dCTP using a G50 column prepared in 1X Tris-EDTA (TE; 10 mM Tris-Cl, 1 mM EDTA), pH 8.0. The specific incorporation was measured by diluting 2 µl of purified probe in 10 ml scintillation fluid (ScintiSafe™ Econo1, Fisher) and counting on a Beckman LS6000IC scintillation counter. The probe was boiled for three minutes, cooled on ice for five minutes, diluted in 5 ml prewarmed Church buffer, and added to the prehybridized membrane. After overnight hybridization at 65˚C, the membrane was washed twice, 15 minutes each at room temperature, in 1X SSC/0.1% SDS and then twice, 15 minutes each at 65˚C, in 0.2X SSC/0.1% SDS. The membrane was wrapped in plastic wrap and exposed to BioMax MS film (Kodak) anywhere from overnight to one week. Film was developed using a Kodak X-OMAT 3000RA processor.

2.2.6 Verification of Cell Lines Harboring Acceptor Locus

To verify functionality of the tk gene, five wells each of G418-resistant (neo^{R}), pML2-infected 167b and 166a clones (two per line), as well as naïve 167b and 166a cells, were seeded in 24-well plates. One day later, gancyclovir (GCV; 9-(1,3-dihydroxy-2-

propoxymethyl)guanine; Sigma) was added at concentrations of 0, 1, 10, 100, and 1,000 μM. Three days after GCV addition, cells were trypsinized with 0.125% trypsin/EDTA and counted using a hemacytomter.

The function of the CreER fusion gene was monitored by transfection with the Cre reporter pZ/AP ((418); kind gift of Andras Nagy, Samuel Lunenfeld Research Institute, Toronto, Ontario, Canada). Clones and naïve cells were plated in duplicate in two 24-well plates so they would be 50% confluent at the time of transfection. Twenty-four hours post-plating, each well was transfected with 0.20 μg DNA using FuGENE-6. The next day, one well per plate of each duplicate was treated with 1 μM 4-hydroxytamoxifen (4HT) while the second well was treated with the same volume of vehicle (100% ethanol) as control. Forty-eight hours following treatment, one plate was stained for β-galactosidase (β-gal) activity and the other for alkaline phosphatase (APAP) activity. For β-gal staining, cells were washed once with cold PBS+ and fixed for 15 minutes in 0.05% glutaraldehyde (Sigma). Cells were washed three times with PBS+, incubating in the second wash for 10 minutes. Cells were incubated overnight and in the dark at 37˚C in staining solution (10 mM $K_3Fe(CN)_6$, 10 mM $K_4Fe(CN)_6$, 2 mM $MgCl_2$, 1 mg/ml X-gal). For APAP staining, cells were washed twice with ice-cold PBS+ and fixed for 45 seconds in ice-cold 3.7% formaldehyde in methanol. After the cells were gently washed with sterile deionized water, they were incubated anywhere from two hours to overnight in the dark at room temperature in staining solution (0.25 mg/ml Fast Violet B Salt (Takara), 0.20 mg/ml Napthol AS-MX Phosphate, pH 8.6 (Sigma)). The percentage of cells stained was determined upon examination of plates using microscope.

The integrity of the *lox* sites upon genomic integration was determined by PCR amplification and subsequent sequencing of clones 167b 3.5 and 166a 11.4. The sequence surrounding the *lox511* site was amplified with primer pair MAL40 (5'-CGTTGGGTTACCTTCTGCTC-3')/MAL44 (5'-GGGCGTACTTGGCATATGAT-3') using the following PCR conditions: 94˚C for 3 minutes, 20 cycles of 94˚C for 1 minute, 68˚C for 1 minute, and 72˚C for 1 minute, 15 cycles of 94˚C, 60˚C for 1 minute, and 72˚C for 1 minute, followed by a 5 minute extension at 72˚C. The products were isolated by gel purification after electrophoresis through a 2.0% agarose/0.5X TBE gel. Sequencing was performed on two independent samples for each line at the Genomics

Core Facility, Program in Human Genetics, University of California San Francisco using primer MAL40. The *loxP* region was amplified with primer pair MAL43 (5'-CCTACAGGTGGGGTCTTTCA-3')/MAL53 (5'-ATCGCATTCCTTGCAAAAGT-3') using the following PCR conditions: 94˚C for 3 minutes, 35 cycles of 94˚C for 1 minute, 60˚C for 1 minute, and 72˚C for 1 minute, followed by a 5 minute extension at 72˚C. Sequencing was performed as for *lox511* with the exception of using primer MAL53 for sequencing.

2.3 Results

2.3.1 Retroviral Acceptor Locus Vector

pML2 (Figure 2.4) is the retroviral vector used to create an acceptor locus in TERT(+) 3C-167b and TERT(-) 3C-166a cells and contains the following relevant elements: (1) a hybrid 5' LTR comprised of the cytomegalovirus (CMV) type I enhancer and the mouse sarcoma virus (MSV) promoter, (2) the retroviral packaging signal ψ, (3) the Cre recombinase recognition site *lox511*, (4) the CMV immediate early promoter (CMV_{IEP}) driving expression of both a neomycin phosphotransferase(*neo*)/herpes simplex virus (HSV) thymidine kinase (*tk*) fusion gene under control of the HSV *tk* promoter (tkNeo), and a Cre recombinase/estrogen receptor (CreER) fusion gene, (5) a second Cre recombinase recognition site, *loxP*, and (6) an MMLV 3' LTR lacking the U3 enhancer region and containing the 1.2 kb chicken β-globin insulator cHS4. The ability of CMV_{IEP} to control expression of both the *neo/tk* and CreER fusion genes is mediated by an internal ribosomal entry site (IRES); the placement of an IRES between two genes allows them to be co-transcribed as a bicistronic mRNA and then translated in a CAP-dependent (gene upstream of the IRES, or *neo/tk* in the case of pML2) and CAP-independent (gene downstream of the IRES, or CreER in the case of pML2) manner (419-422).

Following the stepwise assembly of pML2, the integrity of the *lox* sites was verified by sequencing pML2. The *lox* sites were verified functionally by introducing pML2 and the BAC 117B23 cKR to EL350 bacteria, a strain containing Cre recombinase under control of the L-arabinose-inducible *ara*BAD promoter (P_{BAD}) (415). The verification scheme is found in Figure 2.5A. 117B23 cKR contains *loxP* and *lox511* sites oriented in the same direction as pML2. In the presence of L-arabinose, Cre recombinase is expressed and will lead to recombination between the homologous *lox* sites in pML2 and 117B23 cKR. This recombination results in the exchange of DNA between the two plasmids, and, thus, the segregation of the wild-type streptomycin gene ($rpsL^+$) from the chloramphenicol resistance marker of 117B23 cKR. The presence of colonies resistant to both chloramphenicol and streptomycin after arabinose induction verifies the *in vitro* function of the *lox* sites (Figure 2.5B).

2.3.2 Production of Retrovirus and Infection of TERT(+) and (-) Cells

To create retroviral particles, pML2 was introduced to amphotropic Phoenix packaging cells (416) by FuGENE-6-mediated transfection. TERT(+) and TERT(-) cell lines stably expressing the acceptor locus were identified following infection with pML2 proviral particles and 10 days of selection in G418. For both the TERT(+) and TERT(-) cells split 1:2 following infection, the colonies were too close together to be isolated; however, the cells split 1:10 formed discrete, individual colonies. In total, 12 TERT(+) and 12 TERT(-) colonies were isolated, and of these, 11 TERT(+) and 8 TERT(-) clones were able to be expanded. To identify those clones containing a single copy of the acceptor locus integrated at a single site, Southern hybridization was performed by probing *Taq*$^{\alpha}$I-digested gDNA with the 1.2 kb cHS4 fragment (Figure 2.6A). Single-copy, single-site integrants were expected to show two fragments of equal intensity upon hybridization, one at 1,470 bp and one greater than 1,137 bp. Analysis of these 19 clones revealed that five of eleven TERT(+) (Figure 2.6B) and three of eight TERT(-) (Figure 2.6C) clones displayed the expected banding pattern. Of the remaining clones, one TERT(+) and two TERT(-) clones showed a single, high-intensity band, one TERT(-) clone showed two fragments of equal intensity greater than 1.4 kb, and five TERT(+) and two TERT(-) clones showed two or more fragments of varying intensity. Sequencing of the regions surrounding the *loxP* and *lox511* sites of one TERT(+) and one TERT(-) clone confirmed the integrity of the *lox* sites upon integration.

2.3.3 Test of Gancyclovir Sensitivity

Upon integration of the acceptor locus, the cells become sensitive to gancyclovir (GCV) due to the presence of the HSV *tk* gene. To test those TERT(+) and (-) clones stably expressing a single copy of the acceptor locus for *tk* function, cells were exposed to increasing concentrations of GCV (Figure 2.7). Naïve TERT(+) cells (those not expressing the acceptor locus) were unaffected by 1 or 10 μM GCV, but at 100 and 1,000 μM GCV, the survival was only 64% and 36% of untreated cells. Naïve TERT(-) cells

were affected at all GCV concentrations (82%, 59%, and 40% survival at 1, 10, and 100 and 1,000 μM GCV, respectively). Clones expressing the acceptor locus were affected at all GCV concentrations and to a much greater extent than naïve cells. At only 1 μM GCV, acceptor locus clones showed anywhere from 35-60% survival compared to the naïve cultures; by 1,000 μM, acceptor locus-containing cultures showed survival of 1-7% compared to naïve cultures.

2.3.4 Test of CreER Inducibility

The inclusion of a CreER fusion gene in the acceptor locus should permit Cre expression only in the presence of the estrogen agonist 4-hydroxtamoxifen (4HT). The inducibility of CreER in cells containing a single copy of the acceptor locus was tested by transfecting cells with the Cre reporter pZ/AP (418). pZ/AP is a vector containing a CMV promoter, a βgeo (*lacZ/neo*^{R} fusion) gene surrounded by *loxP* sites, and the human placental alkaline phosphatase (hPLAP) coding sequence (Figure 2.8A). In the absence of Cre, the CMV promoter drives expression of βgeo; however, in the presence of Cre, recombination occurs between the *loxP* sites, resulting in the excision of the βgeo gene and expression of the hPLAP gene. Therefore, it would be expected that in the absence of 4HT, cells would stain positive for *lacZ* expression and negative for hPLAP expression, while culturing cells in the presence of 4HT should result in a lack of staining for *lacZ* expression and positive staining for hPLAP expression. Naïve TERT(+) and (-) cells stained intensely blue regardless of 4HT addition (Figure 2.8B and data not shown). Clones expressing the acceptor locus stained intensely blue in the absence of 4HT and red in the presence of 4HT, as expected (Figure 2.8B and data not shown). Addition of 4HT to acceptor locus clones did not completely eliminate the presence of blue cells, although their number was greatly decreased. Both naïve cells and those expressing the acceptor locus showed a minimal number of red cells regardless of the presence of 4HT (Figure 2.8B and data not shown).

2.4 Discussion

In this chapter, the retroviral-mediated creation of TERT(+) and (-) cells harboring a stably integrated, single-copy of an acceptor locus was reported. To create the pML2 retroviral particles, Phoenix cells were used. Phoenix cells are 293T cells engineered to stably express MMLV *gag-pol-pro* and *env* genes from separate genomic loci (416). Expression of the retroviral genes in *trans* (ψ from pML2 and *gag* and *pol-pro* from the cells themselves) results in the packaging of the recombinant provirus into fully infectious particles within 48-72 hours of transfection. These particles can then be used to infect the cells of interest, which in this case are the TERT(+) and (-) 3C-167b and 3C-166a cells, respectively (Figure 2.9). The natural duplication of LTRs upon reverse transcription of retroviral RNA (Figure 2.10A) was harnessed to surround the acceptor locus with the cHS4 insulator by inserting it into the 3' LTR of pML2 (Figure 2.10B). This duplication of LTRs also makes pML2 a self-inactivating (SIN) vector (423). Because it is the U3 region of the 5' LTR that controls viral transcription, the presence of a U3 region lacking promoter activity results in the subsequent loss of viral transcription. The use of the SIN pML2 vector adds another level of safety to the use of retroviruses as mediators of gene transduction. This acceptor locus contains chicken β-globin insulators surrounding a *lox511*/*loxP*-flanked cassette expressing a positive/negative selection marker (tkNeo) and inducible Cre (CreER). By Southern hybridization, as evidenced by two fragments of equal intensity, five TERT(+) (167b 3.1, 3.5, 11.2, 11.4, and 11.6; Figure 2.6B) and three TERT(-) (166a 3.1, 11.1, and 11.4; Figure 2.6C) clones were shown to contain the acceptor locus integrated at a single site. An additional TERT(+) clone, 11.5, and two TERT(-) clones, 3.2 and 3.5, showed only one fragment of high intensity upon hybridization (Figure 2.6B); these clones could also be single-site integrants in which the >1,137 bp fragment is approximately the same size as the 1,470 bp fragment. To determine if these three clones are truly single-site integrants, additional Southern characterization with different restriction endonucleases would need to be performed. While the TERT(-) clone 3.3 (Figure 2.6C) displays two fragments of equal intensity, the expected fragment of 1,470 bp was not found. This is most likely a single-site integrant that has undergone some type of rearrangement upon integration. All

single-site integrants were assumed to be single-copy integrants because even if numerous copies integrated at the same site, Cre/*lox* activity would reduce the total number of copies to one.

The engineering of the acceptor locus to contain heterologous *lox* sites will allow targeted integration of cassettes containing regions of interest via recombinase-mediated cassette exchange (RMCE). The nature of the product formed upon Cre-mediated recombination is dependent on the type, number, and orientation of *lox* sites present (reviewed in (372;424)). If two identical *lox* sites are found in *cis* in the same orientation, Cre-mediated recombination will result in the excision of the DNA sequence located between the *lox* sites (Figure 2.11A); if the *lox* sites are in *cis* but in opposite orientations, recombination will result in the inversion of the intervening sequence (Figure 2.11B). The presence of heterologous *lox* sites in *cis*, regardless of orientation, should prevent Cre-mediated recombination and therefore, produce no change in the DNA sequence (Figure 2.11C). Regardless of their orientation, single *lox* sites in *trans* will result in integration in the presence of Cre (Figure 2.11D); the presence of two *lox* sites in *trans* will result in a replacement event (Figure 2.11E). The acceptor locus contains the heterologous *lox* sites *lox511* and *loxP*, and, in the presence of a second cassette containing the same *lox* sites in the same orientation, Cre will mediate a replacement event. The use of heterologous *lox* sites will prevent unwanted recombination between the *lox* sites of the acceptor locus, which would decrease the efficiency of the desired RMCE event as intramolecular reactions are more efficient than intermolecular reactions (425). However, even if the *loxP* and *lox511* sites do recombine with each other, which is known to occur in mammalian cells (426-428), the arrangement of the *lox* sites such that they are oriented in opposite directions means that the acceptor locus will simply be inverted, not lost, upon Cre-mediated recombination (Figure 2.11F).

The inclusion of the CreER fusion gene in the acceptor locus provides many benefits. Firstly, the Cre recombinase used in the fusion is a mammalian codon-optimized synthetic Cre (iCRE) that shows improved expression and function in mammalian cells compared to the native bacteriophage λ Cre (414). The use of CreER implies that Cre will only be expressed in the presence of estrogen receptor agonists, such as 4-hydroxytamoxifen (4HT). The ability to easily control Cre expression is important

as prolonged expression of Cre has been shown to induce DNA damage and growth inhibition in mammalian cells (429;430). Additionally, the location of CreER between the *lox* sites signifies that after RMCE, Cre expression will be lost. This loss of CreER will prevent the continued exchange of the two cassettes, which could decrease the overall RMCE efficiency. The inclusion of the estrogen receptor necessitates the use of phenol red-free medium when culturing cells expressing the acceptor locus as phenol red is able to bind to the estrogen receptor and induce its downstream effects (431). The appearance of hPLAP-positive cells in pZ/AP-transfected, acceptor locus-containing cells not treated with 4HT indicates that Cre is expressed at a low level in the absence of induction (data not shown). This could induce DNA damage and/or growth inhibition after prolonged culture; however, growth inhibition of TERT(+) and (-) acceptor locus-containing lines has not been noted after as long as four months of continuous culture in phenol red-free medium.

The inclusion of the tkNeo fusion gene permits selection for both the gain and loss of the acceptor locus. The neomycin phosphotransferase gene (*neo*) provides resistance to G418, and therefore, only those cells that have integrated the acceptor locus into their genome will be able to survive in the presence of G418. Therefore, *neo* is a positive selection marker as selection is aimed at those cells which have gained function. The HSV thymidine kinase gene (*tk*) converts GCV to GCV-monophosphate (GCV-MP), permitting its further phosphorylation to di- and triphosphorylated GCV (GCV-DP and GCV-TP, respectively) by endogenous kinases. The cytotoxic effects of GCV lie in the ability of GCV-TP to compete with dGTP for binding to DNA polymerase, leading to impaired DNA synthesis and cell death by apoptosis (432;433). The efficiency with which *tk* induces cell death upon GCV addition has made HSV *tk* a popular choice for the development of cancer-treating suicide vectors (reviewed in (434)). In our case, the HSV *tk* gene will be important for selecting those cells that have undergone RMCE as only those cells which have loss the acceptor locus will survive addition of GCV. In this way, *tk* is a negative selection marker in that selection is aimed at those cells which have lost function. One potential problem with using negative selection via *tk*-mediated metabolism of GCV is that once a *tk*-expressing cell dies, its toxic metabolites are released into the culture medium and can be taken up by other cells that may or may not

express *tk* themselves. In this way, *tk*-negative cells can also be killed by addition of GCV; this effect is known as bystander killing (433). To alleviate bystander killing effects, the cells can be washed during the GCV selection process in an attempt to remove the toxic metabolites before they can be taken up by other cells. Additionally, cells can be treated with fialuridine (FIAU; 1-(2-deoxy-2-fluro-β-D-arabinofuranosyl)-5-iodouracil), a GCV alternative that has been shown to cause less bystander killing (435). (While not shown, FIAU was shown to effectively kill TERT(+) and (-) cells expressing the acceptor locus.)

Flanking the acceptor locus by single copies of the chicken β-globin insulator should protect the locus from transgene silencing and PEV. Even though Cre-mediated targeting of transgenes to *lox* sites integrated into the genome allows transgenes to be expressed in a single copy at a single locus, such targeting does not prevent the surrounding chromatin environment from influencing transgene expression (368;436). As discussed earlier, flanking transgenes by insulators protects them from PEV by blocking distal enhancer and silencer activities. The inclusion of insulators in retroviral vectors has been shown to increase the probability that they will be expressed upon genomic integration by preventing the methylation of the viral LTRs (347). Furthermore, a combination of insulators and RMCE has been shown to significantly reduce transgene silencing during prolonged culture, as well as significantly decreasing PEV among different pre-targeted clones (349). Taken together, these studies imply that surrounding the acceptor locus by single copies of the cHS4 insulator should yield transgene expression that is unaffected by exogenous influences.

The creation of the acceptor locus in genetically related TERT(+) and (-) cell lines is important for studying h*TERT* regulation. It has been established that expression of the same transgene can vary between different strains of mice due to the presence of strain-specific regulatory elements (437-440). This is not surprising as many endogenous genes show variable expression between different mouse strains, including genes involved in the immune response (441-443) and liver-mediated metabolism (444-446). Human genetic polymorphisms have also been noted and implicated in disease susceptibility (reviewed in (447-449)) and liver metabolism (reviewed in (450-452)). Similarly, gene expression profiles among human cell lines of the same cell type but isolated from

different sources have been shown to differ from one another (453;454). These studies indicate that in order to best characterize gene regulation *in vitro*, the cell lines should be as close to genetically identical as possible. The TERT(+) 3C-167b and TERT(-) 3C-166a cells used to create the acceptor locus lines are both derivatives of IMR-90 cells (primary human lung fibroblasts) (234). The 3C-167b and 3C-166a cell lines were obtained after transducing IMR-90 cells with SV40 large T antigen (SV40 T) (192). Introduction of SV40 T abrogates the p53- and pRB-mediated DNA damage response pathways, thereby preventing M1 senescence. Eventually, the cells will reach M2, or crisis, a period characterized by genomic instability. At this point, most cells die, but some are able to escape by activating pathways to maintain their critically shortened telomeres. 3C-167b cells maintain their telomeres by activating *TERT* while 3C-166a cells maintain their telomeres through the alternative lengthening of telomeres (alt) pathway. (The alt pathway is thought to rely on homologous recombination for telomere maintenance (reviewed in (455)). There are some concerns with using post-crisis cells. For instance, even though they share a common precursor (IMR-90), they have gone through genomic instability, and therefore, their final genetic makeup is most likely different. This is supported by the fact that one cell line is TERT(+) while the other is TERT(-). Additionally, these cells are known to be aneuploid ((192) and data not shown), meaning that other genes besides *TERT*, including those involved in *TERT* regulation could be differentially affected in these two lines. Overall, however, these cells should be useful for studying h*TERT* regulation via RMCE.

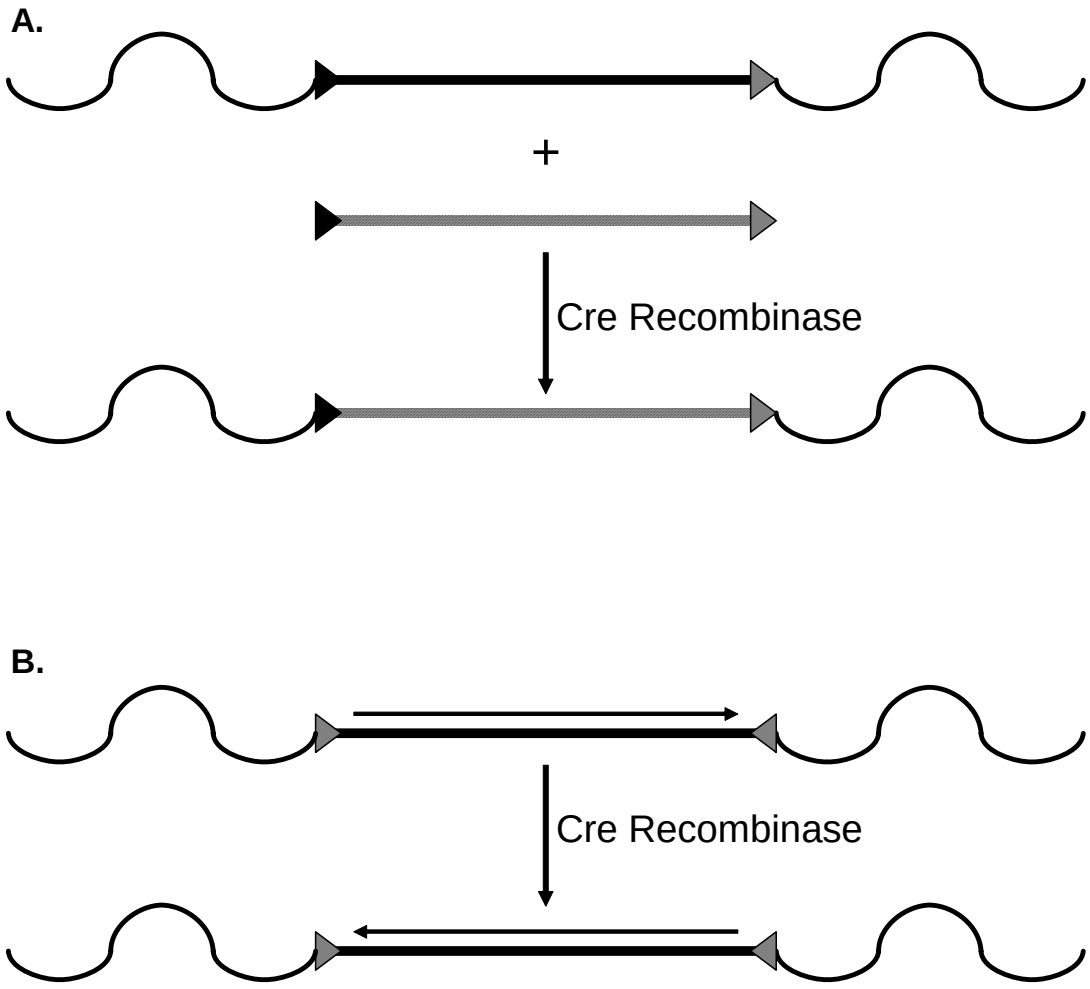

Figure 2.1. Overview of Recombinase-Mediated Cassette Exchange (RMCE). **A.** RMCE requires an acceptor locus (solid black line), minimally harboring a negatively selectable marker, surrounded by heterospecific *lox* sites (black and grey triangles) and integrated into the chromosome (wavy lines). When a DNA fragment of interest (hatched line), surrounded by the same heterospecific *lox* sites in the same orientation, is introduced to cells harboring the acceptor locus in the presence of Cre recombinase results in an exchange of the acceptor locus for the DNA of interest, resulting in the integration of the DNA of interest and the loss of the acceptor locus. **B.** If the acceptor locus is surrounded by the same *lox* sites, but oriented in reverse, the locus will be inverted, not lost, in the presence of Cre. Note: While the diagram shows Cre/*lox*-mediated RMCE, FLP/Frt-mediated recombination can also be used in RMCE.

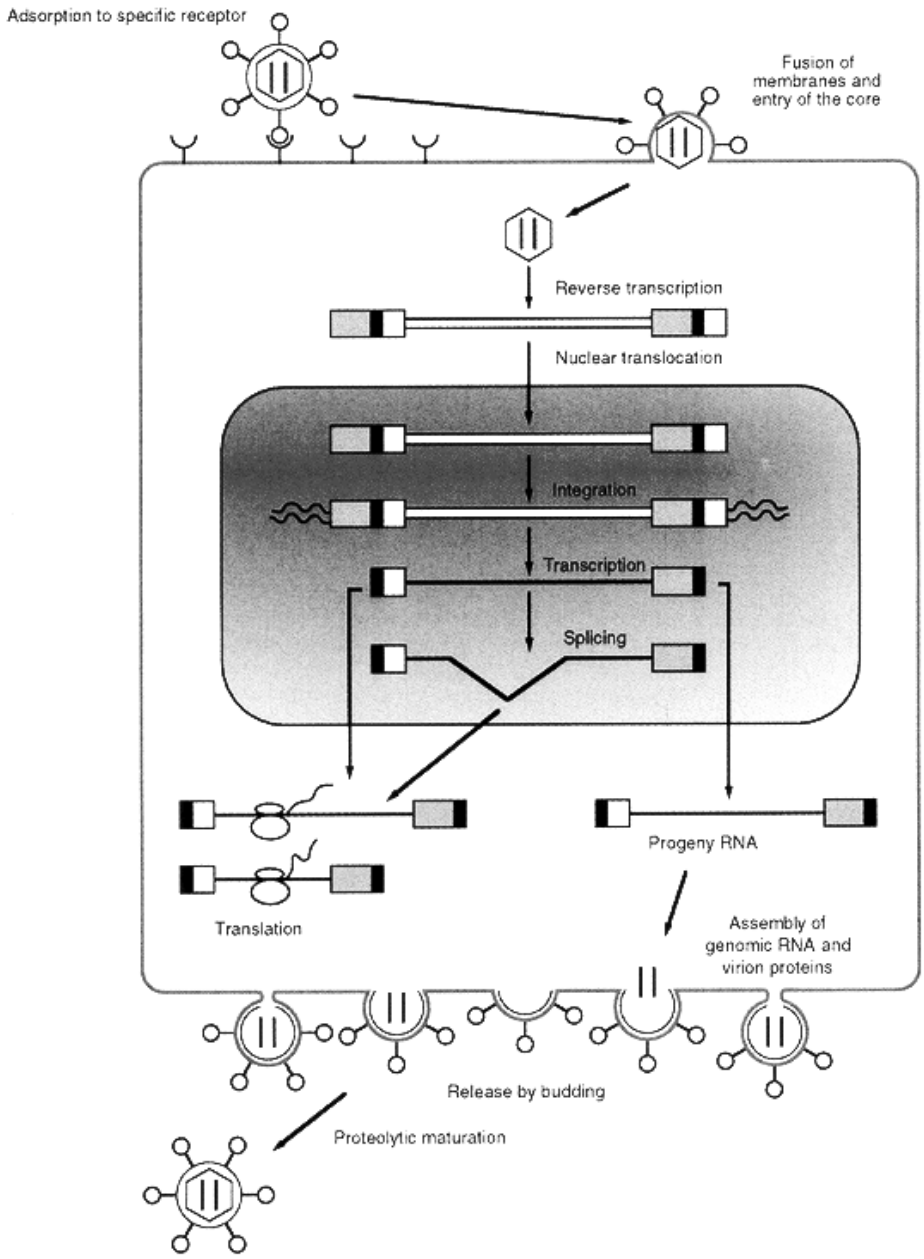

Figure 2.2. The Retroviral Life Cycle. Taken from (456). After receptor-mediated entry in the host cell, the viral RNA undergoes reverse transcription to produce a DNA transcript. This DNA transcript is then translocated to the nucleus where it integrates into the host genome. A portion of the subsequent transcribed RNA is processed for assembly into infectious particles. Another portion of the RNA is spliced and translated to produce the proteins necessary for virion assembly and release.

A. lox511.F 5'-GATCTATAACTTCGTATAGTATACATTATACGAAGTTATGGATCCT-3'

lox511.R 5'-CTAGAGGATCCATAACTTCGTATAATGTATACTATACGAAGTTATA-3'

lox511 Linker 5'-GATCT**ATAACTTCGTATAGTATACATTATACGAAGTTAT**GGATCCT-3'
3'-A**TATTGAAGCATATCATATGTAATATGCTTCAATA**CCTAGGAGATC-5'

B. loxP.F 5'-TCGAGATAACTTCGTATAATGTATGCTATACGAAGTTATCAG-3'

loxP.R 5'-CTGATAACTTCGTATAGCATACATTATACGAAGTTATC-3'

loxP Linker 5'-TCGAG**ATAACTTCGTATAATGTATGCTATACGAAGTTAT**CAG-3'
3'-C**TATTGAAGCATATTACATACGATATGCTTCAATA**GTC-5'

Figure 2.3. Oligos Used to Create *lox511* and *loxP* Linkers. **A.** Oligonucleotides lox511.F and lox511.R were ordered from Integrated DNA Technologies and annealed to create a linker containing the *lox511* Cre recombinase recognition site; the actual recognition site is bolded. The 5' overhang is compatible with ends produced by restriction endonuclease digestion with *Bgl*II while the 3' recessed end is compatible with ends produced by digestion with *Xba*I. **B.** Oligonucleotides loxP.F and loxP.R ordered from Integrated DNA Technologies and annealed to create a linker containing the *loxP* Cre recombinase recognition site; the actual recognition site is bolded. The 5' overhang is compatible with ends produced by restriction endonuclease digestion with *Xho*I while the 3' end is compatible with any endonuclease that produces blunt ends upon cleavage.

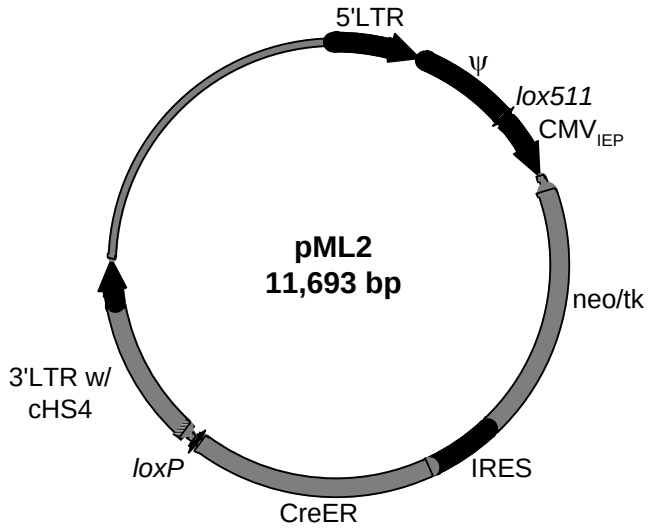

Figure 2.4. The Retroviral Vector pML2. pML2 was used to create an acceptor locus in TERT(+) 3C-167b and TERT(-) 3C-166a cells. It contains a hybrid 5' LTR, the retroviral packaging signal ψ, the Cre recombinase recognition sites *lox511* and *loxP*, the CMV immediate early promoter (CMV_{IEP}), a neomycin/HSV-thymidine kinase (tkNeo) fusion gene, a fusion of Cre recombinase to the estrogen receptor (CreER), an internal ribosomal entry site (IRES) to allow CMV_{IEP} to control both tkNeo and CreER, and a 3'LTR containing the cHS4 insulator. Note: Intermediate plasmids used in the construction of pML2 can be found in Figures A1 and A2 of Appendix A.

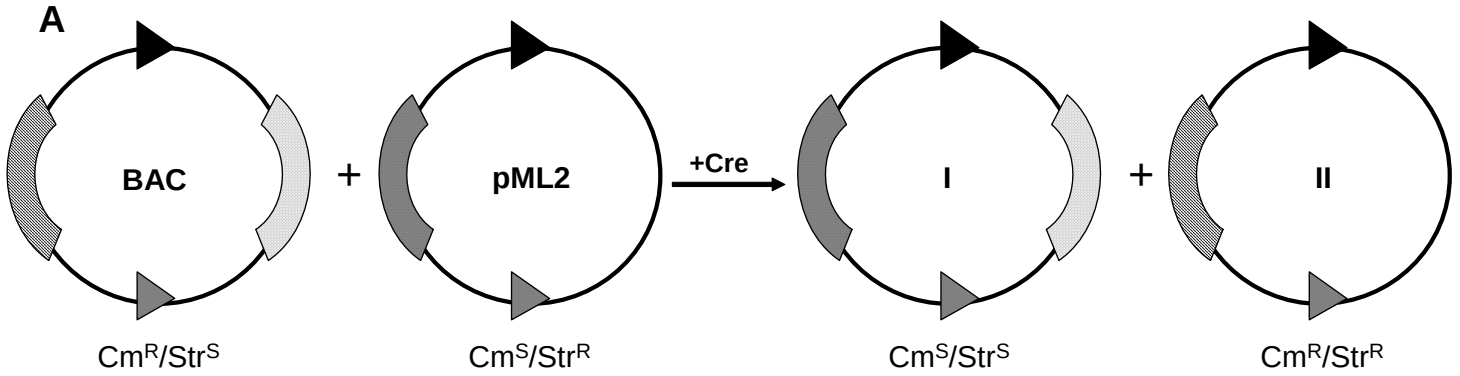

B

Resistance	+ Arabinose	- Arabinose
Cm	+	+
Cm and Strep	+	-

Figure 2.5. *lox* Site Verification. **A.** Experimental scheme to verify *lox* sites *in vitro*. The BAC contains a *lox511* site (black triangle) and a *loxP* site (gray triangle) along with a chloramphenicol resistance marker (hatched line) and the wild type *rpsL* gene (dotted line), which leads to streptomycin sensitivity. pML2 contains the same *lox* sites and an ampicillin resistance marker. Introduction of these plasmids to EL350 bacteria and induction of Cre recombinase by addition of L-arabinose leads to Cre/*lox* recombination and the segregation of the genes for chloramphenicol resistance and streptomycin sensitivity. Therefore, the only way to obtain a colony that is resistant to both chloramphenicol and streptomycin (II) is by Cre/*lox* recombination. **B.** Results of a test of pML2. Actual colony numbers were not counted; results were scored for either the presence (+) or absence (-) of colony growth. These results, representative of two experiments, verify the *in vitro* function of the *lox* sites. Note: Figure not to scale.

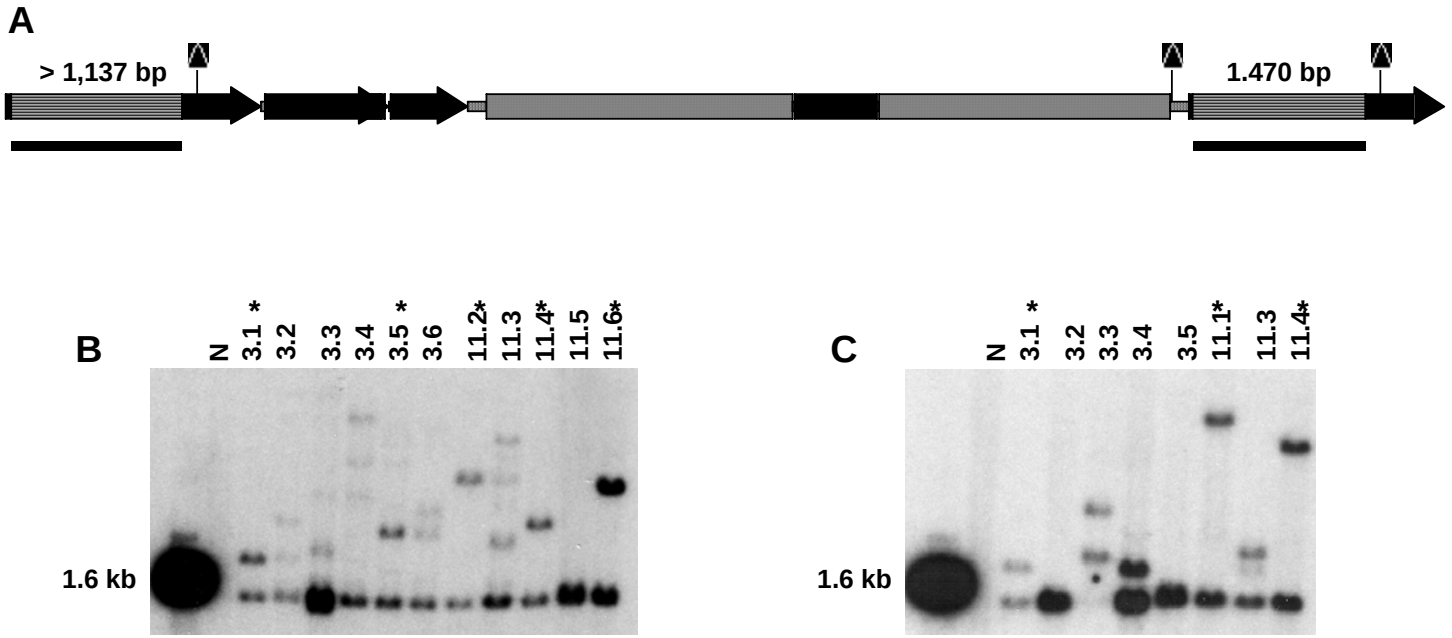

Figure 2.6. Identification of Single-Site Integrants of the Acceptor Locus. Single-site integrants were identified by two fragments of equal intensity upon hybridization with a cHS4 probe. **A.** Schematic of genomic acceptor locus generated by retroviral integration of pML2. Triangles represent *Taq*^{a}I restriction endonuclease recognition sites; the dark line beneath the schematic represents the α-^{32}P-labeled 1.2 kb cHS4 fragment used as a probe. (Additional *Taq*^{a}I sites are present within the acceptor locus but are not included here as they do not affect the expected Southern hybridization pattern.) **B.** TERT(+) clones isolated after retroviral infection of 3C-167b cells with retroviral supernatants 3 and 11. The clones marked with * (3.1, 3.5, 11.2, 11.4, and 11.6) are single-site integrants. C. TERT(-) clones isolated after retroviral infection of 3C-166a cells with retroviral supernatants 3 and 11. The clones marked with * (3.1, 11.1, and 11.4) are single-site integrants.

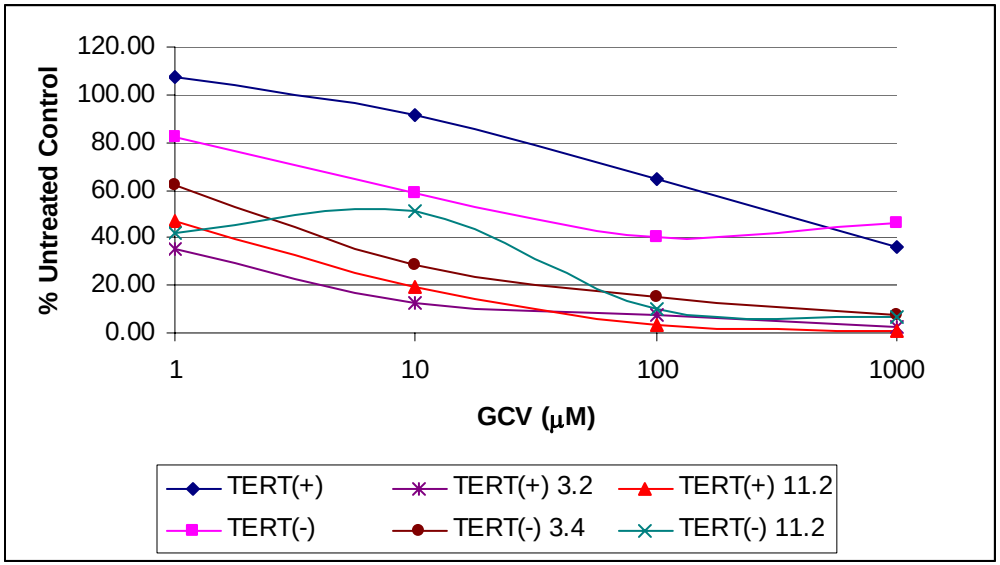

Figure 2.7. Test of Gancyclovir (GCV) Response. 3C-167b and 3C-166a cells without the acceptor locus (TERT(+) and TERT(-), respectively), 3C-167b clones with the acceptor locus (TERT(+) 3.2 and TERT(+) 11.2), and 3C-166a clones with the acceptor locus (TERT(-) 3.4 and TERT(-) 11.2), were plated at equal densities and treated with 0, 1, 10, 100, or 1000 μM GCV. After 48 hours, the cells were trypsinized and counted. Represented is the percentage of cells that survived GCV selection compared to those cells that were not treated with GCV.

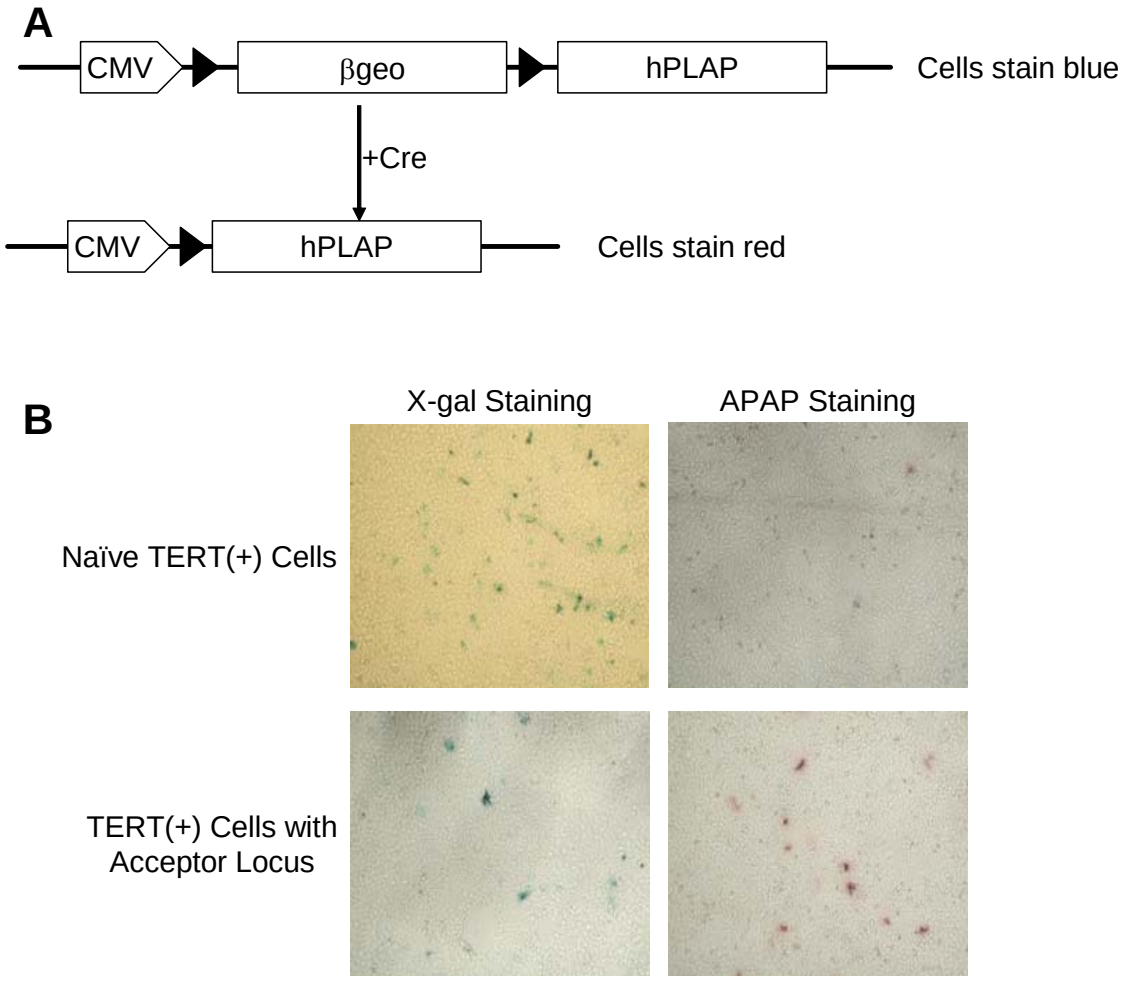

Figure 2.8. Verification of CreER Activity. **A.** Schematic of Cre verification using pZ/AP. In the absence of Cre, the CMV promoter drives expression of the βgeo gene, resulting in the appearance of blue cells upon x-gal staining and a lack of red cells upon alkaline phosphatase staining. After addition of Cre, Cre/*lox*-mediated recombination results in the excision of the βgeo gene, allowing the CMV promoter to control the hPLAP gene, resulting in the appearance of red cells upon alkaline phosphatase staining. **B.** Staining after induction of CreER in naïve TERT(+) cells and TERT(+) cells expressing the acceptor locus. The lack of red cells in naïve cultures verifies the lack of the alkaline phosphatase in the absence of Cre. The decrease in the number of blue cells in the acceptor locus-containing cells and the appearance of red cells is a consequence of Cre excision of the βgeo gene. While not shown, TERT(-) cells showed the same staining pattern. All images are at 40X magnification.

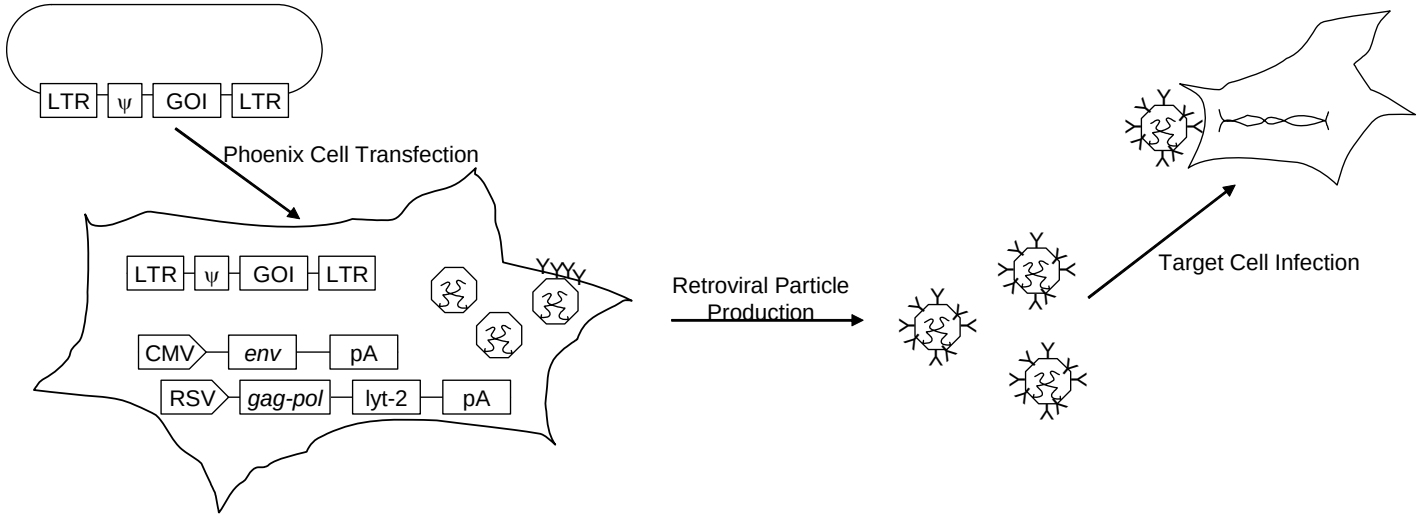

Figure 2.9. Retrovirus Production Using Phoenix Cells. (Figure adapted from (416).) A vector containing a gene of interest (GOI), retroviral LTRs, and a retroviral packaging signal (ψ) is transfected to Phoenix cells. The Phoenix cells contain two separately integrated plasmids expressing the retroviral *env* and *gag/pol* genes. The combination of the *env*, *gag/pol*, LTRs, and ψ allows for the production of enveloped retroviral particles. Upon infection of target cells with the particles, the GOI, surrounded by the LTRs, will integrate into the host genome and become stably expressed (proviral DNA). Note: Figure not to scale.

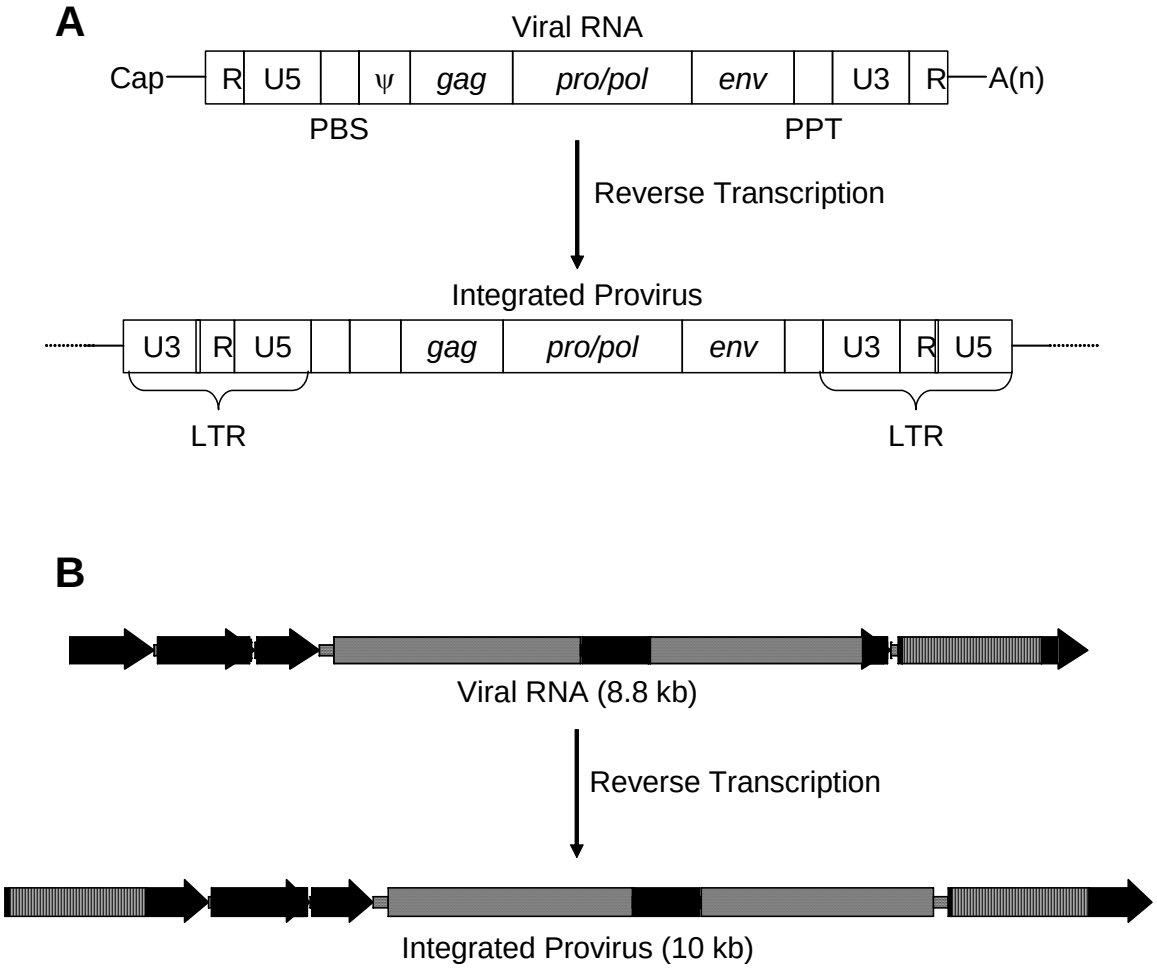

Figure 2.10. Retroviral Reverse Transcription. **A.** Minus strand reverse transcription initiates at the primer binding site (PBS) and proceeds towards the cap. Following RNaseH degradation of the viral RNA R and U5 regions, the newly synthesized DNA (-ssDNA) anneals to the 3' repeat (R) strands and continues -ssDNA synthesis. Plus strand (+ssDNA) synthesis is initiated at the 3' polypyrimidine tract (PPT) of the -ssDNA. Following RNaseH degradation of the viral RNA, the plus and minus ssDNA strands anneal at the PBS and transcription continues. The result is an integrated, double-stranded DNA provirus with the U3 region duplicated at the 5' end and the U5 region duplicated at the 3' end, resulting in identical long terminal repeats (LTRs). **B.** Reverse transcription of pML2 retroviral RNA results in the duplication of the cHS4 insulator at the 5' end, thus insulating the intervening sequence from both the 5' and 3' ends.

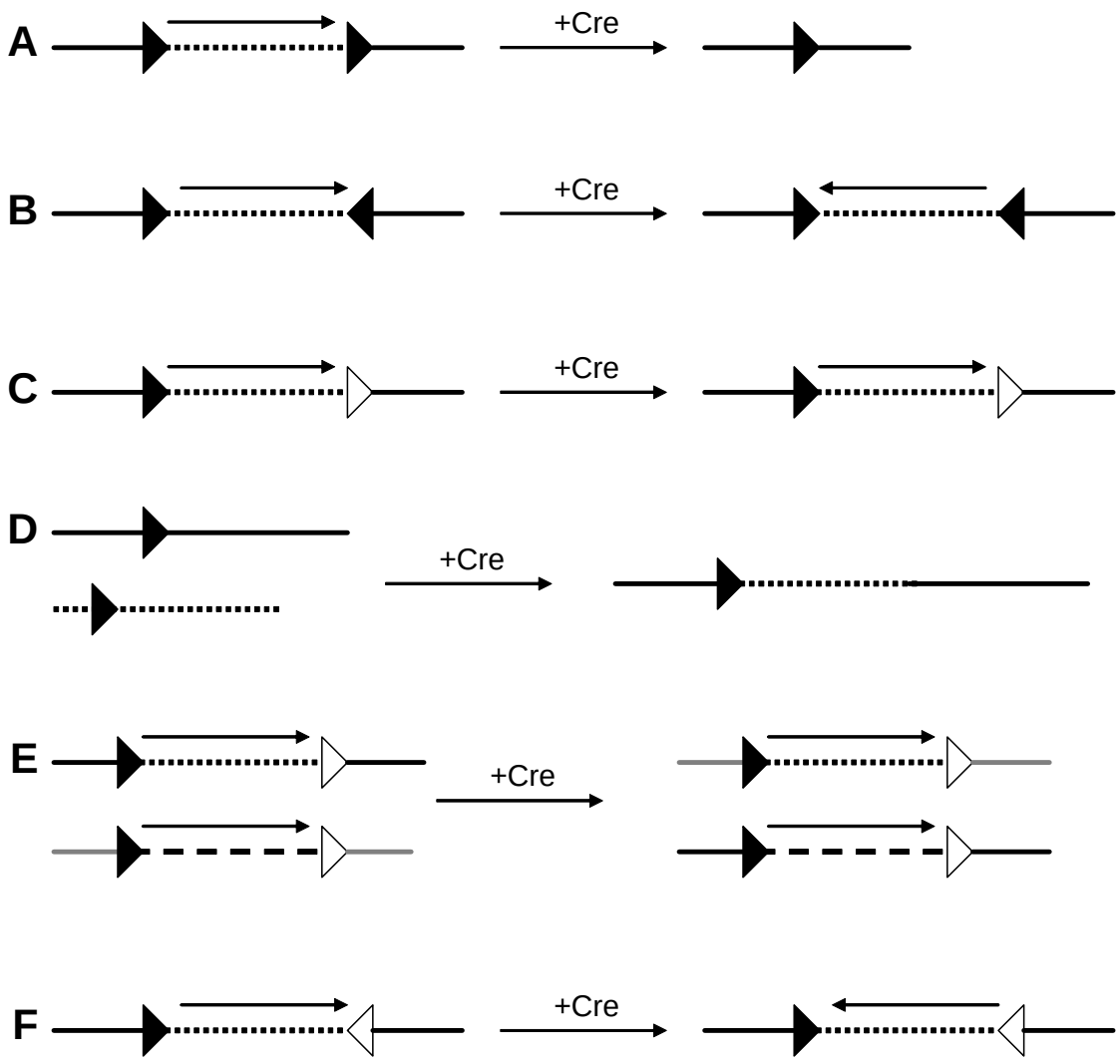

Figure 2.11. Examples of Cre/*lox* Reactions. **A.** The presence of homologous *lox* sites in *cis* in the same orientation results in the excision of the intervening DNA in the presence of Cre. **B.** The presence of homologous *lox* sites in *cis* in the opposite orientation results in the inversion of the intervening DNA in the presence of Cre. **C.** The presence of heterologous *lox* sites, regardless of location or orientation, theoretically results in no recombination in the presence of Cre. **D.** The presence of homologous *lox* sites in *trans* results in the insertion of DNA in the presence of Cre. **E.** The presence of dual *lox* sites in *trans* results in the exchange of the intervening DNA between the two DNA fragments in the presence of Cre. **F.** The presence of heterologous *lox* sites in *cis* in the opposite orientation results in the inversion of the intervening DNA in the presence of Cre.

Chapter 3
MODIFICATION OF HUMAN BAC CONSTRUCTS

3.1 Introduction

Bacterial artificial chromosomes (BACs) are circular vectors based on the *E.coli* F-factor and are capable of stably maintaining genomic inserts of up to 300 kb (270). BACs were originally designed to overcome the limitations of yeast artificial chromosomes (YACs) and eventually became the cloning system of choice for genome sequencing projects (reviewed in (457)). While the instability, chimerism, and purification difficulties of YACs makes them less than ideal for precise sequencing projects, the well-characterized mechanisms of YAC modification make them more tractable for transgene studies involving targeted mutations and/or marker addition (reviewed in (458)). The large size of BACs and PACs makes standard subcloning techniques used to modify small plasmids unfeasible. However, the advent of recombineering, modification techniques based on homologous recombination in the *E.coli* host, has made BACs and PACs more tractable for transgenesis and gene modification (reviewed in (458-460)).

The homologous recombination system most commonly employed by *E.coli* is the RecBCD pathway (reviewed in (461)). In this pathway, RecBCD binds to double-stranded DNA breaks and creates 3' ssDNA overhangs via its nuclease and helicase activity. RecA then coats the ssDNA overhang, rendering it competent for homologous pairing and strand invasion. Once the Holliday junction is formed, either the RuvAB complex or RecG binds to it and induces branch migration, followed by RuvC dimer binding and Holliday junction resolution. The efficiency of RecBCD-mediated homologous recombination is stimulated by the recognition of chi (χ) sites (5'GCTGGTGG-3') by RecBCD; recognition of χ sites causes RecBCD to pause, lose some of its nuclease activity, and stimulate RecA binding. A second homologous recombination system used by *E.coli*, the RecF system, is able to stimulate recombination in *recBC* mutants, although its efficiency is approximately 100-fold lower than the RecBCD pathway (reviewed in (461)). The RecF pathway relies on RecQ to unwind the

DNA; RecJ to generate the 3' ssDNA tail; RecO, RecR, and RecF to stimulate the binding of RecA to the ssDNA tail; RuvAB or RecG to induce branch migration; and RuvC for resolution.

Due to the fact that DH10B, the native host strain for BACs and PACs is *recA*$^-$ (270), the homologous recombination machinery required for recombineering must be provided in *trans*. One such technique is based on a previously published method for creating *E.coli* chromosomal deletions and gene replacements (462;463). In this method, a temperature-sensitive shuttle vector containing the gene of interest surrounded by homology arms of at least 500 bp in length, the wild-type *recA* gene, and a tetracycline resistance marker is transferred to bacteria containing a BAC of interest. Following two homologous recombination events (co-integration followed by resolution), the desired BAC modification is created. Published improvements to this technique include counterselection using less toxic systems based on the *rpsL* and *sacB* genes and shuttle vectors with a non-temperature-sensitive origin of replication (464;465).

The reliance of the above methods on two homologous recombination events requires extensive selection and screening processes to identify correctly modified clones. To circumvent this problem, Jessen et al. developed a method utilizing the ability of χ sites located near the ends of linear DNA fragments to stimulate homologous recombination (466). In this case, instead of providing *recA* in *trans*, the BAC is transferred to the *rec*$^+$ MC1061 bacteria strain, and targeting is performed by introducing a linear piece of DNA containing three χ sites on each end of a fusion of green fluorescent protein (GFP) and the kanamycin resistance-conferring neomycin phosphotransferase gene (*kana*) surrounded by homology arms. Correctly modified clones are formed in one recombination step and are selected for by gain of kanamycin resistance. Because this method requires the integration of *kana*, it is not useful for creating precise deletions or point mutations. To use this system for creating such mutations in PACs, Nistala and Sigmund designed the linear, χ-flanked DNA to contain a *lox511*-flanked chloramphenicol resistance-conferring gene (*cam*) between the homology arms (467). The initial recombination reaction is carried out in MC1016 bacteria harboring a PAC, and integrants are selected by chloramphenicol resistance. To induce the loss of *cam*, the PAC is transferred to Cre-expressing BS591 bacteria; clones that

have undergone Cre/*lox* recombination are selected for their maintenance of kanamycin resistance and loss of chloramphenicol resistance. This method is useful, but does have several drawbacks. First of all, it is not able to be used on BACs without modification as most BAC vectors already contain *cam* (270). Secondly, the use of *lox511* sites precludes the use of later generation BAC vectors, such as pBACe3.6 and pTARBAC1, as they already contain *lox511* sites (271;272). Finally, this system involves three, somewhat cumbersome, transfer steps: 1) from the native, *recA*- DH10B strain to the *rec*+ MC1061 strain, 2) from the *rec*+ MC1061 strain to the Cre-containing BS591 strain, and 3) from the Cre-containing BS591 strain to the *recA*- DH10B strain.

The aforementioned homologous recombination techniques rely on the host recombination machinery and require lengthy homology arms for efficient modification. The Stewart group set out to identify a system in *E.coli* that was capable of mediating homologous recombination between circular DNA and a linear fragment containing homology arms of only 42 bp (468). Homologous recombination between the linear DNA and circular plasmid was only detected in *sbcA*$^-$ strains of bacteria. It was already known that mutations in *sbcA* resulted in the activation of the *recE* and *recT* genes of the cryptic Rac prophage present in *E.coli* strain K12 and that RecE, a 5'-3' exonuclease, and RecT, a DNA annealing protein, were capable of mediating homologous recombination independent of RecA, RecBCD, and RecF (469). To use "ET-recombination" in strains that do not harbor the Rac prophage, which includes the BAC host DH10B, the plasmid pBAD-ETγ was developed. pBAD-ETγ features *recE* under control of the L-arabinose-inducible P_{BAD} promoter, *recT* under control of the constitutive EM7 promoter, and the λ phage *redγ* gene (*gam*) under control of EM7. (The inclusion of *gam* is necessary to prevent degradation of linear DNA fragments by RecBCD (470).) One year later, the Stewart group reported an improvement in specific recombination efficiency (1-3 fold) over their previous system by the creation of a new ET plasmid, pBAD-αβγ (471). In pBAD-αβγ, the λ phage *exo* (*redα*) and *bet* (*redβ*) genes replaced the Rac prophage *recE* and *recT* genes. As was the case with pBAD-ETγ, the exonuclease gene (*exo*) was placed under control of the P_{BAD} promoter and the ssDNA annealing protein gene (*bet*) was placed under control of the constitutive EM7 promoter; *gam* remained under constitutive control as well, but in this case was driven by the Tn5 promoter. A derivative of pBAD-

αβγ is pBAD-RedGam, which contains a *redβ/redα* fusion gene under control of the P_{BAD} promoter and *gam* under control of the constitutive EM7 promoter. A third ET-recombination system was published by the Stewart group in 2000 (472). This system relies on two rounds of ET recombination to create point mutations in a gene of interest. The first step involves the placement of a positive/negative selection cassette (*neo/sacB*) at the site of interest, selected for by the gain of kanamycin sensitivity, while the second step involves the replacement of the selection cassette with the mutation of interest, selected for by the loss of *sacB* sensitivity. Most recently, the Stewart group published a paper indicating that low-copy induction of RecA in *trans* with the ET vectors further increases the recombination efficiency (473).

In addition to the Stewart group, the Ioannou group has been very active in creating ET modification techniques. Ioannou uses a modified form of ET modification, which they call GET recombination, to modify BACs and PACs in the native DH10B host. In GET recombination, the recombinogenic plasmids (pGETrec series of vectors) express the three λ phage Red recombination genes (*exo, bet,* and *gam*) under control of the L-arabinose-inducible P_{BAD} promoter (474). The tight control over *exo*, *bet*, and *gam* allows recombination to be mediated in the native DH10B host without affecting cell viability or recombination efficiency.

The Copeland and Court groups took a slightly different approach to using homologous recombination for BAC modification. Instead of using plasmids to provide the necessary recombination machinery, they integrated a defective λ prophage into the genome of *E.coli* strain ZH1141 (475). The integrated prophage contains an intact p_L operon under control of the temperature-sensitive λ cI-repressor (*cI857*), as well as a deletion of the right arm of the prophage from the *cro* through *bioA* genes. Deletion of the Cro-repressor gene *cro* permits the expression of *exo*, *bet*, and *gam* upon inactivation of the cI-repressor by incubation at 42˚C. Furthermore, deletion of genes between *cro* and *bioA* removes the λ phage lytic genes, permitting stable propagation of the host bacteria at the permissive temperature of 32˚C. In their initial publication, Yu et al. used this system to create point mutations and gene replacements in the endogenous bacterial *galK* gene with homologies as small as 40 bp and activation of *exo*, *bet*, and *gam* for only 7.5 minutes (475). As the λ phage-integrated strains created from ZH1141 could not be

transformed with BACs, the DY380 strain was created by transferring the defective λ prophage to the BAC-permissive strain DH10B (415). DY380 was further modified by inserting *araC*-P_{BAD}*flpe* and *araC*-P_{BAD}*cre* cassettes to create strains EL250 and EL350, respectively. The EL250 and EL350 strains are able to produce FLPe and Cre recombinase upon addition of L-arabinose to the culture, making the system more flexible and able to support additional BAC modifications. As proof of principle, Lee et al. used the EL250 bacterial strain to insert a cassette containing an eGFP/Cre fusion gene and *kana* surrounded by FRT sites (eGFPcre-FRT-kan-FRT) into the mouse *Eno2* locus of a BAC; this insertion was followed by excision of *kana* by arabinose induction of FLPe (415).

Even though the use of EL250 and EL350 strains permits the excision of selectable markers, a FRT or *lox* footprint is still left behind. While these short sequences have not been reported to affect gene expression, methods to create precise deletions and point mutations without any additional changes have been created. One method utilizes short oligonucleotides as the targeting sequence and PCR screening to identify correct recombinants (476). While effective, the lack of a selectable marker makes this method somewhat cumbersome. Another method to create seamless mutations uses two recombineering steps and is based on the ability to both select for and against the endogenous *E.coli galK* gene (477). The bacterial strains SW102, SW105, and SW106 were created from the DY380, EL250, and EL350 strains, respectively, and contain a full-length galactose operon with a mutation in the *galK* gene that prevents the bacteria from using galactose as a carbon source. The first recombineering step corrects this defect by providing *galK* in *trans* upon its integration into the BAC and is selected for by the ability of the bacteria to grow in galactose minimal media. In the second recombineering step, *galK* is replaced by the mutation of interest, resulting in a reversion to galactose sensitivity; those cells that have lost the *galK* gene are selected by addition of glycerol and the galactose analog 2-deoxy-galactose (DOG). The utility of recombineering using the integrated λ phage system is illustrated by the numerous modifications created using the DY380, EL250, and EL350 cell lines. These modifications include reporter construct insertions (297;478), gene deletions (479;480), gene insertions (481;482), and point mutations (483;484). These bacteria strains have

also been used to modify the endogenous *E.coli* chromosome (477) and λ phage itself (485). Additionally, a mini-λ plasmid was created that could be reversibly integrated in any bacteria host to provide homologous recombination capabilities (486).

The ability to easily modify BACs makes them increasingly useful in gene regulation studies. One gene that would benefit from study in a BAC system is human telomerase. Despite almost 25 years of intense study, the exact mechanisms of h*TERT* regulation remain largely unknown. Part of the problem in studying h*TERT* is that transiently-transfected, plasmid-based reporter constructs bearing the h*TERT* promoter do not always faithfully reflect the endogenous telomerase activity (224;234;240). This inability to mimic endogenous expression could be due to the fact that critical regulatory elements are missing from the constructs or because appropriate h*TERT* regulation requires chromatin formation, which transiently-transfected plasmids cannot re-create. The use of BACs would aid in addressing both problems as BACs are larger and would therefore be more likely to contain upstream and downstream regulatory elements and be able to be incorporated into a native chromatin state upon integration into the host cell genome. In this chapter, the creation of BAC-based reporters for human telomerase activity is reported. The reporters were constructed by inserting the firefly and *Renilla reniformis* luciferase open reading frames (ORFs), the puromycin resistance gene, and dual-copy cHS4 insulators into the *TERT*-containing human BAC 117B23 using the DY380 and EL350 strains of bacteria.

3.2 Materials and Methods

3.2.1 Receipt and Verification of RPCI-11.c 117B23

The human *TERT*-containing BAC RPCI-11.c 117B23 (referred to throughout as 117B23) was purchased from Research Genetics and arrived as an agar stab of DH10B bacteria. Bacteria were streaked on LB agar plates containing 12.5 µg/ml chloramphenicol and grown at 37˚C. Individual colonies were picked and seeded in 5 ml LB broth containing 12.5 µg/ml chloramphenicol and grown at 37˚C with shaking. After approximately 18 hours of growth, DNA was prepared using a standard alkaline lysis procedure. Briefly, bacteria were separated from the LB by centrifugation and then resuspended in buffer P1 (50 mM Tris/10 mM EDTA) supplemented with 0.1 mg/ml RNase. Following lysis with an equal volume of buffer P2 (0.2 N NaOH/1% SDS), the protein was precipitated with an equal volume of ice-cold buffer P3 (3 M K/5M acetate). The DNA was precipitated with isopropanol, washed in 70% ethanol, and resuspended in 50 µl TE, pH 8.0. During the isolation procedure, care was taken to avoid shearing of the DNA. The identity and integrity of the BAC was verified by agarose gel electrophoresis after restriction endonuclease digestion with *Bam*HI. PCR was also used to verify BAC integrity (see Tables 3.1 and 3.2 for primers used). Glycerol stocks were prepared for the verified BAC by combining equal volumes of bacteria culture and 30% glycerol; all glycerol stocks were maintained at -80˚C. Large-scale BAC preparations were prepared from 300-500 ml of LB culture using the GenoPure Maxi Kit (Roche) with the manufacturer's recommended modification for low copy-number plasmids.

3.2.2 Creation of *CRR9* Modification Plasmid TOPO MutCRR9

In order to facilitate the insertion of reporter genes and selection cassettes at the CRR9 translational start site, PCR-based mutagenesis was performed to create restriction endonuclease recognition sites in place of the ATG start codon. The PCR-based mutagenesis scheme relied on three different PCR amplifications (Figure 3.1). The first amplification utilized one primer of 20 nt that exactly matched the sequence located ~300

bp upstream of the ATG start codon (primer CRR9.F1) and a second primer that contained 12 nt homologous to the sequence immediately upstream of the ATG start codon, 15 nt of sequence that introduced the *Hind*III and *Bgl*II recognition sites, and 11 nt homologous to the sequence immediately downstream of ATG (primer MutCRR9.R1). The second amplification utilized the complement of primer MutCRR9.R1 (MutCRR9.F1) and primer CRR9.R1, which consisted of 18 nt that exactly matched the sequence located ~300 bp downstream of the ATG start codon. Following the successful amplification and purification of these two PCR products, a third PCR reaction was performed using the products of the first two amplifications as the template and the primer pair CRR9.F1/CRR9.R1. Initial PCR amplification was performed on 117B23 BAC DNA using two primer pairs, CRR9.F1/MutCRR9.R1 and MutCRR9.F1/CRR9.R1. (See Table 3.1 for primer sequences.) Amplification was performed using Herculase polymerase (Stratagene) and touchdown PCR, as follows:

1. 94˚C for 3 minutes
2. 94˚C for 1 minute
3. 65˚C for 1 minute
4. 72˚C for 2 minutes
5. 94˚C for 1 minute
6. 65˚C for 1 minute
7. 72˚C for 1 minute
8. To Step 5 28 times, decreasing step 6 by 0.5˚C each cycle (final = 51˚C)
9. 94˚C for 1 minute
10. 58˚C for 1 minute
11. 72˚C for 1 minute
12. To Step 9 24 times
13. 72˚C for 10 minutes
14. 4˚C for ∞

Products were isolated from four independent reactions per primer pair following agarose gel electrophoresis. These products were referred to as the 5' mutant half (product of primer pair CRR9.F1/MutCRR9.R1) and the 3' mutant half (product of primer pair MutCRR9.F1/CRR9.R1). To create the full-length mutated CRR9 region, PCR was performed using the 5' and 3' mutant halves as template, the primer pair CRR9.F1/CRR9.R1, Herculase polymerase, and touchdown PCR (as outlined above). Full-length products of 597 bp were isolated from four independent reactions.

The full-length mutant CRR9 product was cloned into pCR4Blunt-TOPO using the TOPO Cloning Kit (Invitrogen) according to the manufacturer's instructions. (TOPO cloning is a method to directly clone blunt-ended PCR products into an activated, linearized vector via vaccinia virus DNA topoisomerase I (487).) Plasmids with the PCR insert were identified by restriction endonuclease digestion with *Eco*RI and *Bgl*II/*Not*I and named TOPO-MutCRR9. To verify the integrity of the amplified DNA, sequencing with primers T3 (5'-ATTAACCCTCACTAAAGGGA-3') and T7 (5'-TAATACGACTCACTATAGGG-3') was performed on four independently isolated clones of TOPO-MutCRR9. To create a plasmid that did not contain any unintended mutations, the 331 bp fragment of TOPO-MutCRR9 clone #4 isolated after restriction endonuclease digestion with *Spe*I and *Hind*III was ligated to the 4,224 bp fragment of TOPO-MutCRR9 clone #40 isolated after digestion with *Spe*I and *Hind*III.

3.2.3 Creation of kana/rpsL$^{\pm}$ Selection Cassettes

A positive/negative selectable marker was created by inserting the wild type ribosomal protein S12 (*rpsL*) streptomycin gene in front of the *E.coli* aminoglycoside phosphotransferase gene (*aph*). *rpsL* expression results in streptomycin sensitivity and is referred to as *rpsL*$^{+}$; *aph* expression results in kanamycin resistance and is referred to as *kana*. gDNA was prepared from the DH5α strain of *E.coli* (Invitrogen). The *rpsL*$^{+}$ gene was isolated from gDNA by touchdown PCR amplification (see Section 3.2.2) using Herculase polymerase (Stratagene) and primers MAL23 (5'-GTTGCCATTAAATAGCTCCTGGTAGATCTAGG-3') and MAL24 (5'-GAAGCGTCCTAAGGCTTAATGGTAGATCTAG-3'); these primers introduced one *Bgl*II recognition site on each end of *rpsL*$^{+}$. Two independently isolated, 402 bp products were cloned into pCR4Blunt-TOPO using the TOPO Cloning Kit (Invitrogen) according to the manufacturer's instructions. Clones with the correct PCR product were verified by restriction endonuclease digestion with *Eco*RI and named pTOPO-rpsL^{+}. The *rpsL*$^{+}$ gene was excised from pTOPO-rpsL^{+} by restriction endonuclease digestion with *Bgl*II and inserted into pREP4 (Qiagen) linearized with *Bgl*II to create pREP4-rpsL^{+}. To ensure the appropriate transcription and translation of both *kana* and *rpsL*$^{+}$, *rpsL*$^{+}$ was inserted

upstream of the kana start codon but downstream of its transcriptional start site. pREP4-rpsL$^+$ was verified by restriction endonuclease digestion with *Hind*III/*Sph*I. To verify the functionality of the amplified *rpsL*$^+$ gene, pREP4-rpsL$^+$ was transferred to the DH10B strain of bacteria by electroporation, and subsequent kanamycin-resistant colonies of pREP4-rpsL$^+$ were spotted on LB/agar plates containing kanamycin at 50 μg/ml; kanamycin at 50 μg/ml and streptomycin at 10 μg/ml; and kanamycin at 50 μg/ml and streptomycin at 50 μg/ml. After 24 hours at 37˚C, colony growth was observed. To facilitate further sub-cloning, the 1.74 kb kanamycin/streptomycin cassette (kana/rpsL$^+$) was excised from pREP4-rpsL$^+$ with the restriction endonucleases *Hind*III and *Nru*I and inserted into pSK$^+$ (Stratagene) digested with *Sma*I and *Hind*III; this plasmid was named pSK$^+$kana-rpsL$^+$ and verified by restriction endonuclease digestion with *Hinc*II.

In order to place kana/rpsL$^+$ at the hTERT start codon, the 1.74 kb selection cassette was excised from pSK$^+$kana-rpsL$^+$ with *Xho*I/*Bam*HI and inserted into pYF2 digested with *Xho*I/*Bgl*II to create pYF2-mel; pYF2-mel was verified by restriction endonuclease digestion with *Pst*I. From pYF2-mel, a 2.3 kb fragment containing the kana/rpsL$^+$ cassette was excised with *Sac*II and inserted into pYF10 digested with the same. The resultant plasmid, pYF10-mel, was verified by restriction endonuclease digestion with *Hind*III/*Bgl*II. (pYF2 and pYF10 were created by Yan Fang and contain a mutated hTERT start codon (pYF2) and a firefly luciferase open reading frame inserted at the mutated hTERT start codon (pYF10).) To place the kana/rpsL$^+$ cassette at the CRR9 start codon, the 1.74 kb cassette was excised from pSK$^+$kana-rpsL$^+$ with *Hind*III/*Bam*HI and inserted into TOPO-MutCRR9 digested with *Hind*III/*Bgl*II; the resultant plasmid was named pML3-kana-rpsL$^+$ and verified by restriction endonuclease digestion with *Pst*I and *Alw*NI.

Plasmids containing kana/rpsL$^+$ flanked by DNA homologous to the sequence 5' of the *loxP* and 3' of the *lox511* sites of 117B23 were also prepared. The 1.76 kb fragment of pSK$^+$kana-rpsL$^+$ containing the selection cassette was transferred to pbsII-KS (Stratagene) by restriction endonuclease digestion of both plasmids with *Bam*HI/*Sal*I. The resultant plasmid, pKS-kana-rpsL$^+$, was verified by digestion with *Bam*HI/*Bgl*II and *Sal*I/*Bgl*II. To create the homology arms, oligos (Figures 3.2 and 3.3) containing the appropriate homologous sequence and 5' and 3' overhangs to allow for ligation into pKS-

kana-rpsL$^+$ were pre-annealed by heating to 95˚C in the presence of 1X oligo annealing buffer (10 mM Tris-HCl, pH 8.0, 1 mM EDTA, pH 8.0, 0.1 M NaCl) and slowly cooled to room temperature. A four-way ligation was performed to create a plasmid containing kana/rpsL$^+$ surrounded by homology arms to a region 3' of the *lox511* site by incubating the following fragments with T4 DNA ligase (NEB) overnight at 4˚C: (1) the 1.77 kb fragment of pKS-kana-rpsL$^+$ created by digestion with *Bam*HI/*Xho*I; (2) the 2.89 kb fragment of pbsII-KS created by digestion with *Spe*I/*Kpn*I; (3) the 5' *lox511* homology arm; (4) the 3' *lox511* homology arm. The resultant plasmid, pKS-kana-rpsL$^+$511, was verified by restriction endonuclease digestion with *Xho*I/*Pst*I/*Spe*I, *Bam*HI/*Pst*I, and *Kpn*I/*Pst*I. The same steps were followed to create pKS-kana-rpsL$^+$P, which contains kana/rpsL$^+$ surrounded by homology arms to a region 5' of the *loxP* site. (All kana/rpsL$^+$ plasmids can be found in Figures A3 and A4 of Appendix A.)

3.2.4 Creation of Luciferase Reporter Cassettes

To facilitate the future cloning of reporter cassettes into the start codons of hTERT and CRR9, the firefly and *Renilla reniformis* (referred to as *Renilla* throughout) luciferase open reading frames (ORFs) were subcloned into pSK$^+$. Initially, the *Xba*I restriction endonuclease recognition sites of pGL3-proΔ (modified version of pGL3 (Promega) created by Yan Fang) and pRL-SV40 (Promega) were destroyed by *Xba*I digestion, treatment with Klenow, and self-ligation. The resultant plasmids were named pGL3-proΔX and pRL-SV40ΔX, respectively, and verified by restriction endonuclease digestion with *Hind*III/*Xba*I. The luciferase ORFs were then excised from pGL3-proΔX (1.9 kb) and pRL-SV40ΔX (1.45 kb) with *Hind*III/*Bam*HI and inserted into pSK$^+$ digested with the same to form pSK$^+$FL and pSK$^+$RL, respectively; both plasmids were verified by restriction endonuclease digestion with *Hinc*II. pML-3, TOPO-MutCRR9 with the 1.45 kb *Renilla* luciferase ORF at the CRR9 start codon, was created by digesting pSK$^+$RL with *Hind*III/*Bam*HI and verified by restriction endonuclease digestion with *Eco*RI, *Ban*I, and *Pst*I. In order to place the firefly luciferase ORF at the start codon of CRR9, the 1.9 kb ORF was excised from pSK$^+$FL with *Hind*III/*Bam*HI and ligated to TOPO-MutCRR9 digested with *Bgl*II/*Hind*III. The resultant plasmid was named pML-4

and verified by restriction endonuclease digestion with *Eco*RI. To place the *Renilla* ORF at the hTERT start codon, pYF2 was digested with *Bgl*II and *Xho*I and ligated to the 1.45 kb *Renilla* luciferase ORF isolated after digesting pSK$^+$RL with *Bam*HI/*Xho*I. This plasmid was named pML-2Renilla and verified by restriction endonuclease digestion with *Eco*RI. To create pYF10Renilla, pYF10 was digested with *Sac*II and ligated to the 2.3 kb fragment of pML-2Renilla created by digestion with the same; pYF10Renilla was verified by restriction endonuclease digestion with *Eco*RI/*Xho*I. (All luciferase plasmids can be found in Figures A3 and A5 of Appendix A.)

3.2.5 Creation of *puro* cassettes

Cassettes containing the puromycin resistance-conferring puromcyin N-acetyl transferase gene (*puro*) were constructed in order to provide 117B23 with a positively selectable marker. The plasmid pIGCNpuroII was made by inserting the 1.63 kb mouse phosphoglycerate kinase (mPGK) promoter-driven puromycin cassette, isolated from pLZRSΔSspI+42bp by *Bsp*HI/*Cla*I restriction endonuclease digestion followed by Klenow treatment, into pIGCN21 (415) linearized with *Sma*I and treated with CIP (NEB). Verification of pIGCNpuroII was achieved by restriction endonuclease digestion with *Pst*I. SV40 promoter-driven *puro* was also cloned into pIGCN21, creating pIGCNpuroIII. pIGCNpuroIII was constructed by inserting the 503 bp fragment of pBABEpuroΔ (488) isolated by digestion with *Eco*RI/*Bst*EII into pIGCNpuroII digested with the same, then verified by restriction endonuclease digestion with *Xho*I/*Pvu*II, *Eco*RI/*Pvu*II, and *Eco*RI/*Bst*EII. As pIGCN-based plasmids do not yield large amounts of DNA upon plasmid preparation, the SV40-driven *puro* cassette was removed from pIGCNpuroIII by digestion with *Apa*I/*Sac*I (3.3 kb) and inserted into pSK$^+$ digested with the same. The resultant plasmid, pSK$^+$puroIII, was verified by restriction endonuclease digestion with *Pvu*II and *Apa*I/*Sac*I. A cassette consisting of a fusion of *puro* and the *Renilla* luciferase ORF driven by the *CRR9* promoter (puroRL) was also created. To insert the puroRL at the translational start codon of CRR9, pQCXIX-puroRenilla (created by Joy Ort and harboring an mPGK-driven fusion of *puro* and *Renilla* luciferase) was digested with the restriction endonucleases *Bam*HI/*Pvu*II; following treatment with

Klenow, this 2.9 kb fragment was ligated to pSK$^+$mutCRR9 linearized with *Hind*III and treated with Klenow. The resultant plasmid was named pSK$^+$CRR9puroRL and verified by restriction endonuclease digestion with *Pst*I/*Xba*I. (All *puro* plasmids can be found in Table A6.)

3.2.6 Creation of Dual-Copy cHS4 Cassettes

Plasmids were created to insert two directly repeated copies of the chicken β-globin insulator (cHS4) at either end of 117B23 clones upon linearization with the homing endonuclease PI-*Sce*I. The 2.4 kb fragment containing the dual-copy insulators was removed from pJC13-1 (18) with *Bam*HI/*Sal*I and inserted into pbsII-KS digested with the same to create pKS-2XIns. pKS-2XIns was verified by restriction endonuclease digestion with *Bam*HI/*Bgl*II and *Sal*I/*Bgl*II. To create a plasmid containing homology arms for insertion 3' of the *lox511* site, a four-way ligation was performed with the following fragments: 1) the 2.89 kb fragment of pbsII-KS isolated after restriction endonuclease digestion with *Spe*I/*Kpn*I; 2) the 1.77 kb fragment of pKS-2XIns created by digestion with *Bam*HI/*Xho*I; 3) the 5' *lox511* homology arm (Figure 3.2A); 4) the 3' *lox511* homology arm (Figure 3.2B). The resultant plasmid, pKS-2XIns511 was verified by restriction endonuclease digestion with *Spe*I/*Hind*III, *Bgl*II, *Bgl*II/*Spe*I, *Bgl*II/*Kpn*I, *Bgl*II/*Xho*I, and *Bgl*II/*Bam*HI. A similar plasmid, pKS-2XInsP, was created to contain homology arms for insulator insertion 5' of the *loxP* site. All fragments were the same as those used for pKS-2XIns511 construction except that the 5' and 3' *lox511* homology arms were replaced by the 5' and 3' *loxP* arms (Figure 3.3); verification employed the same set of restriction endonuclease digestions. (All dual-copy insulator plasmids can be found in Figure A9 of Appendix A).

3.2.7 2-Step Recombineering Technique to Introduce Luciferase Reporters and Dual-Copy Insulators to the BAC

The recombineering-competent bacteria strain DY380 (475) was received as an agar stab from the Copeland laboratory at the National Cancer Institute, Frederick, MD.

(The Copeland Group was the kind providers of the bacterial strains DY380, EL250, and EL350 and the plasmid pIGCN21.) The bacteria were amplified in LB media (no antibiotic) at 32˚C and glycerol stocks prepared as above. Electrocompetent bacteria were prepared by growing a liquid culture at 32˚C until the bacteria were in log-phase growth, as determined by the absorbance at a wavelength of 600 nm (A_{600}) reaching between 0.5 and 0.6 OD. Following three washes in 0.2X volumes of ice-cold 10% glycerol, the bacteria were resuspended in 0.01X volumes of ice-cold 10% glycerol, aliquotted into microfuge tubes (50 µl each), snap-frozen in liquid nitrogen, and stored at -80˚C. 117B23 DNA was transferred to electrocompetent DY380 bacteria by electroporation using a 0.1 cm gap cuvette and a BTX ECM-600 electroporator (Harvard Apparatus) set to high voltage mode at 1.75 kV and 189 Ω resistance. Immediately following electroporation, the bacteria were transferred to a 10X volume of SOC medium (20 g/L bacto-tryptone, 5 g/L bacto-yeast extract, 0.5 g/L NaCl, 2.5 mM KCl, 10 mM $MgCl_2$, 20 mM glucose, pH 7.0), recovered at 32˚C with shaking for one hour, plated on LB/agar plates supplemented with 12.5 µg/ml chloramphenicol, and incubated overnight at 32˚C to allow for colony formation. BAC DNA was prepared using alkaline lysis (see Section 3.2.1), and its integrity upon transfer was verified by restriction endonuclease digestion followed by agarose gel electrophoresis. Glycerol stocks of 117B23 in DY380 were prepared and stored at -80˚C.

The DNA cassettes used for recombineering were isolated from 12-15 µg of plasmid DNA by restriction endonuclease digestion. (For a list of the isolated fragments used for recombineering, see Table 3.4.) Following agarose gel electrophoresis, during which the digested DNA was split equally between 12 lanes of a thin agarose gel, the desired fragment was purified using a modified version of the QiaexII protocol, as follows. The twelve individual fragments were split between three microfuge tubes, followed by the addition of the recommended volume of buffer QX1 and 10 µl of resin to each tube. When the agarose was completely melted, the resin in each tube was washed once with 1,000 ml buffer QX1 and twice with 1,000 µl buffer PE. For the third wash, the resin from all three tubes was combined with 1,000 µl PE. The DNA was eluted from the resin by incubating with 10 µl of sterile deionized water for 10 minutes at 50˚C. The concentration of the fragment was measured on a 1:200 dilution and the fragment stored

at -20˚C.

The first step of the two-step recombineering process was to place the kana/rpsL$^+$ cassette at the locus of interest (Figure 3.4). One milliliter of a 5 ml overnight culture of DY380 bacteria harboring the BAC was diluted in 50 ml LB medium containing no antibiotics and grown at 32˚C with shaking for about 3.5-4.0 hours, or when the A_{600} of the culture reached between 0.5 and 0.6 OD. At this point, the homologous recombination machinery was induced by incubating the culture for 15 minutes in a shaking water bath set to 42˚C. Immediately following the 15 minute incubation, the culture was cooled in an ice/water slurry. The bacteria were washed three times with 10 ml ice-cold 10% glycerol, taking care to move as quickly as possible and keeping the bacteria on ice or at 4˚C. Following the glycerol washes, the bacteria were resuspended in 400 µl ice-cold 10% glycerol. For the actual recombineering, 50 µl of induced bacteria were mixed with 1 µl of the purified kana/rpsL$^+$ cassette, transferred to a pre-chilled 0.1 cm gap electroporation cuvette, and electroporated at the conditions outlined above (1.75 kV and 189 Ω). Immediately following electroporation, the bacteria were transferred to 1 ml of SOC and recovered for 1 hour at 32˚C with shaking. After recovery, 20 and 50 µl of concentrated bacteria were plated on LB/agar plates supplemented with 20 µg/ml kanamycin to select for the BACs that took up the kana/rpsL$^+$ cassette. Additionally, 10 µl of a 10^{-4} dilution of bacteria were spread on LB/agar plates supplemented with 12.5 µg/ml chloramphenicol to determine the overall number of bacteria that survived electroporation. Unplated bacteria were stored at 4˚C for at least 24 hours following recovery. The plates were incubated at 32˚C with colony formation becoming visible after approximately 16 hours. To verify those BAC clones that underwent correct homologous recombination, individual colonies were seeded in 5 ml LB medium supplemented with both 12.5 µg/ml chloramphenicol and 20 µg/ml kanamycin and grown overnight at 32˚C with shaking. DNA was prepared by alkaline lysis and digested with appropriate restriction endonucleases. The digestion pattern of the suspected homologous recombinants was compared to the pattern of the parental BAC to verify correct recombinants. Correctly modified BACs were transferred to the DH10B bacterial strain by electroporation as outlined above; glycerol stocks were prepared for the modified BAC in both DY380 and DH10B bacteria.

The second step of the two-step recombineering process was to replace the kana/rpsL$^+$ cassette with the appropriate luciferase cassette (Figure 3.4). A 5 ml overnight LB culture, supplemented with 20 µg/ml kanamycin, was seeded with bacteria from a freshly streaked colony of the modified BAC and grown overnight at 32˚C with shaking. One milliliter of this culture was induced and electroporated as outlined above. Following the one hour recovery period, 10 µl of a 10^{-4} dilution of bacteria were spread on LB/agar plates supplemented with 12.5 µg/ml chloramphenicol to determine the overall number of bacteria that survived electroporation, while 100 µl of a 1:25 dilution was plated on LB/agar supplemented with 12.5 µg/ml chloramphenicol and 1 mg/ml streptomycin to select for bacteria harboring BACs that lost the kana/rpsL$^+$ cassette. To enrich the culture for streptomycin-resistant bacteria, the bacteria were diluted 1:50 in 2 ml LB media supplemented with 1 mg/ml streptomycin and grown at 32˚C with shaking. After two to three hours, 100 µl of this culture was spread on LB/agar plates supplemented with 12.5 µg/ml chloramphenicol and 1 mg/ml streptomycin. Unplated bacteria were stored at 4˚C for at least 24 hours following recovery. All plates were incubated at 32˚C for at least 24 hours. To identify those colonies that underwent homologous recombination, resulting in the replacement of the kana/rpsL$^+$ cassette with the luciferase cassette, whole-cell PCR was performed with primer pairs specific for the desired homologous recombination event. (For a list of primer pairs, see Tables 3.5 and 3.6.) Whole-cell PCR was performed by aliquotting 10 µl of a master cocktail (containing 1X PCR buffer (supplied with Taq), an empirically determined concentration of $MgCl_2$, 0.2 mM dNTPs, 0.2 µM primers, and 0.5 U Taq polymerase (NEB or Promega)) into individual PCR tubes. The mixture was gently pipetted up and down with a standard 1-200 µl pipet tip touched to a bacteria colony; the tip was then ejected into 0.5 ml of LB medium. Following amplification (94˚C for 5 minutes, 30-35 cycles of 94˚C for 30 seconds, 60˚C for 30 seconds, 72˚C for 1 minute, and 72˚C for 5 minutes), 3 µl of the product was electrophoresed through 1.0-2.0% agarose prepared in 0.5X TBE. The cultures corresponding to any correct PCR products were brought up to 5 ml total volume with LB, supplemented with 12.5 µg/ml chloramphenicol, and grown overnight at 32˚C with shaking. These pre-screened clones were further tested by restriction endonuclease digestion after DNA preparation by alkaline lysis. Correctly modified

BAC clones were transferred by electroporation to the DH10B bacterial strain. Glycerol stocks were prepared for BACs in both the DY380 and DH10B strains.

3.2.8 Introduction of *puro* to BAC Using FLPe Recombinase

To modify BACs to express the puromycin resistance gene, one round of recombineering was performed and followed by FLP/FRT-mediated recombination (Figure 3.5). The BAC to be modified was transferred to the EL250 bacteria strain (415) via electroporation using the previously identified conditions. One milliliter of a 5 ml overnight culture of EL250 bacteria harboring the BAC was induced as outlined above for the first step of the 2-step recombineering process. After recovery, 10 µl of a 10^{-4} dilution of bacteria were spread on LB/agar plates supplemented with 12.5 µg/ml chloramphenicol to determine the overall number of bacteria that survived electroporation, while 25 µl of concentrated bacteria were plated on LB/agar plates supplemented with 20 µg/ml kanamycin to select for the BACs that took up the puro/FRT/kana/FRT cassette (see Table 3.4); unplated bacteria were stored at 4˚C for at least 24 hours following recovery. The plates were incubated at 32˚C with colony formation becoming visible after about 16 hours. To verify BAC clones that underwent correct homologous recombination, individual colonies were seeded in 5 ml LB medium supplemented with both 12.5 µg/ml chloramphenicol and 20 µg/ml kanamycin and grown overnight at 32˚C with shaking. DNA was prepared by alkaline lysis and digested with appropriate restriction endonucleases. The digestion pattern of the suspected homologous recombinants was compared to the pattern of the parental BAC to verify those that were correct. In order to remove *kana* from the BAC, a 5 ml LB culture, supplemented with 12.5 µg/ml chloramphenicol and 20 µg/ml kanamycin, was seeded. After overnight growth, 40 µl of this culture was seeded in 2 ml plain LB (1:50 dilution) and grown for 3.5 hours at 32˚C with shaking. At this point, two 1:10 dilutions (total volume 1 ml) were prepared, one with 0.1% L-arabinose and one without. After an additional two hours of growth at 32˚C, 20 µl of 10^{-4} dilutions of each culture were plated on LB/agar plates supplemented with 12.5 µg/ml chloramphenicol and LB/agar plates supplemented with 20 µg/ml kanamycin. After overnight incubation at 32˚C, colony

growth between the LB plates was compared. To verify the loss of *kana*, colonies from the LB/agar plate supplemented with chloramphenicol and plated with bacteria grown in the presence of arabinose were seeded in 5 ml LB supplemented with 12.5 µg/ml chloramphenicol and grown overnight at 32˚C with shaking; DNA was prepared by alkaline lysis and analyzed by restriction endonuclease digestion. Correctly modified BACs were transferred to the DH10B strain of bacteria by electroporation, and glycerol stocks were prepared for BACs in both the DH10B and EL250 strains.

3.2.9 Modification of BAC Vectors

In order to obtain the BAC vector pBACe3.6 (271), 117B23 was digested with the restriction endonuclease *Eco*RI. Following heat inactivation, self-ligation was performed. Correct self-ligations of the vector backbone were verified by restriction endonuclease digestion with *Hind*III/*Bgl*II. The self-ligated product was referred to as pBACe3.6Δstuffer as it did not contain the pUC19 stuffer fragment found in the version of pBACe3.6 available from Research Genetics. Due to the low-copy nature of pBACe3.6Δstuffer, midi preps of this plasmid were prepared using the QiaSpin Midi Kit with the modified low-copy protocol provided by Qiagen. To introduce the pUC stuffer to the re-created BAC vector, pBACe3.6Δstuffer was linearized with *Bam*HI and ligated to the 2.8 kb pUC stuffer fragment isolated by *Bam*HI digestion of a second BAC vector, pTARBAC1 ((272;489); purchased from Research Genetics). The resultant plasmid was named pBACe3.6pUC and verified by restriction endonuclease digestion with *Bam*HI.

pBACe3.6pUC was modified to express either mPGK- or SV40-driven *puro*. To create a BAC vector expressing mPGK-driven *puro*, the 3.4 kb fragment of pIGCNpuroII created by *Sfi*I restriction endonuclease digestion and Klenow treatment was inserted into pBACe3.6pUC linearized with *Sfo*I and treated with CIP. This plasmid was termed pBACe3.6puroFKFpUC and verified by restriction endonuclease digestion with *Pst*I. The SV40 promoter-driven *puro* cassette was introduced to the BAC vector by recombineering in bacterial strain EL250, as outlined in section 3.2.8. To create a plasmid to accept the incoming fragment, pBACepuroFKFpUC was digested with the restriction endonuclease *Rsr*II and self-ligated to create pBACe3.6puroFΔKpUC; this

plasmid was verified by restriction endonuclease digestion with *Hind*III and *Bam*HI. To create a plasmid containing the homology arms necessary for homologous recombination, the 3.7 kb fragment of pBACe3.6puroFKFpUC, created by digestion with *Kpn*I, was inserted into pSK^{+}puroIII digested with *Kpn*I and treated with CIP; the resultant plasmid was termed pSK^{+}puroIIISacB and verified by restriction endonuclease digestion with *Pst*I and *Hinc*II. Following recombineering, the loss of the kanamycin cassette, and thus the creation of pBACeSVpuro, was verified by *Eco*RI restriction endonuclease digestion of DNA prepared from chloramphenicol-resistant colonies.

pTARBAC1 (272;489) was modified to express puroRL. A 3.7 kb DNA fragment containing the *CRR9* promoter-driven *puro*/*Renilla* fusion gene was excised from pSK^{+}CRR9puroRL by restriction endonuclease digestion with *Pvu*II/*Spe*I and inserted into pTARBAC1 digested with *Pml*I/*Nhe*I. The resultant plasmid, pTARpuroRL, was verified by restriction endonuclease digestion with *Pst*I and *Eco*RI. pTARBAC1 was also modified to express mPGK-driven *puro*. An intermediate plasmid, pUC19SacB, was created by excising the 3.7 kb fragment containing the *sacB* gene from pTARBAC1 created by digestion with *Aat*II/*Nhe*I and transferring it to pUC19M digested with *Aat*II/*Xba*I. Next, the 2.5 kb fragment of pLZRSΔSspI+42bp, isolated by restriction endonuclease digestion with *Cla*I/*Bam*HI, was inserted into pUC19SacB digested with the same to create pUC19puroSacB. Finally, the unmodified *sacB* gene of pTARBAC1 was removed by restriction digestion with *Sfi*I/*Bam*HI and replaced with the *sacB* gene harboring mPGK-driven *puro*, which was isolated from pUC19puroSacB by digestion with the same. The final BAC vector expressing *puro* from within *sacB* was named pTARpuroSacB and verified by restriction endonuclease digestion with *Hind*III and *Hinc*II. (All BAC vector modification plasmids can be found in Figures A7 and A8 of Appendix A).

3.3 Results

3.3.1 Identification, Receipt, and Verification of RPCI-11.c 117B23

A search of the University of California Santa Cruz (UCSC) Genome Browser (490) for the human telomerase gene led to the identification of the BAC clone 117B23. Clone 117B23 is part of the RPCI-11 BAC library and contains ~162 kb of genomic DNA from chromosome 5 inserted into the BAC vector pBACe3.6 by partial digestion with the restriction endonuclease *Eco*RI (489). Within 117B23 are the entire *TERT*, *CRR9* and *SLC6A18* coding regions, as well as a part of the *SLC6A19* gene (Figure 3.6). As can be seen in Figure 3.7A, screening of six 117B23 colonies by restriction endonuclease digestion with *Bam*HI revealed that five of the six clones (1, 3, 4, 5, and 6) displayed a digestion pattern similar to the expected. The sixth clone, B2, was missing a fragment at approximately 9 kb, and therefore, was not used in any further studies. PCR amplification was also performed to verify the integrity of the BAC (Tables 3.1 and 3.2 and Figure 3.7B). Successful amplification of regions within the second intron of *TERT*, within the intergenic region between *CRR9* and *TERT*, upstream of *CRR9*, and downstream of *TERT* verified the integrity of 117B23.

3.3.2 Mutation of CRR9 Start Codon and Creation of *CRR9* Homology Arms

The result of the PCR-based mutagenesis scheme was a DNA fragment containing two 300 bp arms homologous to *CRR9* surrounding the *Hind*III and *Bgl*II restriction endonuclease recognition sites (Figure 3.1B). To allow for the cloning of selection and reporter cassettes into the *Hind*III and *Bgl*II restriction endonuclease recognition sites, and subsequent amplification of such products, the plasmid TOPO-MutCRR9 was created by TOPO cloning of the full-length PCR product into pCR4Blunt-TOPO. TOPO-MutCRR9 clones 4, 5, 16, and 44 were sequenced with primers T3 and T7 to check the integrity of the fragment after PCR amplification and cloning. Upon comparison of sequencing results and the sequence found in the human genome database, many errors were revealed in all four clones even though Herculase polymerase is touted

as high-fidelity. As clone 4 did not contain any errors in the first half of the product and clone 40 did not contain any errors in the second half of the product, subcloning between these two clones was performed to create a full-length, mutated CRR9 fragment without any unintended errors. After ligating the non-mutated halves of clones 4 and 40, a copy of TOPO-MutCRR9 was created that did not contain any unintended mutations. This plasmid, referred to throughout as TOPO-MutCRR9, was used as the basis of all *CRR9* recombineering fragments.

3.3.3 Recombineering Cassettes

The creation of kana/rpsL$^+$ selection cassettes for each desired BAC modification was necessary to perform the two-step recombineering procedure. Insertion of *rpsL*$^+$ upstream of *kana* did not destroy the ability of *kana* to confer resistance to kanamycin as bacteria (strain DH5α) containing pREP4-rpsL$^+$ were able to grow in its presence. Transfer of pREP4-rpsL$^+$ to the streptomycin-sensitive DH10B bacterial strain and its subsequent growth in the presence of streptomycin verified that *rpsL*$^+$ was also functional upon insertion into pREP4. Four kana/rpsL$^+$ selection cassettes were necessary for completing the desired BAC modifications. To ease the isolation of these cassettes, plasmids containing kana/rpsL$^+$ surrounded by appropriate homology arms were created for the *CRR9* locus (pML3-kana-rpsL$^+$), the *TERT* locus (pYF10- kana-rpsL$^+$), the region immediately downstream of the *lox511* site (pKS-kana-rpsL$^+$511), and the region 250 bp upstream of the *loxP* site (pKS-kana-rpsL$^+$P). Similar plasmids were created for the FL and RL ORFs; these are pYF10-mel (RL at *TERT*), pML3 (RL at *CRR9*), and pML4 (FL at *CRR9*). In order to insert two directly-repeated copies of the chicken β-globin insulator (cHS4) on either end of 117B23 after linearization with the homing endonuclease PI-*Sce*I, plasmids were created containing homology arms to the region immediately downstream of the *lox511* site and 250 bp upstream of the *loxP* site. Table 3.4 summarizes the relevant characteristics of the plasmids created for BAC recombineering.

3.3.4 Recombineering to Create Human BAC-Based Luciferase Reporters

The recombineering techniques used to modify the human *TERT*-containing BAC 117B23 were performed in the bacteriophage λ-containing bacterial strains DY380 and EL250 and based on the method outlined by the Copeland and Court groups (415;475). The insertion of the luciferase ORFs into the start codons of *CRR9* and *TERT*, as well as insertion of the dual-copy insulators interior of the *lox* sites, was accomplished through two rounds of homologous recombination. The insertion of *puro* into either the vector portion of the BAC or *sacB* was performed by one round of homologous recombination followed by FLP-mediated recombination. Table 3.7 displays the total number of colonies obtained after each round of recombination, the number of clones screened by whole-cell PCR and/or restriction endonuclease digestion, and the total number of correctly modified clones. Table 3.8 displays the results of the FLP/FRT-mediated excision of *kana* from the modified BACs. After the completion of each recombineering step, careful analysis of multiple clones was performed to ensure there were no unexpected/unintended changes in the BAC DNA sequence. A typical result from the restriction endonuclease digestion analysis of kanamycin-resistant colonies obtained from the first step of recombineering is shown in Figure 3.8A. A typical result from the restriction endonuclease digestion analysis of streptomycin-resistant colonies prescreened by whole-cell PCR is shown in Figure 3.8B. Figure 3.8C shows the restriction endonuclease digestion pattern of the unmodified BAC, the modified BAC 117B23 cRtF, and all three intermediates. Occasionally, analysis revealed shortening of VNTR 2-1st; an example of this phenomenon is shown in Figure 3.8D. The eight iterations of the BAC presented in Table 3.9 were used in the genome targeting experiments outlined in Chapter 4.

3.3.5 Modification of the BAC Vectors pBACe3.6 and pTARBAC1

The vectors pBACe3.6 (Figure 1.4B) and pTARBAC1 (Figure 1.4C) were modified to express *puro* driven by either the mPGK or viral SV40 promoter. The modified BAC vectors were created by either standard subcloning or by recombineering

and served as a source of recombineering fragments for BAC modification (Section 3.3.4); they also served as proof-of-principle reagents for genome targeting (Chapter 4). Table 3.10 shows the modified BAC vectors and the technique used for their creation.

3.4 Discussion

In this chapter, the recombineering-mediated creation of a BAC-based, human telomerase reporter was outlined. The chosen BAC clone, RCPI-11.c 117B23, contains ~162 kb of genomic DNA from human chromosome 5 and encompasses the full-length coding regions of *CRR9*, *TERT*, and *SLC6A18* and a portion of *SLC6A19* (Figure 3.6). *SLC6A18* and *SLC6A19* encode orphan transporters of the solute carrier 6 (SLC6) family of proteins, a large, highly conserved family of Na^+ co-transporters specific for neurotransmitters, amino acids, and osmolytes (reviewed in (491;492)). *SLC6A19*, also known as *XT2s1* and *XTRP2s1*, encodes the neutral amino acid transporter B^0AT1 and is expressed only in the kidney and small intestine (reviewed in (492)). *SLC6A18*, also known as *XT2* and *XTRP2*, is expressed solely in kidney proximal tubules. Currently, *SLC6A18* has no known function, although *Xt2* knockout mice show amino aciduria and increased blood pressure (reviewed in (492)). *CRR9* encodes the cisplatin resistance-related 9 protein and was initially identified as a gene upregulated in the cisplatin-resistant ovarian tumor cell line 2008/C13*5.25, even though it was found to be associated with cisplatin-induced apoptosis in these cells (493). A later study comparing drug resistance in various renal cell carcinoma cell lines showed that while *CRR9* expression levels were decreased in carcinoma cells compared to normal renal epithelial cells, the overall expression level remained high and did not correlate with cisplatin sensitivity (494). In fact, expression profiling of mRNA (495) and cDNA (496) revealed *CRR9* to be highly expressed in all normal and tumor tissues and cancer cell lines tested.

There are numerous benefits to using BACs as reporters for h*TERT*. As previously mentioned, artificial chromosomes have been shown to mimic endogenous gene expression when used as transgenes. This is hypothesized to be due to the inclusion of all necessary regulatory elements within their large genetic capacity (reviewed in (263)). The potential inclusion of all appropriate regulatory elements and the neutral effect of reporter genes make the use of BAC reporters to study h*TERT* particularly appealing as these reporters are expected to mimic endogenous *TERT* expression upon their transfer to TERT(+) and (-) human cell lines. Human *TERT* reporters mimicking endogenous *TERT* expression would serve as an important advance in the field of

telomerase regulation as previous work has shown that small, transiently transfected reporters do not always replicate endogenous *TERT* expression (224;234;240). The BAC chosen for modification, RPCI-11.c 117B23 (Figure 3.6), is particularly useful for numerous reasons. Firstly, the entire BAC sequence has been assembled and can be downloaded (490). Secondly, *TERT* is located in the middle of the genomic portion of the BAC, making it more likely that all necessary up- and downstream regulatory elements will be present. Finally, the ubiquitous, high-level expression of *CRR9* in all human cells allows it to be used as an internal control in genome targeting experiments (Chapters 4 and 5).

The human *TERT*-containing BAC 117B23 was modified using a two-step recombineering technique based on the system of Lee et al. (415). One of the biggest benefits to using a two-step technique is the ability to create seamless changes in the BAC. Recombineering in the DY380 and EL250 bacterial strains is very efficient, as evidenced by the ability of 50 bp homology arms to efficiently mediate the insertion of the dual-copy insulators (Table 3.7). In the *TERT* reporter system outlined here, the two-step recombineering technique permits the luciferase reporters to be controlled by the endogenous, non-mutated promoters in the absence of potentially contaminating selectable markers. This is important as one goal of the project is to study gene regulation; therefore, excess sequence is undesirable as its presence may affect gene expression.

Other techniques are available for eliminating undesirable excess sequence during clone modification. For example, instead of using a positive/negative selection cassette in conjunction with two-step modification, a selectable marker surrounded by *lox* or FRT sites can be included as part of the initial cassette. Introduction of Cre or FLP recombinase results in the excision of the selectable marker and the concomitant maintenance of one recognition site. In the creation of the h*TERT* BAC reporters outlined here, FLP/FRT-mediated recombination was used to introduce *puro* to the BAC vector backbone. While there is no evidence in the literature indicating that *lox* or FRT sites have any effect on gene expression, their use in creating iterative BAC modifications is limited to the number of known non-recombining pairs of recognition sites. On the other hand, the two-step technique allows for an unlimited number of

modifications to a single BAC as no *lox* or FRT sites are required and no selection markers are left behind. The seamless nature of the two-step technique also implies that it can be used to create any type of change desired, including the insertion of reporter genes (as already performed) and the creation of point mutations and precise deletions. Examples of future modifications that could be performed with 117B23 clones include the mutation or deletion of binding sites for potential regulatory factors, including those for Sp1/Sp3 (199;208), E-box proteins (199;204), AP-1 (216), WT1 (217), and Menin (218).

There is also the possibility that minisatellites, or variable number of tandem repeats (VNTRs), are involved in *TERT* regulation. Minisatellites are tandem repeats of sequence, typically GC-rich, with a period of 6-100 bp, and span upwards of 0.5 kb (reviewed in (497)). Minisatellites are found throughout the human genome and, as summarized by Vergnaud and Denoeud (497) and Bois (498), have been found to be part of open reading frames; to contribute to gene regulation by affecting transcription factor binding, splicing, and imprinting; to comprise chromosome fragile sites; and to be located near recurrent translocation breakpoints. The high degree of polymorphism in minisatellites has made them indispensable tools for DNA fingerprinting, linkage analysis, and population studies. As might be expected from tandemly repeated regions, human minisatellites are known to be hypermutable, and certain polymorphisms have been implicated in diseases, most notably diabetes and obesity (499;500). While the exact mechanisms of minisatellite instability are not completely clear, one hypothesis with considerable experimental evidence is that the instability is due to mitotic and/or meiotic recombination (reviewed in (498)).

Sequence analysis of three clones containing h*TERT* (GenBank accession numbers AF128893 and AF128894 (501) and AY007685 (502)) identified five *TERT* VNTRs: two in intron 2 (VNTR 2-1st/MSiv2A, and 2-2nd/MSiv2B), two in intron 6 (VNTR 6-1st and 6-2nd/MSiv6), and one in intron 12 (TR 12). Comparison of genomic DNA of from 53 lung cancer patients and 72 cancer-free controls led to the identification of a sixth *TERT* minisatellite, MNS16A, located downstream of the *TERT* coding sequence (503). As can be seen in Table 3.11, PCR analysis of genomic DNA from unrelated individuals revealed all *TERT* VNTRs except TR 12 to be polymorphic.

Attempts to correlate the length of *TERT* VNTRs with cancer have provided mixed results. In one study, a screen of 33 colon carcinoma samples revealed no correlation between the lengths of VNTRs 2-1st and 6-2nd and cancer (501). On the other hand, a second study in which five individual tumor samples (colon, testis, skin, stomach, and kidney) were screened showed changes in VNTRs 6-1st and 6-2nd (502). In a third screen, individuals with two long alleles of MNS16A were two-times more likely to have lung cancer those with two short alleles or one long and one short allele (503). While these screens provide some information on the correlation between *TERT* VNTRs and cancer, the populations screened were very small, especially in the case of Leem et al.; therefore, further study is necessary before any conclusions can be drawn. The use of the BAC reporter system may be very useful in identifying the role of *TERT* minisatellites, particularly VNTR 2-1st, in *TERT* regulation.

During the analysis of modified BACs, shortening of *TERT* VNTR 2-1st was sometimes observed as an artifact following recombineering (Table 3.7). The loss of VNTR 2-1st sequence is most likely due to the active λ phage homologous recombination machinery necessary for recombineering and not the cells themselves. In this case, the repeats of the VNTR act as homology arms and are therefore able to recombine with each other, leading to the loss of repeats. Support for this hypothesis is the lack of VNTR 2-1st shortening observed during FLP/FRT-mediated excision of *kana*. There is also precedence for this in the literature as a previously identified, highly repetitive sequence found in a 100 kb PAC was shown to undergo shortening in the presence of RecA or RecE and RecT (464). Indeed, one of the reasons DH10B was chosen as the BAC host was because it is *recA*$^{-}$ (270). It is not surprising that VNTR 2-1st was the only *TERT* VNTR shown to undergo rearrangements as it is known that not all minisatellites show the same degree of mutability (reviewed in (497) and (498)). On one hand, the spontaneous loss of VNTR 2-1st is beneficial as if enough clones are screened, one with a shortened VNTR will most likely be found and can be used to study the effect of different alleles on *TERT* expression. However, normally shortening is not desired, and care must be taken to ensure that the clone chosen for future manipulation or genome targeting harbors a full-length VNTR 2-1st. While not tested, it is possible that shortening the period during which the recombination genes are active could decrease the chance of

minisatellite shortening. (Yu et al. showed that induction periods as short as 7.5 minutes were able to support successful recombineering of the endogenous *E.coli* chromosome, although they recommended a 15 induction (475).)

While the two-step modification technique outlined in Section 3.2 is very useful for creating seamless modifications in BACs, there are potential improvements that could make the process more efficient. The most time-consuming part of the two-step process is identifying those clones that have correctly replaced the kana/rpsL$^+$ selection cassette with the cassette of interest. The identification of correct clones is complicated by two factors, namely the inability of *rpsL*$^+$ to completely sensitize bacteria to streptomycin and the act of negative selection itself. The incomplete streptomycin-resistance of bacteria expressing *rpsL*$^+$ is a published phenomenon (504-506) and means that bacteria expressing *rpsL*$^+$ do not die, but instead grow at a slower rate. In an experimental setting, all bacteria spread on LB/agar plates supplemented with streptomycin will be able to grow to some degree, resulting in the appearance of large, streptomycin-resistant colonies on a lawn of smaller, streptomycin-sensitive bacteria. To aid in the discrimination of truly streptomycin-resistant bacteria from those that are streptomycin-sensitive, we have employed a high concentration of streptomycin (1 mg/ml), as well as an enrichment period during which recombineered bacteria are grown in a streptomycin-containing liquid culture before plating. Other possible ways to improve the discrimination between streptomycin-resistant and sensitive colonies would be to use a stronger promoter or to include the tetracycline-resistance gene *tetA* (506). Alternatively, using the two-step recombineering method outlined by Warming et al. would eliminate the need for *rpsL* altogether as the kana/rpsL$^+$ selection cassette would be replaced with a constitutively active galactokinase gene (*galK*) (477).

As indicated, the second complicating factor in selecting those clones that have successfully integrated the reporter cassette in place of kana/rpsL$^+$ is the nature of negative selection itself. In negative selection, clones are selected for by the loss of a marker, which in this case is the loss of streptomycin sensitivity. Therefore, any event causing the loss of *rpsL*$^+$, whether it is the desired replacement of the selection cassette with the reporter cassette, a random recombination event, or a gene conversion, will result in the formation of a colony. Depending on the efficiency of the desired event,

many clones need to be screened to find one that is the result of selection cassette replacement; adding this complication to the leaky selection of *rpsL* makes finding correct clones somewhat difficult. To help circumvent this problem, we employed whole-cell PCR to pre-screen colonies for the presence of the integrated reporter cassette. Even with this pre-screening, many clones were still the result of unwanted recombination events. However, we found that increasing the homologous recombination efficiency by optimizing the preparation of the recombineering fragment, the preparation of the electrocompetent bacteria, and the electroporation parameters was sufficient to allow for the identification of correct recombinants.

Primer	Sequence
MAL15	5'-GTGTCCCGCTTTGTAATCGT-3'
MAL16	5'-ATCGTCCTGCTCTTGTCCTT-3'
MAL19	5'-GTTTCTGATGCTGTGAGGCA-3'
MAL20	5'-CAAGCCAACTTCTGAGGAGG-3'
JZHU60	5'-CACAGATCCTGGTCCCATCT-3'
JZHU61	5'-GGGTTGCATGTCGCTTATCT-3'
hTERT.HS10F	5'-CCACACAGTGTCATGGCAGA-3'
hTERT.HS10R	5'-TCATTTTAGGTCAAACGGACAA-3'

Table 3.1. Sequence of Primers Used to Verify the Integrity of BAC 117B23. Primers MAL15, MAL16, MAL19, MAL20, hTERT.HS10F, and hTERT.HS10R were purchased from IDT, Inc.; primers JZHU60 and JZHU61 were synthesized by The Pennsylvania State University College of Medicine Macromolecular Core.

Primer Pair	Location	Product Size
MAL15/MAL16	5' of *CRR9*	596 bp
MAL19/MAL20	3' of *TERT*	826 bp
JZHU60/JZHU61	Intron 2 of *TERT*	551 bp
hTERT.HS10F/hTERT.HS10R	Intergenic *CRR9/TERT*	949 bp

Table 3.2. Primer Pairs Used in PCR Verification Assays. These primer pairs were used to verify the integrity of the human BAC 117B23 received from Research Genetics. The location and size of the amplified product is listed.

Primer	Sequence
CRR9.F1	5'-CCAGGAAAGGTTCCATCTCG-3'
CRR9.R1	5'-GGCCGAGACTCCGTTTCC-3'
MutCRR9.F1	5'-GCGGGGCCGCCAAGCTTACGTAGATCTGGAGCGGCCGC-3'
MutCRR9.R1	5'-GCGGCCGCTCCAGATCTACGTAAGCTTGGCGGCCCCGC-3'

Table 3.3. CRR9 Modification Primers. The primers CRR9.F1, CRR9.R1, MutCRR9.F1, and MutCRR9.R1 were used to mutate the human CRR9 start codon and insert restriction endonuclease recognition sites in its place. All primers were purchased from IDT, Inc.

Plasmid	Enzyme(s)	Fragment Size (bp)	5' Arm (bp)	3' Arm (bp)	Purpose
pYF10-mel	*Bst*EII	2,707	441	483	Insert selection cassette in TERT
pYF10Renilla	*Bst*EII	2,410	441	478	Insert *Renilla* luciferase ORF in TERT
pYF10-hRLuc	*Bst*EII	2,399	441	483	Insert hRL ORF in TERT
pYF10	*Bst*EII	2,882	441	478	Insert firefly luciferase in TERT
pML3-kana-rpsL+	*Eco*RI	2,350	298	284	Insert selection cassette in CRR9
pML-3	*Eco*RI	2,057	298	284	Insert *Renilla* luciferase ORF in CRR9
pML-4	*Eco*RI	2,552	298	284	Insert firefly luciferase in CRR9
pBACe3.6puroFKF	*Eco*RI/*Eco*RV	5,192	1,062	761	Insert PGK-*puro* in 117B23 (*sacB* gene)
pBACeSVpuroFKF	*Spe*I	4,708	997	563	Insert SV40- *puro* in 117B23 (*sacB* gene)
pSK+CRR9puroRL	*Sph*I/*Spe*I	3,437	178	316	Insert puro^{R}/*Renilla* luciferase fusion in CRR9
pSK+puroIIISacB	*Eco*RV/*Sac*I	4,327	330	1,000	Insert SV40- *puro* in pBACe3.6
pIGCN-puroIII+Arms	*Sfi*I/*Xho*I/*Pvu*I	2,984	42	42	Insert SV40- *puro* in 117B23
pKS-kana-rpsL+511	*Spe*I/*Kpn*I	1,878	50	50	Insert selection cassette 3' of 117B23 *lox511* site
pKS-kana-rpsL+P	*Spe*I/*Kpn*I	2,548	50	50	Insert selection cassette 3' of 117B23 *loxP* site
pKS-2XIns511	*Spe*I/*Kpn*I	1,878	50	50	Insert dual copy insulators 5' of 117B23 *lox511* site
pKS-2XInsP	*Spe*I/*Kpn*I	2,548	50	50	Insert dual copy insulators 5' of 117B23 *loxP* site

Table 3.4. Recombineering Fragments. The fragments used for recombineering were isolated from the plasmids listed above with the indicated restriction endonucleases ("Enzyme(s)"); the sizes of the fragments are listed. All fragments were used for 2-step recombineering except for pBACeSVpuroFKF and pSK^{+}CRR9puroRL, which were used for 1-step recombineering followed by arabinose induction.

Primer	Sequence
CRR9.R1	5'-GGCCGAGACTCCGTTTCC-3'
FLuc.F1	5'-AGAACTGCCTGCGTGAGATT-3'
FLuc.R1	5'-ATCCAGATCCACAACCTTCG-3'
hRLuc.F3	5'-AAGCTGCAGAAGTTGGTCGT-3'
hRLuc.R3	5'-GGAGTCCAGCACGTTCATTT-3'
Ins.L	5'-CTAGAGCCCCATCCTCACTG-3'
Ins.R	5'-GAAGAGCTTGCCTGGAGAGA-3'
loxP.InsL	5'-GTGCGCATAGAAATTGCATC-3'
PA.F1	5'-GGGAGGTGTGGGAGGTTTT-3'

Table 3.5. Sequence of Primers Used for Whole-Cell PCR Analysis of Recombineered BACs.

Primer Pair	Region	Insert	Product Size
PA.F1/CRR9.R1	CRR9	puroRL	406 bp
PA.F1/CRR9.R1	CRR9	FL or RL	350 bp
FLuc.F1/FLuc.R1	TERT	FL	494 bp
hRLuc.F3/hRLuc.R3	TERT	hRL	334 bp
Ins.L/Ins.R	lox511	2X cHS4	368 bp
loxP.InsL/Ins.R	loxP	2X cHS4	397 bp

Table 3.6. Primer Pairs Used for Whole-Cell PCR Analysis. For each primer pair, the region of interest, the cassette inserted at the region of insert ("Insert"), and the expected size of the amplified product ("Product Size") is indicated.

Starting Clone	Fragment Source	Total Colonies	Screened by PCR	Screened by Digestion	Number Correct	Final Clone
Naïve	pYF10-mel	10	-	10	10	tKR
tKR #1	pYF10	-	80	7	6	tF[a]
tF #4	pML3-kana-rpsL+	~37,000	-	6	6	cKRtF
cKRtF #4	pML-3	-	40	8	4	cRtF
cKRtF #4	pSK+CRR9-puroRL	-	80	3	3	cPRLtF
cRtF #19-1	pBACe3.6puroFKF	~4,200	-	7	7	cRtFpFKF
cRtF #19-1	pBACeSVpuroFKF	1	-	1	1	cRtFsSVPFKF
cRtF #19-1	pBACeSVpuroFKF	457	-	4	2	cRtFsSVPFKF
cRtF #19-1	pSK+puroIIISacB	~4,300	-	4	4	cRtFvSVPFKF
Naïve	pML3-kana-rpsL+	~1,200	-	6	6	cKR
cKR #1	pSK+CRR9-puroRL	-	80	7	2	cPRL
cPRL #39	pYF10-mel	~4,000	-	6	5	cPRLtKR
cPRLtKR #2	pYF10	-	40	6	5[b]	cPRLtF
cKR #1	pML-4	-	80	5	5[c]	cF
cF #5	pYF10-mel	~1,200	-	5	5	cFtKR
cFtKR #2	pYF10-hRLuc	-	40	4	3	cFtHR
cFtHR #30	pBACeSVpuroFKF	~230	-	5	3	cFtHRsSVPFKF
cFtHR #30	pSK+puroIIISacB	~17,000	-	5	4[d]	cFtHRvSVPFKF
cFtHRsSVP #2	pKS-kana-rpsL+511	~8,000	-	5	3[e]	cFtHRsSVP KR511
cFtHRsSVP KR511 #9	pKS-2XIns511	-	40	15	6	cFtHRsSVP Ins511
cFtHRsSVP Ins511 #7-1	pKS-kana-rpsL+P	~3,000	-	5	5[f]	cFtHRsSVP Ins511KRP
cFtHRsSVP Ins511KRP #2	pKS-2XInsP	-	40	9	1	cFtHRsSVP Ins511InsP

Table 3.7. Summary of BAC Recombineering. For each clone, the recombineering fragment used to create the final clone is indicated. Entries in the "Total Colonies" column marked with "-" represent those obtained through negative selection, and therefore, colonies were not counted. Entries in the "Screened by PCR" column marked with "-" represent those obtained through positive selection, and therefore, PCR was not performed. [a]This clone contained a shortened VNTR 2-1st, although this was not determined before proceeding with recombineering. The following clones displayed VNTR 2-1st shortening: [b]2/5; [c]1/5; [d]1/4; [e]1/3; [f]1/5.

	-Arabinose		+Arabinose				
Starting Clone	**Cm^R Colonies**	**$Kana^R$ Colonies**	**Cm^R Colonies**	**$Kana^R$ Colonies**	**Colonies Screened**	**Number Correct**	**Final Clone**
cRtFpFKF #1	340	300	320	36	4	4	cRtFpF
cRtFsSVPFKF #1	264	240	496	17	3	2	cRtFsSVP
cRtFsSVPFKF #1	~500	~500	~500	2	4	3	cRtFsSVP
cRtFvSVPFKF #3	~500	~500	~600	3	4	4	cRtFvSVP
cFtHRsSVPFKF #3-1	1,512	1,336	1,320	25	5	5	cFtHRsSVP
cFtHRvSVPFKF #4	~1,200	~1,200	~900	17	5	5	cFtHRvSVP

Table 3.8. Summary of FLP/FRT-Mediated Removal of *kana*. Parallel cultures of each starting clone were treated equally except for the addition of L-arabinose to one of the cultures. The colonies screened were picked from LB/agar plates supplemented with 12.5 μg/ml chloramphenicol and plated with bacteria induced with L-arabinose. Those clones displaying a correct restriction endonuclease pattern are indicated as "Number Correct." Cm^R: chloramphenicol-resistant. $Kana^R$: kanamycin-resistant.

Name	*CRR9*	*TERT*	*sacB*	Vector	*lox*511/*lox*P
cRtF	*Renilla*	Firefly	-	-	-
cPRtF	Puro/*Renilla*	Firefly	-	-	-
cRtFPuro	*Renilla*	Firefly	mPGK-Puro	-	-
cRtFsSVP	*Renilla*	Firefly	SV40-Puro	-	-
cRtFvSVP	*Renilla*	Firefly	-	SV40-Puro	-
cFtHRsSVP	Firefly	h*Renilla*	SV40-Puro	-	-
cFtHRvSVP	Firefly	h*Renilla*	-	SV40-Puro	-
cFtHRsSVPIns	Firefly	h*Renilla*	SV40-Puro	-	2X cHS4

Table 3.9. Fully Modified Versions of the Human BAC 117B23. All modifications were performed using recombineering, either by the 2-step method (insertion of luciferase ORFs and dual-copy insulators) or by FLP/FRT excision (insertion of puromycin resistance genes). In the "Name" column, lower case letters represent the place of insertion and upper case letters represent what was inserted; therefore, "cFtHRsSVP" refers to the BAC with the firefly luciferase ORF inserted at *CRR9*, the h*Renilla* luciferase ORF inserted at *TERT*, and SV40-driven *puro* inserted in the *sacB* gene of the vector. "*Renilla*" refers to the original coding sequence of *Renilla reniformis* and "h*Renilla*" refers to the human codon usage-optimized version of *Renilla*. "mPGK-Puro" refers to mPGK promoter-driven *puro*, "SV40-Puro" refers to SV40 promoter-driven *puro*, and "Puro/*Renilla*" refers to the fusion of *puro* and *Renilla* luciferase in which both are driven by the *CRR9* promoter.

BAC Vector	Modification Technique
pTARpuroRL	Subcloning
pTARpuroSacB	Subcloning
pBACe3.6puroFKFpUC	Subcloning
pBACeSVpuroFKF	Recombineering
pBACeSVpuro	FLP/FRT

Table 3.10. Modified BAC Vectors. For each version of pTARBAC1 (pTARpuroRL and pTARpuroSacB) and pBACe3.6 (pBACe3.6puroFKFpUC, pBACeSVpuroFKF, and pBACeSVpuro), the modification technique is indicated. "Subcloning" refers to standard subcloning by restriction endonuclease digestion and ligation. "Recombineering" refers to the use of homologous recombination. "FLP/FRT" refers to FLP/FRT-mediated recombination.

Name	Location	Repeat Motif	Period	Number of Alleles
VNTR 2-1 (MSiv2A)	Intron 2	GAGTGAGGCGTGGTCCCCGGGTGTC CCTGTCACGTGCAGGGT	42 bp	6
VNTR 2-2 (MSiv2B)	Intron 2	C(T)G(T)GTGAGCTGGATGTGC(T)GGT GTCC(T)GGATGGTGCAGGCTT(T)GGG GTGAGGTCGCCAGGCCCTG	61 bp	4
VNTR 6-1	Intron 6	GTGGGATTGGTTTTCATGTGCGGGGT AGGTGGGGATCT	38 bp	8
VNTR 6-2	Intron 6	GGGGTCTGATGTGTGGTGACTGTGGA TGGCGGTCGT	36 bp	30
TR 12	Intron 12	TGGGCATCCGCGTCCACTCCCTCTCC TG	28 bp	1
MNS16A	Downstream of Exon 16	TCCTCTTAT(CAT)CTCCCAGTCTCATC	26 bp	4

Table 3.11. VNTRs Found In The Human Telomerase Gene. In the repeat motif column, nucleotides indicated by parentheses are not found in every repeat. The average repeat length is shown in the period column. Information in this table was gleaned from (501-503).

Figure 3.1. PCR-based Mutagenesis Scheme for CRR9. **A.** The native sequence surrounding the human *CRR9* ATG start codon. (The start codon is indicated by a box.) **B.** The modified CRR9 region in which the ATG start codon has been replaced with sequence introducing the restriction endonuclease recognition sites for *Hind*III and *Bgl*II. The CRR9.F1 and CRR9.R1 primers are indicated by boxes, and the sequence corresponding to the MutCRR9.F1 and MutCRR9.R1 primers is underlined.

A.

MAL69 5'-CTAGTGTAGACTTAATTAAGGATCGATCCGGCGCGCCAATAGTCATGCCCCGCGC-3'

MAL70 5'-GATCGCGCGGGGCATGACTATTGGCGCGCCGGATCGATCCTTAATTAAGTCTACA-3'

5' *lox511* Arm 5'-CTAGTGTAGACTTAATTAAGGATCGATCCGGCGCGCCAATAGTCATGCCCCGCGC-3'
3'-ACATCTGAATTAATTCCTAGCTAGGCCGCGCGGTTATCAGTACGGGGCGCGCTAG-5'

B.

MAL89 5'-TCGACCACCGGAAGGAGCTGACTGGGTTGAAGGCTCTCAAGGGCATCGGTCGAGGGTAC-3'

MAL90 5'-CCTCGACCGATGCCCTTGAGAGCCTTCAACCCAGTCAGCTCCTTCCGGTGG-3'

3' *lox511* Arm 5'-TCGACCACCGGAAGGAGCTGACTGGGTTGAAGGCTCTCAAGGGCATCGGTCGAGGGTAC-3'
3'-GGTGGCCTTCCTCGACTGACCCAA CTTCCGAGAGTTCCCGTAGCCAGCTCC-5'

Figure 3.2. Creation of *lox511* Homology Arms. **A.** The oligonucleotides MAL69 and MAL70 were ordered from Integrated DNA Technologies; upon oligo annealing, the homology arm located 5' of the *lox511* site in 117B23 is formed. The 5' overhang of the annealed oligo is compatible with ends produced by restriction endonuclease digestion with *Spe*I while the 3' recessed end of the annealed oligo is compatible with ends produced by digestion with *Bam*HI. **B.** The oligonucleotides MAL89 and MAL90 were also ordered from Integrated DNA Technologies, and upon their annealing, the homology arm located 3' of the *lox511* site in 117B23 is formed. The 5' overhang of the annealed oligo is compatible with ends produced by restriction endonuclease digestion with *Xho*I while the 3' overhang is compatible with ends produced by digestion with *Kpn*I.

A.

MAL73 5'-CTAGTGTCGGACAGTGCTCCGAGAACGGGTGCGCATAGAAATTGCATCAACGCAT-3'

MAL74 5'-GATCATGCGTTGATGCAATTTCTATGCGCACCCGTTCTCGGAGCACTGTCCGACA-3'

5' *loxP* Arm 5'-CTAGTGTCGGACAGTGCTCCGAGAACGGGTGCGCATAGAAATTGCATCAACGCAT-3'
3'-ACAGCCTGTCACGAGGCTCTTGCCCACGCGTATCTTTAACGTAGTTGCGTACTAG-5'

B.

MAL91 5'-TCGAATAGCGCTAGCAGCACGCCATAGTGACTGGCGATGCTGTCGGAATGGACGGGTAC-3'

MAL92 5'-CCGTCCATTCCGACAGCATCGCCAGTCACTATGGCGTGCTGCTAGCGCTAT-3'

3' *loxP* Arm 5'-TCGAATAGCGCTAGCAGCACGCCATAGTGACTGGCGATGCTGTCGGAATGGACGGGTAC-3'
3'-TATCGCGATCGTCGTGCGGTATCACTGACCGCTACGACGCCTTATTCCTGCC-5'

Figure 3.3. Creation of *loxP* Homology Arms. **A.** The oligonucleotides MAL73 and MAL74 were ordered from Integrated DNA Technologies; upon oligo annealing, the homology arm located 5' of the *loxP* site in 117B23 is formed. The 5' overhang of the annealed oligo is compatible with ends produced by restriction endonuclease digestion with *Spe*I while the 3' recessed end of the annealed oligo is compatible with ends produced by digestion with *Bam*HI. **B.** The oligonucleotides MAL91 and MAL92 were also ordered from Integrated DNA Technologies, and upon their annealing, the homology arm located 3' of the *loxP* site in 117B23 is formed. The 5' overhang of the annealed oligo is compatible with ends produced by restriction endonuclease digestion with *Xho*I while the 3' overhang is compatible with ends produced by digestion with *Kpn*I.

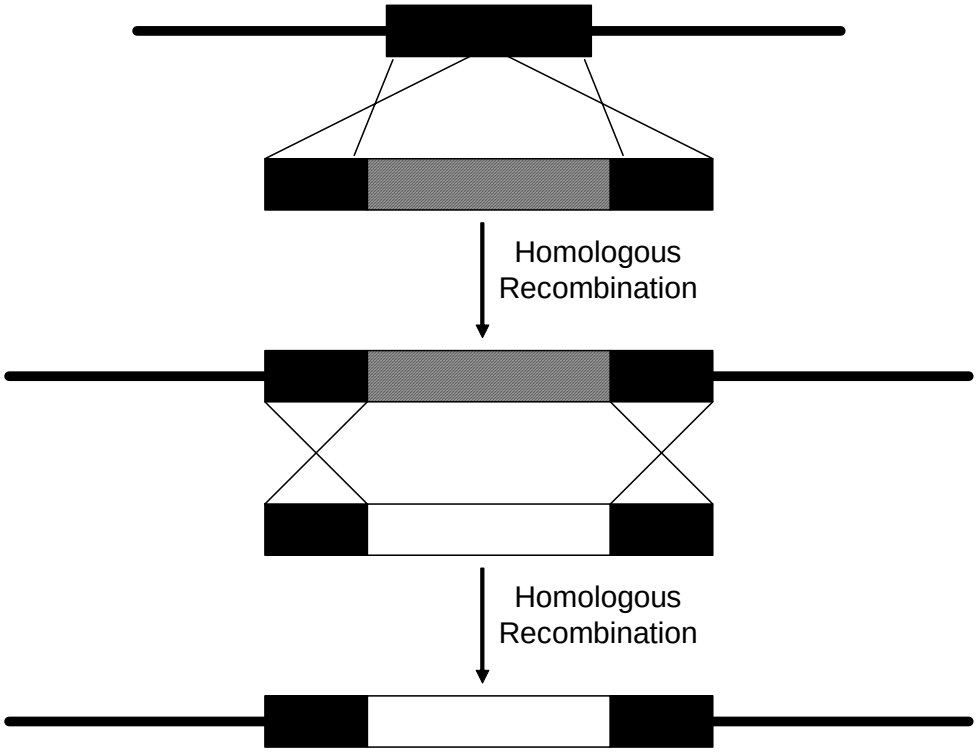

Figure 3.4. 2-Step Recombineering. All steps occur in either the DY380, EL250, or EL350 bacterial strain, all of which contain the λ phage homologous recombination machinery; these strains are streptomycin-resistant due to a mutation in *rpsL*. A kana/rpsL$^+$ selection cassette (hatched box) is designed to contain homology arms to the gene or region of interest (solid box). Activation of the homologous recombination machinery by incubation results in the insertion of the kana/rpsL$^+$ cassette, rendering the bacteria kanamycin-resistant and streptomycin-sensitive. A second round of homologous recombination is completed in order to replace the kana/rpsL$^+$ cassette with the change of interest (white box), causing a reversion to streptomycin-resistance. This technique was used to insert the luciferase ORFs at the *CRR9* and *TERT* loci and the dual-copy insulators interior to the *lox511* and *loxP* sites. Note: Figure not drawn to scale.

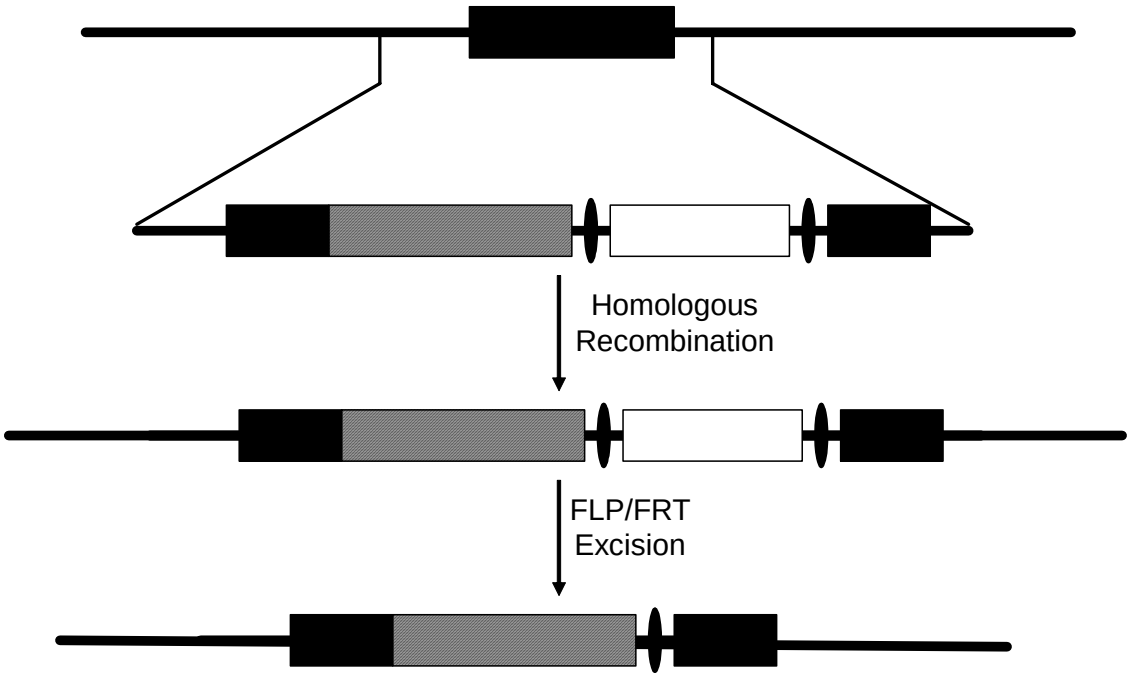

Figure 3.5. FLP/FRT-Mediated Insertion of *puro*. All steps occur in the EL250 bacterial strain, which contains λ phage homologous recombination machinery and arabinose-inducible FRT recombinase. In the first step, a cassette containing homology arms to the region of interest (black boxes), the desired change (hatched line), and two FRT sites (black ovals) surrounding *kana* (white box) was inserted into the region of interest after activation of the homologous recombination, rendering the cells kanamycin-resistant. In the second step, arabinose is added to the cultures to induce FLP recombinase, resulting in the excision of kana. FLP/FRT-mediated recombination is very efficient (see Table 3.8) and therefore, positive selection is not required. This technique was used to insert *puro* into the vector backbone. Note: Figure not drawn to scale.

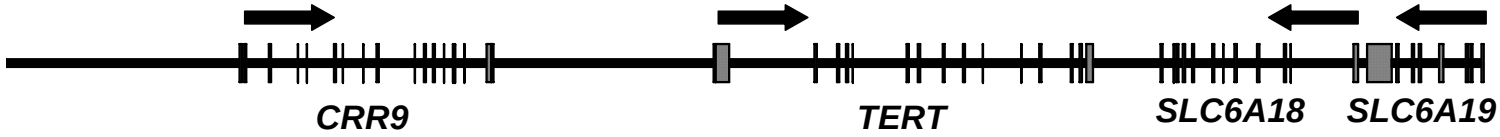

Figure 3.6. The Genomic Loci of the Human BAC RPCI-11 117B23. The BAC consists of ~162 kb of genomic DNA from human chromosome 5p15.33 and contains the full-length coding sequence for the *CRR9*, *TERT*, and *SLC6A18* genes, as well as the partial coding sequence of the *SLC6A19* gene. The arrows represent the direction of transcription.

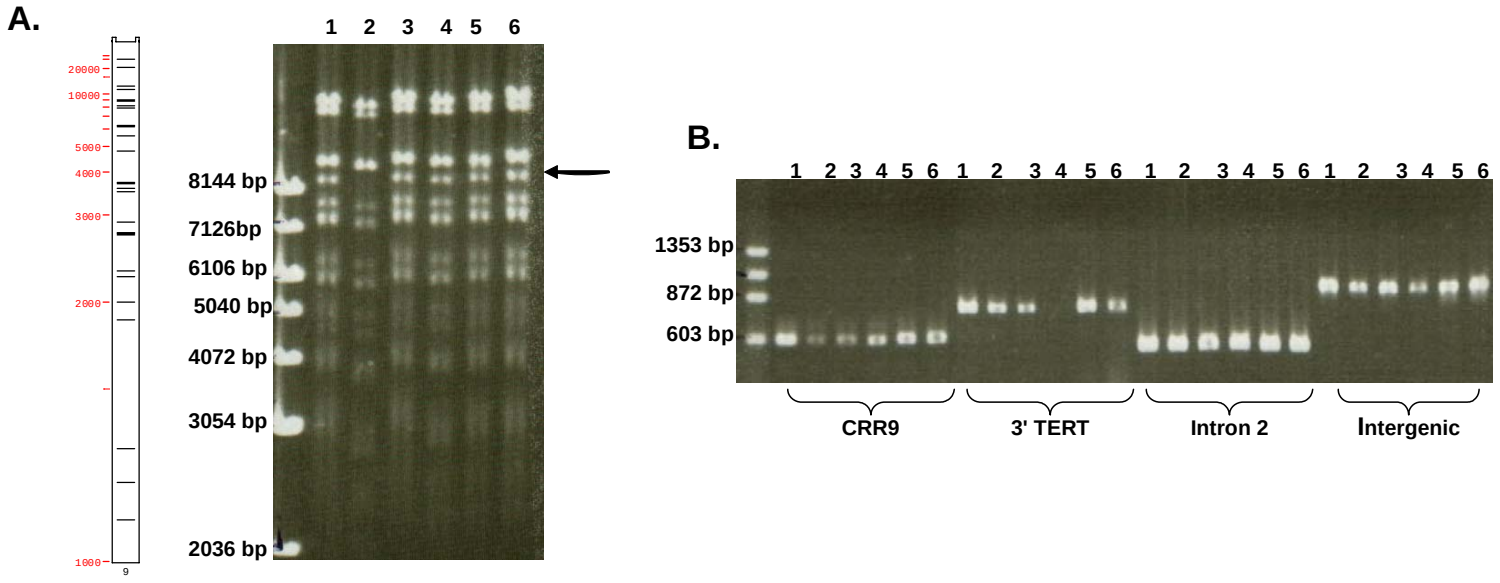

Figure 3.7. Initial Screening of RPCI-11.c 117B23. **A.** DNA from the human BAC RPCI-11 117B23 was digested with the restriction endonuclease *Bam*HI and electrophoresed through a 0.7% agarose gel (0.5X TBE). The expected banding pattern is found in the left panel and the ethidium bromide-stained gel in the right panel. All clones revealed approximately the same pattern as expected, except for colony B2, which is missing a fragment at ~9kb (indicated by arrow). **B.** PCR amplification of BAC DNA was performed using primer pairs specific for *CRR9* ("CRR9"), specific for the region downstream of *TERT* ("3' TERT"), specific for intron 2 of *TERT* ("Intron 2"), and specific for the intergenic region between *CRR9* and *TERT* ("Intergenic"). Primer specificities are found in Tables 3.1 and 3.2.) As can be seen in the ethidium bromide-stained agarose gel, the expected products are visible for all clones, except for clone 4. Clone 4 is lacking the expected product for the region downstream of *TERT*. Based on these results, clones 2 and 4 were discarded.

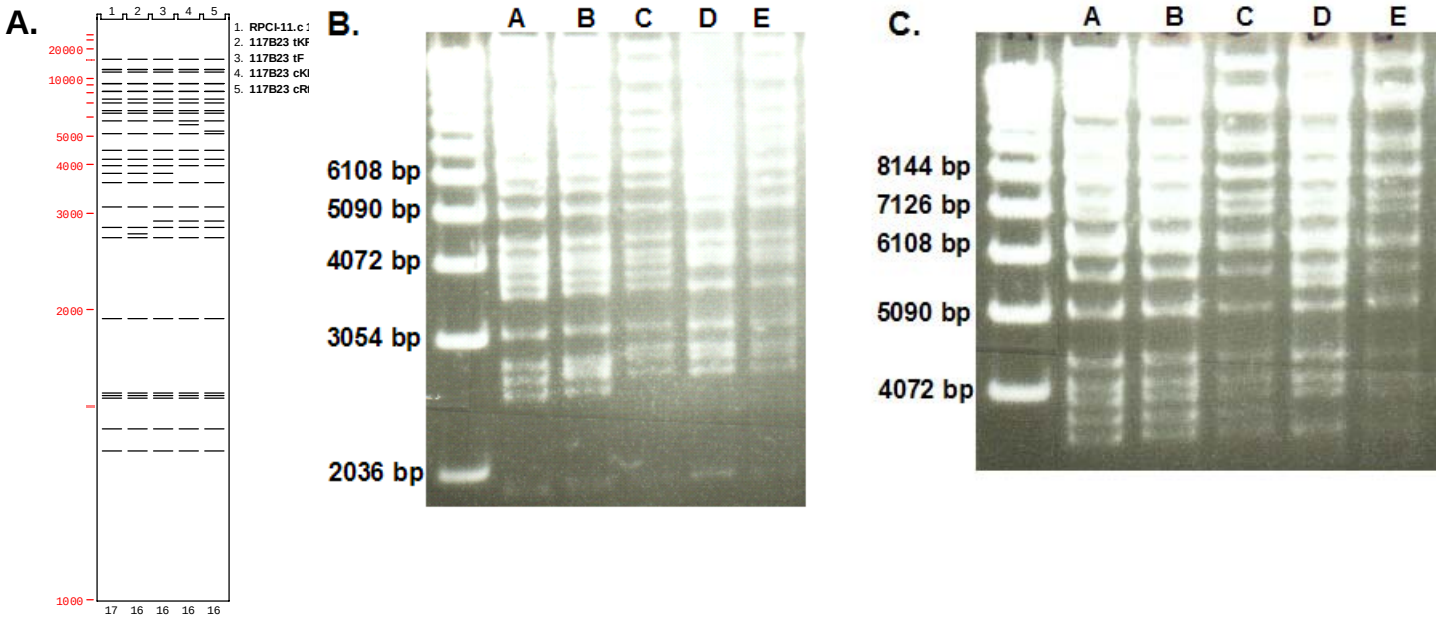

Figure 3.8. Restriction Endonuclease Digestion Verification of Recombineering. *Bst*EII was used to digest the original, unmodified BAC ("A"), the BAC modified to contain kana/rpsL$^+$ at *TERT* ("B"), the BAC modified to contain FL at *TERT* ("C"), the BAC modified to contain FL at *TERT* and kana/rpsL$^+$ at *CRR9* ("D"), and the BAC modified to contain FL at *TERT* and RL at *CRR9* ("E"). The fully modified BAC is referred to as 117B23 cRtF. **A.** Predicted fragments after digestion with *Bst*EII. From A to B, the 922 bp fragment is expected to shift to 2,702 bp. From B to C, the 2,702 bp fragment to 2,882 bp. From C to D, the 3,788 bp fragment is expected to shift to 5,534 bp. From D to E, the 5,534 bp fragment is expected to shift to 5,242 bp. **B and C.** Ethidium bromide-stained agarose gel of *Bst*EII-digested BAC DNA.

Chapter 4
GENOME TARGETING WITH CIRCULAR BAC VECTORS AND BACS

4.1 Introduction

The mechanisms underlying control of human telomerase expression have remained elusive despite almost 25 years of study. One of the biggest problems in studying human telomerase is the lack of a powerful model system. While mice are typically used as models for human genetics and disease, the biology of murine telomeres and telomerase differs significantly from those of humans (see Sections 1.2.2 and 1.3.4 and Table 1.2). The lack of a mouse model for human telomerase biology would be less problematic if telomerase activity could be accurately modeled in cultured, human somatic cells. Unfortunately, transiently expressed h*TERT* reporter constructs do not always mimic the endogenous telomerase activity of the cells; in certain cases, reporter activity is seen in both TERT(+) and TERT(-) cells (see Section 1.3.6; (224;234;240)). Potential reasons for the inability of transiently expressed hTERT reporters to mimic endogenous telomerase activity include the lack of all necessary regulatory elements and the inability of transiently-expressed reporter constructs to form a native chromatin environment.

In order to fully understand how h*TERT* is regulated, a better reporter system is necessary. The ideal h*TERT* reporter system would be comprised of genetically related TERT(+) and (-) cells engineered to express a reporter gene from the endogenous *TERT* locus. In this system, *TERT* would remain under the control of its native promoter, enhancers, and silencers and would be maintained in its native chromatin environment. Therefore, any changes in reporter activity upon the modification of potential regulatory elements could be directly attributable to the modified element. Unfortunately, the creation of this ideal system would require multiple gene targeting events via homologous recombination, a naturally occurring process that is severely limited in human cells (reviewed in (507-509)).

The best alternative to modifying the endogenous locus is to create a pseudo-endogenous locus using an artificial chromosome. The large size of artificial chromosomes implies they are more likely to contain all the up- and downstream regulatory elements required for appropriate gene expression and be incorporated into chromatin (see Sections 1.3.4, 3.1, and 3.4). Even though BAC-based transgenes have been shown to recapitulate endogenous expression patterns upon random integration (reviewed in (263)), the ability to express all BAC reporters from the same genomic position would help eliminate questions of PEV and chromosomal silencing; such a system would result in the creation of a truly pseudo-endogenous locus. Fortunately, through the use of recombinase-mediated cassette exchange (RMCE), it is possible to repeatedly target constructs to the same genomic position.

In this chapter, the introduction of BAC-based human telomerase reporters to TERT(+) and (-) human fibroblasts containing an RMCE-competent acceptor locus is reported. The luciferase activity of clones containing stably integrated BAC DNA was assayed, and the level of this activity was compared between the TERT(+) and (-) cells. The integrity of the BAC DNA was determined by Southern analysis and/or PCR amplification of relevant markers. (Due to the volume of work presented, this chapter is organized somewhat differently than Chapters 2 and 3.)

4.2 Materials and Methods

4.2.1 Preparation of Transfection-Quality BAC DNA

High quality BAC DNA was prepared from 300-500 ml LB cultures of DH10B bacteria using the GenoPure Maxi Kit (Roche) according to the manufacturer's recommended protocol for low copy-number plasmids. In certain cases, an additional ethanol precipitation was performed. Integrity of the BAC was verified by restriction endonuclease digestion of 500 ng DNA with *Bst*EII and/or *Hinc*II, followed by gel electrophoresis through 0.7% agarose prepared in 0.5X TBE. For short-term storage, the BAC was kept at 4˚C; for longer storage, the DNA was stored as an ethanol precipitate at -80˚C.

4.2.2 Introduction of DNA to Cell Lines Harboring Acceptor Locus

Unless otherwise stated, all dishes used to plate cells were tissue culture grade plastic. The standard medium for the TERT(+) and (-) cell lines was EMEM (CellGro) supplemented with either 10% FBS (HyClone) or 10% Bovine Growth Serum (HyClone Bovine Calf Serum supplemented with chemically defined components to stimulate cell growth and proliferation; HyClone), 1X glutaMAX (Gibco), and 1X MEM non-essential amino acid solution (Sigma). The standard medium for CV1 cells (African green monkey kidney cell line) was DMEM (CellGro or Gibco) supplemented with 10% FBS, 1X glutaMAX (Gibco), and 1X pen/strep/Gln. Circular BAC DNA, as well as BAC vector DNA, was introduced to TERT(+) and (-) cells harboring the acceptor locus via transfection using FuGENE-6 (Roche), Lipofectamine2000 (Invitrogen), or GenePorter2 (Genlantis); BAC DNA was also introduced by electroporation. FuGENE-6 transfection was performed as per the manufacturer's recommendations with the following modifications: a ratio of 2.4 µl FuGENE-6 reagent to 1 µg DNA was used, the FuGENE-6 reagent was diluted with OptiMEM (Invitrogen), and the FuGENE-6/DNA complex was diluted three-fold with OptiMEM before addition to the cells. (As a general reference, 0.5 µg BAC was used per each well of a 12-well plate.) Lipofectamine2000

transfection was performed as per the manufacturer's recommendations with the following modifications: a ratio of 2.4 µl Lipofectamine2000 reagent to 1 µg DNA was used and three hours post-transfection, the cells were washed one time with PBS and fed with standard medium. (As a general reference, 1 µg BAC was transfected to one well of a 12-well plate.) Transfection with GenePorter2 was performed as per the manufacturer's instructions for the original GenePorter reagent. (As a general reference, per well of a 12-well plate, a total of 1.5 µg DNA was diluted to 250 µl with OptiMEM and mixed with 6 µl GenePorter2 reagent diluted to 250 µl with OptiMEM.)

4.2.3 Test of Cre Recombinase Efficiency

Cre recombinase efficiency and cytotoxicity was assessed by co-transfecting the DNA of interest with pCAGGS-Cre (β-actin promoter and CMV enhancers; (510)), pBS185 (CMV promoter; (511)), or pCBM (β-actin promoter; (364)), or by treating the cultures with 1 µM 4HT. The function of the three Cre plasmids in a transient assay was measured by co-transfecting TERT(+) cells containing the acceptor locus (167b 3.5) with equal nanogram amounts of the Cre reporter pZ/AP (418) and the respective Cre plasmids. The ability of 4HT to induce CreER activity from the acceptor locus was measured by transfecting the cells with the same nanogram amount of pZ/AP and treating the cells with 1 µM 4HT 24 hours-post-transfection. All transfections were performed in duplicate in 12-well plates. Forty-eight hours post-transfection, half of the duplicate wells were stained with x-gal to monitor β-galactosidase activity , while the other half of the wells were stained with Fast Violet B Salt to monitor APAP activity. (See Section 2.2.6 for the staining methods.)

The effect of the three Cre plasmids on stable integration of BAC vectors, as well as their ability to mediate RMCE, was tested by co-transfection (using FuGENE-6) in naïve TERT(+) cells (167b) and TERT(+) cells expressing the acceptor locus (167b 3.5). Two experiments were performed by co-transfecting 1 µg each of circular pTARpuroSacB and the Cre plasmids in 6-well plates; a third experiment was performed by co-transfecting 400 ng circular pTARpuroSacB and 200 ng Cre plasmid in 12-well plates. Forty-eight hours post-transfection, the cells were expanded to 6 cm and 6-well

plates, respectively. Twenty-four hours after expansion, the cells were treated with 250 ng/ml puromycin and allowed to form colonies. For one of the experiments initiated in a 6-well dish and the experiment initiated in a 12-well plate, individual colonies from each Cre plasmid co-transfection were counted and then pooled together in a 6 cm dish. Cells were harvested when they reached confluency, and gDNA was prepared. For the second experiment initiated in a 6-well plate, individual colonies were counted and cloned to one well of a 24-well plate using cloning cylinders. The clones were sequentially expanded to one well of a 6-well plate and one 6 cm dish. Cells were harvested when they reached confluency, and gDNA was prepared. In all three of these experiments, two wells were co-transfected with salmon sperm DNA in place of the Cre plasmids in order to transfect each well with the same total amount of DNA. Twenty-four hours post-transfection, one of these wells was treated with 1 μM 4HT to induce CreER activity from the acceptor locus. In all other respects, the wells were treated the same.

To test the effect of different 4HT concentrations on stable colony formation and RMCE mediation, naïve TERT(+) and acceptor locus-containing TERT(+) cells (167b and 167b 3.5, respectively) were transfected in 6-well plates with 1 μg of circular BAC vector pBACe3.6puroFKF. One hour after transfection, cells were treated with either 0, 1, 2.5, or 5 μM 4HT. Twenty-four hours post-transfection, the cells were split evenly between two wells of a 6-well plate, maintaining the same 4HT concentrations. Forty-eight hours after expansion, the 4HT was removed; the cells were then treated with 250 ng/ml puromycin. Sixteen days after transfection, six colonies from the wells treated with 5 μM 4HT were cloned to two wells of a 24-well plate; one well was treated with 500 ng/ml puromycin, while the second was treated with 600 μg/ml G418. Clones were sequentially expanded to 6-well and 6 cm dishes, and then harvested for gDNA preparation. At the same time, the wells treated with 1 and 2.5 μM 4HT were treated with 20 μM GCV and monitored for cell death.

Colony formation was also assessed by co-transfection of circular pBACe3.6puroFKF with the Cre plasmids. Naïve TERT(+) and acceptor locus-containing TERT(+) cells (167b and 167b 3.5, respectively) were plated in 10 cm dishes and transfected via FuGENE-6 reagent with 3 μg each of pBACe3.6puroFKF and the Cre plasmids. Twenty-four hours post-transfection, each plate was split evenly between two

new 10 cm plates, and forty-eight hours later, the cells were treated with 250 ng/ml puromycin. Sixteen days after transfection, five colonies from the pCAGGS-Cre co-transfection and 12 colonies each from the pBS185 and pCBM co-transfection were cloned to two wells of a 24-well plate; one well was treated with 500 ng/ml puromycin, while the second was treated with 600 μg/ml G418. Clones were sequentially expanded to 6-well plates and 6 cm dishes, and then harvested for gDNA preparation.

4.2.4 Isolation of Stably Transfected Clones

Twenty-four hours after transfection, cells were trypsinized and expanded. Those cells transfected in 12-well plates were expanded 1:1 to 6-well plates, while cells transfected in 6-well plates were evenly divided between three wells of a 6-well plate. The day after expansion (48 hours post-transfection), the cells were treated with 250 ng/ml puromycin for four to six days. Following a two day period of growth in standard medium, the puromycin was re-added for the duration of culture. Once individual colonies were large enough, they were cloned to one well of a 24-well plate using cloning cylinders. When the clones reached approximately 90-100% confluence, they were split equally between three wells of a 24-well plate; 24 hours after this split, one well was treated with 250 ng/ml puromycin, the second well with 400 μg/ml G418, and the third well with 25 μM gancyclovir (GCV). When selection was complete, the puromycin-resistant cells were expanded sequentially to one well of a 6-well plate and a 6 cm dish. Genomic DNA was prepared from 95-100% confluent 6 cm cultures.

4.2.5 Luciferase Assays

The firefly and *Renilla* luciferase activities were measured using the Dual-Luciferase® Reporter Assay System (Promega) and either a DLReady Femtomaster FB12 luminometer (Zylux Corporation) equipped with a DPU-414 thermal printer (Seiko Instruments, Inc.) or a DLReady Sirius luminometer equipped with an internal thermal printer (Berthold Detection Systems). Transient luciferase activity was measured 48 hours post-transfection from cells aliquotted to 24-well plates. Luciferase activity of

stable integrants was measured on cells plated in either 12- or 24-well plates throughout the culture period. The luciferase assays were performed according to the manufacturer's instructions, with minor modifications. Briefly, cells were washed once with PBS and lysed in 1X Passive Lysis Buffer (PLB) by adding 50-100 µl buffer per well of a 24-well plate or 100 µl buffer per well of a 12-well plate and gently rocking at room temperature for 15-30 minutes. To measure firefly luciferase activity, 5 µl of cell lysate was added to 25 µl Luciferase Assay Buffer II (LARII) pre-aliquotted to microfuge tubes, gently mixed by pipetting up and down, and placed in the luminometer; when all samples were processed, 25 µl Stop & Glo solution (S&G) was added, gently mixed by pipetting up and down, and placed in the luminometer to measure *Renilla* luciferase activity. As a control for background autoluminescence, 5 µl of 1X PLB was analyzed along with the samples.

4.2.6 PCR Analysis of Stable Integrants

PCR was performed on approximately 50 ng of gDNA prepared from the isolated clones. Each 10 µl PCR reaction contained 1X PCR buffer, DMSO (if necessary), the appropriate concentration of $MgCl_2$ (empirically determined), 0.3 mM dNTPs, 0.2 µM primers, and 0.5 U *Taq* DNA polymerase (NEB or Promega). Amplification was performed with 30 cycles of 30 seconds denaturation, 30 seconds annealing, and one minute extension. For the identity of the primers and specific amplification parameters for each, please see Table 4.1.

4.2.7 Southern Hybridization Analysis of Stable Integrants

Three micrograms of gDNA was digested with 10 U of *Bam*HI, *Bst*EII, *Eco*0109I, *Hind*III, or *Pvu*II in a total volume of 30 µl anywhere from 5 hours to overnight. For the electrophoresis, transfer, hybridization, washing, and detection methods, see Section 2.2.5. The blots were hybridized with various probes (summarized in Table 4.2). All probes were labeled as per Section 2.2.5. The insulator probe was prepared by restriction endonuclease digestion of pUC19M-cHS4, followed by gel purification. The firefly and

h*Renilla* luciferase probes were prepared by PCR amplification, followed by gel purification.

4.3 Experimental Design

4.3.1 Transient Luciferase Activity

To verify that luciferase ORFs inserted in the human BAC 117B23 were expressed, the luciferase activity was assayed 48 hours post-transfection using the Dual-Luciferase® Reporter Assay System (Promega) and measured as relative light units per second (RLU/s). Activity was assessed for naïve TERT(+) and (-) cells, acceptor locus-containing TERT(+) and (-) cells, and CV1 cells. The activity of BACs transfected by FuGENE-6, Lipofectamine2000, and GenePorter2 reagents was also compared.

4.3.2 Cre Recombinase Optimization/Proof of Principle

To optimize the induction of Cre recombinase and prove that the acceptor locus was able to support RMCE, four means were tested in a transient transfection assay with the Cre reporter pZ/AP (418). Of these four, three were plasmids (pCAGGS-Cre (510), pBS185 (511), and pCBM (364)) and one was induction of CreER from the acceptor locus by addition of 4HT to the culture medium. To test the ability of the four means of Cre induction to mediate RMCE, as well as their effect on the overall health of the cultures, co-transfections of the three Cre plasmids were performed with four different RMCE-competent BAC vectors, as well as treatment of transfected cells with 4HT. Following transfection, cells were selected with puromycin. Puromycin-resistant colonies were cloned and expanded in order to monitor their sensitivity to G418 and GCV, to measure their luciferase activity, and to harvest gDNA for PCR and Southern analysis. Each individual clone was characterized by its G418 and GCV sensitivity, its luciferase activity, the presence of PCR products specific for the acceptor locus, the presence of PCR products specific for the recombined locus, and/or Southern hybridization patterns of relevant markers present on the BAC.

4.3.3 Cre/*lox*-Mediated Integration of h*TERT* BAC Reporters

To test the ability of modified BACs to undergo RMCE, TERT(+) and (-) cell lines containing the acceptor locus were co-transfected with Cre plasmids and BAC DNA, as well as transfected with BAC DNA alone and then treated with 4HT. Following transfection, cells were selected with puromycin. Puromycin-resistant colonies were cloned and expanded in order to monitor their sensitivity to G418 and GCV, to measure their luciferase activity, and to harvest gDNA for PCR and Southern analyses. Each individual clone was characterized by its G418 and GCV sensitivity, its luciferase activity, the presence of PCR products specific for the acceptor locus, the presence of PCR products specific for the recombined locus, and Southern hybridization patterns of relevant markers present on the BAC.

4.4 Results and Discussion

In this chapter we addressed the hypothesis that BACs would be able to be targeted to a preexisting acceptor locus. To test this hypothesis, we attempted to target h*TERT*-containing BACs modified to express luciferase ORFs (see Chapter 3) to the preexisting acceptor locus (see Chapter 2) via recombinase-mediated cassette exchange (RMCE) using Cre recombinase and *loxP* and *lox511* recognition sites.

4.4.1 Luciferase Activity From Transiently Transfected BACs

Before attempting to target the BAC reporters to the acceptor locus, their ability to express luciferase activity after transient transfection was tested. (We already knew the TERT(+) and (-) cells containing the acceptor locus were transfectable based on the success of experiments performed with pZ/AP (see Section 2.3.4).) As can be seen in Figure 4.1A, TERT(+) acceptor locus-containing cells did express both firefly and *Renilla* luciferase activity 48 hours after transfection with circular BAC DNA expressing *Renilla* and firefly luciferase from the *CRR9* and *TERT* loci, respectively. Although the TERT(+) cells did express luciferase activity, CV1 cells transfected under the same conditions showed luciferase activity that was one order of magnitude greater. Testing of additional TERT(+) acceptor locus-containing lines revealed that all expressed approximately the same luciferase activity after transfection with a BAC modified to express a fusion of *puro* and *Renilla* luciferase and firefly luciferase from the *CRR9* and *TERT* loci, respectively (Figure 4.1B). Figure 4.1B also shows that TERT(+) cells containing the acceptor locus and those without expressed approximately the same levels of luciferase activity. It should also be noted that TERT(-) cells consistently expressed lower levels of luciferase activity than TERT(+) cells when assayed in parallel (Appendix B and data not shown).

4.4.2 Optimization of Cre Recombinase Induction and Verification of RMCE in TERT(+) and (-) Cells Containing the Acceptor Locus

In order to verify that the preexisting acceptor locus was capable of supporting RMCE, various plasmids based on the BAC vectors pBACe3.6 (Figure 1.4A; (271)) and pTARBAC1 (Figure 1.4B; (272)) were used. These modified BAC vectors were chosen for the initial characterization as they were minimally modified (see Section 3.3.5) and contained no genomic inserts, therefore making them smaller and more transfectable (see Appendix B, Figure B3 for comparison of luciferase activity after transfection with plasmid and BAC DNA.) We hypothesized that the smaller size of the BAC vectors would result in an increased number of molecules present in the cells, and therefore an increased efficiency of RMCE. Initial attempts at creating RMCE integrants using three different BAC vectors lacking a positively selectable marker failed to produce any GCV-resistant colonies (data not shown). The lack of GCV-resistant colonies was most likely due to a combination of the low efficiency of RMCE and selection based on HSV *tk*. If RMCE does not occur at a high frequency, the number of cells harboring the acceptor locus will greatly outnumber those that do not. This is problematic as the addition of GCV to cells containing the *tk* gene causes them to release toxic metabolites into the culture medium that can then be taken up by cells not expressing *tk*, causing them to die as well; this effect is known as bystander killing. Bystander killing, a well-documented phenomenon of GCV/*tk* selection systems, is mediated by gap junctional communication and has been exploited for suicide vectors (433;434;512-514). While not shown, extensive efforts to optimize the conditions for selection of *tk* loss, including the density of cells, the time in GCV, and replacement of GCV with the less toxic fialuridine (FIAU) (435), were performed. The results of these experiments revealed that while negative selection of HSV *tk* with GCV was most likely feasible, the technique was cumbersome and time-consuming.

To circumvent problems with GCV-mediated selection of RMCE integrants, vectors containing the positively selectable marker *puro* were developed. By including *puro*, the cells can first be selected with puromycin. As selection with puromycin selects only for gain of *puro* and not RMCE itself, secondary selection with GCV can be used as

a follow-up to select those puromycin-resistant clones that are truly RMCE integrants. Support for this strategy comes from a study that showed staggered positive-negative selection increased the efficiency with which RMCE integrants were identified (515). Induction of CreER with 4HT and puromycin selection of acceptor locus-containing cells transfected with a BAC vector containing a fusion of the *Renilla* luciferase ORF and *puro* under control of the minimal *CRR9* promoter (puroRL) failed to produce any colonies (Table C1 of Appendix C).

As random integration of this vector would also produce puromycin-resistant colonies and we knew that acceptor locus-containing cells transfected with this vector showed luciferase activity (data not shown), we thought that perhaps there was a problem with the 4HT-mediated induction of CreER from the acceptor locus. To test this hypothesis, the vector expressing puroRL was co-transfected with pCAGGS-Cre, a plasmid containing Cre recombinase under control of the chicken β-actin promoter and CMV enhancers (510). This co-transfection also failed to produce any puromycin-resistant colonies (Table C1 of Appendix C). To test whether there was a problem with this vector, a BAC vector containing *puro* under control of the mPGK promoter was transfected in parallel with the original *puro*-containing vector. The formation of puromycin-resistant colonies from cells transfected with mPGK-*puro* but not puroRL indicates that even though the minimal *CRR9* promoter was able to drive *Renilla* luciferase activity in transient transfection assays (Figure 4.1B, Figure B1 of Appendix B, and data not shown), it was unable to produce a high enough expression level of *puro*, preventing cells from surviving puromycin addition.

Although transfection of acceptor locus-containing cells with two different vectors containing mPGK-*puro* and induction of CreER from the acceptor locus or from pCAGGS-Cre produced puromycin-resistant colonies, the total number was less than expected. Furthermore, the cells that did survive were somewhat unhealthy, and none were RMCE integrants (Tables C1 and C2 of Appendix C). We thought the problem might be that Cre expression induced from the acceptor locus may not be strong enough to mediate efficient RMCE and that Cre expression from pCAGGS-Cre may be too strong and therefore, cytotoxic (429). To test this hypothesis, four means of Cre recombinase induction were tested: 1) co-transfection with pCAGGS-Cre, 2) co-

transfection with pBS185 (CMV promoter; (511)), 3) co-transfection with pCBM (β-actin promoter; (364)), and 4) optimization of CreER from the acceptor locus. All four of these means were equally efficient at mediating the Cre/*lox*-mediated loss of βgeo from the transiently transfected Cre reporter pZ/AP (418) (data not shown). However, when the cells were transfected with mPGK-*puro* vectors and selected with puromycin, clear differences were observed. After transfection but before the addition of puromycin, all cultures looked the same. Within three days of puromycin addition, those cells co-transfected with pCAGGS-Cre showed increased cell death over those co-transfected with pBS185 or pCBM or induced for CreER. In terms of colony formation and overall cell health (size of colonies and their density), the order of effectiveness was pCBM > pBS185 ≈ 4HT > pCAGGS-Cre with 27, 18, 16, and 9 puromycin-resistant colonies, respectively, from a total of three experiments (Tables 4.4 and 4.5 and C3 of Appendix C). Similar results were obtained with a second vector containing mPGK-*puro* (Table C3 of Appendix C). As the strength of Cre expression from the plasmids, based on their promoters and enhancers, is pCAGGS-Cre > pBS185 > pCBM, these results seem to support the cytotoxicity of excess Cre expression (429).

In addition to the increased number of puromycin-resistant colonies observed after co-transfection with pCBM, it was more efficient at mediating RMCE; pBS185 and 4HT treatment had approximately the same efficiency. From a total of five experiments performed with two different vectors expressing mPGK-*puro*, 0/11 stable integrants obtained after transfection with pCAGGS-Cre, 5.88% (1/17) of stable integrants obtained after transfection with pBS185, 13.16% (5/38) of stable integrants obtained after transfection with pCBM, and 4.00% (1/25) of stable integrants obtained after induction of CreER were determined to be the result of RMCE after PCR analysis. (Examples of PCR analysis can be found in Figures 4.2 and 4.3.) Based on this information, pCBM co-transfection and 4HT induction of the acceptor locus were used in future experiments.

4.4.3 Importance of Maintaining G418 Selection

To test the ability of staggered positive/negative selection to increase the efficiency of identifying RMCE integrants, acceptor locus-containing cells were

transfected with vectors containing mPGK-*puro*, induced for Cre activity, and selected with puromycin. Addition of 20 μM GCV to whole plates of puromycin-resistant colonies resulted in no cell death. Cloning of individual puromycin- and GCV-resistant colonies, followed by G418 selection, resulted in all clones being G418-sensitive. However, upon PCR analysis with primer pairs specific for both the acceptor locus and the recombined locus failed to produce any specific products. Isolation of individual colonies before addition of GCV resulted in the majority of puromycin- and GCV-resistant, G418-sensitive ($Puro^R/Neo^S/GCV^R$) still not being RMCE integrants (Table 4.5). Overall, of the 113 $Puro^R/Neo^S/GCV^R$ clones obtained from acceptor locus lines not maintained in G418 prior to transfection, only three (2.7%) were the result of RMCE (Figure 4.2, Table 4.5, and Tables C2 and C3 of Appendix C). Theoretically, clones resistant to puromycin and GCV and sensitive to G418 should be RMCE integrants. In actuality, this combination of drug sensitivities only indicates the loss of the acceptor locus, which can occur through either RMCE or the loss of the chromosomal portion harboring the locus. While a negative result, attempts to amplify fragments specific for the acceptor locus in these non-RMCE $Puro^R/Neo^S/GCV^R$ integrants failed (Figure 4.2), supporting the theory that these cells had lost the acceptor locus due to chromosomal loss. To test the hypothesis that these $Puro^R/Neo^S/GCV^R$ were the loss of the acceptor locus, experiments were performed in acceptor locus-containing cells continuously cultured in the presence of G418 prior to transfection. Of the 27 tested $Puro^R/Neo^S/GCV^R$ clones obtained by transfection of cells maintained in G418 prior to transfection, all 27 (100%) were RMCE integrants (Figure 4.3 and Tables C4 and C5 of Appendix C). These results lend direct support to the theory that chromosomal loss was a problem in these cells. While normal cells would not tolerate chromosomal loss, the TERT(+) and (-) cell lines used in these studies contain stably integrated SV40 large T and small t antigens and therefore do not have functional p53- and pRb-mediated DNA damage response pathways (reviewed in (516)). As a consequence of abrogated DNA damage responses and survival through crisis, these cells are hyperdiploid ((192) and data not shown) and can obviously survive chromosomal abnormalities. Therefore, it is not surprising that these cells can lose the acceptor locus in the absence of selective pressure. Loss of transgenic loci in the absence of selection pressure is a documented phenomenon

(517-519).

Overall, RMCE integrants were observed in 1) TERT(+) cells containing the acceptor locus co-transfected with a BAC vector containing mPGK-*puro* and either pBS185 or pCBM; 2) in TERT(+) cells containing the acceptor locus transfected with a BAC vector containing mPGK-*puro* and CreER activation from the acceptor locus; 3) in TERT(+) cells containing the acceptor locus co-transfected with a BAC vector containing SV40-*puro* and pCBM; and 4) TERT(-) cells containing the acceptor locus co-transfected with pBACeSVpuro and pCBM. (See Tables 4.5 and C1-C5 of Appendix C.) Additionally, the TERT(+) acceptor locus-containing line 167b 3.1 and the TERT(-) acceptor locus-containing line 166a 11.1 produced the most stable and RMCE integrants (see Tables C4 and C5 of Appendix C) and BAC vectors containing SV40-*puro* produced more stable integrants than BAC vectors containing mPGK-*puro* (compare Tables C1-C3 to Tables C4 and C5).

4.4.4 Attempts to Target Circular BAC Reporters Via RMCE

Once it was proven that the TERT(+) and (-) acceptor locus-containing cells were able to support RMCE of BAC vector-based plasmids and be transiently transfected by luciferase ORF-containing hTERT BAC reporters, we attempted to target, via RMCE, these BAC reporters to the preexisting acceptor locus. Despite numerous attempts using various BAC reporters, different transfection reagents, and different selection schemes, we were unable to obtain RMCE-mediated BAC integrants (see Tables C5-C11). Additionally, the majority of these clones lacked expression of both luciferase markers. The initial BACs used for targeting attempts expressed *Renilla* luciferase from the *CRR9* locus and firefly luciferase from the *TERT* locus. Transfection of acceptor locus-containing TERT(+) cells with a BAC also expressing mPGK-*puro* from within *sacB* of the vector portion resulted in 21 stable integrants, of which only one (4.76%) expressed both luciferase activities. Transfection of these same cells with a BAC expressing SV40-*puro* from within *sacB* of the vector portion resulted in 29 stable integrants, none of which expressed both luciferase activities. Transfection of TERT(-) cells with this same BAC construct failed to produce any stable integrants.

As *Renilla* luciferase is more sensitive than firefly luciferase and *TERT* is the gene of interest, we decided to design BAC reporters expressing the h*Renilla* luciferase ORF from *TERT* and the firefly luciferase ORF from *CRR9*. Transfection of TERT(+) cells with a BAC also expressing SV40-*puro* from within *sacB* of the vector portion resulted in 29 stable integrants, of which three (10.34%) expressed both luciferase activities. Although one of these integrants was $Puro^R/Neo^S/GCV^R$, PCR analysis revealed it was not the result of RMCE. Transfection of one TERT(-) acceptor locus line with this same BAC produced no stable integrants, but transfection of a second TERT(-) resulted in five stable integrants. Of these five clones, three (60%) showed both luciferase activities; even though two of these integrants were $Puro^R/Neo^S/GCV^R$, they were not the result of RMCE. Transfection of TERT(+) acceptor locus-containing cells with a BAC expressing SV40-*puro* from the region interior of the *lox511* site resulted in one stable integrant, which did not express any luciferase activity. Transfection of TERT(-) cells containing the acceptor locus with this same BAC resulted in no colony formation.

4.4.5 Possible Reasons For Failure of RMCE-Mediated Integration of BAC Reporters

The exact reasons for the inability of BAC reporters to undergo RMCE are unknown, but many different factors are surely involved. One problem is the low transfection efficiency of BAC DNA. The luciferase activity of TERT(+) cells after transfection with plasmid DNA is greater than the activity after transfection with BAC DNA by more than one order of magnitude (See Figure B3 of Appendix B). The promoter and enhancer elements present on pGL3proΔ and pRL-GL3proΔ and the greater number of molecules transfected contribute to the high luciferase activity, but they do not account for all of the difference (data not shown). The negative effect of large DNA constructs on transfection efficiency and transgene expression is a documented phenomenon (30). Another contributing factor is the sensitivity of BAC DNA to shearing and breakage. Even though BACs are more resistant to these mechanical forces than YACs, they are still problematic. To try and reduce mechanical forces, the BAC DNA was manipulated as little as possible and pipetted with large bore pipette tips. Even

with these extra precautions, the BAC is most likely fragmented during its passage from the cytoplasm to the nucleus. In a study of CV1 cells transfected by DEAE-dextran, it was shown that transfected DNA underwent double-stranded breaks approximately every 5-15 kb (520). If these same parameters applied to transfection and/or electroporation in our TERT(+) and (-) cell lines, the BAC reporter could be fragmented into as many as 34 pieces. Even if all of these fragments reassembled in order, they would most likely do so with small insertions or deletions (521-523). Such insertions or deletions could have severe consequences for data interpretation if they occurred within an important regulatory region. Direct support for the fragmentation of BAC DNA upon transfection comes from a study showing that only 57% of primary human fibroblasts showed expression of two markers present on the BAC (524). In a second study, analysis of human MCF-7 cells stably transfected with a BAC retrofitted to express *neo* revealed that not all clones were positive for markers of the genomic portion of the BAC (525).

Another reason for the failure of RMCE could be the cells themselves. It is well-established that certain cell lines are more easily transfectable than others (see Figure B1 of Appendix B), so it stands to reason that different cell lines would have different rates of stable integration as well. In one study, it was shown that mouse LM cells integrated approximately 10-fold more exogenous DNA (57 kb versus 4.5 kb) upon calcium phosphate-mediated transfer than monkey Vero and human HeLa and GM4312A cells (517). These differences could be due to the cellular response to the exogenous DNA, which is likely to differ between cell lines due to their different complements of genetic factors. In one recent study, it was shown that the introduction of exogenous, double-stranded plasmid DNA, regardless of the transfection technique, caused a sharp increase in genes involved in DNA repair in CHO-K1 cells, but not in human HEK293 cells, which already expressed many of these genes at a high level in the absence of transfected DNA (526). While this study did not address stable integration of exogenous DNA, it does highlight the differential response to foreign DNA in cell lines of different origin. Furthermore, while BACs have been used as transgenes, most studies have involved transgenic mice, and therefore, the BACs have been introduced to ES cells. In cases where the BACs have been introduced to human cells, the integrity of integrated DNA has either not been completely analyzed (527), or if it has, some degree of breakage has

been noted, as discussed above (524;525).

Similar to the lack of data on stably integrated BAC DNA in human cells is the lack of data on RMCE in human cells. Of the 13 published studies employing RMCE, only one employed human cells (HeLa; (380)). In theory, there is no reason that RMCE should not work in human cells; however, there are factors unique to our system that could make it less efficient. To fully understand how these unique factors might impact RMCE in our system, it is useful to consider the process of RMCE itself. While a simplified version of RMCE is represented in Figure 2.1, the actual replacement reaction proceeds through two steps (Figure 4.4). Initially, the BAC is integrated alongside the acceptor locus via Cre-mediated recombination through one of the two *lox* sites. Following this integration, resolution can proceed through either pair of *lox* sites. If the resolution occurs through the same *lox* sites as the integration, the BAC will be excised and the acceptor locus maintained (indicated by red line in Figure 4.4). If resolution occurs through the opposite pair of *lox* sites, the acceptor locus will be lost, leaving behind the BAC in its place (indicated by blue line in Figure 4.4). Theoretically, resolution could occur through either pair of *lox* sites, although the desired reaction is probably favored as the *loxP* sites are in closer proximity than the *lox511* sites (10 kb versus 170 kb).

One potentially complicating factor in our system is the choice of *lox* sites. Our use of the *loxP* and *lox511* sites was dictated by their preexisting presence on the BAC itself. While the *loxP* and *lox511* Cre recognition sites are incompatible in prokaryotes (528), they are more promiscuous in mammalian cells (377;426;529). The simplest consequence of this promiscuity, in our system, is inversion of the DNA located between the *lox* sites as the *loxP* and *lox511* sites are in the reverse orientation (Figure 2.1B). These simple inversions would not be expected to have an effect on RMCE efficiency because the intervening DNA is functional in either orientation. Complications arise when one considers the possible products of initial integration and resolution mediated through heterospecific sites. The potential products of heterospecific Cre/*lox* recombination occurring after initial integration mediated through specific *lox* sites are shown in Figure 4.5. While none of these recombination events would preclude resolution into the desired product, the relative efficiencies of these heterospecific

reactions are unknown. Therefore, if Cre is able to mediate a higher level of recombination between heterospecific *lox* sites located in closer proximity than between matched *lox* sites located further apart, overall RMCE efficiency would be decreased due to the preferential recombination between the *loxP* site of the BAC and the *lox511* site of the acceptor locus (Figure 4.5). Further complications arise when considering the possible products of initial integration mediated through heterospecific *lox* sites (Figure 4.6).

Another complicating factor when considering possible outcomes is at which stage of the cell cycle RMCE occurs in (reviewed in (367)). During G1, the cells contain only one copy of the acceptor locus, and therefore, the only possible Cre-mediated reactions are inversion of the acceptor locus, inversion of the genomic portion of the BAC, or the desired RMCE. However, once the cells complete S phase and proceed to G2, they now have two copies of the acceptor locus. The number of possible Cre-mediated recombination products is now increased because the *lox* sites of the acceptor locus can interact with one another, potentially causing chromosomal translocations and/or loss of the acceptor locus (Figure 4.7). The possible products that could arise in the presence of the BAC during G2 are numerous as well and could further complicate analysis. Overall, while none of these factors individually could cause a failure of RMCE, taken together and considered along with the low transfection efficiency of BACs, they provide serious hurdles to obtaining RMCE-mediated BAC reporter integrants in our TERT(+) and (-) cell lines.

Primer	Sequence
MAL40	5'-CGTTGGGTTACCTTCTGCTC-3'
MAL41	5'-TTCAACCCAGTCAGCTCCTT-3'
MAL42	5'-GCCGATACTTCATTGGCATT-3'
MAL43	5'-CCTACAGGTGGGGTCTTTCA-3'
MAL44	5'-GGGCGTACTTGGCATATGAT-3'
MAL53	5'-ATCGCATTCCTTGCAAAAGT-3'
MAL54	5'-TCATACACGGTGCCTGACTG-3'
MAL59	5'-GCTCAAAGAGCAGCGAGAAG-3'
MAL60	5'-CTAGCAGCACGCCATAGTGA-3'
MAL61	5'-TAGCGGCCGCAAATTTATTA-3'
MAL62	5'-ATTACATCCCTGGGGGCTTT-3'
MAL63	5'-GACGATGAGCGCATTGTTAG-3'
MLVF2'	5'-AATTTTTGCTTTCGGTTTGG-3'

Primer Pair	Specificity	5' or 3' End	Size	Cycles/Temp
MLVF2'/MAL61	RMCE	5'	726	35/65°C
MAL40/MAL41	RMCE	5'	448	35/65°C
MAL42/MAL43	RMCE	3'	586	35/65°C
MAL54/MAL43	RMCE	3'	234	15/68°C 20/60°C
MAL63/MAL62	RMCE	3'	314	15/68°C 20/60°C
MAL60/MAL59	RMCE	3'	599	35/65°C
MAL40/MAL44	Acceptor Locus	5'	573	20/68°C 15/60°C
MAL53/MAL43	Acceptor Locus	3'	232	35/60°C

Table 4.1. Primer Pairs Used to Analyze Stable Integrants by PCR Amplification. The primer sequences are shown in the top panel while the primer pairs are shown in the bottom panel. Primer pairs are specific for either an RMCE event ("RMCE") or for the acceptor locus ("Acceptor Locus"). "5' or 3' End" refers to the end of the acceptor locus or integrated DNA. "Cycles/Temp" refers to the number of amplification cycles and annealing temperature used. Primer pair MAL60/MAL59 also required a final concentration of 10X DMSO. All amplification was performed with 2 mM $MgCl_2$, except for pair MAL53/MAL43, which was performed with 5 mM $MgCl_2$.

Probe	Source	Size
cHS4	pUC19M-cHS4	1.2 kb
Firefly Luciferase	pML4	332 bp
h*Renilla* Luciferase	pYF10-hRL	219 bp

Table 4.2. Probes Used for Southern Hybridization Analysis of Stable Integrants. The cHS4 probe was isolated from pUC19M-cHS4 by restriction endonuclease digestion with *Spe*I and *Bam*HI. The firefly luciferase probe was created by PCR amplification of pML4 using the primers FL.F (5'-TTTTCCGTCATCGTCTTTCC-3') and FL.R (5'-TCAAAGAGGCGAACTGTGTG-3'). The h*Renilla* luciferase probe was created by PCR amplification of pYF10-hRL using the primers hRL.F (5'-TCGTCCATGCTGAGAGTGTC-3') and hRL.R (5'-CTAACCTCGCCCTTCTCCTT-3').

Experiment	pCAGGS-Cre	pBS185	pCBM	1 μM 4HT	No Cre
I	5	12	16	12	12
II	0	1	3	0	7
III	4	5	8	4	3
Total	9	18	27	16	22

Table 4.3. Comparison of Different Methods of Cre Induction on the Formation of Stable Integrants. Cells of the TERT(+) acceptor locus line 167b 3.5 were transfected with the RMCE-competent plasmid pTARpuroSacB. Cre recombinase was introduced by either co-transfection with a Cre-expressing plasmid (pCAGGS-Cre, pBS185, or pCBM) or induction of CreER from the acceptor locus by treatment with 1 μM 4HT. Cells, including those not expressing Cre recombinase ("No Cre"), were selected with 250 ng/ml puromycin, and the number of puromycin-resistant clones was assessed for three different experiments.

				Puro			Puro + GCV		
DNA (Amount)	**Cre Induction**	**Number of Cells**	**Total Expts.**	**Screened/ Total**	**Neo^R**	**RMCE Integrants**	**Screened/ Total**	**Neo^R**	**RMCE Integrants**
pBACe3.6puroFKFpUC (0.5 μg)	pCAGGS-Cre	2.12E+05	1	0/0	-	-	-	-	-
pBACe3.6puroFKFpUC (0.5 μg)	pBS185	2.12E+05	1	4/5	2	1	3/4	1	0
pBACe3.6puroFKFpUC (1.75 μg)	pCBM	8.46E+05	2	5/34	1	1	3/9	1	0
pBACe3.6puroFKFpUC (0.5 μg)	5 μM 4HT	2.12E+05	1	4/4	1	1	0/0	-	-

Table 4.4. Comparison of Selection with Puromycin Alone Versus Puromycin and GCV. Following transfection of the TERT(+) acceptor locus line 167b 3.5, the cells were split 1:4; half were treated with puromycin, while the second half were treated with puromycin and GCV. Of the total number of colonies, a select number were cloned ("Screened/Total") and tested for their resistance to G418 ("Neo^R"). All screened clones were also amplified for gDNA harvest and screened by PCR amplification. The number of clones found to be RMCE integrants are indicated. Note: All cell numbers are approximate. Cells were maintained in the absence of G418 prior to transfection.

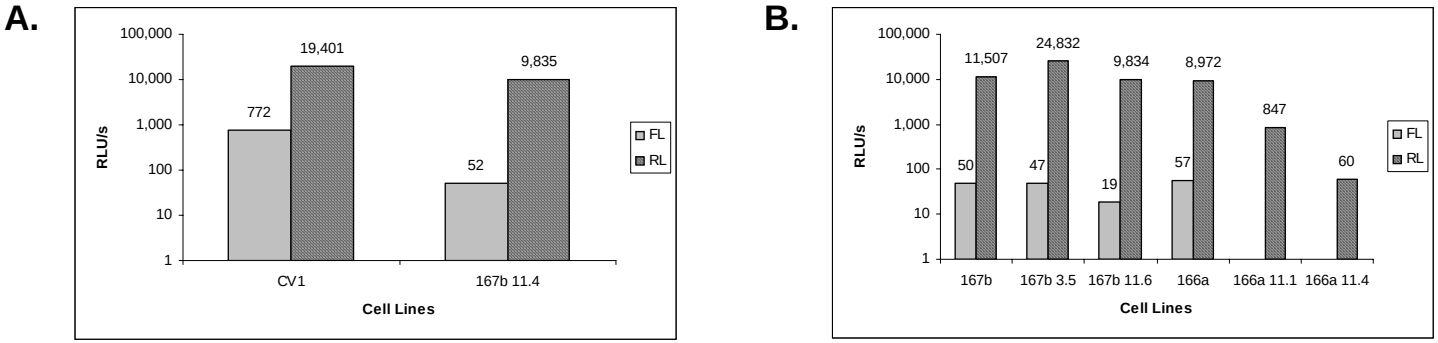

Figure 4.1. Transient Luciferase Activity of h*TERT* BAC Reporters. **A.** The firefly and *Renilla* luciferase activity of CV1 Cells and the TERT(+) acceptor locus-containing line 167b 11.4 48 hours post-transfection of circular 117B23 cRtFsP. **B.** The firefly and *Renilla* luciferase activity of naïve TERT(+) and (-) cells (167b and 166a, respectively) and two TERT(+) and (-) lines containing the acceptor locus (167b 3.5 and 11.5 and 166a 11.1 and 11.4, respectively) 48 hours post-transfection of circular 117B23 cPRLtF. Notes: All luciferase activity is plotted on a logarithmic scale. In both **A** and **B**, FL is a reporter of TERT and RL is a reporter of CRR9.

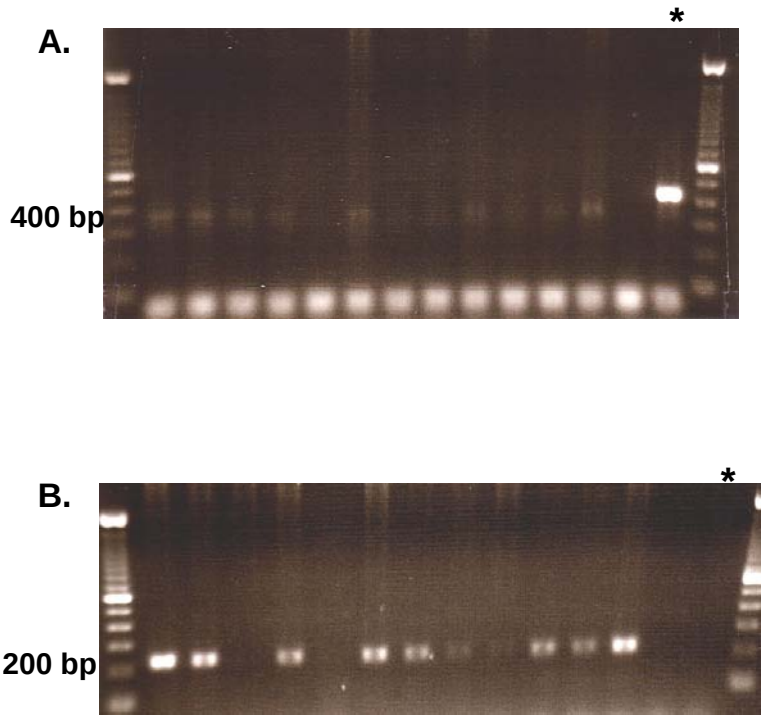

Figure 4.2. PCR Amplification of Puromycin-Resistant Clones Obtained After Transfection of the TERT(+) Line 167b 3.5 with Circular pTARpuroSacB. **A.** PCR amplification using the RMCE-specific primer pair MAL40/MAL41. Amplification with this primer pair results in the amplification of a product of 448 bp if the DNA is integrated through RMCE. The lane marked with "*" is an RMCE recombinant. **B.** PCR amplification using the acceptor locus-specific primer pair MAL53/MAL43. Amplification with this primer pair results in the amplification of a product of 232 bp if the acceptor locus is present in the cells. The lane marked with "*" does not show this product. These results identify this clone as an RMCE integrant.

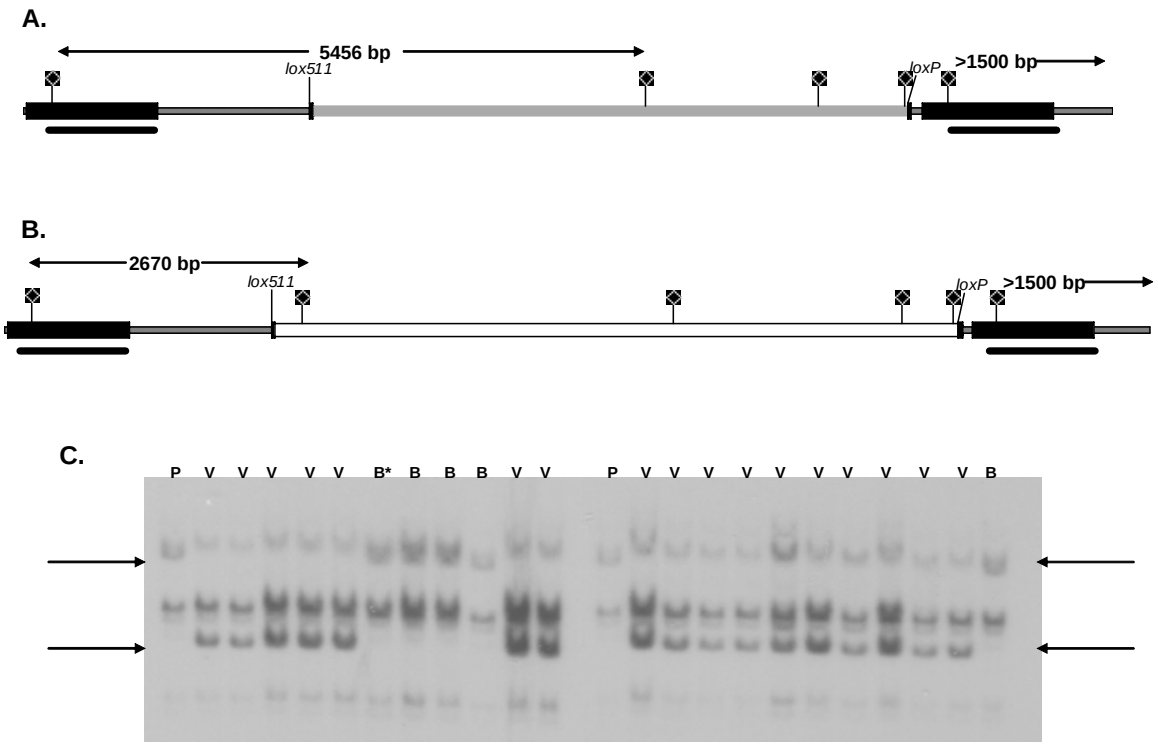

Figure 4.3. Southern Analysis of Stable Integrants That Arose From Acceptor Locus-Containing TERT(+) Cells Continuously Cultured in G418 Prior to Transfection. **A.** The integrated acceptor locus is expected to produce two fragments upon hybridization: one at 5,456 bp and one >1,510 bp. **B.** Upon RMCE-mediated integration of pBACeSVpuro, the 5,456 bp fragment is lost and replaced by one of 2,670 bp; the >1,510 bp band is unaffected. In both **A** and **B**, the probe is represented by a black line and the *Hind*III recognition sites by a diamond. **C.** gDNA prepared from stable integrants of a BAC vector containing SV40-*puro* (pBACeSVpuro), as well as integrants of a BAC reporter (117B23 cFtHRvSVP), digested with *Hind*III and hybridized with a probe specific to cHS4. All vector integrants were $Puro^R/Neo^S/GCV^R$. All BAC integrants were $Puro^R/Neo^R/GCV^S$ except for one that was $Puro^R/Neo^S/GCV^R$ (indicated by "*"). While nonspecific fragments are present, it can plainly be seen that all $Puro^R/Neo^S/GCV^R$ vector integrants ("V") are true RMCE integrants while the $Puro^R/Neo^R/GCV^S$ BAC integrants ("B") maintained the acceptor locus, as expected. Clone B* seems to have lost the acceptor locus, perhaps during the cloning process. Samples marked by "P" are parental acceptor locus-containing cells.

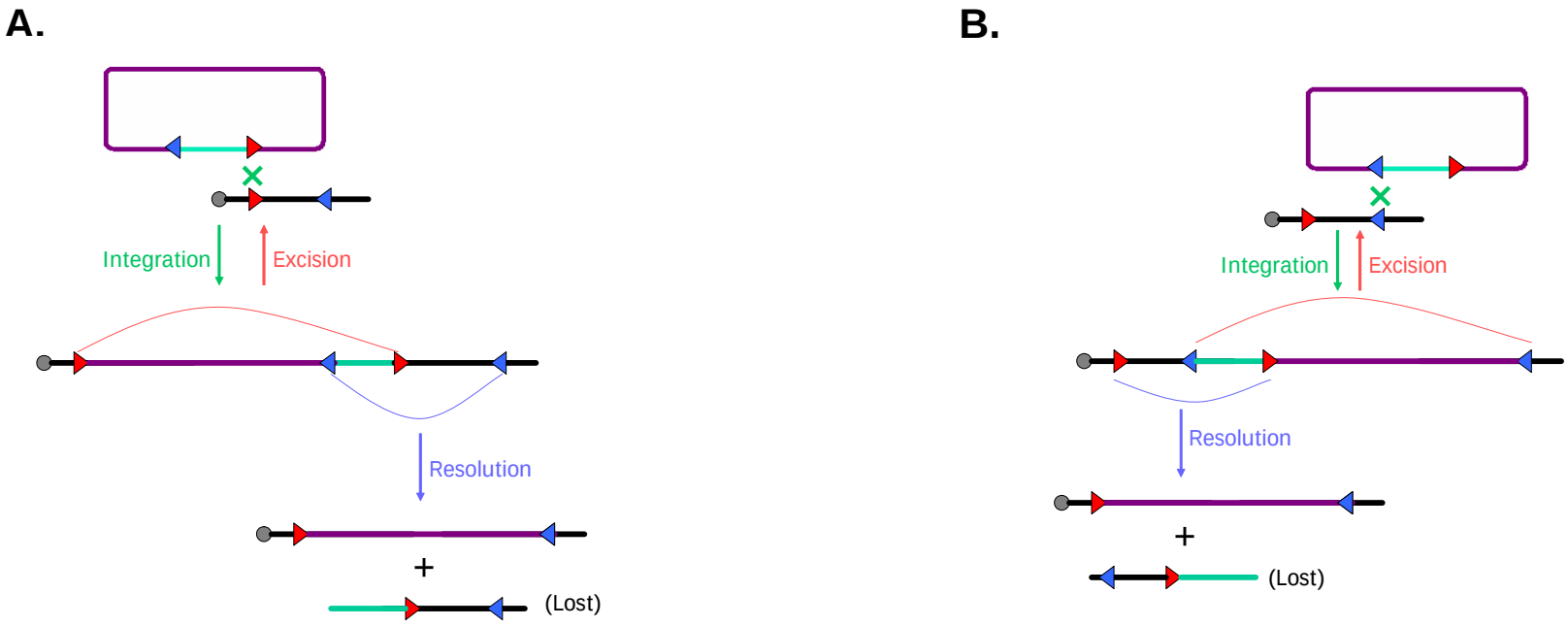

Figure 4.4. RMCE Proceeds Through Two Cre-mediated Recombinations. In the first, the BAC (represented in purple (genomic insert) and green (vector portion)) is integrated alongside of the integrated acceptor locus (black line) by recombination between either the *lox511* sites (**A**) or *loxP* sites (**B**). If Cre causes a recombination event between this same pair of *lox* sites (represented by the red line), the BAC will be excised and the acceptor locus reformed. If Cre recombination instead occurs through the other pair of *lox* sites (represented by the blue line), the acceptor locus will be lost and the BAC integrated in its place. Note: Figure not to scale.

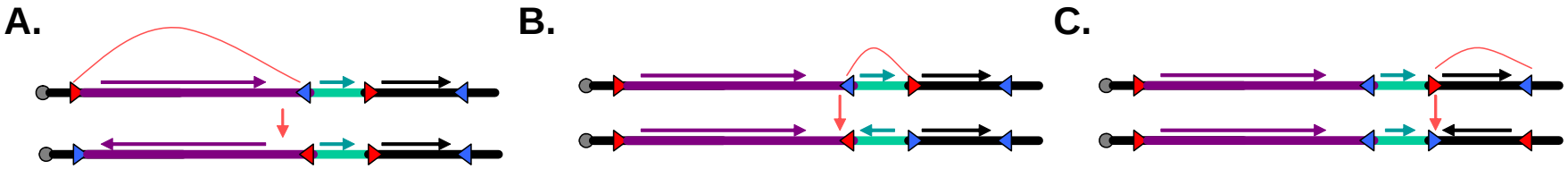

Figure 4.5. Heterospecific Cre/*lox*-mediated Recombination Following Initial Integration. The initial integration products, represented by the top line of **A-C**, are the result of Cre/*lox*-mediated recombination through the *lox511* sites (red triangles), although similar products could be visualized if initial integration proceeded through the *loxP* sites. Due to the promiscuity of the *lox511* and *loxP* sites, several additional Cre-mediated recombinant products are possible. These include recombination between the *lox511* and *loxP* sites of the BAC (**A**), recombination between the *loxP* site of the BAC and the *lox511* site of the acceptor locus (**B**), and recombination between the *lox511* and *loxP* sites of the acceptor locus (**C**). Note: Figures not to scale.

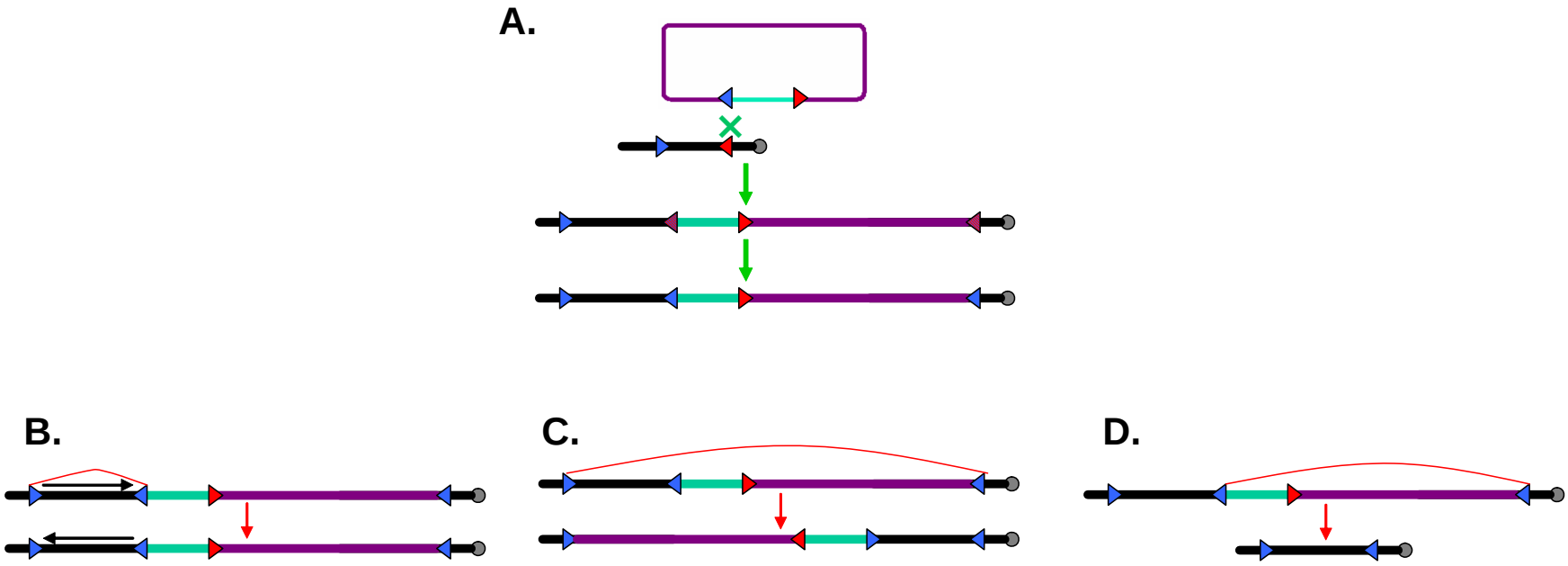

Figure 4.6. Initial Integration of BAC Reporter Mediated by Heterospecific *lox* Sites. **A.** Integration of the BAC reporter mediated through a *loxP* site (blue) of the BAC and the *lox511* site (red) of the acceptor locus will result in the creation of two *lox* sites containing C-A nucleotide mismatches (red and blue striped triangles of middle panel). Through DNA mismatch repair, the adenine will most likely be converted to guanine (530), creating wild-type *loxP* sites (blue triangles, bottom panel). **B-C** represent three of the possible Cre-mediated reactions that could occur following heterospecific integration. Note: Figures not to scale.

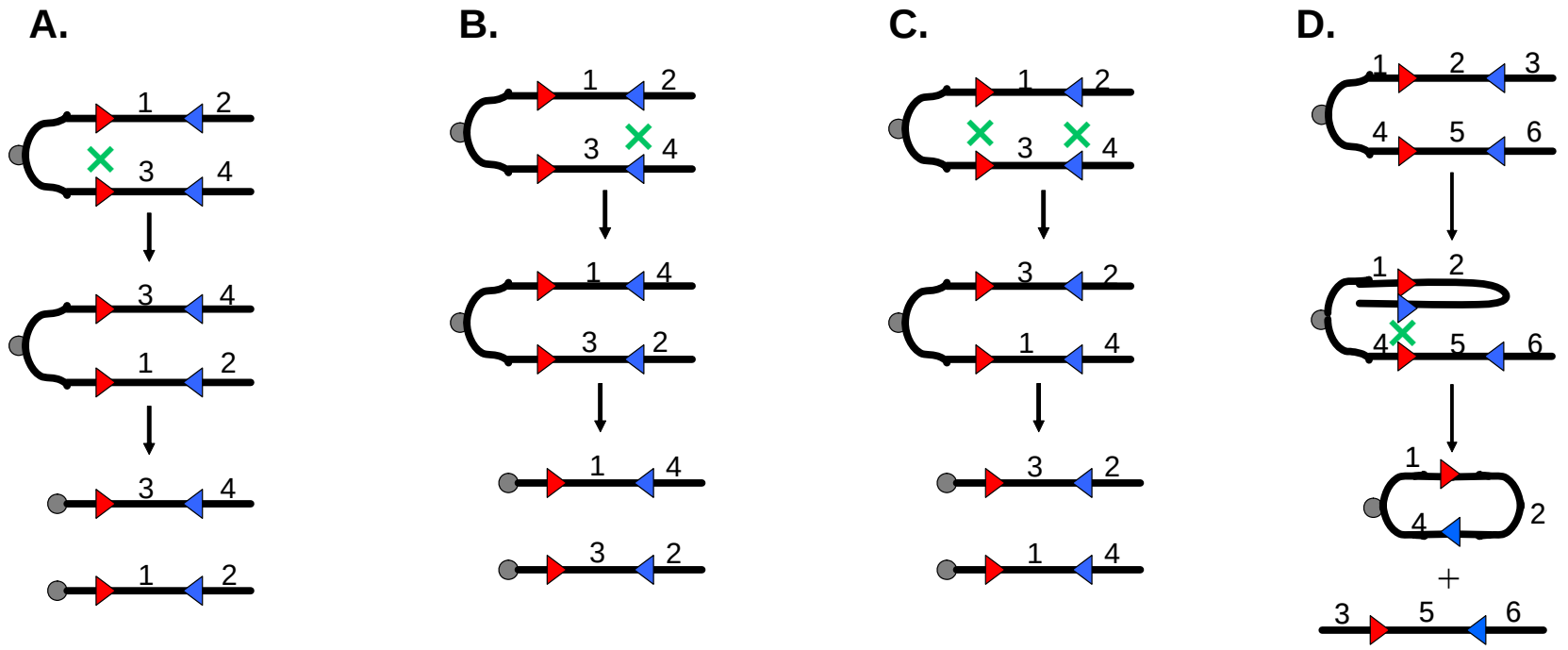

Figure 4.7. Potential Products Formed From Cre/*lox*-mediated Recombination of the Acceptor Locus During G2. **A-C**. Recombination between specific *lox* sites of sister chromatids results in the maintenance of the locus without any effect on the ability to undergo RMCE. **D.** Recombination between the *loxP* site (blue) of one chromatid and the *lox511* site (red) of the second chromatid results in the creation of a circular chromosome and loss of the acceptor locus, precluding RMCE. Notes: Not all possible products are shown. Figure not to scale.

Chapter 5
INTEGRATION OF PI-*Sce*I-LINEARIZED BACS

5.1 Introduction

The initial hypothesis of the project was that h*TERT* reporters constructed from a BAC and targeted to a preexisting acceptor locus via RMCE would mimic endogenous telomerase expression. However, as shown in Chapter 4, we were unable to obtain RMCE-mediated integrants of the BACs, and therefore, the original hypothesis was unable to be addressed. Due to the inability to target BAC reporters to the preexisting acceptor locus, we turned to studying random integrants of the BAC DNA. We theorized that this was possible as large transgenes randomly inserted into the mouse genome have been shown to recapitulate endogenous expression ((275;277;290); reviewed in (263)). To help eliminate the possibility of PEV and heterochromatin spreading, BAC reporters were prepared that contained two directly repeated copies of the cHS4 insulator immediately interior to each *lox* site of the BAC (Figure 5.1).

In this chapter, we address the hypothesis that h*TERT* BAC reporters linearized with the homing endonuclease PI-*Sce*I and randomly integrated into the genome of TERT(+) and (-) cells containing the acceptor locus are able to mimic endogenous telomerase activity. (This chapter is organized in the same way as Chapter 4.)

5.2 Materials and Methods

For the materials and methods used to prepare transfection-quality BAC DNA, see Section 4.2.1. For the standard culturing conditions and techniques used to transfect the TERT(+) and (-) cells and the CV1 cells, see Section 4.2.3. All experiments were performed in the TERT(+) acceptor locus line 167b 3.1 and the TERT(-) acceptor locus line 166a 11.1 as these two lines were shown to form more stable integrants and undergo RMCE of BAC vectors at a higher rate than other acceptor locus-containing lines (see Section 4.4.4 and Table C4 of Appendix C). Additionally, all experiments were performed with BAC reporters expressing firefly luciferase from *CRR9*, h*Renilla* luciferase from *TERT*, and SV40-*puro* from either *sacB* or the vector region immediately interior of *lox511*. Those experiments performed with reporters also containing dual-copy insulators are noted. Specific details are noted in the figure legends.

5.2.1 Linearization of BAC DNA with *PI-Sce*I

Approximately 20-30 µg of high quality BAC DNA was linearized in a 300 µl reaction with 20 U of the homing endonuclease *PI-Sce*I (NEB) by incubating at 37˚C anywhere from 5 hours to overnight. To monitor the quality of the DNA, 5 µl of the digest was subjected to pulse field gel electrophoresis (PFGE) through 1.0% agarose prepared with 05.X TBE using a CHEF-DRII apparatus (Bio-Rad). The PFGE parameters were as follows: 24 hour run time, 200 volts, initial switching time of 1 second, final switching time of 25 seconds, and switching ratio of one.

5.2.2 Electroporation of BAC DNA

Linearized BAC and BAC vector DNA was introduced to cells either via transfection by FuGENE-6 or electroporation. The DNA was not purified after linearization; therefore, the transfected DNA included components of the reaction mixture. For FuGENE-6 transfection of linearized BAC DNA, cells were transfected as previously indicated, with the following modifications: a ratio of 3 µl FuGENE-6

reagent to 2 µg DNA was used and the amount of BAC DNA was increased to 6 µg/well of a 12-well plate. For electroporation, 400 µl of cells (at a density of 4 x 10^6 cells/ml resuspended in OptiMEM) were electroporated in a 0.2 cm cuvette with 5 µg linearized BAC DNA using a BTX ECM-600 electroporator (Harvard Apparatus) set to low voltage mode, a capacitance of 500 µF, a resistance of 13 Ω, and a charging voltage of 150 V. Following electroporation, the cells were incubated on ice for 10 minutes and then transferred to a 10 cm dish with 8 ml standard medium. (These conditions were determined empirically. Results of the optimization process are found in Figures B7 and B8 of Appendix B.)

5.2.3 Isolation of Stably Transfected Clones

Forty-eight hours post-electroporation, the cells were treated with 250 ng/ml puromycin for four to six days. Following a period of two days growth in standard medium, puromycin was re-added for the duration of culture. Once individual colonies were large enough, they were cloned to one well of a 24-well plate using cloning cylinders. When the clones reached 90-100% confluence, they were sequentially expanded to one well of a 12-well plate and one well of a 6-well plate. Genomic DNA was prepared was prepared from 100% confluent wells of a 6-well plate. Frozen stocks were prepared from 100% confluent wells of a 6-well plate by washing the cells once in 1X PBS, resuspending in 1 ml standard medium supplemented with 5% DMSO, and storing in cryovials in liquid nitrogen.

5.2.4 Luciferase Assays

All materials and methods outlined in Section 4.2.5 apply for random integration with the exception that transient luciferase activity was measured 24 hours post-electroporation.

5.2.5 Southern Hybridization Analysis of Isolated Clones

Southern hybridization was performed as per Section 4.2.7. The probes used to hybridize the blots are summarized in Table 5.1. The expected hybridization fragments are shown in Figures 5.5 and 5.9.

5.2.6 PCR Analysis of Isolated Clones

PCR was performed on approximately 50 ng of gDNA prepared from the isolated clones. Each 10 µl PCR reaction contained 1X PCR buffer, the appropriate concentration of $MgCl_2$ (empirically determined), 0.3 mM dNTPs, 0.2 µM primers, and 0.5 U *Taq* DNA polymerase (Denville Scientific). Amplification was performed with 35 cycles of 30 seconds denaturation, 30 seconds annealing, and 45 seconds extension. For the identity of the primers and specific amplification parameters for each, please see Table 5.2.

5.3 Experimental Design

5.3.1 PI-*Sce*I-Mediated Linearization of BAC Reporters

The luciferase activity after transient FuGENE-6-mediated transfection of linearized BAC DNA was compared to that of circular BAC DNA. The linearization of the BAC reporters with the homing endonuclease PI-*Sce*I also allowed the quality of the BAC DNA to be assessed. As can be seen in Figure 5.2A, clean, intact BAC DNA appears as a single fragment located at approximately the expected molecular weight and shows minimal smearing at lower molecular weights. BAC DNA that has been fragmented appears as a less distinct band at the expected molecular weight and shows substantial smearing at lower molecular weights (Figure 5.2B). Only clean, intact BAC DNA was used for integration studies.

5.3.2 Cre/*lox*-mediated Integration of PI-*Sce*I-Linearized BAC Reporters

To determine if linearized BAC reporters were able to undergo RMCE, TERT(+) and (-) cells were co-transfected with pCBM and PI-*Sce*I-linearized BAC DNA. Following transfection with FuGENE-6 (Roche), cells were selected with puromycin. Puromycin-resistant colonies were cloned and expanded in order to monitor their sensitivity to G418 and GCV, to measure their luciferase activity, and to harvest gDNA for PCR and Southern analysis. Each individual clone was characterized by its G418 and GCV sensitivity, its luciferase activity, the presence of PCR products specific for the acceptor locus, the presence of PCR products specific for the recombined locus, and Southern hybridization patterns of relevant markers present on the BAC.

To determine if DNA introduced by electroporation was able to undergo RMCE, TERT(+) and (-) cells were co-electroporated with pCBM and PI-*Sce*I-linearized BAC DNA. Following electroporation, cells were selected with puromycin. Puromycin-resistant colonies were cloned and expanded in order to monitor their sensitivity to G418 and GCV, to measure their luciferase activity, and to harvest gDNA for PCR and Southern analysis. Each individual clone was characterized by its G418 and GCV

sensitivity, its luciferase activity, the presence of PCR products specific for the acceptor locus, the presence of PCR products specific for the recombined locus, and/or Southern hybridization patterns of relevant markers present on the BAC.

5.3.3 Random Integration of PI-*Sce*I-Linearized BAC Reporters

To determine if randomly integrated BAC reporters were able to mimic endogenous telomerase activity, TERT(+) and (-) cells were electroporated with PI-*Sce*I-linearized BAC reporters. To determine if the presence of dual-copy insulators had any effect on whether or not the BAC reporters would mimic endogenous telomerase expression, TERT(+) and (-) cells were electroporated with PI-*Sce*I-linearized BAC reporters and compared to the same cells electroporated with the same BAC that additionally contained dual-copy insulators interior of both the *lox511* and *loxP* sites. Following electroporation, cells were selected with puromycin. Puromycin-resistant colonies were cloned and expanded in order to measure their luciferase activity and to harvest gDNA for PCR and Southern analyses. Each individual clone was characterized by its luciferase activity, the amplification of PCR products specific to the BAC, and/or Southern hybridization patterns of relevant markers present on the BAC.

5.4 Results and Discussion

In this chapter we addressed the hypothesis that stably integrated, h*TERT* reporters are able to mimic endogenous telomerase activity in genetically related TERT(+) and (-) cell lines. To test this hypothesis, we introduced PI-*Sce*I-linearized, h*TERT*-containing BACs modified to express luciferase ORFs (see Chapter 3) to the preexisting acceptor locus (see Chapter 2) via electroporation. In this chapter we also addressed the hypothesis that randomly integrated, linearized BAC reporters containing dual-copy insulators on either end would be less susceptible to PEV and heterochromatin silencing and therefore, more likely to recapitulate endogenous telomerase expression. To test this hypothesis, we compared the results of electroporation of BACs containing the insulators to the results of those that did not.

5.4.1 Luciferase Activity of PI-*Sce*I-Linearized BAC Reporters

As was discussed in Sections 4.4.4 and 4.4.5, very few stable integrants obtained after transfection of circular h*TERT* BAC reporters expressed both luciferase activities, and none were RMCE integrants. We hypothesized that the problem could be that the circular BAC DNA was breaking somewhere between the *CRR9* and *TERT* loci, thus separating the luciferase ORFs from each other and preventing RMCE from occurring as desired. Furthermore, we thought that this problem could be eliminated by linearizing the BAC at a site that would not interfere with RMCE prior to its introduction to the cells. The location of a recognition site for the homing endonuclease PI-*Sce*I immediately upstream of *lox511* allowed us to linearize the BAC reporters without separating the luciferase ORFs from one another or preventing RMCE (Figure 5.3). Unfortunately, the efficiency of transfection and electroporation of linearized DNA is not as efficient as that of circular DNA (531). Because BACs are already less efficiently transfected than small plasmids and our TERT(+) and (-) cells are less efficient at taking up the DNA (Section 4.4.1), we wanted to ensure that linearized BAC reporters were able to be successfully delivered to the TERT(+) and (-) cells. As can be seen in Figure 5.4A, both TERT(+) and TERT(-) cells showed luciferase activity 48 hours after transfection with a BAC

reporter linearized with PI-*Sce*I, although this activity was one order of magnitude less than cells transfected in parallel with the same BAC vector in its circular form. TERT(+) and (-) cells also expressed transient luciferase activity after electroporation of the linearized BAC reporter (Figure 5.4B). Based on the fact that linearized BAC DNA is able to be introduced to cells at a high enough efficiency to produce luciferase activity, future experiments were performed with PI-*Sce*I-linearized BAC reporters. The use of linearized transgenes is not a new concept as most transgenes are linearized prior to their introduction to mouse ES cells (532;533).

5.4.2 Attempts to Target PI-*Sce*I-Linearized BAC Reporters via RMCE

Using transfection with FuGENE-6, we attempted to target linearized BAC reporters to the preexisting acceptor locus via RMCE. Co-transfection of TERT(+) cells with pCBM and linearized BAC DNA resulted in two stable integrants, neither of which expressed luciferase activity nor were RMCE integrants based on their drug sensitivity. The same experiment performed in TERT(-) cells failed to produce any stable integrants after puromycin selection (Table C12 of Appendix C).

To determine if electroporation was able to support RMCE of linearized BAC reporters, TERT(+) and (-) cells were electroporated with pCBM and the linearized BAC reporter. Electroporation of TERT(+) cells resulted in the formation of 29 stable integrants. Only two (6.90%) of these stable integrants expressed both luciferase activities, and none were RMCE integrants based on their drug sensitivity. Electroporation of TERT(-) cells resulted in 17 stable integrants, but none expressed both luciferase activities or were the result of RMCE based on their drug sensitivity (Table C13 of Appendix C). Based on these results, it seems that linearized BACs are no more able to undergo RMCE than circular BACs, although it is possible that with further experimentation and optimization it would be possible to obtain RMCE integrants of PI-*Sce*I-linearized BAC reporters.

5.4.3 Random Integration of PI-*Sce*I-Linearized BAC Reporters

Because we were unable to target BAC reporters to the preexisting acceptor locus through RMCE, we looked to random integration of linearized BAC reporters to address the hypothesis that h*TERT* reporters constructed from BACs are able to mimic endogenous telomerase expression in genetically related TERT(+) and (-) cells. In the course of the experiments outlined in Chapter 4, random integrants were generated (see Table C13 of Appendix C). However, because these random integrants were created using circular BAC reporters, they were not useful for addressing the hypothesis (see Section 4.5.1). Generation of random integrants in TERT(+) and (-) cells via transfection of linearized BAC reporters was inefficient (Table C13 of Appendix C). Based on these results and those of Sections 5.4.1 and 5.4.2, future attempts at generating random integrants were performed using reporters introduced to the TERT(+) and (-) cells by electroporation.

The characterization of the stable integrants began during the expansion period by the repeated assessment of luciferase activity. Each individual clone was characterized by the presence or absence of both firefly and h*Renilla* luciferases, originating from the *CRR9* and *TERT* loci, respectively. The clones were internally consistent from one assay to the next; i.e., if a clone expressed h*Renilla* luciferase in one assay it expressed it in all assays (see Tables D7-D10 of Appendix D). This indicates the stability of the integrated DNA and the lack of silencing over periods as long as 88 days post-electroporation (see Table D1 of Appendix D).

The next step in the analysis of the stable integrants was to assess the gDNA for the presence of the firefly and h*Renilla* loci through Southern hybridization. A number of outcomes are possible when comparing the results of Southern hybridization and luciferase activity. Using the TERT(+) clones 401-419 (Figure 5.6) and the TERT(-) clones 301-329 (Figure 5.7), the interpretation of each of these scenarios will be addressed. (Data on additional clones is found in Appendix D). The most straight-forward result is when a clone expresses luciferase activity and shows a fragment of the expected size when hybridized with a probe specific for that luciferase ORF. Of the 11 TERT(+) and eight TERT(-) clones that expressed firefly and/or h*Renilla* luciferase

activity, eight (72.73%) and eight (100%) displayed a fragment of the expected size after hybridization with the same luciferase probe. Alternatively, a clone could express luciferase activity but not show the expected fragment upon hybridization with a luciferase probe; the three remaining TERT(+) clones fall into this category. One possible reason for the lack of specific hybridization is a failure of Southern analysis, most likely due to inferior gDNA quality. A second possible reason for the lack of specific hybridization is that the DNA underwent truncation and/or rearrangement upon integration, and therefore, the hybridized fragment is shifted. To distinguish between these two possibilities, the gDNA can be hybridized with a probe specific for a housekeeping gene such as β-actin. If the β-actin probe results in a fragment of the expected size, it could be concluded that the gDNA itself is fine and that the locus may have been rearranged; if hybridization with the probe fails, it can be concluded that the quality of the gDNA is sub-optimal. Alternatively, PCR with a primer pair specific to the luciferase ORF could be used to amplify the gDNA; results would be interpreted in a fashion similar to those of β-actin hybridization. PCR analysis of the three TERT(+) clones that failed to hybridize to the expected probe is shown in Figure 5.8A. The presence of a PCR product of the correct size for one of these clones indicates that the DNA underwent truncation or rearrangement upon insertion. The lack of a PCR product of the correct size for a second clone indicates its gDNA quality is poor. For true verification, Southern analysis with a housekeeping gene should be performed.

While not exhibited by any of the clones represented in Figures 5.6 and 5.7, a third possibility is that a stable integrant lacking luciferase activity shows a fragment of the expected size when hybridized with a luciferase-specific probe. There are numerous possible explanations for data such as this, and the explanations may be slightly different depending on which luciferase is in question and how much of the surrounding sequence is present. Possible explanations include PEV (if there are no insulators, if the insulators are unable to prevent PEV, or if only a small portion of the BAC containing the luciferase ORF integrated near a strong silencer), heterochromatin-induced silencing (see argument for PEV), and recapitulation of endogenous activity (i.e., gDNA of TERT(-) cells containing a stably integrated, intact BAC would be expected to hybridize to the h*Renilla* luciferase probe but not express h*Renilla* luciferase activity).

5.4.4 Do Randomly Integrated, PI-*Sce*I-linearized BAC Reporters Mimic Endogenous Telomerase Expression?

In order to assess whether or not PI-*Sce*I-linearized h*TERT* reporters are able to mimic endogenous telomerase expression in genetically related TERT(+) and (-) cells, the stable integrants were further characterized by PCR and/or additional Southern analysis. This additional analysis was necessary to make a correlation between the presence of the locus and its expression and draw sound conclusions on the ability of stably integrated BAC reporters to mimic endogenous h*TERT* activity. Because we are hypothesizing that chromatin and/or distant regulatory elements are critical to appropriate telomerase regulation, only those clones containing an intact BAC are useful for analysis. Therefore, the only clones that were considered for future analysis were 1) those clones that expressed both firefly and h*Renilla* luciferase activity and displayed fragments of the expected size upon hybridization and 2) those that showed specific hybridization of both fragments in the absence of firefly and/or h*Renilla* luciferase activity. Examination of the data from all electroporations performed with PI-*Sce*I-linearized BAC reporters (Figures 5.6 and 5.7 and Appendix D), regardless of the presence of dual-copy insulators or the location of SV40-*puro*, resulted in the identification of eight TERT(-) and 20 TERT(+) clones that warranted further study (Table 5.3).

PCR analysis of these 28 clones was performed with five diagnostic primer pairs (Table 5.2). All primer pairs successfully amplified products of the expected size except for InsL.2/MAL61, the primer pair specific for the presence of the insulators interior to *lox511*. Attempts to use a second primer pair for this end, MAL61/MAL59, also failed, and therefore, no PCR data was collected for the presence of the dual-copy insulators at the extreme 5' end of the linearized BAC reporters. The results of amplification with the remaining primer pairs are presented in Table 5.4. As can be seen, four of the five clones that could show product for all four markers clearly did. Two of these clones were TERT(+) (415 and 416) and two were TERT(-) (517 and 518). Of the remaining clones, nine showed products only for the luciferase ORFs, ten showed products for the luciferase ORFs and *cam*, two showed products for firefly luciferase only, and two more

showed specific products for FL and RL and an ambiguous product for *cam*. Overall, specific products for all available loci were able to be amplified from 12 clones.

Table 5.5 shows a comparison of the luciferase activity, presence of specific hybridization fragments, and PCR product amplification for each clone; the raw luciferase data can be found in Tables D1-D6 of Appendix D. The data in Table 5.5 reveals that those clones that expressed firefly luciferase activity but did not show a fragment of the expected size upon hybridization with a firefly luciferase probe were permissive for PCR amplification of the expected product with a primer pair specific for the firefly luciferase ORF. These results imply that the DNA is either rearranged or truncated in the area surrounding *CRR9*. As *CRR9* is located near the 5' terminus of the linearized BAC, it is possible that truncation resulted in a separation of adjacent *Bst*EII recognition sites that is too large to observe using the standard Southern techniques employed. To better address this concern, Southern hybridization could be performed on gDNA digested with one or more additional restriction endonucleases, providing a more detailed analysis of the integrated DNA.

By assessing the results of PCR amplification, Southern hybridization of firefly and h*Renilla* luciferase probes, and presence of luciferase activity, there are 12 clones that potentially contain an intact BAC and therefore have the ability to address whether or not PI-*Sce*I-linearized h*TERT* reporters constructed from BACs are able to mimic endogenous *TERT* activity in genetically related TERT(+) and (-) cells. Of these 12 clones, five are TERT(-) (505, 513, 517, 525, and 701) and seven are TERT(+) (3, 30, 41, 46, 209, 415, and 416). To thoroughly assess the integrity of the integrated BACs, Southern hybridization needs to be performed as fragment hybridization provides information on thousands of base pairs, as opposed to only the hundreds of base pairs provided by PCR amplification. Attempts to perform Southern hybridization with a probe specific to *cam* have been unsuccessful as the hybridizing fragment is expected to be greater than 6,431 bp; the use of a different restriction endonuclease would be necessary to obtain Southern data for *cam*. As of now, the representative integrants of Figures 5.6 and 5.7 have been hybridized with the cHS4 insulator probe (Figures 5.10 and 5.11). Careful analysis of the complex hybridization pattern of the previously identified clones 415, 416, 517, and 525 reveals the presence of all the fragments specific

for the integration of both the 5' and 3' ends of the linearized BAC (5,704 bp and 1,390 bp fragments, respectively), although clone 517 seemed to do so with a rearrangement of the acceptor locus (evidenced by the shift of the 2,589 bp fragment to ~5.5 kb). (More detailed analysis of the hybridization patterns is found in the legends of Figures 5.10 and 5.11.)

Based on the current data, it does not seem as if the randomly integrated, PI-*Sce*I-linearized h*TERT* BAC reporters are able to mimic the endogenous telomerase status of the TERT(+) and (-) cells. This conclusion is based on the fact that all 12 clones containing a seemingly intact BAC, regardless of the presence or absence of dual-copy insulators, expressed a high level of firefly luciferase activity and a low level of h*Renilla* luciferase activity. If the BAC was able to recapitulate endogenous telomerase expression, both firefly and h*Renilla* luciferase would be expressed at a high level in TERT(+) cells while only firefly luciferase activity would be expressed in TERT(-) cells. (These are the expected results because the firefly luciferase ORF is integrated at the start codon of the ubiquitously expressed *CRR9* gene (495;496) and the h*Renilla* luciferase ORF is integrated at the start codon of the differentially expressed *TERT* gene (see Section 1.3.4).)

While these results indicate that the BAC reporters are unable to recapitulate the telomerase expression of the crisis-derived TERT(+) and (-) fibroblasts, the BAC may actually be mimicking the telomerase status of normal fibroblasts. In 2003, Masutomi et al. reported that contrary to the established dogma, TERT was transiently expressed at a low level in BJ, TIG-3, and WI-38 presenescent fibroblasts (534). Using various experiments, they showed that this transient TERT expression occurred during S-phase of the cell cycle, and while the level was not sufficient to support telomerase activity, the expression was necessary for normal proliferation and cellular lifespan, as well as telomere capping. A later study by the same group indicated that transient TERT expression was critical to regulating the overall chromatin status and DNA damage response of the cells (535). The verification of this transient, low-level *TERT* expression in IMR-90 fibroblasts (536;537) raises the possibility that the low-level h*Renilla* luciferase activity observed in the TERT(+) and (-) clones could be representative of the endogenous, low-level TERT transcription in human fibroblasts. The fact that this TERT

expression occurs only transiently during S-phase of the cell cycle may also help to explain why the ratios of firefly to h*Renilla* luciferase expression, representative of the expression levels of *CRR9* and *TERT*, respectively, differ between clones and between different measurements of the same clone (Table 5.6). Ideally, if the BAC was integrated intact in a single copy and not subject to PEV, the ratio of firefly to h*Renilla* luciferase expression would be the same amongst all clones. However, because the cells were not synchronized prior to measurement, nor were they harvested at the same confluency each time, there was most likely a different proportion of cells in S-phase in different clones at different timepoints, and therefore, the expression of h*Renilla* luciferase was different. To formally test this hypothesis, the cells could be synchronized by serum starvation and harvested for luciferase activity assessment at different time points after synchronization. If the BAC was recapitulating telomerase expression patterns of normal fibroblasts, the ratio of firefly to h*Renilla* luciferase activity of cells in S-phase would be expected to be lower than the firefly to h*Renilla* ratio of cells in other stages of the cell cycle.

The fact that the BAC reporter is seemingly unable to duplicate the telomerase activation of the TERT(+) cells is not necessarily surprising when one considers their origin. As discussed in Chapter 2 and Section 4.4.3, the TERT(+) and (-) cells used in these studies are immortal clones that arose after IMR-90 fibroblasts stably expressing SV40 large T and small t antigens underwent crisis (192). These clones are known to be hyperdiploid ((192) and data not shown), and therefore, the telomerase activity of the TERT(+) cells could be due to amplification of the locus and/or translocation of the locus to a position under the influence of a strong promoter or enhancer. In fact, Southern analysis performed in the Zhu laboratory revealed there was a breakpoint near the *TERT* locus in the crisis-derived TERT(+) cells. Preliminary fluorescence *in situ* hybridization (FISH) analysis of the TERT(+) cells with a probe prepared from the same BAC used to create the reporter (117B23) revealed that there were at least four copies of the *TERT* locus in these cells (Figure 5.12). Therefore, it is likely that the telomerase activity observed in these cells is a result of translocation and duplication, not a fundamental change in the locus itself.

These results seem to indicate that perhaps the TERT(+) and (-) cells chosen for these studies may not be the best choice. In addition to their hyperdiploid karyotype with

TERT duplications and/or translocations, their low transfection efficiency (discussed in Section 4.4.5) and seeming propensity to fragment the BAC upon its entry into the cells are big concerns. As discussed in Section 5.4.1, it was hypothesized that forcing the BAC reporter to break at a predetermined site that would not interfere with the genomic insert would increase the number of clones that were the result of integration of intact BACs. Unfortunately, this may not be the case. Even though the integrity of the PI-*Sce*I-linearized BAC DNA was verified by PFGE prior to electroporation, the majority of clones still did not express an intact BAC. Out of a total of 186 stable integrants obtained by electroporation of cleanly linearized BAC reporters, only 12 (6.45%) were intact, as determined by luciferase assays and PCR amplification and Southern hybridization with primers and probes specific for the luciferase ORFs, the dual-copy insulators, and *cam* (Figures 5.5 and 5.6 and Appendix D). This seems to indicate that there is some intrinsic pathway in the cells that results in the fragmentation of the BAC. (See 4.4.5 for further discussion on the fragmentation of transfected DNA.)

Another reason the BAC reporters may not recapitulate endogenous telomerase expression is because the necessary regulatory regions are not encompassed by the BAC. (While this may be unlikely due to the fact that the natural state of *TERT* is repression and the locus seems to be mostly repressed in both TERT(+) and (-) cells, this concern will be addressed for the sake of thoroughness.) Even though this BAC seems ideal for the study of *TERT* (see Section 3.4), it may still be missing important regulatory sequence that is located beyond the BAC ends. There is evidence in the literature indicating regulatory elements can be located as far as 1 Mb from their target (388-390). Alternatively, even if the BAC looks to be completely intact upon Southern hybridization analysis with all appropriate probes, there could still be microdeletions and rearrangements that are not detected. If these changes occur in a region necessary for appropriate TERT regulation, the results become very difficult to interpret. Even though BACs are hypothesized to re-form the native chromatin environment upon integration at a transgenic locus, it is not necessarily known that they will do so. Therefore, if the state of the chromatin is critical for appropriate h*TERT* regulation, as hypothesized (235), the failure of the BAC to recapitulate the endogenous chromatin environment will result in its failure to mimic endogenous telomerase expression. By performing DNaseI

hypersensitivity studies on the DNA of stable integrants with a probe specific for h*Renilla*, it might be possible to determine if the BAC does recapitulate the endogenous chromatin environment. (A paper in press from the Zhu laboratory indicates that a modified BAC reporter expressing *Renilla* luciferase from *CRR9*, firefly luciferase from *TERT*, and mPGK-*puro* from within *sacB* stably integrated into murine ES cells does recapitulate the endogenous h*TERT* chromatin environment (538)).

Overall, the currently available results seem to suggest that human telomerase reporters based on BACs are unable to mimic endogenous luciferase activity. Further experiments are necessary to support this preliminary conclusion. These future experiments should include attempts to increase the scale of the experiments in order to obtain more stable integrants, analysis of the chromatin status of intact, integrated BAC DNA, and attempts to use a different model system. (Additional information concerning potential future experiments can be found in Chapter 6.)

Probe	Source	Size
cHS4	pks-2X Ins	1.2 kb
Firefly Luciferase	pML4	332 bp
h*Renilla* Luciferase	pYF10-hRL	219 bp
cam	pBACeSVpuro	519 bp
β-actin	Human gDNA	499 bp

Table 5.1. Probes Used for Southern Hybridization Analysis of Stable Integrants. The cHS4 probe was isolated from pks-2X Ins by restriction endonuclease digestion with *Xba*I. The *cam* probe was created by PCR amplification of pBACeSVpuro using the primers Cm.F (5'-TCCGGCCTTTATTCACATTC-3') and Cm.R (5'-GGGCACCAATAA CTGCCTTA-3'). The β-actin gene probe was created by PCR amplification of human gDNA with the primers Actin.F (5'-AGAGCGAGAGCGAGATTGAG-3') and Actin.R (5'-GACTTCTAAGTGGCCGCAAG-3'). For the creation of the firefly and h*Renilla* luciferase probes, see the legend of Table 4.2.

Primer	Sequence
Cm.F	5'-TCCGGCCTTTATTCACATTC-3'
Cm.R	5'-GGGCACCAATAA CTGCCTTA-3'
FL.F	5'-TTTTCCGTCATCGTCTTTCC-3
FL.R	5'-TCAAAGAGGCGAACTGTGTG-3'
hRL.F	5'-TCGTCCATGCTGAGAGTGTC-3'
hRL.R	5'-CTAACCTCGCCCTTCTCCTT-3'
Ins.L2	5'-TTGGATCTGGATGAGCACTG-3'
loxP.InsL	5'-GTGCGCATAGAAATTGCATC-3'
Ins.R	5'-GAAGAGCTTGCCTGGAGAGA-3'
MAL61	5'-AAGCGGCCGCAAATTTATTA-3'

Primer Pair	Specificity	Size	Temp
Cm.F/Cm.R	*cam*	519 bp	60ºC
FL.F/FL.R	Firefly Luciferase	332 bp	60ºC
hRL.F/hRL.R	h*Renilla* Luciferase	219 bp	63ºC
Ins.L2/MAL61	Dual-copy Insulators @ *lox511* end	434 bp	60ºC
loxP.InsL/Ins.R	Dual-copy Insulators @ *loxP* end	396 bp	60ºC

Table 5.2. Primer Pairs Used to Analyze Stable Integrants by PCR Amplification. The sequence of the individual primers is shown in the top panel while the specific primer pairs used for amplification are shown in the bottom panel. "Temp" refers to the annealing temperature. All amplifications were performed with 1.5 mM $MgCl_2$ in the reaction mixture.

		Firefly Luciferase (*CRR9* Locus)		hRenilla Luciferase (*TERT* Locus)	
	Clone	**Activity**	**Southern**	**Activity**	**Southern**
TERT(-) No Ins	111	+	a	-	a
	322	+	+	+	+
	529	+	a	+	a
	505	+	+	+	+
	513	+	+	+	+
	701	+	+	+	+
TERT(-) With Ins	517	+	+	+	+
	525	+	+	+	+
TERT(+) No Ins	3	+	+	+	+
	12	-	+	-	+
	18	+	+	+	+
	30	-	+	-	+
	34	-	-	-	+
	37	+	+	+	+
	41	+	+	+	+
	46	+	a	+	+
	209	+	+	-	+
	211	+	+	+	+
	215	+	-	+	+
	223	+	+	+	+
	401	+	-	+	+
	402	+	+	+	+
	405	+	+	+	+
	406	+	+	+	+
	601	+	+	+	+
TERT(+) With Ins	415	+	+	+	+
	416	+	+	+	+
	606	+	-	+	-

Table 5.3. Stable Integrants Identified for Further Study. For each clone, the firefly (reporter for *CRR9*) and h*Renilla* (reporter for *TERT*) luciferase activity is shown, as well as the presence of specific fragments upon hybridization with a luciferase-specific probe. a: Clones not assessed by Southern analysis.

	Clone	FL	RL	Cm	loxP
TERT(-) No Ins	111	+	-	-	b
	322	+	+	-	b
	529	+	+	-	b
	505	+	+	+	b
	513	+	+	+	b
	701	+	+	+	b
TERT(-) With Ins	517	+	+	+	+
	525	+	+	+	+
TERT(+) No Ins	3	+	+	+	b
	12	+	+	-	b
	18	+	+	-	b
	30	+	+	+	b
	34	+	+	+	b
	37	+	+	-	b
	41	+	+	+	b
	46	+	+	+	b
	209	+	+	a	b
	211	+	+	-	b
	215	+	+	+	b
	223	+	+	-	b
	401	+	+	+	b
	402	+	+	-	b
	405	+	+	-	b
	407	+	+	-	b
	601	+	+	a	b
TERT(+) With Ins	415	+	+	+	+
	416	+	+	+	+
	606	+	-	-	-

Table 5.4. Summary of PCR Amplification of Selected Stable Integrants. The 28 stable integrants identified for further characterization were used as the template for PCR amplification of FL (reporter for *CRR9*), RL (reporter for *TERT*), *cam* ("Cm"), and the dual-copy insulators inserted interior of *loxP* ("loxP"). Attempts to amplify the dual-copy insulators inserted interior of *lox511* were unsuccessful. a: The presence of the product is ambiguous for this clone. b: No product is expected as these clones are the result of integration of BACs that do not contain the dual-copy insulators. Overall, fifteen clones were able to support amplification of all possible markers, indicating these clones may contain an intact copy of the BAC reporter. While not shown, amplification of PI-*Sce*I-linearized BAC DNA resulted in products of the expected size for all primer pairs; amplification of gDNA from 166a 11.1 and 167b 3.1 cells resulted in no specific product formation.

		FL (*CRR9* Locus)			RL (*TERT* Locus)		
	Clone	**Activity**	**Southern**	**PCR**	**Activity**	**Southern**	**PCR**
TERT(-) No Ins	111	+	a	+	-	a	-
	322	+	+	+	+	+	+
	529	+	a	+	+	a	+
	505	+	+	+	+	+	+
	513	+	+	+	+	+	+
	701	+	+	+	+	+	+
TERT(-) With Ins	517	+	+	+	+	+	+
	525	+	+	+	+	+	+
TERT(+) No Ins	3	+	+	+	+	+	+
	12	-	+	+	-	+	+
	18	+	+	+	+	+	+
	30	-	+	+	-	+	+
	34	-	-	+	-	+	+
	37	+	+	+	+	+	+
	41	+	+	+	+	+	+
	46	+	a	+	+	+	+
	209	+	+	+	-	+	+
	211	+	+	+	+	+	+
	215	+	-	+	+	+	+
	223	+	+	+	+	+	+
	401	+	-	+	+	+	+
	402	+	+	+	+	+	+
	405	+	+	+	+	+	+
	406	+	+	+	+	+	+
	601	+	+	+	+	+	+
TERT(+) With Ins	415	+	+	+	+	+	+
	416	+	+	+	+	+	+
	606	+	-	+	+	-	-

Table 5.5. Comparison of Luciferase Activity, Specific Hybridization, and PCR Product Amplification of Selected Clones. The data in this table was compiled from Tables 5.3 and 5.4, and therefore, FL is the reporter for *CRR9* and RL is the reporter for *TERT*. a: Indicates clones were not hybridized with this probe.

		Measurement 1			Measurement 2			Measurement 3		
	Clone	FL (CRR9)	RL (TERT)	FL/RL	FL (CRR9)	RL (TERT)	FL/RL	FL (CRR9)	RL (TERT)	FL/RL
TERT(-) No Ins	505	41,017	1,976	20.76	-	-	-	-	-	-
	513	183,910	573,276	0.32	-	-	-	-	-	-
	701	155,440	1,735	89.59	-	-	-	-	-	-
TERT(-) With Ins	517	3,367	821	4.10	5,031	352	14.29	-	-	-
	525	146,352	1,346	108.73	125,313	399	314.07	-	-	-
TERT(+) No Ins	3	88,109	4,844	18.19	103,446	21,631	4.78	88,428	19,925	4.44
	30	59,198	1,099	53.87	-	-	-	-	-	-
	41	76,439	12,547	6.09	333,919	75,163	4.44	438,862	40,994	10.71
	46	16,205	59	274.66	152,273	407	374.14	89,115	900	99.02
	209	5,525	27	204.63	-	-	-	-	-	-
TERT(+) With Ins	415	33,090	134	246.94	28,603	222	128.84	-	-	-
	416	42,043	818	51.40	92,772	1,056	87.85	-	-	-

Table 5.6. Ratio of Firefly to h*Renilla* Luciferase Activity in the Potentially Intact Integrants. For each clone, the firefly and h*Renilla* luciferase values represented are in RLU/s. The firefly to h*Renilla* luciferase activity ratio represents the relative activity of the *CRR9* and *TERT* loci in each individual clone at the indicated measurement.

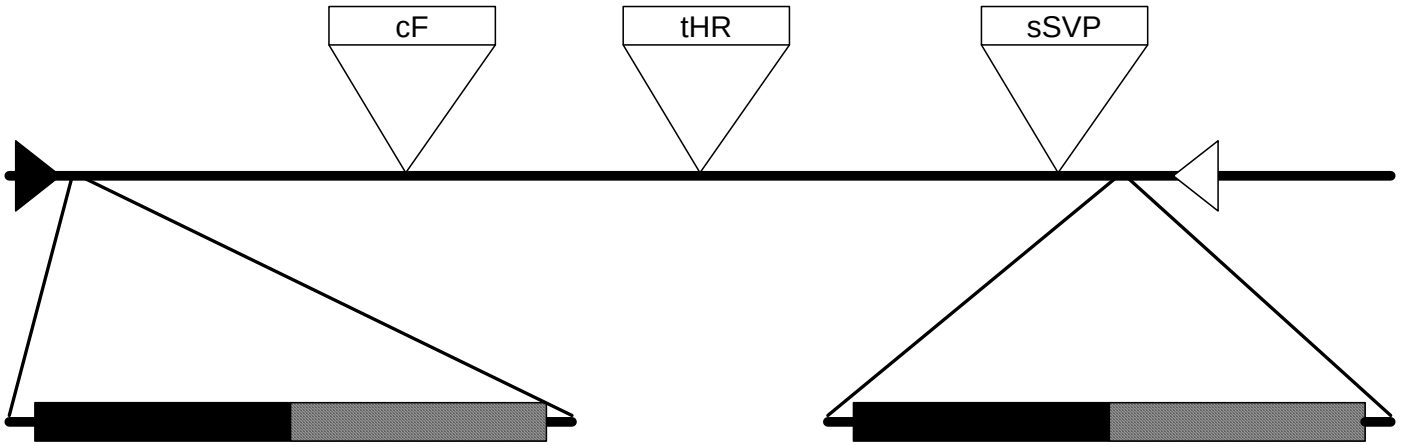

Figure 5.1. h*TERT* BAC Reporter with Dual-Copy Insulators. The h*TERT*-containing BAC 117B23 was modified to express firefly luciferase from the *CRR9* locus ("cF"), h*Renilla* luciferase from the *TERT* locus ("tHR"), SV40-*puro* from within *sacB* of the BAC vector sequence ("sSVP"), and dual-copy insulators interior of the *lox* sites (solid and hatched boxes). At the 5' end, the insulators are immediately adjacent to *lox511* (closed triangle). At the 3' end, the insulators are 250 bp upstream of *loxP* (open triangle).

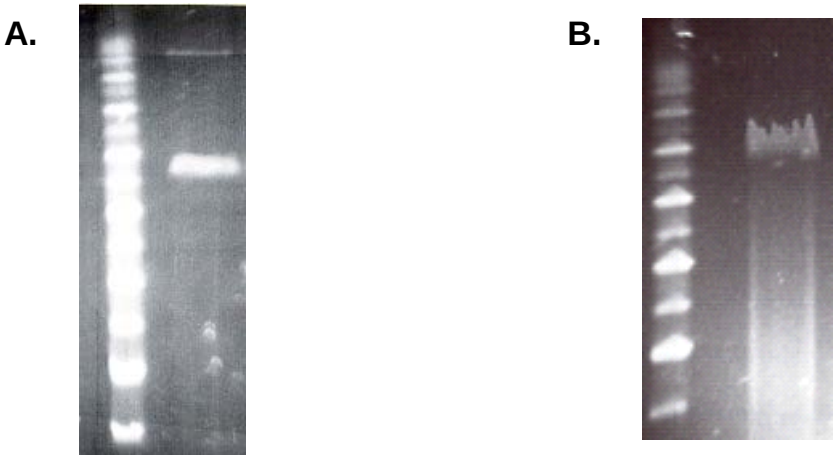

Figure 5.2. Examples of BAC DNA Electrophoresed by PFGE. PI-*Sce*I-linearized BAC DNA was electrophoresed through 1% agarose prepared in 0.5X TBE using PFGE and the parameters indicated in Section 4.2.2. **A.** Ethidium bromide-stained gel of clean, non-degraded BAC DNA. **B.** Ethidium bromide-stained gel of degraded BAC DNA.

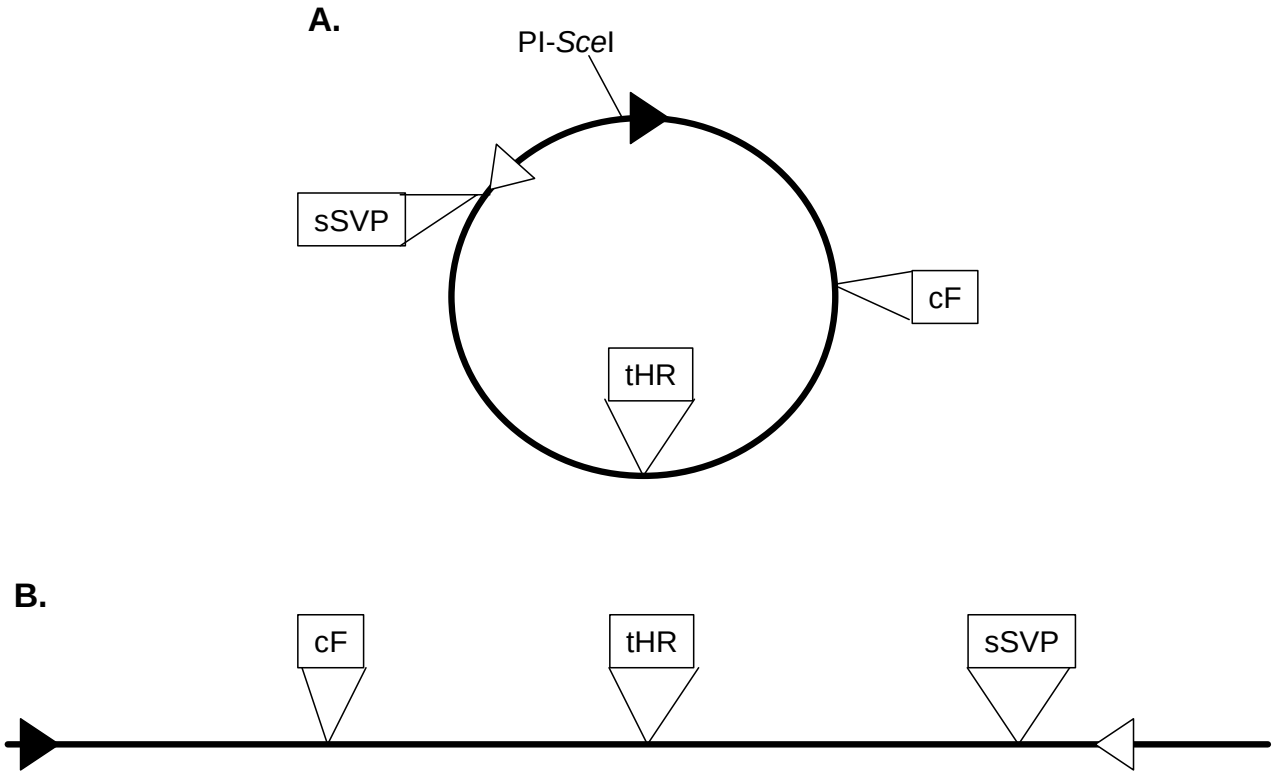

Figure 5.3. Linearization of BAC Reporters With PI-*Sce*I. **A.** The circular BAC reporter represented here expresses firefly luciferase from *CRR9* ("cF"), h*Renilla* luciferase from *TERT* ("tHR"), and SV40-*puro* from *sacB* ("sSVP"). The location of the PI-*Sce*I homing endonuclease recognition site is indicated. **B.** After linearization with PI-*Sce*I, the luciferase ORFs remain adjacent to each other and the *lox* sites are maintained in the orientation required for RMCE. Notes: In both **A** and **B**, l*ox511* is represented as a black triangle and *loxP* as a white triangle. Figure not to scale.

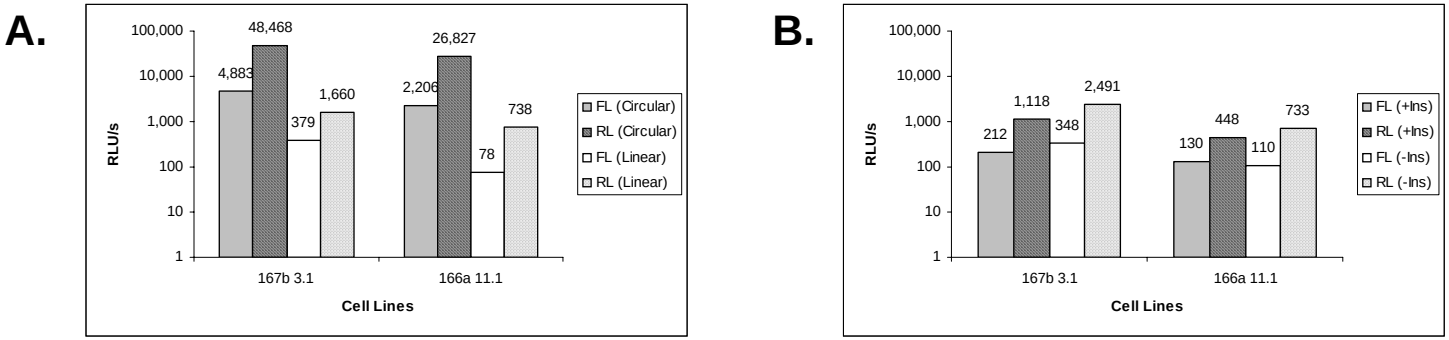

Figure 5.4. Transient Luciferase Activity of PI-*Sce*I-Linearized h*TERT* BAC Reporters. **A.** The firefly (reporter for *CRR9*) and *Renilla* (reporter for *TERT*) luciferase activity of the TERT(+) acceptor locus-containing line 167b 3.1 and TERT(-) line 166a 11.1 48 hours post-transfection of either circular or PI-*Sce*I-linearized 117B23 cFtHRvSVP. **B.** The firefly (reporter for *CRR9*) and *Renilla* (reporter for *TERT*) luciferase activity of 167b 3.1 and 166a 11.1 cells 24 hours post-electroporation of PI-*Sce*I-linearized 117B23 cFtHRsSVP or 117B23 cFtHRsSVP2xIns. Note: All luciferase activity is plotted on a logarithmic scale and corrected for background autoluminescence.

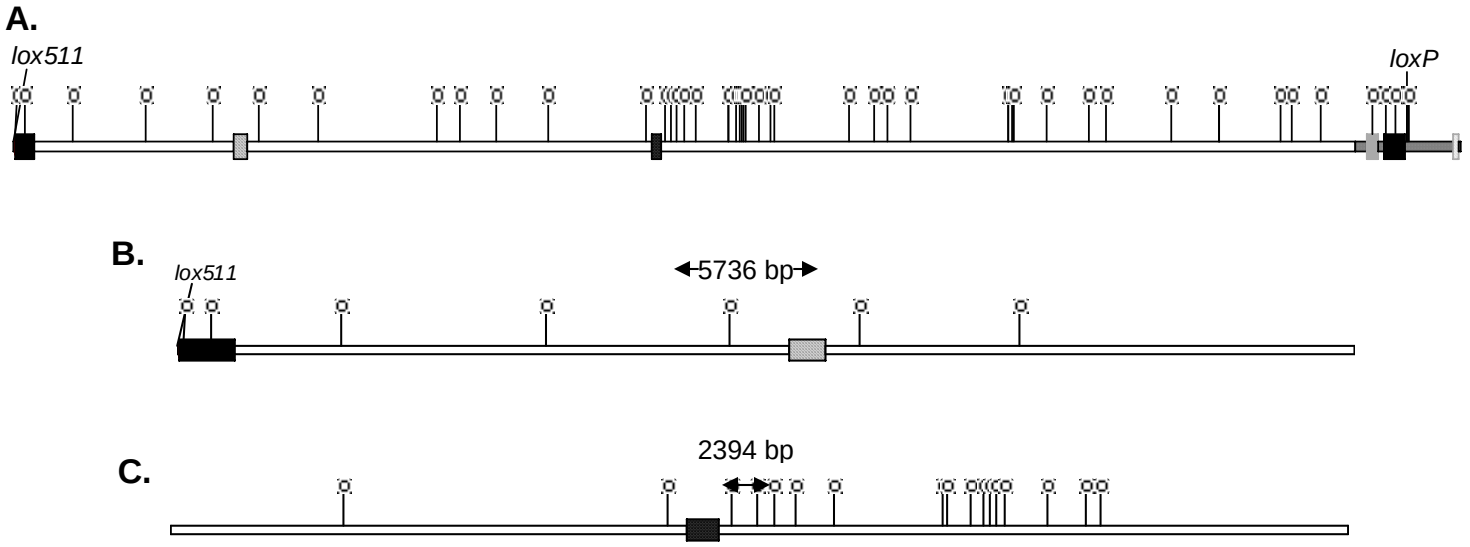

Figure 5.5. Fragments Expected Upon Southern Hybridization with FL- and hRL-Specific Probes. In **A-C**, the PI-*Sce*I-linearized version of a BAC expressing firefly luciferase from *CRR9* (black hatched box), h*Renilla* luciferase from *TERT* (dotted box), SV40-*puro* from *sacB* (solid gray box), and dual-copy cHS4 insulators interior of the *lox* site (solid black boxes). Additionally, genomic sequence is represented as white boxes and vector sequence as thin, patterned boxes. *Bst*EII restriction endonuclease recognition sites are represented as white circles. **A.** Overall view of the linearized reporter. The location of the *loxP* and *lox511* sites is indicated; *cam* is represented as a hatched gray box. **B.** The genomic region surrounding firefly luciferase integrated at *CRR9*. An intact BAC will produce a fragment of 5,736 bp upon hybridization with a firefly luciferase probe. **C.** The genomic region surrounding h*Renilla* luciferase integrated at *TERT*. An intact BAC will produce a fragment of 2,394 bp upon hybridization with an h*Renilla* luciferase probe. Note: Figures not to scale.

A.

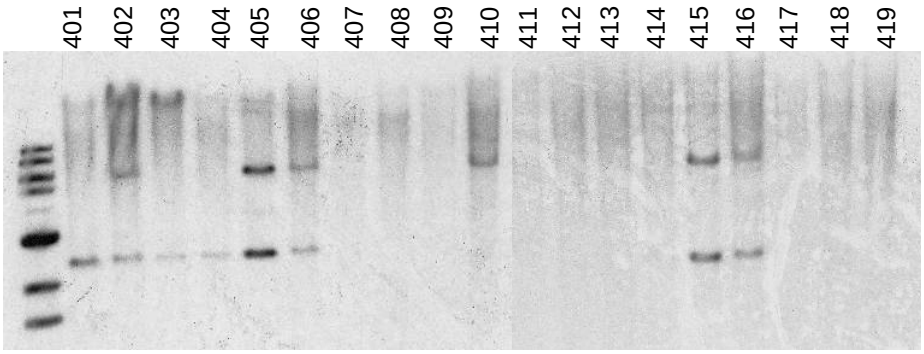

B.

Clone	Activity		Southern	
	FL	RL	FL	RL
401	+	+	-	+
402	+	+	+	+
403	-	+	-	+
404	-	+	-	+
405	+	+	+	+
406	+	+	+	+
407	-	-	-	-
408	-	-	-	-
409	-	-	-	-
410	+	-	+	-
411	-	-	-	-
412	-	-	-	-
413	-	-	-	-
414	+	-	-	-
415	+	+	+	+
416	+	+	+	+
417	-	-	-	-
418	+	-	-	-
419	-	-	-	-

Figure 5.6. Correlation of Luciferase Activity and Presence of Specific Hybridization Fragments for TERT(+) Cells. Cells of the TERT(+) acceptor locus-containing line 167b 3.1 were electroporated with PI-*Sce*I-linearized 117B23 cFtHRsSVP with and without dual-copy insulators. Stable integrants were obtained through puromcyin selection, tested for luciferase activity, and expanded for gDNA harvest. **A.** Southern hybridization with probes specific for firefly (FL) and h*Renilla* luciferase (RL) of gDNA digested with *Bst*EII. The expected fragment size for FL (*CRR9*) is 5,736 bp; the expected fragment size for RL (*TERT*) is 2,394 bp. **B.** Table representing the near-perfect correlation of luciferase activity and presence of the locus. Only two clones do not match; both clones 401 and 419 expressed firefly luciferase activity but did not show a hybridization fragment of the expected size. The most likely reason for the lack of a specific fragment is that the 5' end of the BAC was truncated, causing the loss of the terminal *Bst*EII site. Loss of this site implies that the hybridizing fragment will be greater than the expected size, and could perhaps not be visualized under the Southern conditions employed.

A.

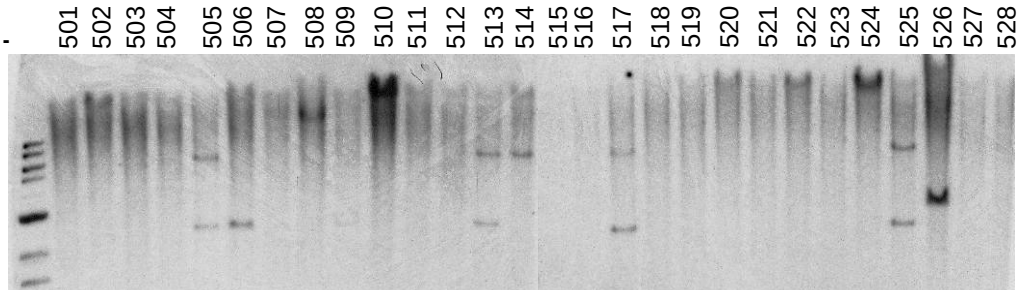

B.

Clone	Activity		Southern	
	FL	RL	FL	RL
501	-	-	-	-
502	-	-	-	-
503	-	-	-	-
504	-	-	-	-
505	+	+	+	+
506	-	+	-	+
507	-	-	-	-
508	-	-	-	-
509	-	+	-	+
510	-	-	-	-
511	-	-	-	-
512	-	-	-	-
513	+	+	+	+
514	+	-	+	-
515	-	-	-	-
516	-	-	-	-
517	+	+	+	+
518	-	-	-	-
519	-	-	-	-
520	-	-	-	-
521	-	-	-	-
522	-	-	-	-
523	-	-	-	-
524	-	-	-	-
525	+	+	+	+
526	-	+	-	+
527	-	-	-	-
528	-	-	-	-

Figure 5.7. Correlation of Luciferase Activity and Presence of Specific Hybridization Fragments for TERT(-) Cells. Cells of the TERT(-) acceptor locus-containing line 166a 11.1 were treated as the 167b 3.1 cells (see legend of Figure 5.5). **A.** Southern hybridization with probes specific for firefly (FL) and h*Renilla* luciferase (RL) of gDNA digested with *Bst*EII. The expected fragment size for FL (*CRR9*) is 5,736 bp; the expected fragment size for RL (*TERT*) is 2,394 bp. The RL fragment for clone 526 is larger than expected, indicating a deletion or rearrangement in the integrated DNA. **B.** Table representing the perfect correlation of luciferase activity and presence of the locus.

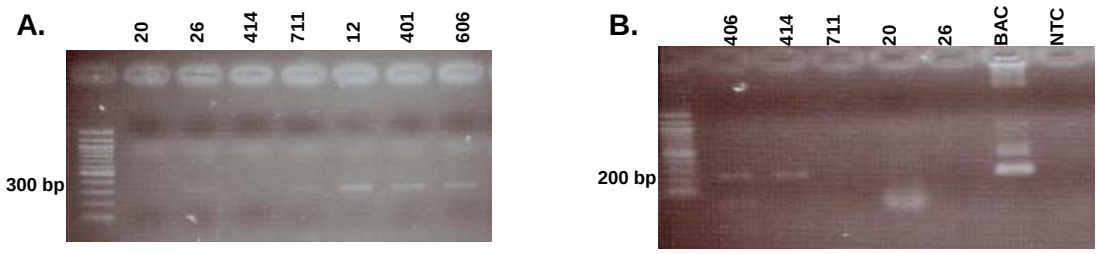

Figure 5.8. PCR Amplification to Address Clones Expressing Luciferase Activity But Not a Specific Band Upon Hybridization. **A.** PCR amplification with the firefly luciferase-specific primer pair FL.F/FL.R of clones stably expressing firefly luciferase activity but not a fragment upon Southern hybridization. Clones 26, 711, 12, and 401 all exhibit the expected product of 334 bp, indicating the BAC DNA was most likely truncated or rearranged in the region of *CRR9*. Clones 20 and 414 lacked a specific product, indicating the quality of the gDNA is not high enough to support analysis. Clone 606 served as the positive control. **B.** PCR amplification with the h*Renilla* luciferase-specific primer pair hRL.F/hRL.R of clones stably expressing firefly luciferase activity but not a fragment upon Southern hybridization. Clones 406 and 414 showed specific hybridization bands and therefore, served as positive controls, as did PI-*Sce*I-linearized BAC reporter DNA. NTC is the non-template control. The specific product (219 bp) failed to be amplified in clones 20 and 26, indicating the gDNA quality may be sub-par.

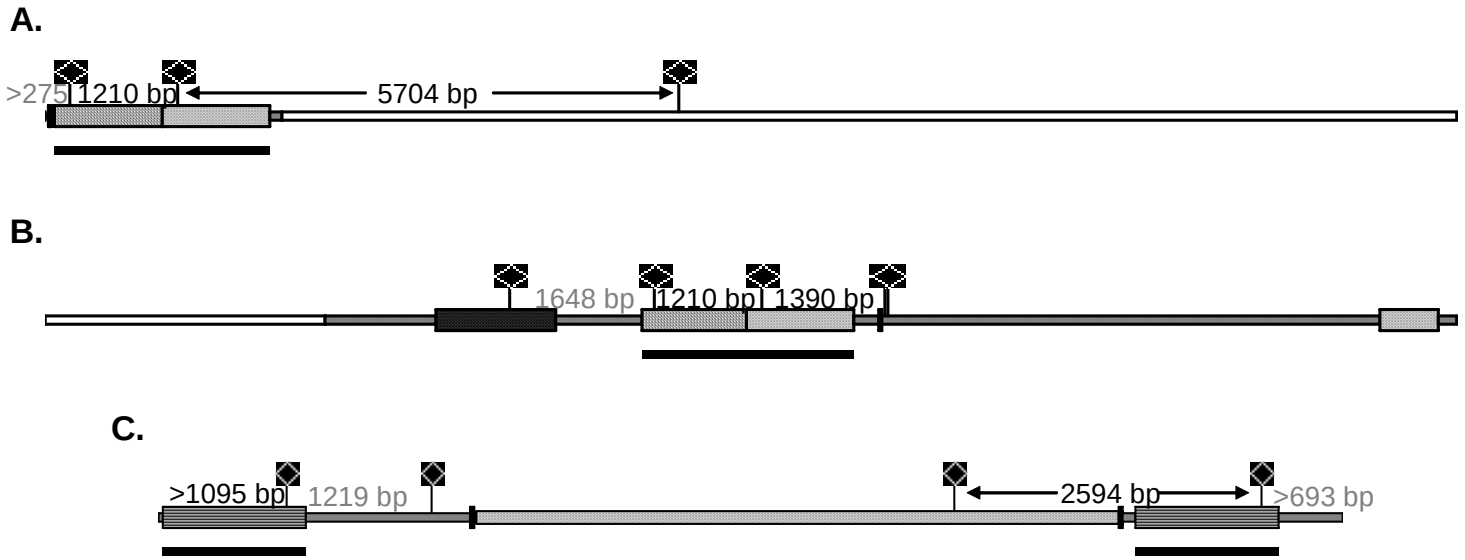

Figure 5.9. Fragments Expected Upon Southern Hybridization with an Insulator-Specific Probe. For general information, see legend of Figure 5.5. In **A-C**, all *Bst*EII restriction endonuclease recognition sites are represented as diamonds; the location of the probe is indicated below the schematic. **A.** Dual-copy insulators (dotted and hatched boxes) located interior of the *lox511* site (solid box). 16,000 bp of sequence is represented. Fragments of 1,210 and 5,704 bp are expected if the *lox511* end is present. An additional fragment of >275 bp may also be present, although its intensity will be less than that of the other two fragments. **B.** Dual-copy insulators (dotted and hatched boxes) located interior of the *loxP* site (solid box). 16,000 bp of sequence is represented. Fragments of 1,210 and 1,390 bp are expected if the *loxP* end is present. An additional fragment of 1,648 bp is also expected, but its intensity will be less than that of the other two fragments. **C.** The acceptor locus contains single-copy insulators (vertically striped boxes) on either end. Fragments of >1,095 and 2,594 bp are expected if the acceptor locus is maintained. Additional fragments of 1,219 and >693 bp are also expected, although their intensity will be decreased.

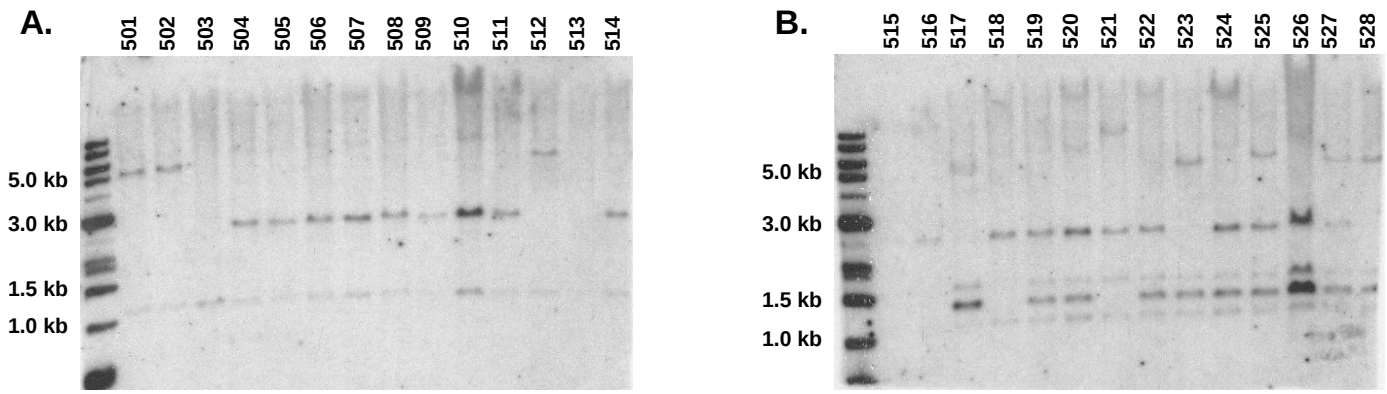

Figure 5.10. Southern Hybridization of TERT(-) Stable Integrants with Insulator Probe. The expected hybridization pattern is found in Figure 5.9. **A.** Clones 501-514 were obtained after integration of a BAC lacking the insulators. The 2,594 and1,219 bp fragments arising from integration of the acceptor locus are clearly observed for all clones except 501-503, 512, and 514. Clone 513 lacks both acceptor locus fragments; the specific hybridization of the probes for firefly and h*Renilla* luciferase (Figure 5.7A) indicates this clone lost the acceptor locus during expansion. Clone 503 shows only the 1,219 bp fragment, indicating there was a partial loss of the acceptor locus or a rearrangement. Clones 501, 502, and 512 all show the 1,210 bp fragment with the 2,594 bp fragment shifted to ~5.5 kb. This indicates some sort of rearrangement of the acceptor locus and could indicate that these clones are not independent of one another. (None of these three clones exhibited fragments specific for either luciferase ORF (Figure 5.7A). **B.** Clones 515-528 were obtained after integration of a BAC containing the insulators. Clones 515, 516, and 518 only show the fragments specific to the acceptor locus, indicating the BAC ends were not present. Clones 517, 523, and 528 are similar to clones 501, 502, and 512 in that the 2,594 bp fragment of the acceptor locus is shifted to ~5.5 kb. The diagnostic fragment for the dual-copy insulators located at the 5' end of the BAC is 5,704 bp; this fragment is seen in clones 517, 525, and 527. The diagnostic fragment for the dual-copy insulators located at the 3' end is 1,390 bp; this fragment is seen in all clones but 515, 516, 518, and 521. A less intense fragment of 1,648 bp is also expected to arise from the 3' end of the BAC; this fragment is seen in the same clones as the 1,390 bp fragment, as well as in clone 521. The presence of the 1,648 bp fragment in the absence of the 1,390 bp fragment in clone 521 indicates that perhaps the BAC was truncated somewhere in the first copy of the insulator.

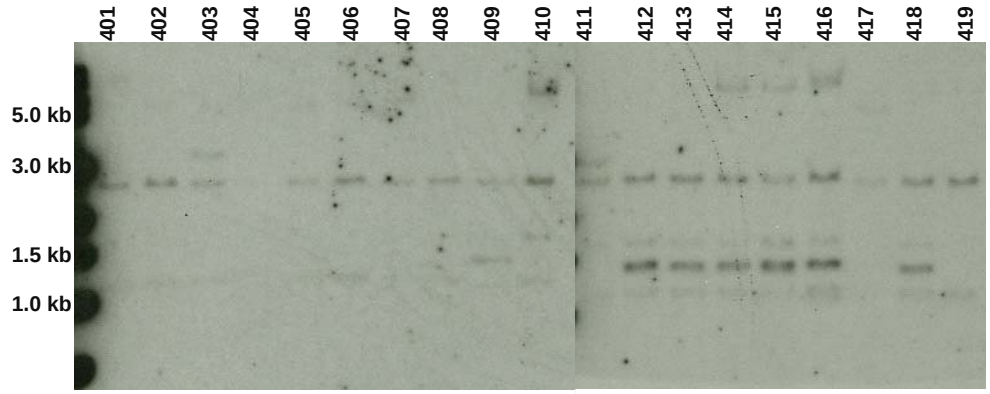

Figure 5.11. Southern Hybridization of TERT(+) Stable Integrants with Insulator Probe. The expected hybridization pattern is found in Figure 5.9. Clones 401-408 were obtained after integration of a BAC lacking the insulators. Clones 409-419 were obtained after integration of a BAC containing the insulators. The 2,594 and1,219 bp fragments arising from integration of the acceptor locus are visible for all clones except 404; the specific hybridization of the probe for h*Renilla* luciferase (Figure 5.6A) indicates this clone lost the acceptor locus during expansion. The fragment located at ~3.5 kb in clone 403 represents some sort of rearrangement of the acceptor locus. The diagnostic fragment for the dual-copy insulators located at the 5' end of the BAC is 5,704 bp; this fragment is seen in clones 410, 414, 415, and 416. The diagnostic fragment for the dual-copy insulators located at the 3' end is 1,390 bp; this fragment is seen in all clones but 410, 411, 417, and 419. A less intense fragment of 1,648 bp is also expected to arise from the 3' end of the BAC; this fragment is seen in the same clones as the 1,390 bp fragment, as well as in clone 410. The presence of the 1,648 bp fragment in the absence of the 1,390 bp fragment in clone 410 indicates that perhaps the BAC was truncated somewhere in the first copy of the insulator. Clones 411, 417, and 419 only show the fragments specific to the acceptor locus, indicating the BAC ends were not present.

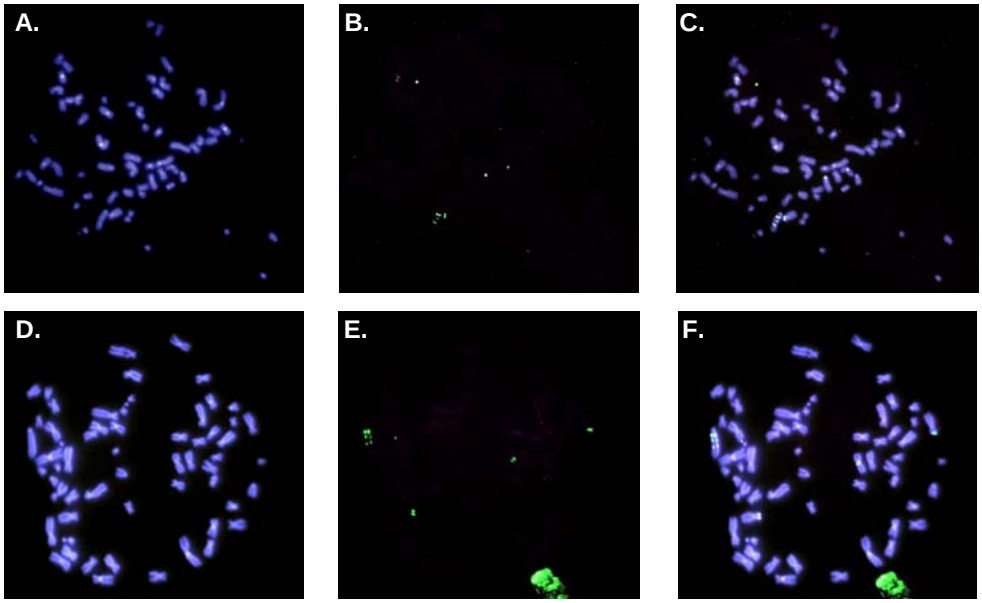

Figure 5.12. FISH Analysis of TERT(+) Cells. Chromosome spreads were prepared from proliferating TERT(+) cells after their arrest with colcemid. The results of FISH analysis using biotin-dUTP-labeled 117B23 as the probe are shown for two different nuclei (A-C and D-F). Chromosomes were visualized with DAPI (represented in blue) while 117B23 hybridization was visualized with avidin conjugated to AlexaFluor 488 (Molecular Probes, represented in green). A and D show the DAPI-stained chromosomes, B and E show the probe hybridization, and C and F are the merges of A and B and D and E, respectively. All images were captured on an Eclipse E1000 microscope (Nikon) equipped with an Orca model C4742-95 digital camera (Hamamatsu). Images were captured using Image-Pro plus 4.1 software (Media Cybernetics). For each field, the magnification is 400X.

CHAPTER 6

GENERAL DISCUSSION

6.1 Overview

The ends of all eukaryotic chromosomes are comprised of tandemly repeated sequences known as telomeres. Along with their host of associated proteins, telomeres form a protective cap that prevents critical genetic information from being lost during DNA replication and prevents end-to-end fusion of the linear eukaryotic chromosomes. Eukaryotes have the ability to lengthen their telomeres through the activity of telomerase, a ribonucleoprotein complex able to synthesize telomeric DNA. The telomerase RNA component (TERC) serves as the template for the addition of telomeric repeats by the telomerase reverse transcriptase (TERT). While all eukaryotes possess a telomerase reverse transcriptase, the expression of telomerase activity is species-dependant. In humans, telomerase activity is highly regulated. During embryogenesis and early development, telomerase activity is high. However, in the adult, telomerase activity is restricted to cells of the germline, some hematopoietic precursors, and the stem cells of tissues with a high turnover rate. The absence of telomerase activity has been shown to be due to the lack of expression of the TERT component as TERC is ubiquitously expressed in all cells at all times while only those cells displaying telomerase activity express TERT. The lack of an mRNA transcript of the *TERT* gene implies that TERT expression, and therefore telomerase activity, is regulated primarily at the level of *TERT* transcription.

Despite almost 25 years of study, the precise mechanisms governing human telomerase regulation have remained elusive. One of the main reasons for this is the lack of a powerful model system. While mouse genes are often used to characterize the regulation of their human counterparts, the more permissive expression of mouse telomerase (*Tert*) and the much longer telomeres of mouse chromosomes make it difficult to extrapolate information learned from *Tert* regulation to that of *TERT*. Furthermore, while gene regulation is often studied by using transiently transfected reporter constructs

containing promoter and/or potential regulatory elements of the gene of interest, the inability of small, transiently transfected *TERT* reporters to mimic endogenous telomerase expression makes them less useful. Based on these observations and others that indicated the status of chromatin surrounding *TERT* might be important for its appropriate regulation, we decided to evaluate the use of *TERT* promoters created from bacterial artificial chromosomes (BACs). We hypothesized that due to their large size, BACs would contain all necessary regulatory elements and therefore, upon their integration into the genome, would be able to faithfully mimic the telomerase expression of the host cell. In order to test this hypothesis, we created luciferase reporters from a human *TERT*-containing BAC and introduced them to genetically related TERT(+) and (-) cells engineered to contain an acceptor locus capable of specifically integrating the BAC through recombinase-mediated cassette exchange (RMCE). These luciferase reporters contained the firefly and *Renilla reniformis* luciferase open reading frames (ORFs) inserted into the start codons of *TERT* and *CRR9*, the gene immediately 5' of *TERT*. As *CRR9* has been shown to be ubiquitously expressed in all cells, the luciferase reporter inserted at its start codon serves as an internal control. Additional modifications to the BAC included the insertion of *puro* and the insertion of dual-copy cHS4 insulators interior of the *lox511* and *loxP* sites.

The competence of the acceptor locus to mediate RMCE was verified by the creation of RMCE-mediated stable integrants of plasmids based on the base BAC vectors. Attempts to target circular and PI-*Sce*I-linearized h*TERT* BAC reporters to the genome via RMCE were unsuccessful. The exact reasons for the failure are unknown, but possible contributing factors include low transfection efficiency, BAC fragmentation, the choice of *lox* sites, and the cells themselves. Electroporation of PI-*Sce*I-linearized BAC reporters to the acceptor locus-containing TERT(+) and (-) cells resulted in the formation of 186 stable integrants after puromcyin selection. Analysis of these clones by Southern hybridization with probes specific for firefly and h*Renilla* luciferase and performance of luciferase assays resulted in the identification of 28 clones that warranted further characterization. Of these 28, five TERT(-) and seven TERT(+) clones were identified that were possibly the result of integration of an intact BAC. Comparison of luciferase activity in these clones revealed that all clones expressed high-level firefly and

low-level h*Renilla* luciferase activities, seemingly indicating that PI-*Sce*I-linearized BACs introduced to the genome of genetically related TERT(+) and (-) cells are unable to recapitulate the expression of endogenous *TERT*. Possible reasons for the failure of these BAC reporters to faithfully mimic endogenous expression include the way in which the TERT(+) cells gained telomerase activity, undetected microdeletions and rearrangements of the BAC DNA, the lack of necessary *TERT* regulatory sequence due to its location outside of the BAC ends, and the inability of stably integrated BACs to re-form the endogenous chromatin locus.

6.2 Improvements to the Methodology

6.2.1 Choice of *lox* Sites

The targeting of h*TERT* BAC reporters to a preexisting acceptor locus in genetically related TERT(+) and (-) cells represents the ideal system in which to study telomerase regulation. One potential reason for the failure of RMCE of BAC reporters is the *lox* sites employed. Due to their preexisting presence on RPCI-11.c 117B23 (489), the *lox511* and *loxP* Cre recombinase recognition sites were chosen for RMCE. However, as discussed in detail in Section 4.4.5, *lox511* and *loxP* are not completely heterologous in mammalian systems, and can therefore recombine with each other, potentially decreasing the overall RMCE efficiency. *lox* sites that are truly incompatible with one another have been identified (377;528), and their use might serve to increase the overall RMCE efficiency, allowing for the targeting of the BAC reporters. To employ different *lox* sites in our system, it would be necessary to replace the *lox511* site of the BAC with one that is completely unable to recombine with *loxP*. This replacement could be accomplished through the use of the two-step recombineering technique outlined in Chapter 3. The acceptor locus would also have to be remade with the new *lox* site. This would require the re-creation of pML2 (Chapter 2) and could be accomplished through either standard subcloning or two-step recombineering. Following the re-creation of pML2, it would be necessary to create retroviral stocks, re-infect naïve 3C-167b and 3C-166a (TERT(+) and (-), respectively) cells, and screen for single-copy, single-site integrants.

6.2.2 Choice of Cell Lines

From a standpoint of both RMCE and random integration, the choice of a different set of TERT(+) and (-) cells could be beneficial. While the TERT(+) and (-) cells employed were derived from the same parental cell line (see Chapter 2), making them genetically related as desired, their passage through crisis due to the expression of SV40 large T antigen could make them less desirable as a model system (see Section

5.4.4). Another set of TERT(+) and (-) cells that have been employed in studying human telomerase regulation are the TERT(+) GM00639 and TERT(-) GM00847 fibroblasts (224). Therefore, we could introduce our h*TERT* BAC reporters to these cell lines and monitor the integration of intact copies of the reporters and whether or not these intact reporters mimic endogenous telomerase activity. Unfortunately, these cell lines are not derived from the same parental cell line and were also transformed by SV40 and survived crisis; therefore, they are not genetically identical and if passage through crisis is problematic, then they are not a better model system than the cells used in the outlined studies. One way to circumvent these issues would be to study the expression of the BAC reporters in models of hematopoietic or ES cell differentiation. In these model systems, the undifferentiated cells express high levels of telomerase activity, but the differentiated cells do not. These studies could help elucidate whether or not the BAC reporters are able to recapitulate endogenous patterns of telomerase activity. (Dr. Zhu has published a paper concerning transgenic h*TERT* expression patterns in mouse ES cells (538). Differentiation studies using U937 and HL60 hematopoietic cells are also in progress in Dr. Zhu's the laboratory.)

6.2.3 Introduction of BAC DNA to Cells of Interest

Optimizing the introduction of the BAC DNA will also be useful in drawing conclusions concerning whether or not h*TERT* BAC reporters are able to mimic endogenous telomerase expression. While improving the method of transfection will not affect the fragmentation of DNA that occurs once the DNA enters the cells (see Section 4.4.5), the ability to introduce more molecules of the BAC to each cells may increase the chance that an intact molecule will integrate into the genome, either randomly or through RMCE. Increasing the overall number of integrants containing intact BAC DNA will add more credence to any conclusions due to the increased power of the experiments.

As outlined in Chapter 4 and Appendix B, extensive efforts to optimize the introduction of circular BAC DNA were performed. These techniques included the commercially available transfection reagents FuGENE-6 (Roche), Lipofectamine2000 (Invitrogen), and GenePorter2 (Genlantis). Less extensive attempts to optimize the

introduction of PI-*Sce*I-linearized BAC DNA included transfection by FuGENE-6 and electroporation (Chapter 5 and Appendix B). Even though the transient expression of BAC reporters does not necessarily indicate the efficiency of genomic integration, it is a measure of the number of molecules successfully introduced to the cells. It would be useful to determine the efficiency of Lipofectamine2000- and GenePorter2-mediated transfection of PI-*Sce*I-linearized BAC DNA. If their efficiency was greater than that of FuGENE-6-mediated transfection or electroporation, it might be of benefit to use these reagents to introduce the BAC DNA. As can be seen in Figure B4 of Appendix B, GenePorter2-mediated transfection of circular BAC DNA resulted in transient luciferase activity that was at least two orders of magnitude greater than that of DNA introduced by FuGENE-6. If this same difference in efficiency were noted for linearized DNA, it would be worthwhile to use this reagent in a large-scale experiment addressing the expression of linearized BAC reporters in TERT(+) and (-) cells.

Other techniques are available for introducing DNA to cells, and many have been used in conjunction with BAC DNA. Many of these methods rely on the condensation of the BAC DNA prior to it introduction to the cells as condensation has been shown to increase the efficiency of BAC transfection (527). One method involves the use of psoralen-inactivated adenoviral particles to deliver BAC DNA condensed with polyethyenimine (PEI) (539). This method was used to successfully introduce an intact BAC of 170 kb into HeLa cells and primary human fibroblasts. PEI condensation has also been used in conjunction with Lipofectamine to transfect CHO cells (540). The LID technique has also been used to successfully introduce plasmids up 242 kb in size to 293 and MRC5-V2 (SV40-immortailzed human fetal lung fibroblasts) cells (524). The LID technique relies on the creation of delivery particles consisting of Lipofectin, an integrin-targeting peptide, and the DNA of interest. Recently, techniques have been developed to retrofit BACs with herpes simplex virus type I (HSV-1) replicons and Epstein-Barr virus (EBV) amplicons in order to deliver BACs to mammalian cells as infectious particles referred to as “iBACs” (541). While this system has many beneficial properties, the size of the genomic insert is limited to ~153 kb due to the packaging requirement. Therefore, if the BAC of interest is larger than 153 kb, it would have to be truncated in order to be able to be packaged. This could be problematic if the regions for appropriate regulation

are located outside of these limits. (For instance, this system may not be useful for studying telomerase regulation.)

6.3 Future Directions

The absence of telomerase expression in most adult somatic cells and its reactivation in 85-90% of human cancers makes h*TERT* a potential target for cancer therapeutics and/or an attractive cancer biomarker (reviewed in (542)). Additionally, the correlation between shortened telomere lengths, senescence, and aging makes telomerase an interesting topic for aging studies (543). In order to fully appreciate and realize these potential uses of h*TERT*, it would be helpful to have a clear, complete understanding of its regulation in normal cells. Therefore, it is important to continue the studies outlined in this document, both as originally outlined and employing the improvements outlined in Sections 2.4, 4.4, 5.4, and 6.2.

If the results of these future studies support the preliminary conclusion that BAC-based h*TERT* reporters are unable to recapitulate endogenous telomerase expression upon their stable integration into the genome of TERT(+) and (-) cells, it would be necessary to try and identify the necessary factors. It is possible that these factors could be located outside the BAC ends, and therefore, the use of different BACs that cover additional sequence located up-and downstream of *TERT* would be useful. A search of the UCSC genome browser resulted in the identification of three additional BAC clones encompassing the entire *TERT* locus (490). As can be seen in Table 6.1, two of these BAC clones contain additional sequence upstream of *TERT* but less sequence downstream than 117B23; the third clone contains additional sequence up- and downstream. Modification of these BACs in a manner similar to that of 117B23 may help identify the sequences necessary to confer appropriate telomerase expression to BAC reporters in TERT(+) and (-) cells. Once the necessary sequence is identified, it would be possible to recombineer the BACs, as outlined in Section 3.4, to determine what part of the sequence is critical for appropriate telomerase regulation, and therefore, what may be a useful target for future studies on cancer and aging.

Clone	Start	End	Size (bp)	Downstream (bp)	Upstream (bp)
RP11-117B23	1,260,045	1,422,139	162,094	-	-
RP11-990A6	1,169,186	1,371,084	201,898	90,859	-51,055
CTD-3080P12	1,169,264	1,371,407	202,143	90,781	-50,732
CTD-2524G15	1,225,754	1,429,867	204,113	34,291	7,728

Table 6.1. Comparison of BAC Clones Encompassing h*TERT*. A total of four BACs encompassing the entire human telomerase locus were identified by searching the UCSC Human Genome Database (490). The BAC used in the studies outlined in this document, RP11-117B23, is shown in the first line of the table. The three additional BACs are also represented. "Start" and "End" refer to the genomic position of the beginning and end of the BAC clone, with position 1 referring to the telomere of 5p. As can be seen, all three BACs contain additional sequence downstream (towards the telomere) of *TERT*, while only one BAC contains additional sequence upstream (towards the centromere) of *TERT*; the remaining two clones contain less upstream sequence.

APPENDIX A

PLASMIDS AND VECTORS CREATED AND USED IN THE COMPLETION OF THE THESIS

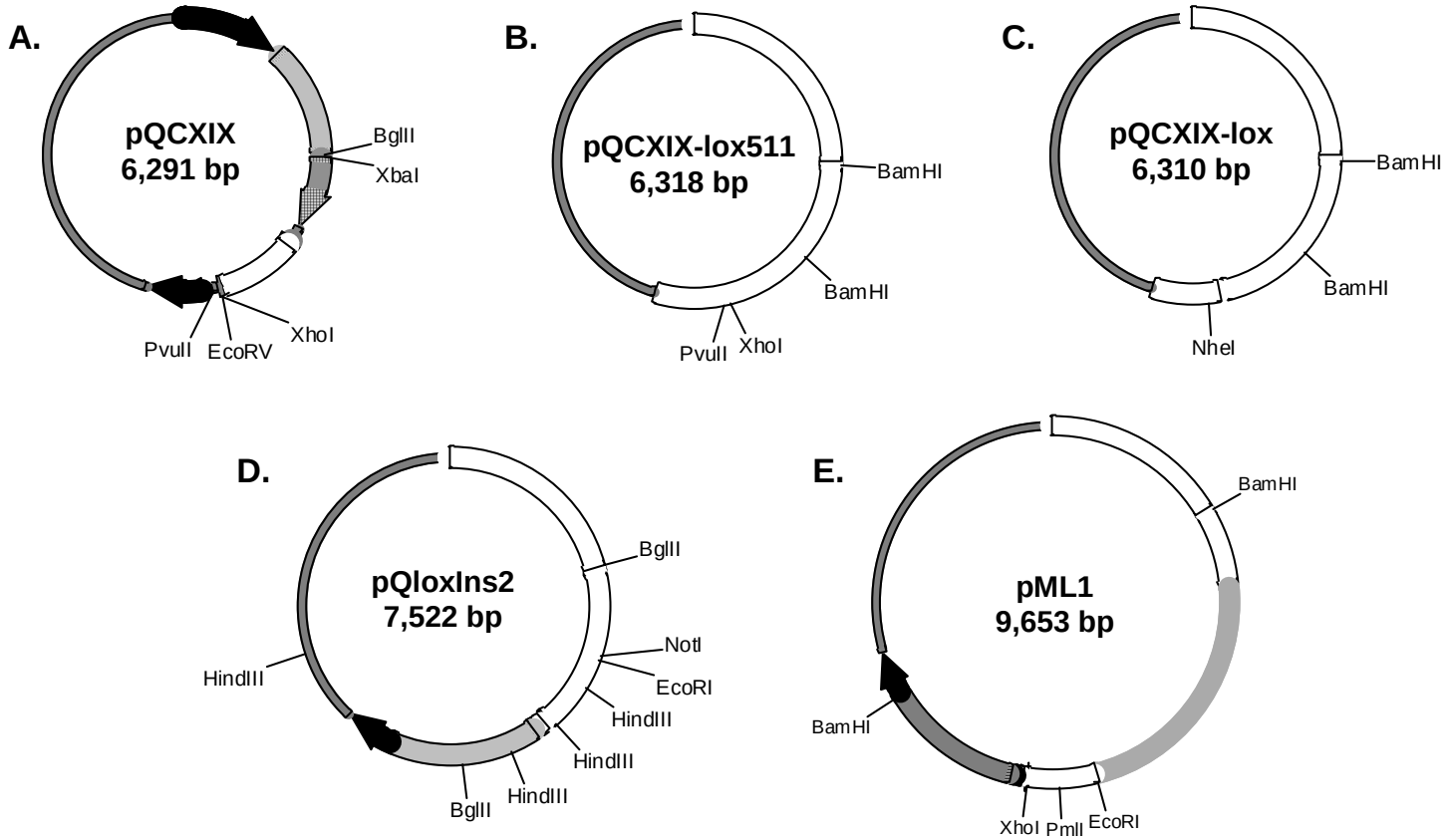

Figure A1. Intermediate Plasmids Used to Create pML2. For each plasmid, relevant restriction endonuclease recognition sites are shown. **A.** The original vector pQCXIX was purchased from Clontech and contains a 5' and 3' LTR (black arrows), the retroviral packaging signal ψ (gray), the CMV_{IEP} promoter (hatched arrow), and an IRES (white). In **B-F**, the portion of pQCXIX from the beginning of the 5' LTR to the end of the 3' LTR is represented in white. **B.** pQCXIXlox511 contains the *lox511* site (black line). **C.** pQCXIXlox contains the *loxP* site (second black line). **D.** pQloxIns2 contains cHS4 (gray) inserted into the 3' LTR (black arrow). **E.** pML1 contains tkNeo (light gray). Note: Figures not to scale with respect to one another.

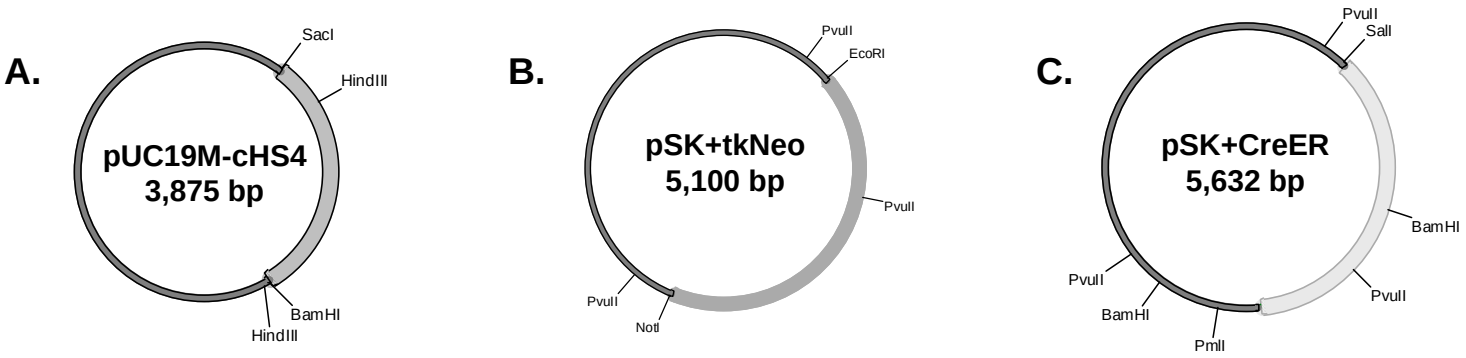

Figure A2. Subcloning Plasmids Used in Creation of pML2. For each plasmid, the insert is indicated by the gray line and relevant restriction endonuclease recognition sites are shown. Note: Figures not to scale with respect to one another.

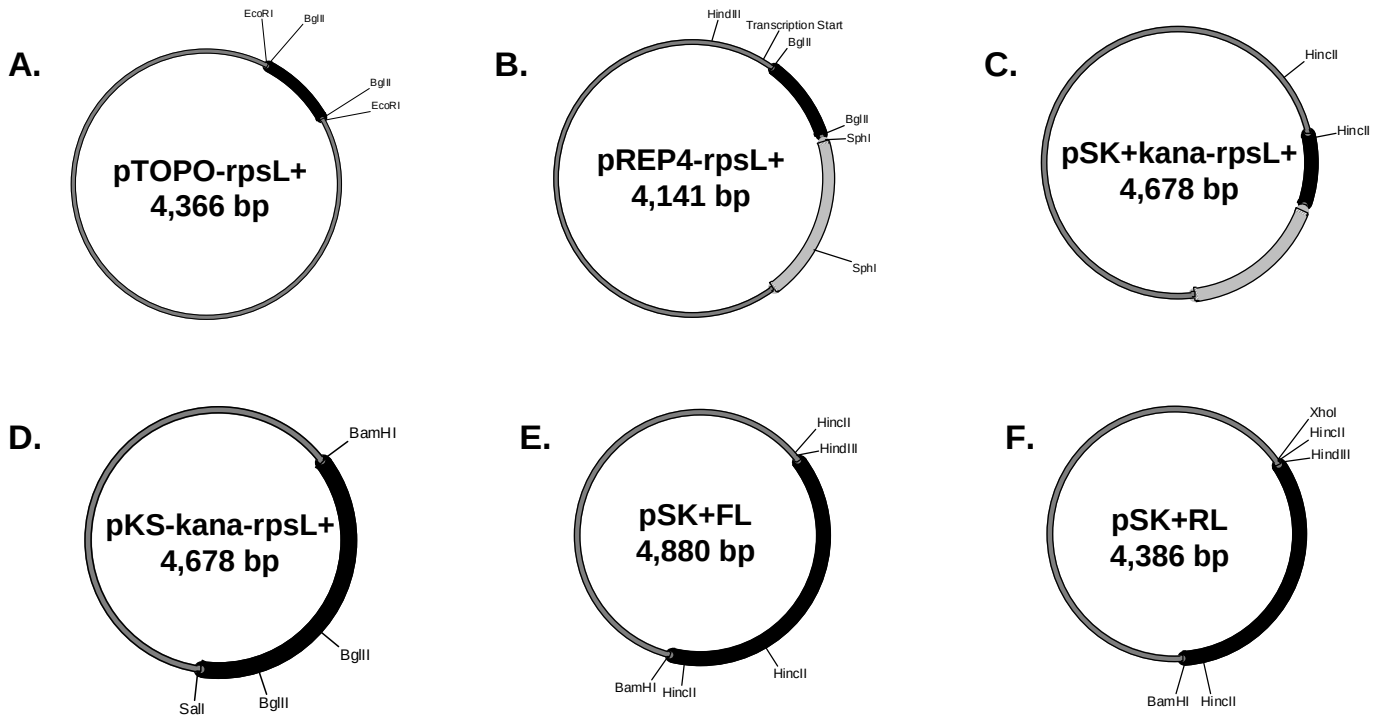

Figure A3. Subcloning Plasmids Used in the Creation of kana/rpsL$^+$ and Luciferase Recombineering Cassettes. For each plasmid, relevant restriction endonuclease recognition sites are shown. In **A-C**, *rpsL*$^+$ is represented in black and *kana* in gray. In **D-F**, the insert is represented in black. Note: Figures are not to scale with respect to each other.

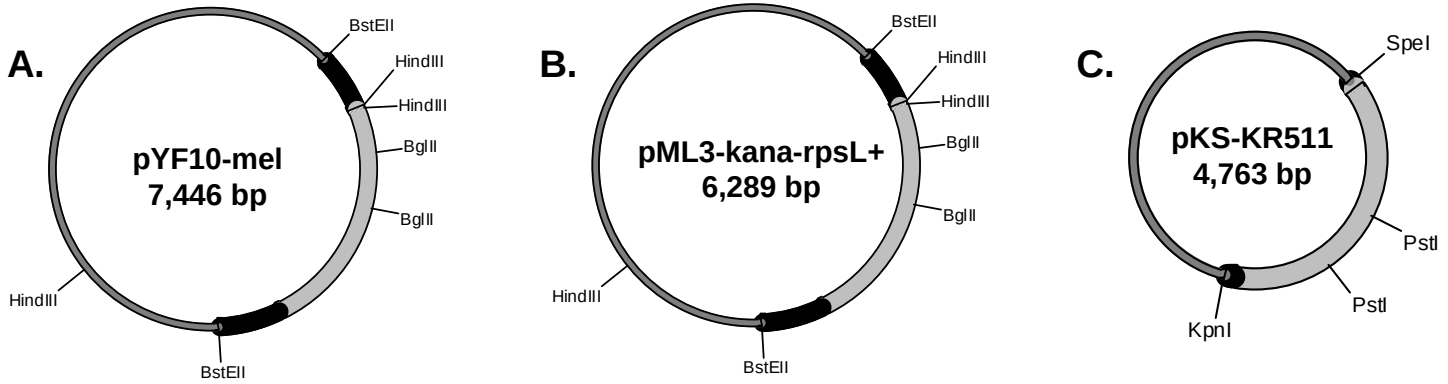

Figure A4. Plasmids Used to Create kana/rpsL$^+$ Selection Cassettes. For each plasmid, the homology arms are represented in black, kana/rpsL$^+$ is represented in gray, and relevant restriction endonuclease recognition sites are shown. **A.** pYF10-mel allows for the insertion of kana/rpsL$^+$ at the TERT start codon. **B.** pML3-kana-rpsL$^+$ allows for the insertion of kana/rpsL$^+$ at the CRR9 start codon. (Created by Renee Dusheck.) **C.** pKS-kana-rpsL$^+$511 allows for the insertion of kana/rpsL$^+$ interior of *lox511*. While not shown, pKS-kana-rpsL$^+$P allows for the insertion of kana/rpsL$^+$ interior of *loxP*.

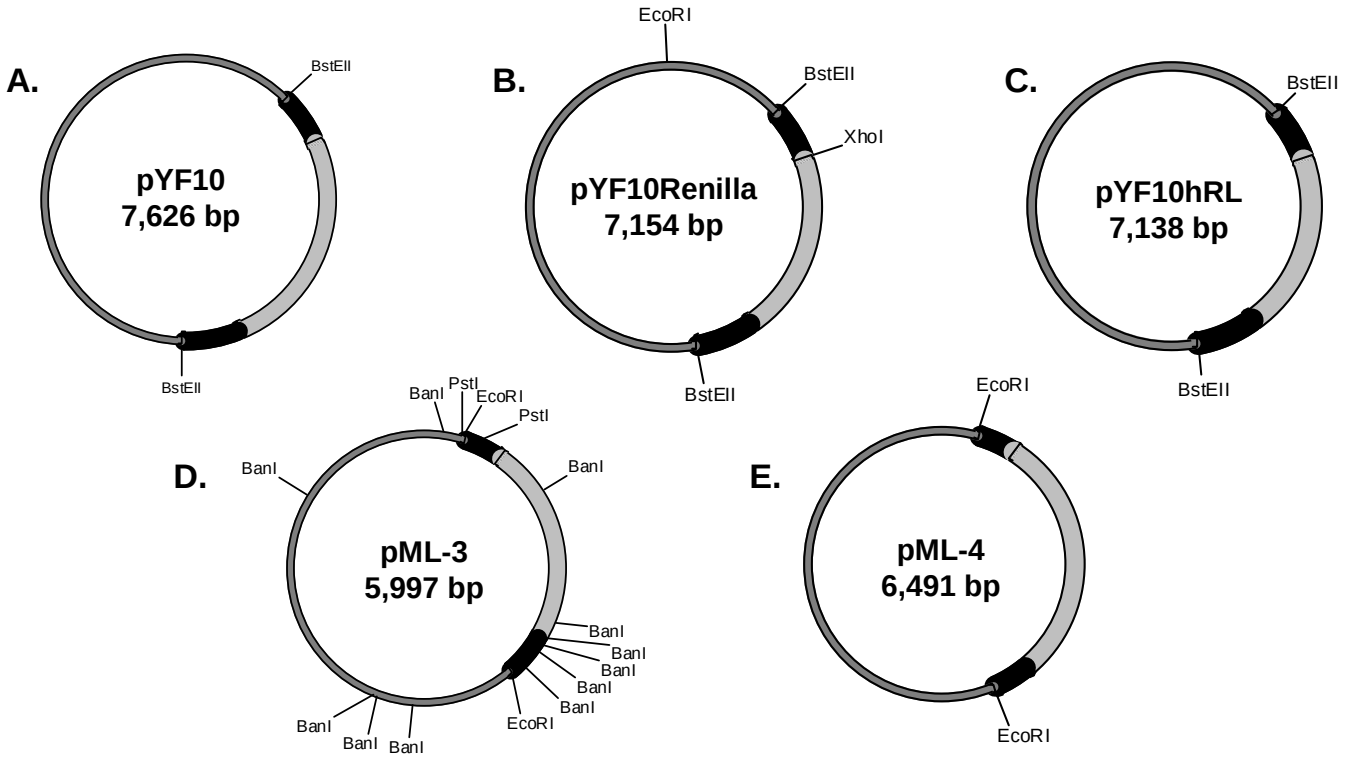

Figure A5. Plasmids Used to Create Luciferase Cassettes. For each plasmid, the homology arms are represented in black, the luciferase ORFs are represented in gray, and relevant restriction endonuclease recognition sites are shown. **A.** pYF10 allows for the insertion of FL at the TERT start codon. (Created by Yan Fang.) **B.** pYF10-Renilla allows for the insertion of RL at the TERT start codon. **C.** pYF10-hRenilla allows for the insertion of hRL at the TERT start codon. (Created by Shuwen Wang.) **D.** pML-3 allows for the insertion of RL at the CRR9 start codon. (Created by Renee Dusheck.) **E.** pML-4 allows for the insertion of FL at the CRR9 start codon. Note: Figures not to scale with respect to one another.

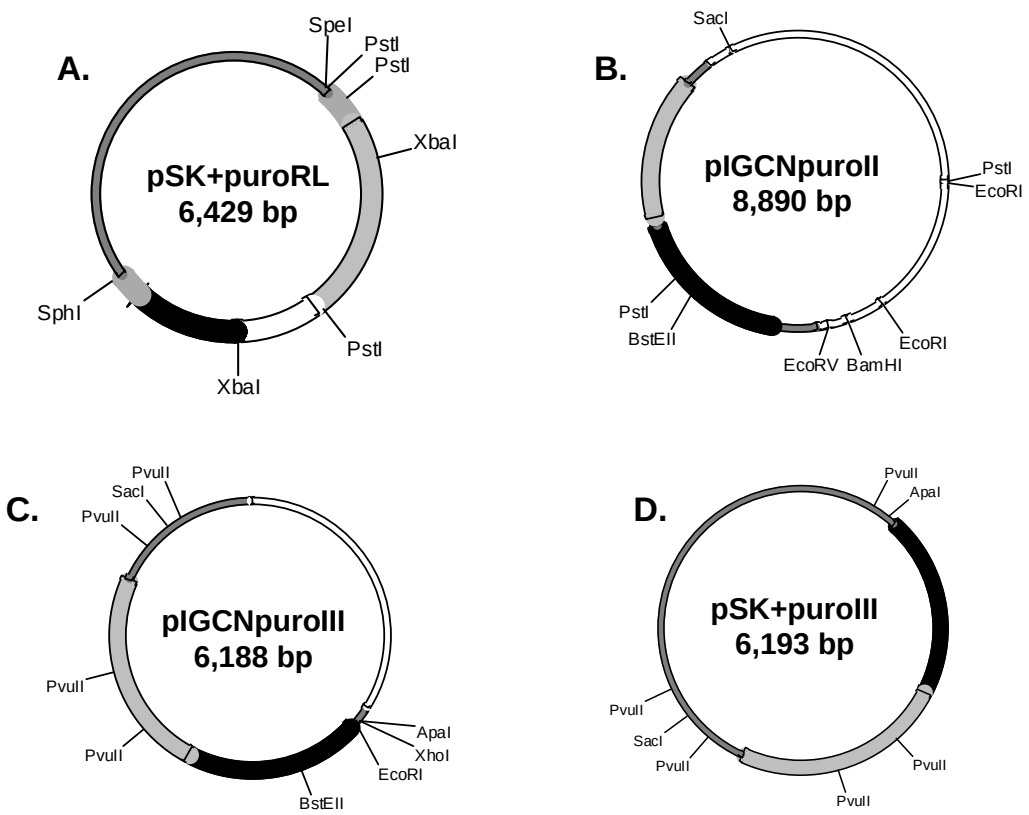

Figure A6. Subcloning Plasmids Used for Creation of Puromycin Cassettes. For each plasmid, relevant restriction endonuclease recognition sites are shown. **A.** pSK^{+}puroRL contains *puro* (gray), and IRES (white) and RL (black). Homology arms to CRR9 are also indicated in gray. **B.** pIGCNpuroII contains mPGK-driven *puro* (black) and *kana* surrounded by FRT sites (gray). Unknown sequence is represented in white. **C.** pIGCNpuroIII contains SV40-driven *puro* (black) and *kana* surrounded by FRT sites (gray). Unknown sequence is represented in white. **D.** pSK^{+}puroIII contains SV40-driven *puro* (black) and *kana* surrounded by FRT sites (gray). Note: Figures not to scale with respect to one another.

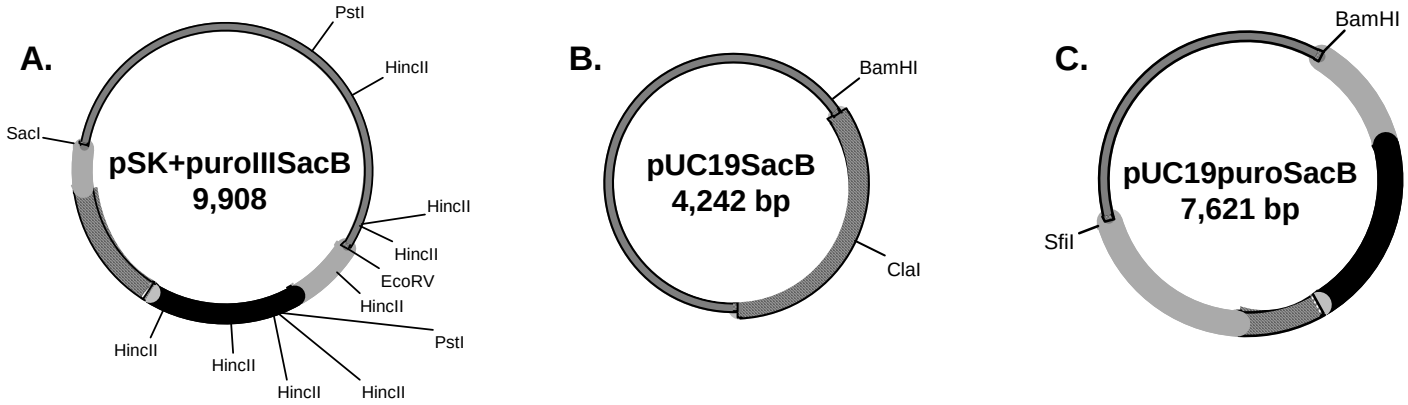

Figure A7. Subcloning Plasmids Used for BAC Vector Modification. For each plasmid, relevant restriction endonuclease recognition sites are shown. **A.** pSK^{+}puroIIISacB contains *sacB* (hatched) and *puro* (black). Other homologous regions are indicated in gray. **B.** pUC19SacB contains *sacB*. **C.** pUC19puroSacB contains *sacB* (hatched) and *puro* (black). Other homologous regions are indicated in gray. Note: Figures not drawn to scale with respect to one another.

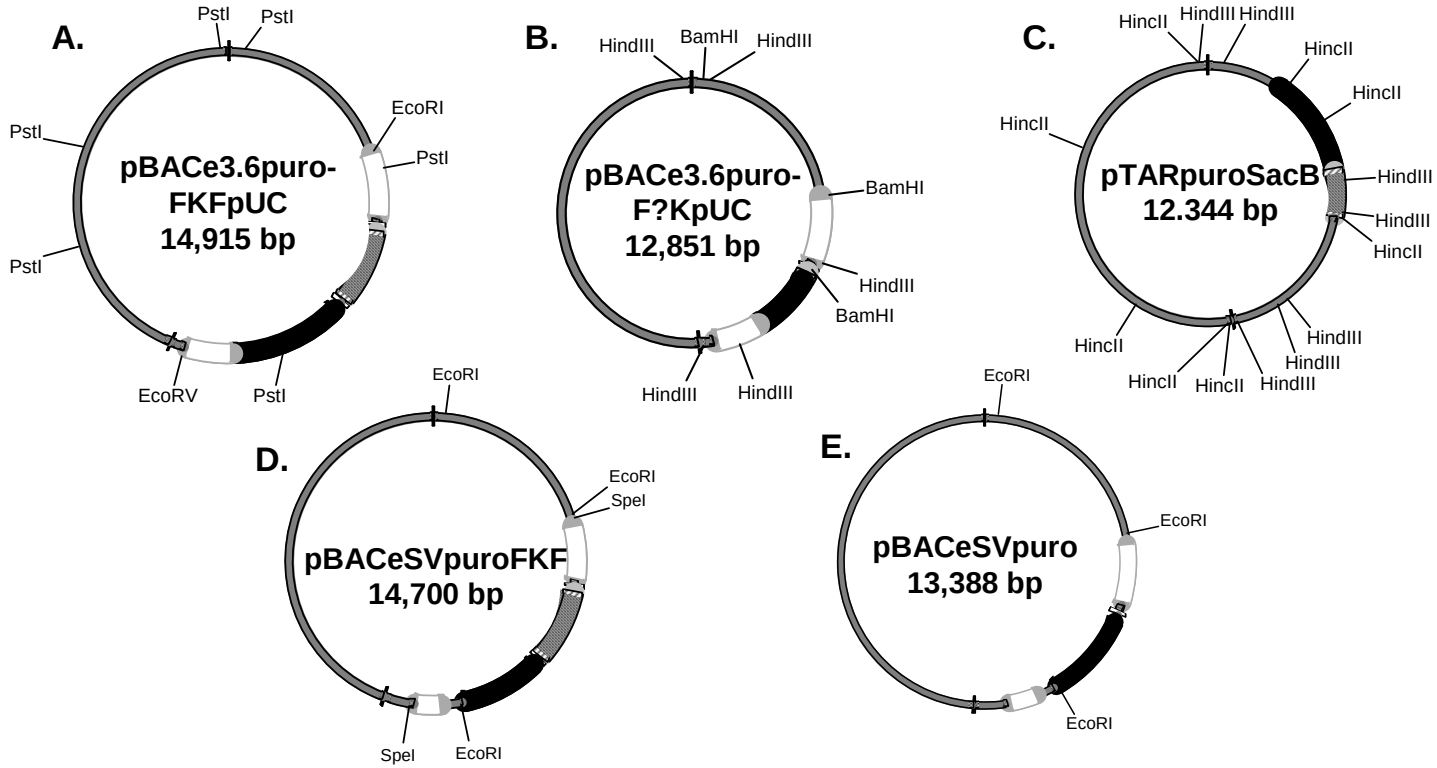

Figure A8. Modified BAC Vectors. For each vector, relevant restriction endonuclease recognition sites are shown and the *lox* sites are represented as black lines. **A.** pBACe3.6puroFKFpUC contains *puro* (black) and *kana* surrounded by FRT sites (hatched). Homology arms are in white. **B.** pBACe3.6puroFΔKpUC is the same as pBACe3.6puroFKFpUC with a deletion of *kana*. **C.** pTARpuroSacB contains *puro* (black) inserted upstream of *sacB* (hatched). **D.** pBACeSVpuroFKF contains *puro* (black) and *kana* surrounded by FRT sites (hatched). Homology arms are in white. **E.** pBACeSVpuro is the result of FLP/FRT-mediated excision of *kana*. Note: Figures are not to scale with respect to each other.

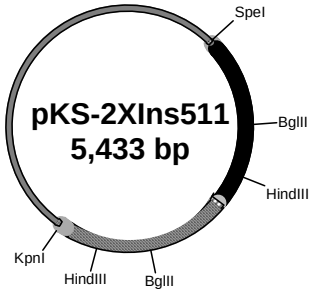

Figure A9. Plasmid Used for Dual-copy Insulator Insertion. pKS-2XIns511 contains two copies of cHS4 (one represented as black, one represented as hatched) surrounded by homology arms (gray) to the region interior of *lox511*. pKS-2XInsP looks the same, although the homology arms are specific for the region interior of *loxP*.

APPENDIX B

LUCIFERASE ASSAYS

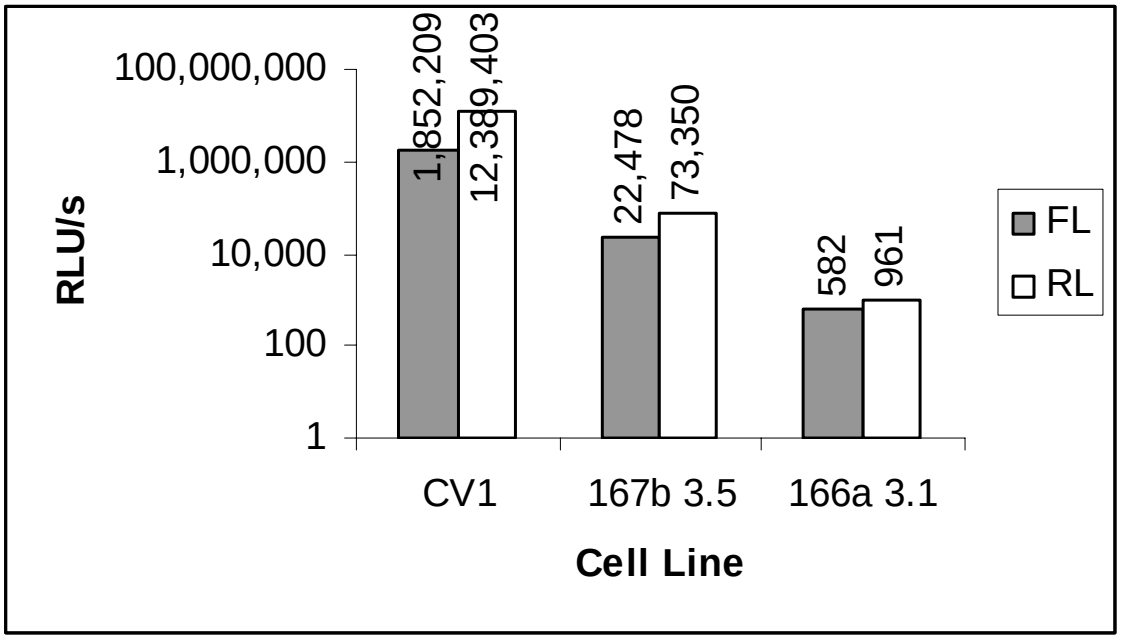

Figure B1. Comparison of Transfection Efficiency Among Three Cell Lines. All transfections were performed in duplicate in 24-well plates using FuGENE-6 (Roche). Each transfection employed 125 ng pYF10 and 100 ng pTARpuroRL. Luciferase activity was measured 48 hours post-transfection using the Dual-Luciferase® Reporter Assay System (Promega). The firefly luciferase activity ("FL") is a read-out of pYF10 while *Renilla* luciferase activity ("RL") is a read-out of pTARpuroRL. All values shown were corrected for background autoluminescence (48 RLU/s for FL and 111 RLU/s for RL). Note: Results are displayed on a logarithmic scale.

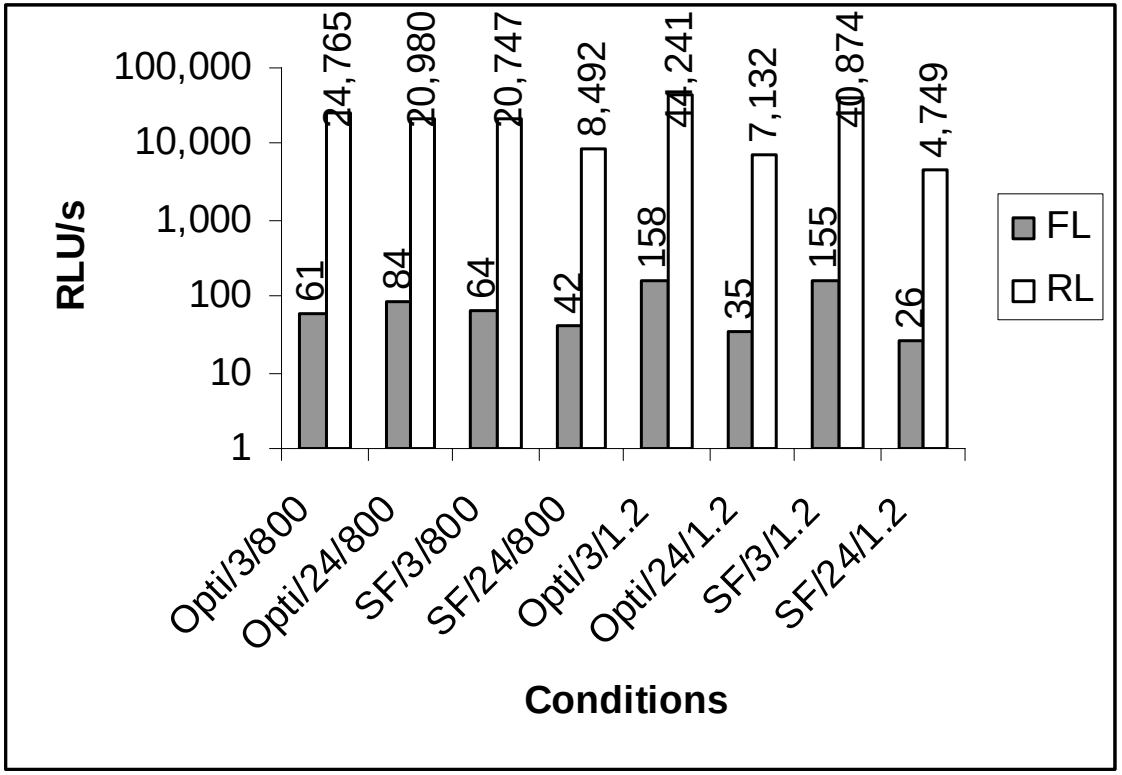

Figure B2. Optimization of Lipofectamine2000-Mediated Transfection of 117B23 cRtFsP. All transfections were performed in TERT(+) 167b 3.5 cells in 12-well plates. For each condition listed as "A/B/C", A refers to the medium used to prepare the transfection mixture (OptiMEM ("Opti) or serum-free EMEM ("SF"), B refers to the amount of time (in hours) the cells were incubated with the transfection mixture, and C refers to the amount of DNA used (800 ng versus 1.2 μg). Firefly luciferase activity ("FL") is a read-out of *TERT* expression and *Renilla* luciferase activity ("RL") is a read-out of *CRR9* expression. All luciferase readings are corrected for autoluminescence (138 RLU/s for FL and 188 RLU/s for RL). Note: Results are presented on a logarithmic scale.

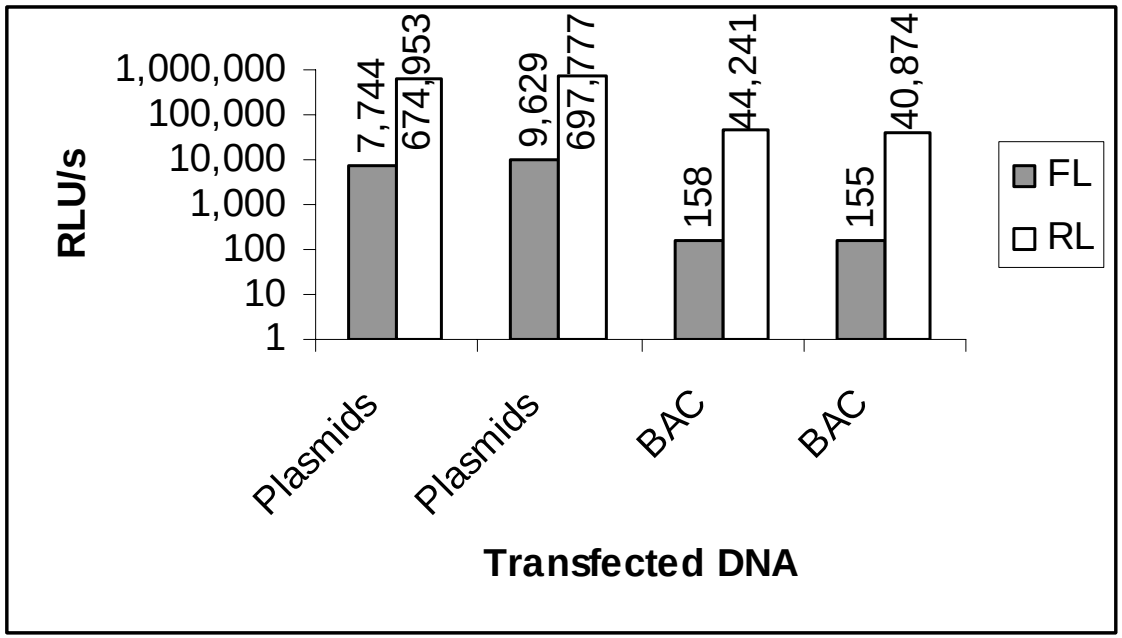

Figure B3. Comparison of Luciferase Activity After Transfection of Plasmid and BAC DNA. Each transfection was performed in TERT(+) 167b 3.5 cells plated in a 12-well plate using Lipofectamine2000. The plasmids used for transfection were 250 ng pGL3proΔ (FL activity) and 100 ng pRL-GL3proΔ (RL activity); the BAC used for transfection was 1.2 µg 117B23 cRtFsP. The luciferase values shown were corrected for autoluminescence (138 RLU/s for FL and 188 RLU/s for RL). Note: All values are shown on a logarithmic scale.

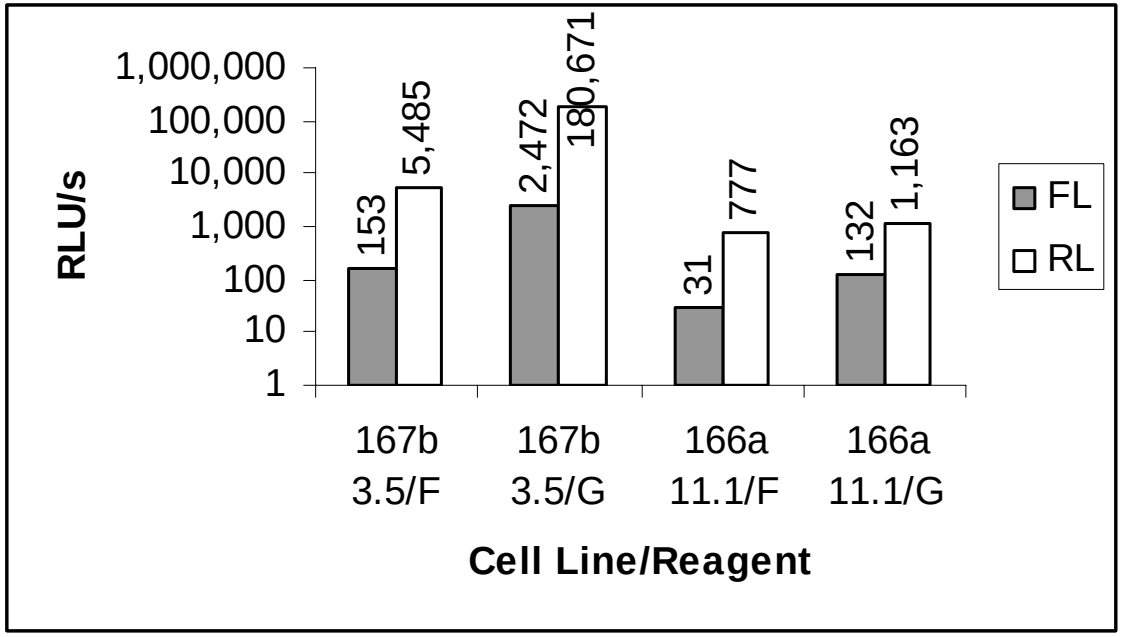

Figure B4. Comparison of Luciferase Activity After BAC Transfection with FuGENE-6 and GenePorter2. Each transfection was performed in one well of a 12-well plate with 117B23 cFtHRsSVP, and therefore, FL is the reporter for *CRR9* and RL is the reporter for *TERT*. For FuGENE-6 ("F"), 0.5 μg of BAC was transfected per well; for GenePorter2 ("G"), 1.5 μg of BAC was transfected per well. All luciferase activity was corrected for autoluminescence (265 RLU/s for FL and 884 RLU/s for RL). Note: All values are shown on a logarithmic scale.

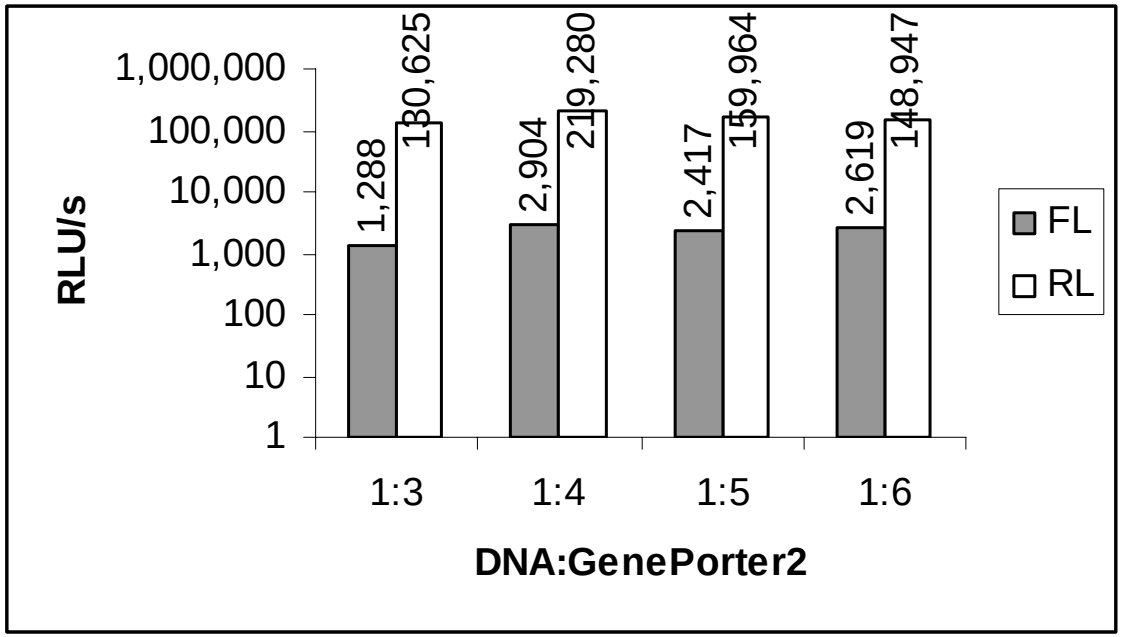

Figure B5. Optimization of GenePorter2-Mediated Transfection. Each transfection was performed in one well of a 12-well plate with 1.5 μg 117B23 cFtHRsSVP, and therefore, FL is the reporter for *CRR9* and RL is the reporter for *TERT*. "DNA:GenePorter2" refers to the ratio of DNA (μg) to GenePorter2 reagent (μl) used for transfection. All luciferase activity was corrected for autoluminescence (317 RLU/s for FL and 1,183 RLU/s for RL). Note: Luciferase activity is displayed on a logarithmic scale.

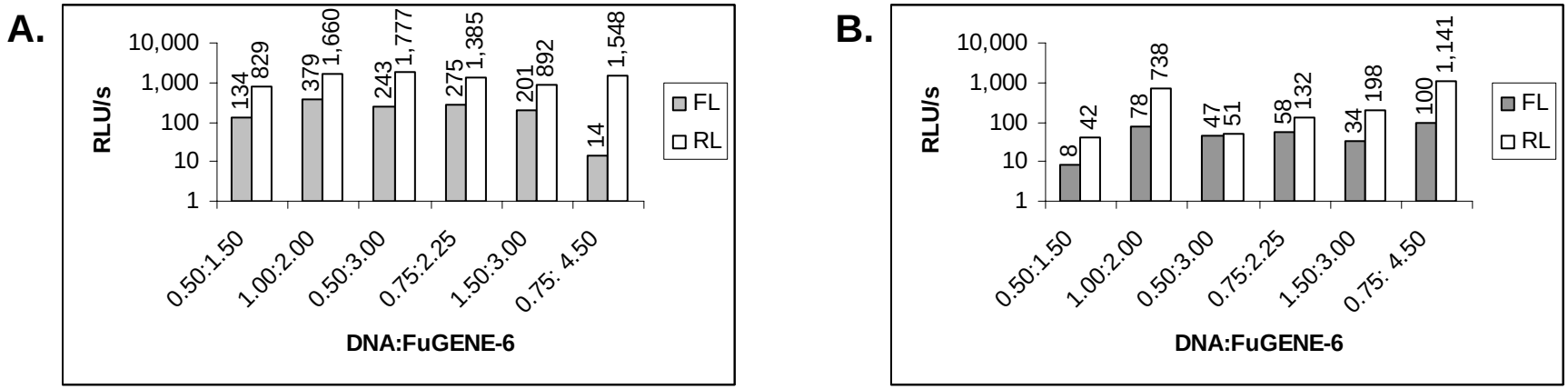

Figure B6. Optimization of FuGENE-6-Mediated Transfection of PI-*Sce*I-linearized BAC. Each transfection was performed in one well of a 12-well plate with 117B23 cFtHRvSVP, and therefore, FL is the reporter for *CRR9* and RL is the reporter for *TERT*. The DNA:FuGENE-6 ratio is represented as μg DNA to μl FuGENE-6. **A.** TERT(+) 167b 3.1 cells. **B.** TERT(-) 166a 11.1 cells. All luciferase activity was corrected for autoluminescence (39 RLU/s for FL and 110 RLU/s for RL). Note: Luciferase activity is presented on a logarithmic scale.

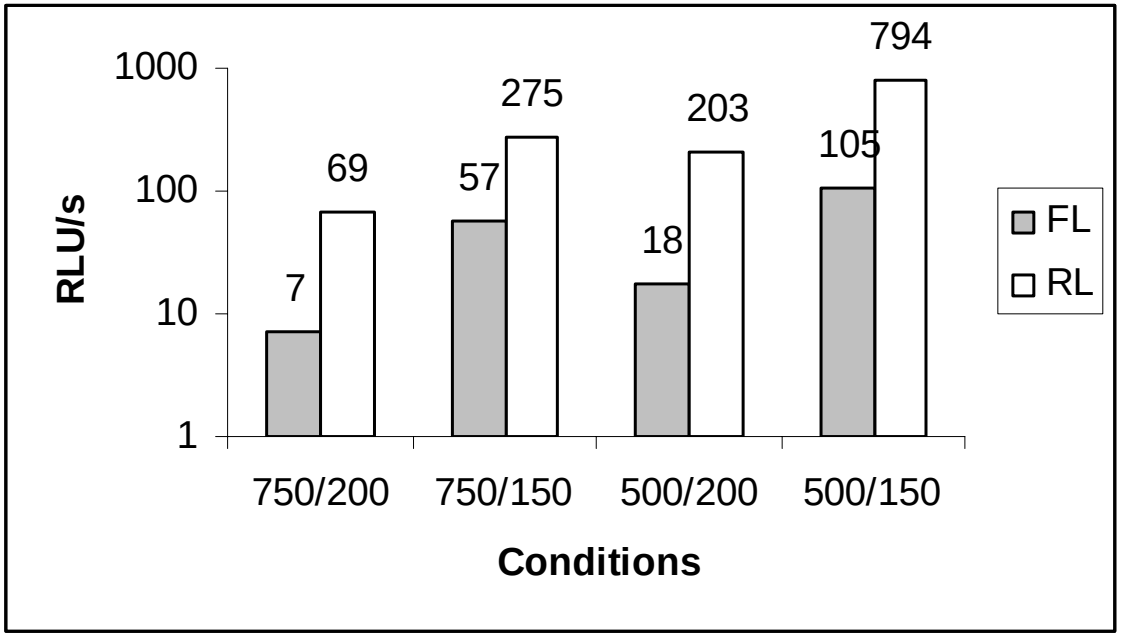

Figure B7. Determination of Optimal Capacitance and Charging Voltage for Electroporation of PI-*Sce*I-linearized 117B23 cFtHRvSVP. For all electroporations listed, $1.6x10^6$ cells were electroporated at a density of $4x10^6$ cells/ml in a 2 mm gap cuvette with 4 μg DNA at 13 Ω resistance. For each condition listed as "A/B," A refers to the capacitance (μF) and B refers to the charging voltage (V). FL is the reporter for *CRR9* and RL is the reporter for *TERT*. All luciferase activities were corrected for autoluminescence (104 RLU/s for FL and 215 RLU/s for RL). Note: Luciferase activity is presented on a logarithmic scale.

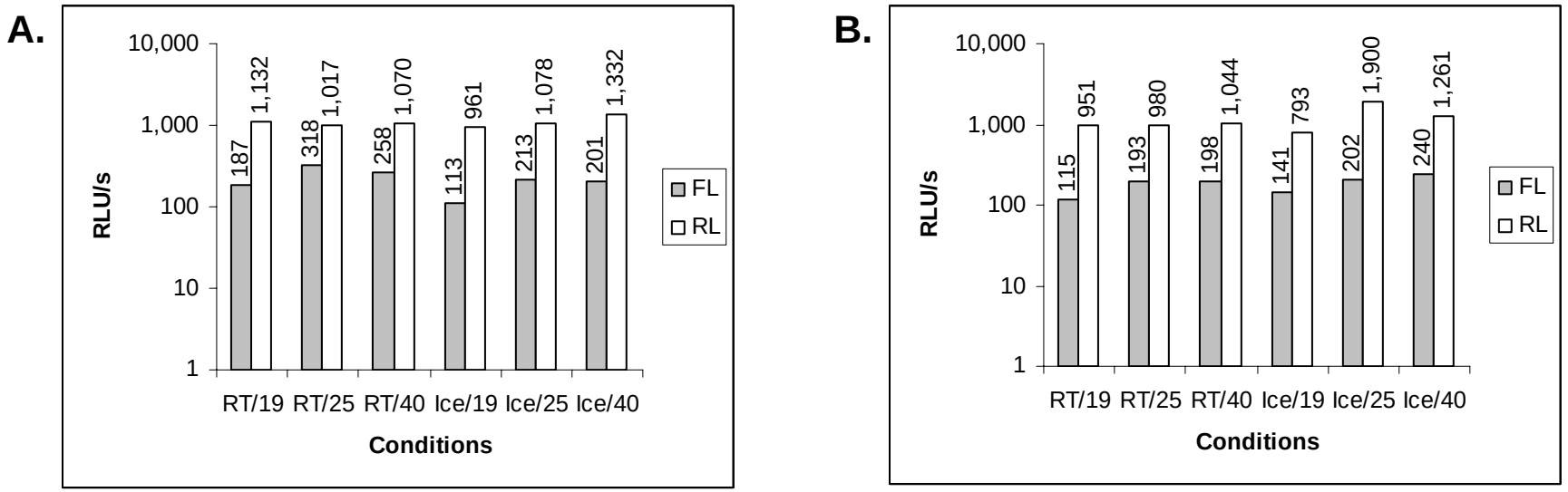

Figure B8. Optimization of BAC Electroporation. For all electroporations listed, $1.6x10^6$ cells were electroporated at a density of $4x10^6$ cells/ml with 4 μg PI-*Sce*I-linearized 117B23 cFtHRvSVP in a 2 mm gap cuvette at a capacitance of 500 μF, a charging voltage of 150 V, and a resistance of 13 Ω. For each condition represented as "A/B," A represents the temperature at which the cells were incubated for 10 minutes post-electroporation and B represents the number of hours after electroporation the assay was performed. In **A**, the cells were resuspended in OptiMEM; in **B**, the cells were resuspended in PBS. FL is the reporter for *CRR9* and RL is the reporter for *TERT*. All luciferase activity was corrected for autoluminescence (189 RLU/s for FL and 289 RLU/s for RL). Note: All luciferase activity is represented on a logarithmic scale.

APPENDIX C

RESULTS OF GENOMIC INTEGRATIONS USING CIRCULAR DNA

DNA (Amount)	Cre Induction	Transfxn. Method	Number of Cells	Total Expts.	Stable Integrants	RMCE Integrants
pTARpuroRL (10 μg)	1 μM 4HT	Cal. Phos.	6.32E+05	2	-	-
pTARpuroRL (400 ng)	1 μM 4HT	FuGENE-6	6.43E+04	1	-	-
pTARpuroRL (200 ng)	1 μM 4HT	FuGENE-6	6.43E+04	1	-	-
pTARpuoRL (200 ng)	1 μM 4HT + pCAGGS-Cre	FuGENE-6	6.43E+04	1	-	-
pTARpuroSacB (10 μg)	1 μM 4HT	Cal. Phos.	6.32E+05	2	+	-
pTARpuroSacB (400 ng)	1 μM 4HT	FuGENE-6	6.43E+04	1	+	-
pTARpuroSacB (200 ng)	1 μM 4HT	FuGENE-6	6.43E+04	1	+	-
pTARpuroSacB (200 ng)	1 μM 4HT + pCAGGS-Cre	FuGENE-6	6.43E+04	1	+	-

Table C1. Comparison of Colony Formation After Transfection with BAC Vectors Containing *puro*. The TERT(+) acceptor locus line 167b 3.5 was transfected with BAC vectors containing a *CRR9*- or PGK-driven puromycin resistance gene (pTARpuroRL and pTARpuroSacB, respectively). After transfection, cells were selected with puromycin and scored for the presence ("+") or absence ("-") of puromycin-resistant colonies ("Stable Integrants"). Those cultures showing puromycin-resistant clones were expanded for gDNA harvest and tested by PCR analysis for RMCE ("RMCE Integrants"). Note: All cell numbers are approximate. Cells were maintained in the absence of G418 prior to transfection.

				250 ng/ml Puromycin			500 ng/ml Puromycin		
DNA (Amount)	**Cre Induction**	**Number of Cells**	**Total Expts.**	**Screened/Total**	**GCV^R**	**RMCE Integrants**	**Screened/Total**	**GCV^R**	**RMCE Integrants**
pTARpuroSacB (8.2 μg)	pCAGGS-Cre	7.09E+05	2	Pooled/23	All	0	Pooled/21	All	0
pBACe3.6puroFKFpUC (8.2 μg)	pCAGGS-Cre	7.09E+05	2	Pooled/27	All	0	Pooled/23	All	0
pBACe3.6puroFKF (200 ng)	pCAGGS-Cre	7.71E+04	1	Pooled/3	All	0	1/1	All	0

Table C2. Optimization of Puromycin Concentration. The total number of stable and RMCE integrants was determined after selection of the TERT(+) acceptor line 167b 3.5 with different concentrations of puromycin. One day post-transfection, the cultures were split 1:2; one culture was treated with 250 ng/ml puromycin while the second was treated with 500 ng/ml puromycin. After counting the number of puromycin-resistant colonies formed, all colonies were pooled and selected with GCV or FIAU. No cells died in the presence of either drug. After harvest for gDNA, PCR analysis was performed to monitor the number of RMCE integrants. Not: All cell numbers are approximate. Cells were maintained in the absence of G418 prior to transfection.

DNA (Amount)	Cre Induction	Number of Cells	Total Expts.	Stable Integrants	Number Screened	RMCE Integrants
pTARpuroSacB (2.4 μg)	pCAGGS-Cre	5.71E+05	3	9	9	0
pTARpuroSacB (2.4 μg)	pBS185	5.71E+05	3	18	17	0
pTARpuroSacB (2.4 μg)	pCBM	5.71E+05	3	27	24	2
pTARpuroSacB (2.4 μg)	1 μM 4HT	5.71E+05	3	16	16	0
pBACe3.6puroFKF (3.5 μg)	pCAGGS-Cre	2.30E+06	2	6	5	0
pBACe3.6puroFKF (3.5 μg)	pBS185	2.30E+06	2	>104	15	1
pBACe3.6puroFKF (3.5 μg)	pCBM	2.30E+06	2	>120	14	3
pBACe3.6puroFKF (3.5 μg)	5 μM 4HT	2.30E+06	2	30	9	1

Table C3. Comparison of Different Methods of Cre Induction. The ability of 4HT-mediated induction of CreER from the acceptor locus and Cre induction from the three plasmids pCAGGS-Cre, pBS185, and pCBM was tested in the TERT(+) acceptor locus line 167b 3.5. Following transfection with FuGENE-6, cells were selected with puromycin. The total number of puromycin-resistant clones is represented by "Stable Integrants". The indicated number of clones, "Number Screened," were amplified for gDNA and screened by PCR analysis for an RMCE event. Note: All cell numbers are approximate. Cells were maintained in the absence of G418 prior to transfection.

Cell Line (DNA)	Transfxn. Method	Number of Cells	Stable Integrants	Survivors/ Attempted	Neo^R Clones	GCV^R Clones	RMCE Integrants
167b 3.1 (200 ng)	FuGENE-6	1.03E+05	30	12/16	10	2	2
167b 3.5 (200 ng)	FuGENE-6	1.03E+05	10	2/9	2	0	0
167b 11.2 (200 ng)	FuGENE-6	1.03E+05	7	3/7	3	0	0
167b 11.4 (200 ng)	FuGENE-6	1.03E+05	1	0/1	-	-	-
166a 3.1 (200 ng)	FuGENE-6	8.25E+04	7	0/7	-	-	-
166a 11.1 (200 ng)	FuGENE-6	8.25E+04	7	1/7	1	0	0
166a 11.4 (200 ng)	FuGENE-6	8.25E+04	2	0/2	-	-	-
167b 3.1 (800 ng)	GenePorter2	2.18E+05	17	3/12	1	2	2
167b 3.5 (800 ng)	GenePorter2	2.18E+05	0	-	-	-	-
167b 11.2 (800 ng)	GenePorter2	2.18E+05	5	1/5	1	0	0
167b 11.4 (800 ng)	GenePorter2	2.18E+05	7	0/7	-	-	-
166a 3.1 (800 ng)	GenePorter2	1.40E+05	4	0/4	-	-	-
166a 11.1 (800 ng)	GenePorter2	1.40E+05	0	-	-	-	-
166a 11.4 (800 ng)	GenePorter2	1.40E+05	1	0/1	-	-	-

Table C4. Comparison of Colony Formation Efficiency in Different TERT(+) and TERT(-) Acceptor Locus Cell Lines and Transfection by FuGENE-6 and GenePorter2. After co-transfection with pBACeSVpuro and pCBM, cells were selected with puromcyin and the total number of colonies was scored ("Stable Integrants"). Individual colonies were picked, although not all picked colonies survived after cloning ("Survivors/Attempted"). The surviving clones were screened for resistance to G418 ("Neo^R Clones") and GCV ("GCV^R Clones"). Clones that were resistant to puromcyin and GCV and sensitive to G418 ($Puro^R/Neo^S/GCV^R$) were amplified for gDNA harvest and analysis by PCR amplification. The number of clones that were shown to be the result of RMCE are indicated. Transfection of the same cell lines with pBACeSVpuro and treatment with 2.5 μM 4HT failed to produce any $puro^R$ colonies. Note: All cell numbers are approximate. Cells were maintained in 400 μg/ml G418 prior to transfection.

Cell Line	Amt. Vector/ Amt. Cre	Number of Cells	Stable Integrants	Survivors/ Attempted	Neo^R Clones	GCV^R Clones	RMCE Integrants
167b 3.1	100 ng/150 ng	1.29E+05	~40[a]	18/24	17	1	1
167b 3.1	100 ng/150 ng	1.29E+05	8[b]	6/8	0	6	6
167b 3.1	125 ng/125 ng	1.29E+05	~40[a]	10/24	10	0	0
167b 3.1	125 ng/125 ng	1.29E+05	9[b]	8/9	0	8	8
166a 11.1	100 ng/150 ng	1.65E+05	26[a]	6/22	2	4	4
166a 11.1	125 ng/125 ng	1.65E+05	33[a]	7/24	3	4	4

Table C5. Comparison of Differing Ratios of Vector to Cre Recombinase. TERT(+) and (-) cells expressing the acceptor locus (167b 3.1 and 166a 11.1, respectively) were transfected by FuGENE-6 with pBACeSVpuro ("Vector") and pCBM ("Cre"). Cells were initially selected with puromycin ([a]) or puromycin and GCV ([b]) ("Stable Integrants"). The indicated number of colonies was cloned ("Attempted") and the actual number that survived the cloning attempt ("Survivors") are indicated. The surviving clones were screened for resistance to G418 ("Neo^R Clones") and GCV ("GCV^R Clones"). Clones were expanded for gDNA harvest and screening by PCR amplification. Those clones that were shown to be RMCE integrants are indicated. Note: All cell numbers are approximate. Cells were maintained in 400 μg/ml G418 prior to transfection.

Amt. BAC DNA	Cre Induction	Transfxn. Method	Number of Cells	Stable Integrants	FL and RL Activity	RMCE Integrants
2.50 μg	5 μM 4HT	Lipofectamine2000	6.35E+05	0[a]	-	-
1.25 μg	1.25 μg pBS185	Lipofectamine2000	6.35E+05	0[a]	-	-
1.25 μg	1.25 μg pCBM	Lipofectamine2000	6.35E+05	1[a]	0	0
5.00 μg	5 μM 4HT	Lipofectamine2000	7.11E+05	0[a]	-	-
2.50 μg	2.50 μg pBS185	Lipofectamine2000	7.11E+05	2[a]	0	0
2.50 μg	2.50 μg pCBM	Lipofectamine2000	7.11E+05	6[a]	0	0
5.00 μg	5 μM 4HT	Lipofectamine2000	7.11E+05	0[b]	-	-
2.50 μg	2.50 μg pBS185	Lipofectamine2000	7.11E+05	0[b]	-	-
2.50 μg	2.50 μg pCBM	Lipofectamine2000	7.11E+05	6[b]	1	0
1.00 μg	1 μM 4HT	FuGENE-6	2.47E+05	5[a]	0	0

Table C6. Attempts to Create RMCE Integrants Using the Circular BAC Reporter 117B23 cRtFsP. All transfections were performed in the TERT(+) acceptor locus-containing cell line 167b 3.5. The number of colonies that survived cloning after selection with puromycin ("a") or puromycin and GCV ("b") is indicated ("Stable Integrants"). The number of these stable integrants that expressed both firefly (reporter of *TERT*) and *Renilla* (reporter for *CRR9*) luciferase activity are indicated; clones that only showed one of the two luciferase activities are not indicated. PCR amplification analysis revealed none of the clones to be the result of RMCE. Note: All cell numbers are approximate. Cells were maintained in the absence of G418 prior to transfection.

Amt. BAC DNA	Cre Induction	Transfxn. Method	Number of Cells	Stable Integrants	Neo^R Integrants	GCV^R Integrants	FL and RL Activity	RMCE Integrants
1.00 μg	1.0 μM 4HT	FuGENE-6	2.82E+05	0	-	-	-	-
1.00 μg	2.5 μM 4HT	FuGENE-6	2.82E+05	0	-	-	-	-
1.00 μg	5.0 μM 4HT	FuGENE-6	2.82E+05	0	-	-	-	-
0.875 μg	0.125 μg pCBM	FuGENE-6	2.82E+05	0	-	-	-	-
4.00 μg	1.0 μM 4HT	Lipofectamine2000	1.42E+06	7	1	6	0	0
4.00 μg	2.5 μM 4HT	Lipofectamine2000	1.42E+06	4	0	4	0	0
4.00 μg	5.0 μM 4HT	Lipofectamine2000	1.42E+06	3	0	3	0	0
3.50 μg	0.50 μg pCBM	Lipofectamine2000	1.42E+06	8	0	8	0	0

Table C7. Comparison of Different Methods of Cre Induction and Their Effect on RMCE-Mediated Integration of the Circular BAC Reporter 117B23 cRtFsSVP. Cells of the TERT(+) acceptor locus-containing line 167b 3.5 were transfected by either FuGENE-6 or Lipofectamine2000. The number of puromycin-resistant colonies that survived cloning is indicated ("Stable Integrants"). These puromycin-resistant clones were also screened for their resistance to G418 ("Neo^R Integrants") and GCV ("GCV^R Integrants"). While some clones displayed either firefly (reporter for *TERT*) or *Renilla* (reporter for *CRR9*) luciferase activity, none displayed both. None of the clones were found to be the result of RMCE upon PCR analysis. While not shown, the same experiment was performed in the TERT(-) acceptor locus-containing line 166a 11.1 (~$8.59x10^5$ cells/Lipofectamine2000 transfection and ~2.71x105 cells/FuGENE-6 transfection; no puromycin-resistant clones were obtained from these transfections. Notes: All cell numbers are approximate. Cells were maintained in the absence of G418 prior to transfection.

Amt. BAC DNA	Cre Induction	Cell Line	Number of Cells	Stable Integrants	Neo^R Integrants	GCV^R Integrants	FL and RL Activity	RMCE Integrants
1.50 μg	2.5 μM 4HT	167b 3.1	4.11E+05	0	-	-	-	-
1.35 μg	0.15 μg pCBM	167b 3.1	4.11E+05	1	1	0	0	0
1.50 μg	2.5 μM 4HT	166a 11.1	2.64E+05	0	-	-	-	-
1.35 μg	0.15 μg pCBM	166a 11.1	2.64E+05	0	-	-	-	-

Table C8. Test of the Ability of 2.5 mM 4HT and pCBM Co-transfection to Mediate RMCE of the Circular BAC Reporter 117B23 cFtHRvSVP. Both TERT(+) and (-) cells containing the acceptor locus, 167b 3.1 and 166a 11.1 respectively, were transfected with the indicated amount of DNA using GenePorter2. The number of colonies that survived cloning after selection in puromycin are indicated as "Stable Integrants." These puromycin-resistant clones were also tested for their resistance to G418 ("Neo^R Integrants") and GCV ("GCV^R Integrants"). This clone did not express any luciferase activity and was shown by PCR analysis to be the result of random integration. Notes: All cell numbers are approximate. Cells were maintained in 400 μg/ml G418 prior to transfection.

Amt. BAC DNA	Cre Induction	Cell Line	Number of Cells	Stable Integrants	Neo^R Integrants	GCV^R Integrants	FL and RL Activity	RMCE Integrants
1.00 μg	1.0 μM 4HT	167b 3.1	2.31E+05	0	-	-	-	-
0.90 μg	90 ng pCBM	167b 3.1	2.31E+05	0	-	-	-	-
10.80 μg	1.08 μg pCBM	167b 3.1	2.31E+05	8	8	0	0	0
1.00 μg	1.0 μM 4HT	166a 11.1	1.49E+05	0	-	-	-	-
0.90 μg	90 ng pCBM	166a 11.1	1.49E+05	0	-	-	-	-
10.80 μg	1.08 μg pCBM	166a 11.1	1.49E+05	0	-	-	-	-

Table C9. Test of the Ability of Lipofectamine2000-Mediated Transfection of the Circular BAC Reporter 117B23 cFtHRsSVP to Undergo RMCE. Both TERT(+) (167b 3.1) and TERT(-) (166a 11.1) cells containing the acceptor locus were transfected with the indicated amounts of circular BAC DNA. The number of puromycin-resistant colonies that survived cloning are indicated as "Stable Integrants." The resistance of these puromycin-resistant clones to G418 ("Neo^R Integrants") and GCV ("GCV^R Integrants") is also indicated. None of these clones expressed any luciferase activity, and none were RMCE integrants. Notes: All cell numbers are approximate. Cells were maintained in 400 μg/ml G418 prior to transfection.

Amt. BAC DNA	Cre Induction	Cell Line	Number of Cells	Stable Integrants	Neo^R Integrants	GCV^R Integrants	FL and RL Activity	RMCE Integrants
1.00 μg	2.5 μM 4HT	167b 3.5	5.99E+05	1	0	1	-	-
0.875 μg	0.125 μg pCBM	167b 3.5	5.99E+05	0	-	-	-	-
1.50 μg	1.0 μM 4HT	167b 3.1	2.31E+05	0	-	-	-	-
1.35 μg	0.15 μg pCBM	167b 3.1	2.31E+05	2	2	0	0	0
1.50 μg	2.5 μM 4HT	167b 3.1	1.80E+05	0	-	-	-	-
1.35 μg	0.15 μg pCBM	167b 3.1	1.80E+05	6	6	0	0	0
16.20 μg	1.80 μg pCBM	167b 3.1	2.47E+06	3	3	0	1	0
1.00 μg	2.5 μM 4HT	166a 11.4	2.38E+05	0	-	-	-	-
0.875 μg	0.125 μg pCBM	166a 11.4	2.38E+05	0	-	-	-	-
1.50 μg	1.0 μM 4HT	166a 11.1	1.49E+05	0	-	-	-	-
1.35 μg	0.15 μg pCBM	166a 11.1	1.49E+05	0	-	-	-	-
16.20 μg	1.80 μg pCBM	166a 11.1	1.58E+06	0	-	-	-	-

Table C10. Test of the Ability of GenePorter2-Mediated Transfection of the Circular BAC Reporter 117B23 cFtHRsSVP to Undergo RMCE. Both TERT(+) (167b 3.1 and 3.5) and TERT(-) (166a 11.1 and 11.4) cells containing the acceptor locus were transfected with the indicated amounts of circular BAC DNA. The number of puromycin-resistant colonies that survived cloning are indicated as "Stable Integrants." The resistance of these puromycin-resistant clones to G418 ("Neo^R Integrants") and GCV ("GCV^R Integrants") is also indicated. Only one clone expressed both firefly (reporter for *CRR9*) and h*Renilla* (reporter for *TERT*) luciferase activity, but none were RMCE integrants. Notes: All cell numbers are approximate. Cells were maintained in 400 μg/ml G418 prior to transfection.

Amt. BAC DNA	Cre Induction	Cell Line	Number of Cells	Stable Integrants	Neo^R Integrants	GCV^R Integrants	FL and RL Activity	RMCE Integrants
1.00 μg	2.5 μM 4HT	167b 3.5	3.17E+05	0	-	-	-	-
0.875 μg	0.125 μg pCBM	167b 3.5	3.17E+05	0	-	-	-	-
0.50 μg	1.0 μM 4HT	167b 3.1	2.31E+05	0	-	-	-	-
0.45 μg	0.05 μg pCBM	167b 3.1	2.31E+05	2	1	1	1	0
5.40 μg	0.60 μg pCBM	167b 3.1	2.31E+06	14	14	0	1	0
1.00 μg	2.5 μM 4HT	166a 11.4	1.13E+05	0	-	-	-	-
0.875 μg	0.125 μg pCBM	166a 11.4	1.13E+05	0	-	-	-	-
0.50 μg	1.0 μM 4HT	166a 11.1	6.60E+04	0	-	-	-	-
0.45 μg	0.05 μg pCBM	166a 11.1	6.60E+04	0	-	-	-	-
5.40 μg	0.60 μg pCBM	166a 11.1	1.49E+06	4	3	1	1	0

Table C11. Test of the Ability of FuGENE-6-Mediated Transfection of the Circular BAC Reporter 117B23 cFtHRsSVP to Undergo RMCE. Both TERT(+) (167b 3.1 and 3.5) and TERT(-) (166a 11.1 and 11.4) cells containing the acceptor locus were transfected with the indicated amounts of circular BAC DNA. The number of puromycin-resistant colonies that survived cloning are indicated as "Stable Integrants." The resistance of these puromycin-resistant clones to G418 ("Neo^R Integrants") and GCV ("GCV^R Integrants") is also indicated. Three clones, two 167b 3.1 and one 166a 11.1, expressed both firefly (reporter for *CRR9*) and h*Renilla* (reporter for *TERT*) luciferase activity, but none were RMCE integrants. Notes: All cell numbers are approximate. Cells were maintained in 400 μg/ml G418 prior to transfection.

Amt. BAC DNA	Cre Induction	Cell Line	Number of Cells	Stable Integrants	Neo^R Integrants	GCV^R Integrants	FL and RL Activity	RMCE Integrants
1.80 μg	0.20 μg pCBM	167b 3.1	2.82E+05	0	-	-	-	-
2.70 μg	0.30 μg pCBM	167b 3.1	2.82E+05	1	1	0	0	0
12 μg	1.60 μg pCBM	167b 3.1	2.82E+05	1	1	0	0	0
1.80 μg	0.20 μg pCBM	166a 11.1	1.80E+05	0	-	-	-	-
2.70 μg	0.30 μg pCBM	166a 11.1	1.80E+05	0	-	-	-	-

Table C12. Test of the Ability of FuGENE-6-Mediated Transfection of the PI-*Sce*I-Linearized BAC Reporter 117B23 cFtHRsSVP to Undergo RMCE. Both TERT(+) (167b 3.1) and TERT(-) (166a 11.1) cells containing the acceptor locus were transfected with the indicated amounts of linearized BAC DNA. The number of puromycin-resistant colonies that survived cloning are indicated as "Stable Integrants." The resistance of these puromycin-resistant clones to G418 ("Neo^R Integrants") and GCV ("GCV^R Integrants") is also indicated. Neither of the puromycin-resistant clones expressed luciferase activity, nor were they RMCE integrants. Notes: All cell numbers are approximate. Cells were maintained in 400 μg/ml G418 prior to transfection.

BAC Reporter (Amt.)	Cell Line	Transfxn. Method	Number of Cells	Stable Integrants	Neo^R Integrants	GCV^R Integrants	FL and RL Activity
cRtFsP (2 μg)	167b 3.5†	Lipofectamine2000	6.34E+05	0	-	-	-
cRtFsP (5 μg)	167b 3.5†	Lipofectamine2000	1.42E+06	2	-	-	0
cRtFsSVP (1 μg)	167b 3.5†	FuGENE-6	2.82E+05	0	-	-	-
cRtFsSVP (4 μg)	167b 3.5†	FuGENE-6	1.42E+06	7	0	7	0
cFtHRsSVP (1 μg)	167b 3.5	FuGENE-6	3.17E+05	0	-	-	-
cFtHRvSVP (2 μg)*	167b 3.1	FuGENE-6	2.82E+05	0	-	-	-
cFtHRvSVP (3 μg)*	167b 3.1	FuGENE-6	2.82E+05	5	5	0	0
cFtHRvSVP (12 μg)*	167b 3.1	FuGENE-6	5.64E+05	0	-	-	-
cRtFsSVP (1 μg)	166a 11.1†	FuGENE-6	2.71E+05	0	-	-	-
cRtFsSVP (4 μg)	166a 11.1†	FuGENE-6	8.59E+05	0	-	-	-
cFtHRvSVP (2 μg)*	166a 11.1	FuGENE-6	1.80E+05	0	-	-	-
cFtHRvSVP (3 μg)*	166a 11.1	FuGENE-6	1.80E+05	0	-	-	-
cFtHRsSVP (1 μg)	166a 11.4	FuGENE-6	1.13E+05	0	-	-	-

Table C13. Test of Colony Formation After BAC Reporter Transfection in the Absence of Induced Cre Recombinase. Both TERT(+) (167b 3.1 and 3.4) and TERT(-) (166a 11.1 and 11.4) cells containing the acceptor locus were transfected with the indicated amounts of the various BAC reporters. Those transfections marked by "*" were carried out with PI-*Sce*I-linearized DNA. The number of puromycin-resistant colonies that survived cloning are indicated as "Stable Integrants." The resistance of these puromycin-resistant clones to G418 ("Neo^R Integrants") and GCV ("GCV^R Integrants") is also indicated. None of the puromycin-resistant clones expressed both firefly and *Renilla* luciferase activity. Notes: All cell numbers are approximate. Cells marked by "†" were maintained in the absence of G418 prior to transfection; all others were maintained in 400 μg/ml G418 prior to transfection.

Amt. BAC DNA	Cre Induction	Cell Line	Stable Integrants	FL and RL Activity	RMCE Integrants
5 μg	None	167b 3.1	15	2	-
5 μg	None	167b 3.1	11	2	-
8 μg	None	167b 3.1	13	3	-
5 μg	0.67 μg pCBM	167b 3.1	6	1	0
5 μg	0.67 μg pCBM	167b 3.1	8	1	0
8 μg	1.00 μg pCBM	167b 3.1	15	0	0
5 μg	0.67 μg pCBM	166a 11.1	11	0	0
5 μg	0.67 μg pCBM	166a 11.1	6	0	0
5 μg	0.67 μg pCBM	166a 11.1	0	-	-

Table C14. Stable Integrants Obtained After Electroporation of PI-*Sce*I-linearized 117B23 cFtHRvSVP. TERT(+) and (-) cells containing the acceptor locus (167b 3.1 and 166a 11.1, respectively) were electroporated with the indicated amounts of BAC and pCBM. For each experiment, $1.6x10^6$ cells were electroporated at a density of $4x10^6$ cells/ml. The number of puromcyin-resistant colonies is indicated ("Stable Integrants"), as well as the number of those stable integrants that showed both firefly (reporter for *CRR9*) and h*Renilla* (reporter for *TERT*) luciferase activity. By PCR analysis, none of the stable integrants obtained after co-electroporation with pCBM were found to be RMCE integrants.

BAC	Cell Line	Number of Electro.	Stable Integrants	FL and RL Activity
cFtHRsSVP	167b 3.1	8	26	8
cFtHRsSVP2xIns	167b 3.1	7	24	3
cFtHRsSVP	166a 11.1	8	34	5
cFtHRsSVP2xIns	166a 11.1	8	36	2

Table C15. Stable Integrants Obtained After Electroporation of PI-*Sce*I-linearized BAC DNA. TERT(+) and (-) acceptor locus-containing cells (167b 3.1 and 166a 11.1, respectively) were electroporated in the absence of Cre induction, and therefore, all puromcyin-resistant clones ("Stable Integrants") are the result of random integration. For each electroporation, $1.6x10^6$ cells at a density of $4x10^6$ cells/ml were electroporated with 5 μg BAC DNA. The number of stable integrants that displayed both firefly (reporter of *CRR9*) and h*Renilla* (reporter of *TERT*) luciferase activity are indicated.

APPENDIX D

RESULTS OF GENOMIC INTEGRATIONS USING LINEAR DNA

Clone	Day 39		Day 46		Day 88	
	FL (CRR9)	RL (TERT)	FL (CRR9)	RL (TERT)	FL (CRR9)	RL (TERT)
1	-26	299	25	12	-55	64
2	-	-	14	-20	-3	-13
3	88,109	4,844	103,446	21,631	89,428	19,925
4	1,270	-79	870	61	-	-
5	-	-	22	-8	-	-
6	-13	-40	21	29	-39	2
7	-18	-73	18	-31	-26	4
8	-31	-43	13	-16	-44	-13
9	-39	-50	47	-42	-	-
10	-	-	765	-24	-	-
11	-	-	29	-42	-33	49
12	72,378	67,093	263,587	445,720	-	-
13	-	-	2,252	-67	-	-
14	-	-	3	-37	-38	34
15	-24	-95	10	-38	-	-
16	6	-37	35	6	10	32
17	-26	-37	11	33	-15	21
18	61,615	955	188,589	4,822	648,623	14,707
19	217,518	-72	321,791	-26	238,928	16
20	1,232	402	676	840	-	-
21	-28	-43	64	-21	-35	9
22	70	-10	123	204	-35	-31
23	685	-33	379	-5	-	-
24	-6	-18	18	-36	-48	11

Clone	Day 39		Day 46		Day 88	
	FL (CRR9)	RL (TERT)	FL (CRR9)	RL (TERT)	FL (CRR9)	RL (TERT)
25	28	32	-7	-18	-55	16
26	-	-	9	666	-	-
27	-	-	-	-	-	-
28	-2	-71	13	-10	-54	-29
29	-	-	83	-19	-	-
30	-	-	59,198	1,099	-	-
31	-	-	19	-44	-23	19
32	-	-	21	387	-	-
33	-13	86	1,635	32	-	-
34	-	-	4,803	439	-	-
35	254	44	535	-19	-	-
36	-	-	-	-	-28	1,414
37	17,464	118	45,780	526	17,556	580
38	-	-	23	-37	-	-
39	-2	-79	815	-51	3	9
40	-	-	-	-	-34	37
41	76,439	12,547	333,919	75,163	438,862	40,994
42	-24	-47	11	12	-48	9
43	-	-	65	-32	-	-
44	346	-90	14	-66	-30	19
45	-	-	35	-18	-15	67
46	16,205	59	152,273	407	89,115	900
47	-	-	18	217,651	-	-
48	-	-	30	9	-7	28

Table D1. Luciferase Activity of TERT(+) Stable Integrants Obtained From Electroporation with Linearized BAC DNA Containing SV40-*puro* Proximal to *lox511*. Luciferase activity was assessed using the Dual-Luciferase® Reporter Assay System (Promega). All units are RLU/s. "-" indicates the luciferase activity was not assayed. Background measurements were obtained from assaying the activity of the lysis buffer; the values shown are after background subtraction. For the first assay, FL and RL background was 404 and 646 RLU/s, respectively. For the second assay, FL and RL background was 313 and 523 RLU/s, respectively. For the third assay, FL and RL background was 270 and 418 RLU/s, respectively. The total number of cells or protein was not normalized between clones or between assays. Clone numbers are arbitrary.

Clone	FL (CRR9)	RL (TERT)	FL (CRR9)	RL (TERT)
102	-	-	2	9
103	1	64	6	-17
104	-12	48	42	11
105	-31	16	11	38
106	-30	-49	-2	64
107	-34	8	79	-41
108	-23	42	1	16
109	22,758	87	35,634	-2
110	-27	82	-36	21
111	339,367	68	436,041	0
112	-21	113	17	37
113	-29	45	6	103
114	-19	40	310	96
115	-28	44	-2	-19
116	-	-	9	-2

Table D2. Luciferase Activity of TERT(-) Stable Integrants Obtained From Electroporation with Linearized BAC DNA Containing SV40-*puro* Proximal to *lox511*. Luciferase activity of individual clones was assessed using the Dual-Luciferase® Reporter Assay System (Promega). "-" indicates the luciferase activity was not assayed. Background measurements were obtained from assaying the activity of the lysis buffer; the values shown are after background subtraction. For the first assay, the FL and RL background levels were 238 and 393 RLU/s, respectively. For the second assay, the FL and RL background were 230 and 420 RLU/s, respectively. The total number of cells or protein was not normalized between clones or between assays. All units are RLU/s. Clone numbers are arbitrary.

Clone	FL (CRR9)	RL (TERT)	FL (CRR9)	RL (TERT)
201	-3	872	3	2,114
202	36,958	21	79,425	-15
203	17	461	-13	1,477
204	-21	28	0	26
205	-8	1	-13	-18
206	-17	4	-4	8
207	-31	-13	-1	-6
208	5	-11	-8	-24
409	45	-11	-11	7
410	204,777	50	223,834	18
411	25	22	22	36
412	40	16	8	10
413	26	30	68	90
414	3,293	91	2,831	34
415	33,090	134	28,603	222
416	42,043	818	92,772	1,056
417	54	30	21	16
418	2,602	14	4,383	41
419	17	27	-2	33
606	24,102	20	25,109	10
607	178,936	-15	-	-
608	56	48	33	32
609	24	2,546	44	3,908
610	77	-15	17	9

Table D3. Luciferase Activity of TERT(+) Stable Integrants Obtained From Electroporation with Linearized BAC DNA Containing SV40-*puro* in *sacB* and Dual-Copy Insulators. Luciferase activity of individual clones was assessed using the Dual-Luciferase® Reporter Assay System (Promega). "-" indicates the luciferase activity was not assayed. Background measurements were obtained from assaying the activity of the lysis buffer; the values shown are after background subtraction. For all assays, the FL background level was 262 ± 53 RLU/s; the RL background was 352 ± 46 RLU/s. The total number of cells or protein was not normalized between clones or between assays. All units are RLU/s. Clone numbers are arbitrary.

Clone	FL (CRR9)	RL (TERT)	FL (CRR9)	RL (TERT)
209	-	-	5,525	27
210	-18	-1	82	15
211	9,364	672	93,204	1,400
212	1	1,470	3	6,882
213	-5	0	-2	-4
214	-23	12	2	-10
215	16,502	94	158,699	547
216	-4	29	-4	114
217	-14	29	-10	107
218	6	-17	5	-12
219	-20	-1	-13	7
220	-17	123	-16	730
221	-7	6,801	-20	25,136
222	-35	5,291	3	19,507
223	26,672	189	265,990	2,708
224	-24	-3	-4	-4
401	12,085	5,762	8,695	12,293
402	197,251	8,865	323,015	15,134
403	33	1,880,458	41	2,031,549
404	28	3,546	-34	3,594
405	1,837,371	41,761	1,746,397	67,987
406	22,554	109	87,788	411
407	37	18	111	58
408	41	45	46	53
420	3,010	1	-	-
601	413,339	7,160	275,693	10,921
602	68	32	34	9
603	65	48	36	58
604	18	32	27	20

Table D4. Luciferase Activity of TERT(+) Stable Integrants Obtained From Electroporation With Linearized BAC DNA Containing SV40-*puro* in *sacB*. Luciferase activity of individual clones was assessed using the Dual-Luciferase® Reporter Assay System (Promega). "-" indicates the luciferase activity was not assayed. Background measurements were obtained from assaying the activity of the lysis buffer; the values shown are after background subtraction. For all assays, the FL background level was 262 ± 53 RLU/s; the RL background was 352 ± 46 RLU/s. The total number of cells or protein was not normalized between clones or between assays. All units are RLU/s. Clone numbers are arbitrary.

Clone	FL (CRR9)	RL (TERT)	FL (CRR9)	RL (TERT)
301	-	-	-26	-20
302	6	-7	-2	-13
303	-3	17	-20	1
304	-10	25	-26	-58
305	-2	30	-30	-27
306	-9	-17	-19	-21
307	8	-8	10	-5
308	-	-	-28	-84
309	-	-	-16	66
310	3	9	-24	-16
311	-12	8,932	-18	598
312	-4	12	-8	-30
313	-	-	-49	-51
314	-14	17	-7	-65
315	-1	31,197	-37	5,201
316	-	-	-15	-1
515	10	1	71	46
516	-12	-37	28	40
517	3,367	821	5,031	352
518	-17	-20	14	54
519	-	-	19	25
520	-2	16	66	71
521	-27	-49	35	-18
522	-38	-39	-45	58
523	-8	-22	58	-53
524	-22	-22	47	39
525	146,352	1,346	125,313	399
526	-	-	10	544,166
527	-27	-23	-11	-22
528	-23	32	19	86
708	-	-	21	-3
709	-32	-29	18	11
710	-11	-5	34	13
711	4,748	203	4,327	97
713	-	-	25	-7
714	-	-	50	4,146

Table D5. Luciferase Activity of TERT(-) Stable Integrants Obtained From Electroporation with Linearized BAC DNA Containing SV40-*puro* in *sacB* and Dual-Copy Insulators. Luciferase activity of individual clones was assessed using the Dual-Luciferase® Reporter Assay System (Promega). "-" indicates the luciferase activity was not assayed. Background measurements were obtained from assaying the activity of the lysis buffer; the values shown are after background subtraction. For all assays, the FL background level was 320 ± 54 RLU/s; the RL background was 415 ± 56 RLU/s. The total number of cells or protein was not normalized between clones or between assays. All units are RLU/s. Clone numbers are arbitrary.

Clone	FL (CRR9)	RL (TERT)	FL (CRR9)	RL (TERT)
317	10	19	-9	4
318	23	-20	5	-36
319	-12	-10	14	14
320	-	-	-13	53,818
321	-6	5	-34	-21
322	207,001	712	64,877	148
324	10	-43	-13	-22
325	-16	22	-3	-18
326	-	-	-30	9,278
327	0	27,695	8	-14
328	-9	196,768	-31	37,340
329	12	2,214	-20	3,137
501	-	-	-	-
502	-10	1	37	22
503	-	-	5	27
504	64	7	125	66
505	-	-	41,017	1,976
506	-8	173	41	243
507	15	-22	30	44
508	7	-27	89	24
509	-3	21,335,230	13	21,452,633
510	-21	29	-3	40
511	-22	43	66	16
512	-22	22	5	22
513	-	-	183,910	573,276
514	851,315	4	1,483,269	43
529	110,368	368	175,193	590
701	-	-	155,440	1,735
702	-23	34,341	-24	49,829
703	-39	36	19	0
704	27	4	16	2
705	-5	26	39	-23
706	17	20	26	7
707	-32	28	-15	-2

Table D6. Luciferase Activity of TERT(-) Stable Integrants Obtained from Electroporation with Linearized BAC DNA Containing SV40-*puro* in *sacB*. Luciferase activity of individual clones was assessed using the Dual-Luciferase® Reporter Assay System (Promega). "-" indicates the luciferase activity was not assayed. Background measurements were obtained from assaying the activity of the lysis buffer; the values shown are after background subtraction. For all assays, the FL background level was 320 ± 54 RLU/s; the RL background was 415 ± 56 RLU/s. The total number of cells or protein was not normalized between clones or between assays. All units are RLU/s. Clone numbers are arbitrary.

	Southern		Activity	
Clone	FL	hRL	FL	hRL
1	-	-	-	-
2	-	-	-	-
3	+	+	+	+
4	-	-	-	-
5	-	-	-	-
6	-	-	-	-
7	-	-	-	-
8	-	-	-	-
9	-	-	-	-
10	-	-	-	-
11	-	-	-	-
12	+	+	-	-
13	-	-	-	-
14	-	-	-	-
15	-	-	-	-
16	-	-	-	-
17	-	-	-	-
18	+	+	+	+
19	+	-	+	-
20	-	-	+	+
21	-	-	-	-
22	-	+	-	-
23	-	-	-	-
24	-	-	-	-
25	-	-	-	-
26	-	-	+	+
27	-	-	-	-
28	-	-	-	-
29	-	-	-	-
30	+	+	-	-
31	-	-	-	-
32	-	+	-	-
33	-	-	-	-
34	-	+	-	-
35	-	-	-	-
36	-	+	-	+
37	+	+	+	+
38	-	-	-	-
39	-	-	-	-
40	-	-	-	-
41	+	+	+	+
42	-	-	-	-

Table D7. Summary of Clones 1-42. Clones 1-42 were the result of electroporation of TERT(+) 167b 3.1 cells. The data in this summary table were compiled from luciferase assays of stable integrants and Southern hybridization with probes specific for firefly (reporter for *CRR9*) and h*Renilla* (reporter for *TERT*) luciferase. The clones were scored for either the presence ("+") or absence ("-") of luciferase activity or the specific hybridization fragment.

		Southern		Activity	
Clone	**Ins**	**FL**	**hRL**	**FL**	**hRL**
201	+	-	+	-	+
202	+	+	-	+	-
203	+	-	+	-	+
204	+	-	-	-	-
205	+	-	+	-	-
206	+	-	-	-	-
207	+	-	-	-	-
208	+	-	-	-	-
209	-	+	+	+	-
210	-	a	a	-	-
211	-	+	+	+	+
212	-	-	+	-	+
213	-	-	-	-	-
214	-	-	+	-	-
215	-	-	+	+	+
216	-	-	+	-	+
217	-	-	-	-	-
218	-	-	-	-	-
219	-	-	+	-	+
220	-	-	+	-	+
221	-	-	+	-	+
222	-	-	b	-	+
223	-	a	a	+	+
224	-	-	b	-	-

Table D8. Summary of Clones 201-224. Clones 201-224 are the result of electroporation of TERT(+) 167b 3.1 cells. The data in this summary table were compiled from luciferase assays of stable integrants and Southern hybridization with probes specific for firefly (reporter for *CRR9*) and h*Renilla* (reporter for *TERT*) luciferase. The clones were scored for either the presence ("+") or absence ("-") of luciferase activity or the specific hybridization fragment. The presence or absence of dual-copy insulators ("Ins") is also noted. a: Southern hybridization not performed. b: Results of Southern hybridization unclear.

		Southern		Activity	
Clone	**Ins**	**FL**	**hRL**	**FL**	**hRL**
301	+	-	-	-	-
302	+	-	-	-	-
303	+	-	-	-	-
304	+	-	-	-	-
305	+	-	-	-	-
306	+	-	-	-	-
307	+	-	-	-	-
308	+	-	-	-	-
309	+	-	-	-	-
310	+	-	-	-	-
311	+	-	+	-	+
312	+	-	-	-	-
313	+	-	-	-	-
314	+	-	-	-	-
315	+	-	+	-	+
316	+	-	-	-	-
317	-	-	-	-	-
318	-	-	-	-	-
319	-	-	-	-	-
320	-	-	+	-	+
321	-	-	-	-	-
322	-	+	+	+	+
324	-	-	-	-	-
325	-	-	-	-	-
326	-	-	+	-	+
327	-	-	-	-	-
328	-	-	+	-	+
329	-	-	+	-	+

Table D9. Summary of Clones 301-329. Clones 301-329 are the result of electroporation of TERT(-) 166a 11.1 cells. The data in this summary table were compiled from luciferase assays of stable integrants and Southern hybridization with probes specific for firefly (reporter for *CRR9*) and h*Renilla* (reporter for *TERT*) luciferase. The clones were scored for either the presence ("+") or absence ("-") of luciferase activity or the specific hybridization fragment. The presence or absence of dual-copy insulators ("Ins") is also noted. The Southern hybridization information for clone 308 was obtained from a different membrane (data not shown).

		Southern		Activity	
Clone	**Ins**	**FL**	**hRL**	**FL**	**hRL**
601	-	+	+	+	+
602	-	-	-	-	-
603	-	-	-	-	-
604	-	-	-	-	-
605	-	-	-	-	-
606	+	-	-	+	+
607	+	+	-	a	a
608	+	-	-	-	-
609	+	-	+	-	+
610	+	-	-	-	-
701	-	+	+	+	+
702	-	-	+	-	+
703	-	-	-	-	-
704	-	-	-	-	-
705	-	-	-	-	-
706	-	-	-	-	-
707	-	-	-	-	-
708	+	-	-	-	-
709	+	-	-	-	-
710	+	-	-	-	-
711	+	-	-	+	b
712	+	-	-	-	-
713	+	-	-	-	-
714	+	-	+	-	+

Table D10. Summary of Clones 601-610 And 701-714. Clones 601-604 and 606-610 are the result of electroporation of TERT(+) 167b 3.1 cells. Clones 605 and 701-714 are the result of electroporation of TERT(-) 166a 11.1 cells. The data in this summary table were compiled from luciferase assays of stable integrants and Southern hybridization with probes specific for firefly (reporter for *CRR9*) and h*Renilla* (reporter for *TERT*) luciferase. The clones were scored for either the presence ("+") or absence ("-") of luciferase activity or the specific hybridization fragment. The presence or absence of dual-copy insulators ("Ins") is also noted. a: Luciferase activity not assessed. b: Clone 711 showed low-level h*Renilla* luciferase activity in some assays, but not others (see Figure D5 of Appendix D).

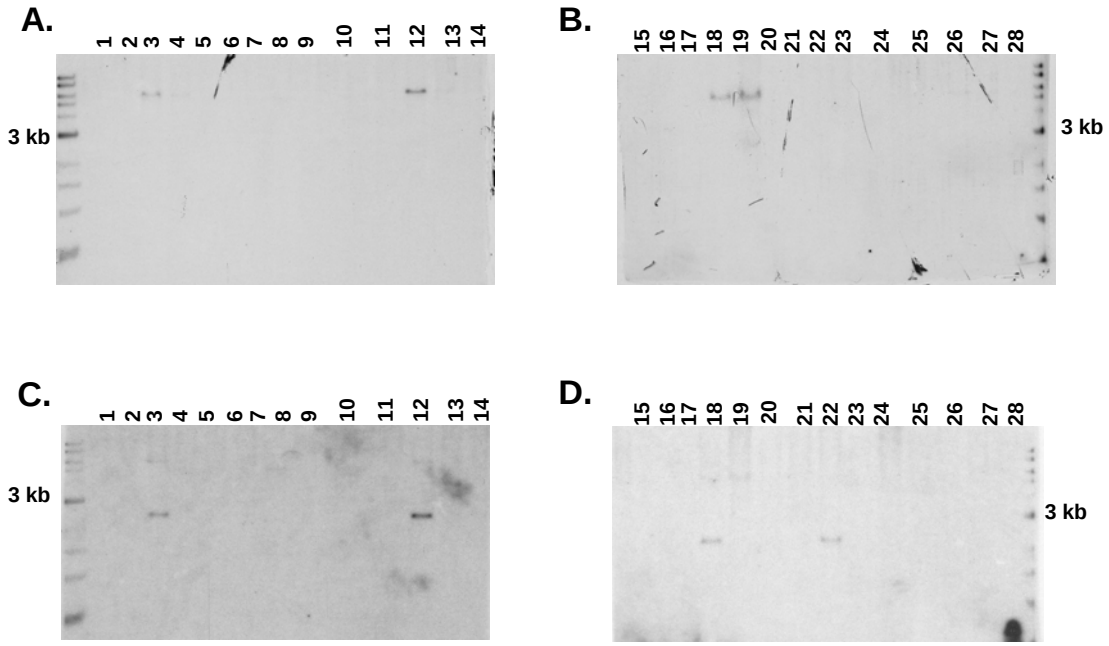

Figure D1. Southern Hybridization of Clones 1-28. Clones 1-28 are stable integrants obtained after electroporation of the TERT(+) acceptor locus-containing cell line 167b 3.1 with a PI-*Sce*I-linearized BAC reporter expressing SV40-*puro* from a position immediately interior to *lox511*. Southern hybridization was performed on gDNA digested with the restriction endonuclease *Bst*EII. **A** and **B**. Hybridization with a probe specific for firefly luciferase (reporter for *CRR9*). The expected hybridization fragment is 5,736 bp and is only seen for clones 3, 12, 18, and 19. **C** and **D**. Hybridization with a probe specific for h*Renilla* luciferase (reporter for *TERT*). The expected hybridization fragment is 2,394 bp and is only seen for clones 3, 12, 18, and 22. Note: The data in this figure is summarized in Table D1.

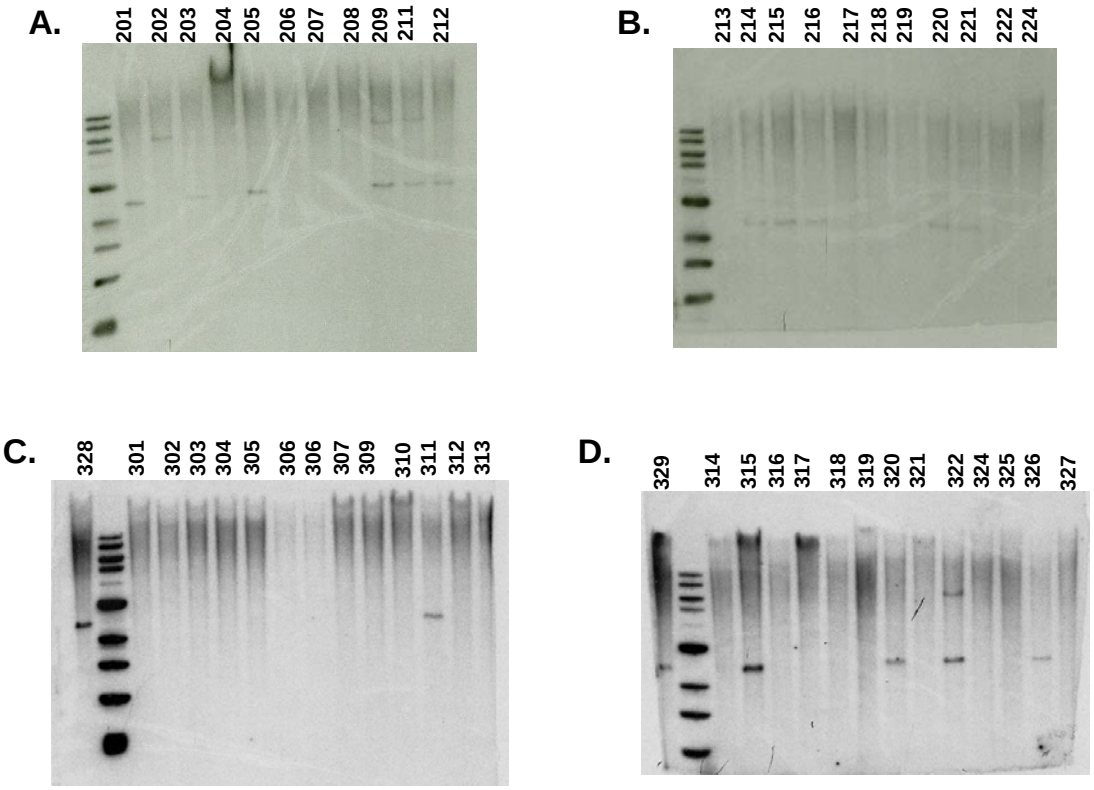

Figure D2. Southern Hybridization of Clones 201-224 and 301-329. Southern hybridization was performed with the firefly (reporter for *CRR9*) and h*Renilla* (reporter for *TERT*) luciferase probes simultaneously on gDNA digested with the restriction endonuclease *Bst*EII. **A** and **B**. Clones 201-208 are stable integrants obtained after electroporation of the TERT(+) acceptor locus-containing cell line 167b 3.1 with a PI-*Sce*I-linearized BAC reporter expressing SV40-*puro* from *sacB* and dual-copy insulators interior to the *loxP* and *lox511* sites. The remaining clones are stable integrants obtained after electroporation with the same BAC in the absence of the dual-copy insulators. **C** and **D**. Clones 301-315 are stable integrants obtained after electroporation of the TERT(-) acceptor locus-containing cell line 166a 11.1 with the PI-*Sce*I-linearized BAC reporter containing the dual-copy insulators. The remaining clones were obtained after electroporation with the same BAC in the absence of dual-copy insulators. Note: The data in this figure is summarized in Tables D2 and D3.

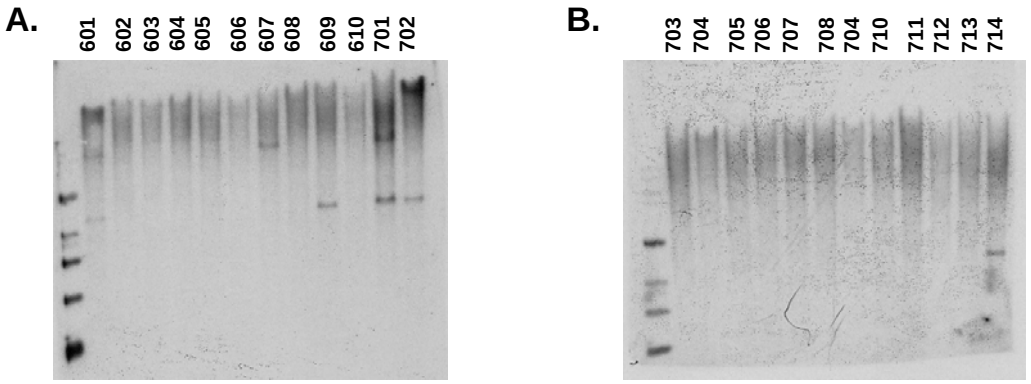

Figure D3. Southern Hybridization of Clones 601-610 and 701-714. Southern hybridization was performed with the firefly (reporter for *CRR9*) and h*Renilla* (reporter for *TERT*) luciferase probes simultaneously on gDNA digested with the restriction endonuclease *Bst*EII. **A** and **B**. Clones 601-604 are stable integrants obtained after electroporation of the TERT(+) acceptor locus-containing cell line 167b 3.1 with a PI-*Sce*I-linearized BAC reporter expressing SV40-*puro* from *sacB*. Clones 606-610 are stable integrants obtained after electroporation of 167b 3.1 cells with a BAC containing dual-copy insulators. Clones 605 and 701-707 are stable integrants obtained after electroporation of the TERT(-) acceptor locus-containing cell line 166a 11.1 with the PI-*Sce*I-linearized BAC reporter. The remaining clones were obtained after electroporation with the same BAC in the presence of dual-copy insulators. Note: The data in this figure is summarized in Table D4.

Reference List

1. Ruvkun G, Hobert O. The taxonomy of developmental control in *Caenorhabditis elegans*. Science 1998;2033-41.

2. Adams MD, Celniker SE, Holt RA, Evans CA, Gocayne JD, Amanatides PG, Scherer SE, Li PW, Hoskins RA, Galle RF, George RA, Lewis SE, Richards S, Ashburner M, Henderson SN, Sutton GG, Wortman JR, Yandell MD, Zhang Q, Chen LX, Brandon RC, Rogers Y-HC, Blazej RG, Champe M, Pfeiffer BD, Wan KH, Doyle C, Baxter EG, Helt G, Nelson CR, Miklos GLG, Abril JF, Agbayani A, An H-J, Andrews-Pfannkoch C, Baldwin D, Ballew RM, Basu A, Baxendale J, Bayraktaroglu L, Beasley EM, Beeson KY, Benos PV, Berman BP, Bhandari D, Bolshakov S, Borkova D, Botchan MR, Bouck J, Brokstein P, Brottier P, Burtis KC, Busam DA, Butler H, Cadieu E, Center A, Chandra I, Cherry JM, Cawley S, Dahlke C, Davenport LB, Daview P, Pablos Bd, Delchr A, Deng Z, Mays AD, Dew I, Dietz SM, Dodson K, Coup LE, Downes M, Dugan-Rocha S, Dunkov BC, Dunn P, Durbin KJ, Evangelista CC, Ferraz C, Ferriera S, Fleishmann W, Fosler C, Gabrielian AE, Garg NS, Gelbart WM, Glasser K, Glodek A, Gong F, Correll JH, Fu Z, Guan P, Harris M, Harris NL, Harvey D, Heiman TJ, Hernandez JR, Houck H, Hostin D, Houston KA, Howland TJ, Wei M-H, Ibegwam C, Jalali M, Kalush F, Karpen GH, Ke Z, Kennison JA, Ketchem KA, Kimmel BE, Kodira CD, Kraft C, Kravitz S, Kulp D, Lai Z, Lasko P, Lei Y, Levitsky AA, Li J, Li Z, Liang Y, Lin X, Liu X, Mattei B, McIntosh TC, McLeod MP, McPherson D, Merkulov G, Milshina NV, Mobarry C, Morris J, Moshrefi A, Mount SM, Moy M, Murphy B, Murphy L, Muzny DM, Nelson DL, Nelson DR, Nelson KA, Nixon K, Nusskem DR, Pacleb JM, Palazzolo M, Pittman GS, Pan S, Pollard J, Puri V, Reese MG, Reinert K, Remington K, Saunders RDC, Scheeler F, Shen H, Shue BC, Siden-Kiamos I, Simpson M, Skupski MP, Smith T, Spier E, Spradling AC, Stapleton M, Strong R, Sun E, Svirskas R, Tector C, Turner R, Venter E, Wang AH, Wnag X, Wang Z-Y, Wassarman DA, Weinstock GM, Weissenbach J, WIlliams SM, Woodage T, Worley KC, Wu D, Yang S, Yao QA, Ye J, Yeh R-F, Zaveri JS, Zhan M, Zhang G, Zhao Q, Zheng L, Zheng XH, Zhong FN, Zhong W, Zhou X, Zhu S, Zhu X, Smith MO, Gibbs RA, Myers EW, Rubin GM, Venter JC. Drosophila melanogaster. Science 2000;2185-95.

3. Consortium IHGS. Initial sequencing and analysis of the human genome. Nature 2001;860-921.

4. Butler JEF, Kadonaga JT. The RNA polymerase II core promoter: a key component in the regulation of gene expression. Genes and Development 2002;2582-92.

5. Breathnack R, Chambon P. Organization and expression of eucaryotic split genes coding for proteins. Annual Reviews in Biochemistry 1981;349-83.

6. Lagrange T, Kapanidis AN, Tang H, Reinberg D, Ebright RH. New core promoter element in RNA polymerase II-dependent transcription: sequence-specific DNA

binding by transcription factor IIB. Genes and Development 1998;34-44.

7. Suzuki Y, Tsunoda T, Sese J, taira H, Mizushima-Sugano J, Hata H, Ota T, Isogai T, Tanaka T, Nakamura Y, Suymama A, Sakaki Y, Morishita S, Okubo K, Sugano S. Identification and characterization of the potential promoter regions of 1031 kinds of human genes. Genome Res 2001;677-84.

8. Burke TW, Kadonaga JT. *Drosophila* TFIID binds to a conserved downstream basal promoter element that is present in many TATA-box-deficient promoters. Genes and Development 1996;711-24.

9. Burke TW, Kadonaga JT. The downstream core promoter element, DPE, is conserved from *Drosophila* to humans and is recognized by $TAF_{II}60$ of *Drosophila*. Genes and Development 1997;3020-31.

10. Smale ST, Baltimore D. The "initiator" as a transcription control element. Cell 1989;103-13.

11. Calhoun VC, Stathopoulos A, Levine M. Promoter-proximal tethering elements regulate enhancer-promoter specificity in the *Drosophila Antennapedia* complex. PNAS 2002;9243-7.

12. Lee F, Hall CV, Ringold GM, Dobson DE, Luh J, Jacob PE. Functional analysis of the steriod hormone control region of mouse mammary tumor virus. Nucleic Acids Res. 1984;4191-206.

13. Klein-Hitpass L, Ryffel GU, Heitlinger E, Cato ACB. A 13 bp palindrome is a functional estrogen responsive element and interacts specifically with estrogen receptor. Nucleic Acids Res. 1988;647-63.

14. Banerji J, Rusconi S, Schaffner W. Expression of a β-globin gene is enhanced by remote SV40 DNA sequences. Cell 1981;299-308.

15. Blackwood EM, Kadonaga JT. Going the distance: a current view of enhancer action. Science 1998;60-3.

16. Brand AH, Breeden L, Abraham J, Sternglanz R, Nasmyth K. Characterization of a "silencer" in yeast: a DNA seuqnce with properties opposite to those of a transcriptional enhancer. Cell 1985;41-8.

17. Geyer PK, Corces VG. DNA position-specific repression of transcription by a Drosophila zinc finger protein. Genes and Development 1992;1865-73.

18. Chung JH, Whiteley M, Felsenfeld G. A 5' element of the chicken β-globin domain serves as an insulator in human erythroid cells and protects against position effects in Drosophila. Cell 1993;505-14.

19. Noma K, Allis CD, Grewal SIS. Transitions in distinct histone H3 methylation

patterns at the heterochromatin domain boundaries. Science 2001;1150-5.

20. Bell AC, West AG, Felsenfeld G. The protein CTCF is required for the enhancer blocking activity of vertebrate insulators. Cell 1999;387-96.

21. Recillas-Targa F, Pikaart MJ, Burgess-Beusse B, Bell AC, Litt MD, West AG, Gaszner M, Felsenfeld G. Position-effect protection and enhancer blocking by the chicken β-globin insulator are separable activities. PNAS 2002;6883-8.

22. Mutskov VJ, Farrell CM, Wade PA, Wolffe AP, Felsenfeld G. The barrier function of an insulator couples high histone acetylation levels with specific protection of promoter DNA from methylation. Genes and Development 2002;1540-54.

23. Pugh BF, Tjian R. Mechanism of transcriptional activation by Sp1: evidence for coactivators. Cell 1990;1187-97.

24. Kirov N, Zhelnin L, Shah J, Rushlow C. Conversion of a silencer into an enhancer: evidence for a co-repressor in dorsal-mediated repression in Drosophila. EMBO J. 1993;3193-9.

25. Goodrich JA, Hoey T, Thut CJ, Admn A, Tjian R. Drosophila TAFII40 interacts with both a VP16 activation domain and the basal transcription factor TFIIB. Cell 1993;519-30.

26. Chrivia JC, Kwok RPS, Lamb N, Hagiwara M, Montiminy MR, Goodman RH. Phosphorylated CREB binds specifically to the nuclear protein CBP. Nature 1993;855-9.

27. Lundblad JR, Kwok RP, Laurance ME, Harter ML, Goodman RH. Adenoviral E1A-associated protein p300 as a functional homologue of the transcriptional co-activator CBP. Nature 1995;85-8.

28. Kanai F, Marignani PA, Sarbassova D, Yagi R, Hall RA, Donowitz M, Hisaminato A, Fujiwara T, Ito Y, Cantley LC, Yaffe MB. TAZ: a novel transcriptional co-activator regulated by interactions with 14-3-3 and PDZ domain proteins. EMBO J. 2000.

29. Paroush Z, Jr. RLF, Kidd T, Wainwright SM, Ingham PW, Brent R, Ish-Horowicz D. Groucho is required for Drosophila neurogenesis, segmentation, and sex determination and interacts directly with hairy-related bHLH proteins. Cell 1994;805-15.

30. Boyd JM, Subramaian T, Schaeper U, Regina ML, Bayley S, Chinnadurai G. A region in the C-terminus of adenovirus 2/5 E1a protein is required for association with a cellular phosphoprotein and important for the negative modulation of T24-ras mediated transformation, tumorigenesis and metastasis. EMBO J. 1993;469-78.

31. Horlein AJ, Naar AM, Heinzel T, Torchia J, Gloss B, Kurokawa R, Ryan A, Kamei Y, Soderstrom M, Glass CK, Rosenfeld MG. Ligand-independent repression by the thyroid hormone receptor mediated by a nuclear receptor co-repressor. Nature 1995;397-404.

32. Wotton D, Lo RS, Lee S, Massague J. A Smad transcriptional corepressor. Cell 1999;29-39.

33. Watt F, Molloy PL. Cytosine methylation prevents binding to DNA of HeLa cell transcription factor required for optimal expression of the adenovirus major late promoter. Genes and Development 1988;1136-43.

34. Kroft TL, Jethanandani P, McLean DJ, Goldberg E. Methylation of CpG dinucleotides alters binding and silences testis-specific transcription directed by the mouse lactate dehydrogenase c promoter. Biology of Reproduction 2001;1522-7.

35. Boyes J, Bird A. DNA methylation inhibits transcription indirectly via a methyl-CpG binding protein. Cell 1991;1123-34.

36. Jones PL, Veenstra GCJ, Wade PA, Vermaak D, Kass SU, landsberger N, Strouboulis J, Wolffe AP. Methylated DNA and MeCP2 recruit histone deacetylase to repress transcription. Nature Genetics 1998;187-91.

37. Wilkins JF. Genomic imprinting and methylation: epigenetic canalization and conflict. Trends in Genetics 2005;356-65.

38. Reik W, Dean W, Walter J. Epigenetic reprogramming in mammalian development. Science 2001;1089-93.

39. Klose RJ, Bird AP. Genomic DNA methylation: the mark and its mediators. Trends in Biochemical Sciences 2006;89-97.

40. Okano M, Bell DW, Haber DA, Li E. DNA methyltransferases Dnmt3a and Dnmt3b are essential for de novo methylation and mammalian development. Cell 1999;247-57.

41. Hendrich B, Guy J, Ramsahoye B, Wilson VA, Bird A. Closely related proteins MBD2 and MBD3 play distinctive but interacting roles in mouse development. Genes and Development 2001;710-23.

42. Hansen RS, Wijmenga C, Luo P, Stanek AM, Canfield TK, Weemaes CMR, Gartler SM. The *DNMT3B* gene is mutated in the ICF immunodeficiency syndrome. PNAS 1999;14412-7.

43. Amir RE, Veyver IBVd, Wan M, Tran CQ, Francke U, Zoghbi HY. Rett syndrome is caused by mutations in X-linked *MECP2*, encoding methyl-CpG-binding protein 2. Nature Genetics 1999;185-8.

44. Nicholls RD, Knoll JHM, Butler MG, Karam S, Lalande M. Genetic imprinting suggested by maternal heterodisomy in non-deletion Prade-Willi syndrome. Nature 1989;281-5.

45. Driscoll DJ, Waters MF, Williams CA, Zori RT, Glenn CC, Avidano KM, Nicholls RD. A DNA methylation imprint, determined by the sex of the parent, distinguishes the Angelman and Prader-Willi syndromes. Genomics 1992;917-24.

46. Driel Rv, Fransz PF, Verschure PJ. The eukaryotic genome: a system regulated at different hierarchical levels. Journal of Cell Science 2003;4067-75.

47. Strahl BD, Allis CD. The language of covalent histone modifications. Nature 2000;41-5.

48. Jenuwein T, Allis CD. Translating the histone code. Science 2001;1074-80.

49. Turner BM. Cellular memory and the histone code. Cell 2002;285-91.

50. Eberharter A, Becker PB. Histone acetylation: a switch between repressive and permissive chromatin. EMBO Rep. 2002;224-9.

51. Racey LA, Byovet P. Histone acetyltransferase in chromatin. Evidence for in vitro enzymatic transfer of acetate from acetyl-coenzyme A to histones. Experimental Cell Research 1971;366-70.

52. Kaneta H, Fujimoto D. A histone deactylase capable of deacetylating chromatin-bound histones. Journal of Biochemistry 1974;905-7.

53. Mahadevan LC, Willis AC, Barratt MJ. Rapid histone H3 phosyphorylation in response to growth factors, phorbol esters, okadaic acid, and protein synthesis inhibitors. Cell 1991;775-83.

54. Kwok RPS, Lundblad JR, Chrivia JC, Richards JP, Bachinger hP, Brennan RG, Roberts SGE, Green MR, Goodman RH. Nuclear protein CBP is a coactivator for the transcription factor CREB. Nature 1994;223-6.

55. Sobulo OM, Borrow J, Tomek R, Reshmi S, Harden A, Schlegelberger B, Housman D, Doggett NA, Rowley JD, Zeleznik-Le NJ. MLL is fused to CBP, a histone acetyltransferase, in therapy-related acute myeloid leukemia with a t(11:16)(q23;p13.3). PNAS 1997;8732-7.

56. Lin RJ, Nagy L, Inoue S, Shao W, Wison H.Miller Jr, Evans RM. Roles of histone deacetylase complex in acute promyelocytic leukaemia. Nature 1998;811-4.

57. Miao F, Natarajan R. Mapping global histone methylation patterns in the coding regions of human genes. Mol Cell Biol 2005;4650-61.

58. Lachner M, O'Carroll D, Rea S, Mechtler K, Jenuwein T. Methylation of histone H3 lysine 9 creates a binding site for HP1 proteins. Nature 2001;116-20.

59. Bannister AJ, Zegerman P, Partridge JF, Miska EA, Thomas JO, Allshire RC, Kousarides T. Selective recognition of methylated lysine 9 on histone H3 by the HP1 chromo domain. Nature 2001;120-4.

60. Lehnertz B, Ueda Y, Derijck AAHA, Braunschweig U, Prez-Burgos L, Kubicek S, Chen T, Li E, Jenuwein T, Peters AHFM. *Suv39h*-mediated histone H3 lysine 9 methylation directs DNA methylation to major satellite repeats at pericentric heterochromatin. Current Biology 2003;1192-200.

61. Fuks F, Hurd PJ, Deplus R, Kouzarides T. The DNA methyltransferases associate with HP1 and the SUV39H1 histone methyltransferase. Nucleic Acids Res. 2003;2305-12.

62. Nishiola K, Chuikov S, Sarma K, Erdjument-Bromage H, Allis CD, Tempst P, Reinberg D. Set9, a novel histone H3 methyltransferase that facilitates transcription by precluding histone tail modifications required for heterochromatin formation. Genes and Development 2002;479-89.

63. Shi Y, Lan F, Matson C, Mulligan P, Whetstine JR, Cole PA, Casero RA, Shi Y. Histone demethylation mediated by the nuclear amine oxidase homolog LSD1. Cell 2004;941-53.

64. Tsukada Y, Fang J, Erdjument-Bromage H, Warren ME, Borchers CH, Tempst P, Zhang Y. Histone demethylation by a family of JmjC domain-containing proteins. Nature 2006;811-6.

65. Yamane K, Toumazou C, Tsukada Y, Erdjument-Bromage H, Tempst P, Wong J, Zhang Y. JHDM2A, a JmjC-containing H3K9 demethylase, facilitates transcription acitvation by androgen receptor. Cell 2006;483-95.

66. Narlikar GJ, Fan H-Y, Kingston RE. Cooperation between complexes that regulate chromatin structure and transcription. Cell 2002;475-87.

67. DiRenzo J, Shang Y, Sif S, Myers M, Kingston R, Brown M. BRG-1 is recruited to estrogen-responsive promoters and cooperates with factors involved in histone acetylation. Mol Cell Biol 2000;7541-9.

68. Zegerman P, Canas B, Pappin D, Kouzarides T. Histone H3 lysine 4 methylation disrupts binding of nucleosome remodelling and deaceylase (NuRD) repressor complex. J.Biol.Chem. 2002;11621-4.

69. Sullivan EK, weirich CS, Guyon JR, Sif S, Kingston RE. Transcriptional activation domains of human heat shock factor 1 recruit human SWI/SNF. Molecular and Cellular Biology 2001;5826-37.

70. Geiman TM, Sankpal UT, Robertson AK, Zhao Y, Zhao Y, Robertson KD. DNMT3B interacts with hSNF2H chromatin remodeling enzyme, HDACs1 and 2, and components of the histone methylation system. Biocehmical and Biophysical Research Communications 2004;544-55.

71. Lemon B, Tjian R. Orchestrated response: a symphony of transcription factors for gene control. Genes and Development 2000;2551-69.

72. Levine M, Tjian R. Transcription regulation and animal diversity. Nature 2003;147-51.

73. Soller M. Pre-messenger RNA processing and its regulation: a genomic perspective. Cellular and Molecular Life Sciences 2006;796-819.

74. Modrek B, Lee CJ. Alternative splicing in the human, mouse and rat genomes is associated with an increased frequency of exon creation and/or loss. Nature Genetics 2003;177-80.

75. Beaudoing E, Gautheret D. Identification of alternate polyadenylation sites and analysis of their tissue distribution using EST data. Genome Res 2001;1520-6.

76. Grabowski PJ, Seiler SR, Sharp PA. A multicomponent complex is involved in the splicing of messenger RNA precursors. Cell 1985;345-53.

77. Grabowski PJ, Sharp PA. Affinity chromatography of splicing complexes: U2, U5, and U4 + U6 small nuclear ribonucleoprotein particles in the spliceosome. Science 1986;1294-9.

78. Keembiyehetty C, Augustin R, Carayannopoulos MO, Steer S, Manolescu A, Cheeseman CI, Moley KH. Mouse glucose transporter 9 splice variants are expressed in adult liver and kidney and are up-regulated in diabetes. Molecular Endocrinology 2006;686-97.

79. Ladd AN, Charlet-B. N, Cooper TA. The CELF family of RNA binding proteins is implicated in cell-specific and developmentally regulated alternative splicing. 21 2001.

80. Skuse GR, Cappione AJ. RNA processing and clinical variability in neurofibromatosis type I (NF1). Human Molecular Genetics 1997;1707-12.

81. Lorson CL, Hahnen E, Androphy EJ, Wirth B. A single nucleotide in the *SMN* gene regulates splicing and is responsible for spinal muscular atrophy. PNAS 1999;6307-11.

82. Pagani F, Buratti E, Stuani C, Bendix R, Dork T, Baralle FE. A new type of mutation causes a splicing defect in *ATM*. Nature Genetics 2002;426-9.

83. Venables JP. Aberrant and alternative splicing in cancer. Cancer Research

2004;7647-54.

84. Kalnina Z, Zayakin P, Sillina K, Line A. Alterations of pre-mRNA splicing in cancer. Genes, Chromosomes, and Cancer 2005;342-57.

85. Venables JP. Unbalanced alternative splicing and its significance in cancer. Bioessays 2006;378-86.

86. Dantonel J-C, Murthy KGK, Manley JL, Tora L. Transcription factor TFIID recruits factor CPSF for formation of 3' end of mRNA. Nature 1997;399-402.

87. Muller HJ, Herskowitz IH. Concerning the healing of chromosome ends in *Drosophila melanogaster*. Am.Nat. 1954;177-208.

88. McClintock B. The stability of broken ends of chromosomes in *Zea mays*. Genetics 1941;234-82.

89. Blackburn EH, Gall JG. A tandemly repeated sequence at the termini of the extrachromosomal rRNA genes in *Tetrahymena*. J.Mol.Biol. 1978;33-53.

90. Shampay J, Szotak JW, Blackburn EH. DNA sequences of telomeres maintained in yeast. Nature 1984;154-7.

91. Richards EJ, Ausubel FM. Isolation of a higher eukaryotic telomere from *Arabidopsis thaliana*. Cell 1988;127-36.

92. Moyzis RK, Buckingham JM, Cram LS, Dani M, Deaven LL, Jones MD, Meyne J, Ratliff RL, Wu J-R. A highly conserved repetitive DNA sequence, $(TTAGGG)_n$, present at the telomeres of human chromosomes. PNAS 1988;6622-6.

93. Larson DD, Spangler EA, Blackburn EH. Dynamics of telomere length variation in *Tetrahymena thermophila*. Cell 1987;477-83.

94. Shampay J, Blackburn EH. Generation of telomere-length heterogeneity in *Saccharomyces cerevisiae*. PNAS 1988;534-8.

95. Cooke HJ, Smith BA. Variability at the telomeres of the human X/Y pseudoautosomal region. Cold Spring Harbor Symp.Quant.Biol. 1986;213-9.

96. Henderson ER, Blackburn EH. An overhanging 3' terminus is a conserved feature of telomeres. Mol.Cell.Biol. 1989;345-8.

97. Makarov V, Hirose Y, Langmore JP. Long G tails at both ends of human chromosomes suggest a C strand degradation mechanism for telomere shortening. Cell 1997;657-66.

98. Griffith JD, Comeau L, Rosenfiled S, Stansel RM, Bianchi A, Moss H, Lange Td.

Mammalian telomeres end in a large duplex loop. Cell 1999;503-14.

99. Munoz-Jordan JL, Cross GA, Lange Td, Griffith JD. T-loops at trypanosome telomeres. EMBO J. 2001;579-88.

100. Cesare AJ, Quinney N, Wilcox S, Subramanian D, Griffith JD. Telomere looping in *P. sativium* (common garden pea). Plant J. 2003;271-9.

101. Nikitina T, Woodcock CL. Closed chromatin at the ends of chromosomes. J.Cell Biol. 2004;161-5.

102. Pluta AF, Dani GM, Spear BB, Zakian VA. Elaboration of telomeres in yeast: recognition and modification of termini from Oxytricha macronuclear DNA. PNAS 1984;1475-9.

103. Lange Td. Shelterin: the protein complex that shapes and safeguards human telomeres. Genes and Development 2005;2100-10.

104. Bianchi A, Stansel RM, Fairall L, Griffith JD, Rhodes D, Lange Td. TRF1 binds a bipartite telomeric site with extreme spatial flexibility. EMBO J. 1999;5735-44.

105. Court R, Chapman L, Fairall L, Rhodes D. How the human telomeric proteins TRF1 and TRF2 recognize telomeric DNA: A view from high-resolution crystal structures. EMBO Rep. 2005;39-45.

106. Li B, Oestreich S, Lange Td. Identification of human Rap1: Implications for telomere evolution. Cell 2000;471-83.

107. Kim SH, Kaminker P, Campisi J. TIN2, a new regulator of telomere length in human cells. Nature Genetics 1999;405-12.

108. Kim SH, Beausejour C, Davalos AR, Kaminker P, Heo SJ, Campisi J. TIN2 mediates functions of TRF2 at human telomeres. J.Biol.Chem. 2004;43799-804.

109. Baumann P, Cech TR. Pot1, the putative telomere end-binding protein in fission yeast and humans. Science 2001;1171-5.

110. Hockemeyer D, Sfeir AJ, Shay JW, Wright WE, Lange Td. POT1 protects telomeres from a transient DNA damage response and determines how human chromosomes end. EMBO J. 2005;2667-78.

111. Ye JZ, Hockenmeyer D, Krutchinsky AN, Loayza D, Hooper SM, Chait BT, Lange Td. POT1-interacting protein PIP1: A telomere length regulator that recruits POT1 to the TIN2/TRF1 complex. Genes and Development 2004;1649-54.

112. Steensel Bv, Smogorzewska A, Lange Td. TRF2 protects human telomeres from end-to-end fusions. Cell 1998;401-13.

113. Bellen M, Datta A, Brown M, Pouliquen J-F, Couppie P, Kazanj M, Nicot C. Increased expression of telomere length regulating factors TRF1, TRF2, and TIN2 in patients with adult T-cell leukemia. International Journal of Cancer 2006.

114. Karlseder J, Broccoli D, Dai Y, Hardy S, Lange Td. p53- and ATM-dependent apoptosis induced by telomeres lacking TRF2. Science 1999;1321-5.

115. Zhu XD, Niedernhofer L, Kuster B, Mann M, Hoeijmakers JH, Lange Td. ERCC1/XPF removes the 3' overhang from uncapped telomeres and represses formation of telomeric DNA-containing double minute chromosomes. Mol.Cell 2003;1489-98.

116. Opresko PL, Kobbe CV, Laine JP, Harrigan J, Hickson ID, Bohr VA. Telomere binding protein TRF2 binds to and stimulates the Werner and Bloom syndrome helicases. J.Biol.Chem. 2002;41110-9.

117. Fagagna Fdd, Reaper PM, Clay-Farrace L, Fiegler H, Carr P, Zglinicki Tv, Saretzki G, Carter NP, Jackson SP. A DNA damage checkpoint response in telomere-initiated senescence. Nature 2003;194-8.

118. Wong K-K, Maser RS, Bachoo RM, Menon J, Carrasco DR, Gu Y, Alt FW, DePinho RA. Telomere dysfunction and Atm deficiency compromises organ homeostasis and accelerates ageing. Nature 2003;643-8.

119. Chang S, Multani AS, Cabrera NG, Naylor ML, Laud P, Lombard D, Pathak S, Guarente L, DePinho RA. Essential role of limiting telomeres in the pathogenesis of Werner syndrome. Nature Genetics 2004;877-82.

120. Du X, Shen J, Kugan N, Furth EE, Lombard DB, Cheung C, Pak S, Luo G, Pignolo RJ, DePinho RA, Guarente L, Johnson FB. Telomere shortening exposes functions for the mouse werner and bloom syndrome gene. Mol Cell Biol 2004;8437-46.

121. Meselson M, Stahl FW. The replication of DNA in Escherichia coli. PNAS 1958;671-82.

122. Greider CW, Blackburn EH. Identification of a specific telomere terminal transferase activity in Tetrahymena extracts. Cell 1985;405-13.

123. Greider CW, Blackburn EH. The telomere terminal transferase of Tetrahymena is a ribonucleoprotein enzyme with two kinds of primer specificity. Cell 1987;887-98.

124. Morin GB. The human telomere terminal transferase enzyme is a ribonucleoprotein that synthesizes TTAGGG repeats. Cell 1989;521-9.

125. Zhuang Y, Weiner AM. A compensatory base change in U1 snRNA suppresses a 5' splice site mutation. Cell 1986;827-35.

126. Parker R, Siliciano PG, Guthrie C. Recognition of the TACTAAC box during mRNA splicing in yeast involves base pairing to the U2-like snRNA. Cell 1987;229-39.

127. Greider CW, Blackburn EH. A telomeric sequence in the RNA of Tetrahymena telomerase required for telomere synthesis. Nature 1989;331-7.

128. Gilley D, Blackburn EH. Specific RNA residue interactions required for enzymatic functions of *Tetrahymena* telomerase. Mol Cell Biol 1996;66-75.

129. Autexier C, Pruzan R, Funk WD, Greider CW. Reconstitution of human telomerase activity and identification of a minimal functional region of the human telomerase RNA. EMBO J. 1996;5928-35.

130. Blasco MA, Lee H, Hande MP, Samper E, Lansdorp PM, DePinho RA, Greider CW. Telomere shortening and tumor formation by mouse cells lacking telomerase RNA. Cell 1997;25-34.

131. Soder AI, Hoare SF, Muir S, Going JJ, Parkinson EK, Keith WN. Amplification, increased dosage and *in situ* expression of the telomerase RNA gene in human cancer. Oncogene 1997;1013-21.

132. Theimer CA, Feigon J. Structure and function of telomerase RNA. Current Opinion in Structural Biology 2006;1-12.

133. Blasco MA, Rizen M, Greider CW, Hanahan D. Differential regulation of telomerase activity and telomerase RNA during multi-stage tumorigenesis. Nature Genetics 1996;200-4.

134. Yi X, Tesmer VM, Savre-Train I, Shay JW, Wright WE. Both transcriptional and posttranscriptional mechanisms regulate human telomerase template RNA levels. Mol Cell Biol 1999;3989-97.

135. Vulliamy T, Marrone A, Goldman F, Dearlove A, Bessler M, Mason PJ, Dokal I. The RNA component of telomerase is mutated in autosomal dominant dyskeratosis congenita. Nature 2001;432-5.

136. Vulliamy T, Marrone A, Szydlo R, Walne A, Mason PJ, Dokal I. Disease anticipation is associated with progressive telomere shortening in families with dyskeratosis congenita due to mutations in *TERC*. Nature Genetics 2004;447-9.

137. Lingner J, Cech TR. Purification of telomerase from *Euplotes aediculatus*: Requirement of a primer 3' overhang. PNAS 1996;10712-7.

138. Lingner J, Hughes TR, Shevchenko A, Mann M, Lundblad V, Cech TR. Reverse transcriptase motifs in the catalytic subunit of telomerase. Science 1997;561-7.

139. Harrington L, Zhou W, McPhail T, Oulton R, Yeung DSK, Mar V, Bass MB,

Robinson MO. Human telomerase contains evolutionarily conserved catalytic and structural subunits. Genes and Development 1997;3109-15.

140. Meyerson M, Counter CM, Eaton EN, Ellisen LW, Steiner P, Caddle SD, Ziaugra L, Beijerbergen RL, Davidoff MJ, Liu Q. *hEST2*, the putative human telomerase catalytic subunit gene, is up-regulated in tumor cells and during immortalization. Cell 1997;785-95.

141. Nakamura TM, Morin GB, Chapman KB, Weinrich SL, Andrews WH, Lingner J, Harley CB, Cech TR. Telomerase catalytic subunit homologs from fission yeast and human. Science 1997;955-9.

142. Martin-Rivera L, Herrera E, Albar JP, Blasco MA. Expression of mouse telomerase catalytic subunit in embryos and adult tissues. PNAS 1998;10471-6.

143. Prowse KR, Greider CW. Developmental and tissue-specific regulation of mouse telomerase and telomere length. PNAS 1995;4818-22.

144. Greenberg RA, Allsopp RC, Chin L, Morin GB, DePinho RA. Expression of mouse telomerase reverse transcriptase during development, differentiation and proliferation. Oncogene 1998;1723-30.

145. Kim NW, Piatyszek MA, Prowse KR, Harley CB, West MD, Ho PLC, Coviello GM, Wright WE, Weinrich SL, Shay JW. Specific association of human telomerase activity with immortal cells and cancer. Science 1994;2011-5.

146. Ulaner GA, Giudice LC. Developmental regulation of telomerase activity in human fetal tissues during gestation. Molecular Human Reproduction 1997;769-73.

147. Wright DL, Jones EL, Mayer JF, Oehninger S, Gibbons WE, Lanzendorf SE. Characterization of telomerase activity in the human oocyte and preimplantation embryo. Molecular Human Reproduction 2001;947-55.

148. Counter CM, Gupta J, Harley CB, Leber B, Bacchetti S. Telomerase activity in normal leukocytes and in hematologic malignancies. Blood 1995;2315-20.

149. Yasumoto S, Kunimura C, Kikuchi K, Tahara H, Ohji H, Yamamoto H, Ide T, Utakoji T. Telomerase activity in normal human epithelial cells. Oncogene 1996;433-9.

150. Wright WE, Piatyszek MA, Rainey WE, Byrd W, Shay JW. Telomerase activity in human germline and embryonic tissues and cells. Developmental Genetics 1996;173-9.

151. Shay JW, Bacchetti S. A survey of telomerase activity in human cancer. European Journal of Cancer 1997;787-93.

152. Tahara H, Yasui W, Tahara E, Fujimoto J, Ito K, Tamai K, Nakayama J, Ishikawa F, Tahara E, Ide T. Immuno-histochemical detection of human telomerase catalytic component, hTERT, in human colorectal tumor and non-tumor tissue sections. Oncogene 1999;1561-7.

153. Morita M, Nakanishi K, Kawai T, Fujikawa K. Telomere length, telomerase activity, and expression of human telomerase reverse transcriptase mRNA in growth plate of epiphyseal articular cartilage in femoral head during normal human development and in thantophoric dysplasia. Human Pathology 2004;403-11.

154. Kyo S, Kanaya T, Takakura M, Tanaka M, Inoue M. Human telomerase reverse transcriptase as a critical determinant of telomerase activity in normal and malignant endometrial tissues. International Journal of Cancer 1999;60-3.

155. Nagao K, Tomimatsu M, Endo H, Hisatomi H, Hikui K. Telomerase reverse transcriptase mRNA expression and telomerase activity in hepatocellular carcinoma. Journal of Gastroenterology 1999;83-7.

156. Kok JBd, Ruers TJM, Muijen GNPv, Bokhoven Av, Willems HL, Swinkels DW. Real-time quantification of human telomerase reverse transcriptase mRNA in tumors and healthy tissues. Clinical Chemistry 2000;313-8.

157. Gunes C, Lichtsteiner S, Vasserot AP, Englert C. Expression of the *hTERT* gene is regulated at the level of transcriptional initiation and repressed by Mad1. Cancer Research 2000;2116-21.

158. Ducrest A-L, Szutorisz H, Lingner J, Nabholz M. Regulation of the human telomerase reverse transcriptase gene. Oncogene 2002;541-52.

159. Miller RA. Gerontology as oncology. Research on aging as the key to the understanding of cancer. Cancer 1991;2496-501.

160. Lee H, Blasco MA, Gottlieb GJ, II JWH, Greider CW, DePinho RA. Essential role of mouse telomerase in highly proliferative organs. Nature 1998;569-74.

161. Rudolph KL, Chang S, Lee H, Blasco M, Gottlieb GJ, Greider C, DePinho RA. Longevity, stress response, and cancer in aging telomerase-deficient mice. Cell 1999;701-12.

162. Harley CB, Futcher BA, Greider CW. Telomeres shorten during ageing of human fibroblasts. Nature 1990;458-60.

163. Allsopp RC, Chang E, Kashefi-Aazam M, Rogaev EI, Piatyszek MA, Shay JW, Harley CB. Telomere shortening is associated with cell division *in vitro* and *in vivo*. Experimental Cell Research 1995;194-200.

164. Lange Td, Shiue L, Myers RM, Cox DR, Naylor SL, Killery AM, Varmus HE.

Structure and variability of human chromosome ends. Molecular and Cellular Biology 1990;518-27.

165. Vaziri H, Dragowska W, Allsopp RC, Thomas TE, Harley CB, Lansdorp PM. Evidence for a mitotic clock in human hematopoetic stem cells: Loss of telomeric DNA with age. PNAS 1994;9857-60.

166. Notaro R, Cimmino A, Tabarini D, Rotoli B, Luzzatto L. *In vivo* telomere dynamics of human hematopoietic stem cells. PNAS 1997;13782-5.

167. Epel ES, Blackburn EH, Lin J, Dhabhar FS, Adler NE, Morrow JD, Cawthon RM. Accelerated telomere shortening in response to life stress. PNAS 2006;17312-5.

168. Cernak I, Savic V, Kotur J, Prokic V, Kuljic B, Grbovic D, Veljovic M. Alterations in magnesium and oxidative status during chronic emotional stress. Magnesium Research 2000;29-36.

169. Irie M, Asami S, Ikeda M, Kasai H. Depressive state relates to female oxidative DNA damage via neutrophil activation. Biocehmical and Biophysical Research Communications 2003;1014-8.

170. Hayley S, Poulter MO, Merali Z, Anisman H. The pathogenesis of clinical depression: Stressor- and cytokine-induced alterations of neuroplasticity. Neuroscience 2005;659-78.

171. Zglinicki Tv, Saretzki G, Docke W, Lotze C. Mild hyperoxia shortens telomeres and inhibits proliferation of fibroblasts: A model for senescence? Experimental Cell Research 1995;186-93.

172. Serra V, Zglinicki Tv, Lorenz M, Saretzki G. Extracellular superoxide dismutase is a major antioxidant in human fibroblasts and slows telomere shortening. J.Biol.Chem. 2003;6824-30.

173. Kurz DJ, Decary S, Hong Y, Trivier E, Akhmedov A, Erusalimsky JD. Chronic oxidative stress compromises telomere integrity and accelerates the onset of senescence in human endothelial cells. Journal of Cell Science 2004;2417-26.

174. Hayflick L, Moorehead PS. The serial cultivation of human diploid cell strains. Experimental Cell Research 1961;585-621.

175. Campisi J. From cells to organisms: can we learn about aging from cells in culture. Experimental Gerontology 2001;607-18.

176. Bodnar AG, Ouellette M, Frolkis M, Holt SE, Chiu C-P, Morin GB, Harley CB, Shay JW, Lichtsteiner S, Wright WE. Extension of life-span by introduction of telomerase into normal human cells. Science 1998;349-52.

177. Karlseder J, Smogorzewska A, Lange Td. Senescence induced by altered telomere

state, not telomere loss. Science 2002;2446-9.

178. Li G-Z, Eller MS, Firoozabadi R, Gilchrest BA. Evidence that exposure of the telomere 3' overhang sequence induces senescence. PNAS 2003;527-31.

179. Stewart SA, Ben-Porath I, Carey VJ, O'Connor BF, Hahn WC, Weinberg RA. Erosion of the telomeric single strand overhang at replicative senescence. Nature Genetics 2003;492-6.

180. Smogorzewska A, Lange Td. Different telomere damage signaling pathways in human and mouse cells. EMBO J. 2002;4338-48.

181. Reddel RR. A reassessment of the telomere hypothesis of senescence. Bioessays 1998;977-84.

182. Klapper W, Parwaresch R, Krupp G. Telomere biology in human aging and aging syndromes. Mechanisms of Ageing and Development 2001;695-712.

183. Serrano M, Blasco MA. Putting the stress on senescence. Current Opinion in Cell Biology 2001;748-53.

184. Zglinicki Tv. Replicative senescence and the art of counting. Experimental Gerontology 2003;1259-64.

185. Ben-Porath I, Weinberg RA. When cells get stressed: an integrative view of cellular senescence. Journal of Clinical Investigation 2004;8-13.

186. Zglinicki Tv, Serra V, Lorenz M, Saretzki G, Lenzen-Grossimlighaus R, Gessner R, Risch A, Steinhagen-Thiessen E. Short telomeres in patients with vascular dementia: an indicator of low antioxidative capacity and a possible risk factor? Lab Investigation 2000;1739-47.

187. Samani NJ, Boultby R, Butler R, Thompson JR, Goodall AH. Telomere shortening in atherosclerosis. Lancet 2001;472-3.

188. Cawthon RM, Smith KR, O'Brien E, Sivatchenko A, Kerber RA. Association between telomere length in blood and mortality in people age 60 years or older. Lancet 2003;393-5.

189. Counter CM, Hirte HW, Bacchetti S, Harley CB. Telomerase activity in human ovarian carcinoma. PNAS 1994;2900-4.

190. Desmaze C, Soria J-C, Freulet-Marriere M-A, Mathieu N, Sabatier L. Telomere-driven genomic instability in cancer cells. Cancer Letters 2003;173-82.

191. Londono-Vallejo JA. Telomere length heterogeneity and chromosome instability. Cancer Letters 2004;135-44.

192. Zhu J, Wang H, Bishop JM, Blackburn EH. Telomerase extends the lifespan of virus-transformed human cells without net telomere lengthening. PNAS 1999;3723-8.

193. Hiyama E, Hiyama K. Telomerase as tumor marker. Cancer Letters 2003;221-33.

194. Keith WN, Bilsland A, Hardie M, Evans TRJ. Drug insight: cancer cell immortality-telomerase as a target for novel cancer gene therapies. Nature Clinical Practice Oncology 2004;88-96.

195. Olaussen KA, Dubrana K, Domont J, Spano J-P, Sabatier L, Soria J-C. Telomeres and telomerase as targets for anticancer drug development. Critical Reviews in Oncology/Hematology 2006;191-214.

196. Horikawa I, Barrett JC. Transcriptional regulation of the telomerase hTERT gene as a target for cellular and viral oncogenic mechanisms. Carcinogenesis 2003;1167-76.

197. Cong Y-S, Wen J, Bacchetti S. The human telomerase catalytic subunit hTERT: organization of the gene and characterization of the promoter. Human Molecular Genetics 1999;137-42.

198. Wick M, Zubov D, Hagen G. Genomic organization and promoter characterization of the gene encoding the human telomerase reverse transcriptase (hTERT). Gene 1999;97-106.

199. Takakura M, Kyo S, Kanaya T, Hirano H, Takeda J, Yutsudo M, Inoue M. Cloning of human telomerase catalytic subunit (hTERT) gene promoter and identification of proximal core promoter sequences essential for trnascriptional activation in immortalized and cancer cells. Cancer Research 1999;551-7.

200. Wang J, Xie LY, Allan S, Beach D, Hannon GJ. Myc activates telomerase. Genes and Development 1998;1769-74.

201. Greenberg RA, O'Hagan RC, Deng H, Xiao Q, Hann SR, Adams RR, Lichtsteiner S, Chin L, Morin GB, DePinho RA. Telomerase reverse transcriptase gene is a direct target of c-Myc but is not functionally equivalent in cellular transformation. Oncogene 1999;1219-26.

202. Kyo S, Takakura M, Taira T, Kanaya T, Itoh H, Yutsudo M, Ariga H, Inoue M. Sp1 cooperates with c-Myc to activate transcription of the human telomerase reverse transcriptase gene (*hTERT*). Nucleic Acids Res. 2000;669-77.

203. Oh ST, Kyo S, Laimins LA. Telomerase activation by human papillomavirus type 16 E6 protein: induction of human telomerase reverse transcriptase expression through Myc and GC-rich Sp1 binding sites. Journal of Virology 2001;5559-66.

204. Oh S, Song Y-H, Yim J, Kim TK. Identification of Mad as a repressor of the

human telomerase (hTERT) gene. Oncogene 2000;1485-90.

205. McMurray HR, McCance DJ. Human papillomavirus type 16 E6 activates TERT gene transcription through induction of c-Myc and release of USF-mediated repression. Journal of Virology 2003;9852-61.

206. Xu D, Popov N, Hou M, Wang Q, Bjorkholm M, Gruber A, Menkel AR, Henriksson M. Switch from Myc/Max to Mad1/Max bidning and decrease in histone acetylation at the *telomerase reverse transcriptase* promoter during differenctiation of HL60 cells. PNAS 2001;3826-31.

207. Li L, He S, Sun J-M, Davie JR. Gene regulation by Sp1 and Sp3. Biochemical Cell Biology 2004;460-71.

208. Won J, Yim J, Kim TK. Sp1 and Sp3 recruit histone deacetylase to repress transcription of the human telomerase reverse transcriptase (hTERT) promoter in normal human somatic cells. JBC 2002;38230-8.

209. Ma H, Urquidi V, Wong J, Kleeman J, Goodison S. Telomerase reverse transcriptase promoter regulation during myogenic differentiation of human RD rhabdomyosarcoma cells. Molecular Cancer Research 2003;739-46.

210. Wooten LG, Ogretmen B. Sp1/Sp3-dependent regulation of human telomerase reverse transcriptase promoter activity by the bioactive sphingolipid ceramide. JBC 2005;28867-76.

211. Horikawa I, Chiang YJ, Patterson T, Feigenbaum L, Leem S-H, Michishita E, Larionov V, Hodes RJ, Barrett JC. Differential cis-regulation of human versus mouse Tert gene expression in vivo: Identification of a human-specific repressive element. PNAS 2005;18437-42.

212. Xu D, Wang Q, Gruber A, Bjorkholm M, Chen Z, Zaid A, Selivanova G, Peterson C, Wiman KG, Pisa P. Downregulation of telomerase reverse transcriptase mRNA expression by wild type p53 in human tumor cells. Oncogene 2000;5123-33.

213. Racek T, Mise N, Li Z, Stoll A, Putzer BM. C-terminal p73 isoforms repress transcriptional activity of the human telomerase reverse transcriptase (hTERT) promoter. J.Biol.Chem. 2005;40400-5.

214. Beitzinger M, Oswald C, Beinoraviciute-Kellner R, Stiewe T. Regulation of telomerase activity by the p53 family member p73. Oncogene 2006;813-26.

215. Verma SC, Borah S, Robertson ES. Latency-associated nuclear antigen of Kaposi's sarcoma-associated herpesvirus up-regulates transcription of human telomerase reverse transcriptase promoter through interaction with transcription factor Sp1. Journal of Virology 2004;10348-59.

216. Takakura M, Kyo S, Inoue M, Wright WE, Shay JW. Function of Ap-1 in transcription of the telomerase reverse transcriptase gene (*hTERT*) in human and mouse cells. Mol Cell Biol 2005;8037-43.

217. Oh S, Song Y, Yim J, Kim TK. The Wilms' tumor 1 tumor suppressor gene represses transcription of the human telomerase reverse transcriptase gene. J.Biol.Chem. 1999;37473-8.

218. Lin S-Y, Elledge SJ. Multiple tumor suppressor pathways negatively regulate telomerse. Cell 2003;881-9.

219. Fujimoto K, Kyo S, Takakura M, Kanaya T, Kitagawa Y, Itoh H, Takahashi M, Inoue M. Identification and characterization of negative regulatory elements of the human telomerase catalytic subunit (hTERT) gene promoter: possible role of MZF-2 in transcriptional repression of hTERT. Nucleic Acids Res. 2000;2557-62.

220. Horikawa I, Oshimura M, Barrett JC. Repression of the telomerase catalytic subunit by a gene on human chromosome 3 that induces cellular senescence. Molecular Carcinogenesis 1998;65-72.

221. Tanaka H, Shimizu M, Horikawa I, Kugoh H, Yokota J, Barrett JC, Oshimura M. Evidence for a putative telomerase repressor gene in the 3p14.2-p21.1 region. Genes, Chromosomes, and Cancer 1998;123-33.

222. Cuthbert AP, Bond J, Trott DA, Gill S, Broni J, Marriott A, Khoudoli G, Parkinson EK, Cooper CS, Newbold RF. Telomerase represor sequences on chromosome 3 and induction of permanent growth arrest in human breast cancer cells. Journal of the National Cancer Institute 1999;37-45.

223. Horikawa I, Cable PL, Mazur SJ, Appella E, Afshari CA, Barrett JC. Downstream E-box-mediated regulation of the human telomerase reverse transcriptase (*hTERT*) gene: transcription evidence for an endogenous mechanism of transcriptional repression. Molecular Biology of the Cell 2002;2585-97.

224. Ducrest A-L, Amacker M, Mathieu YD, Cuthbert AP, Trott DA, Newbold RF, Nabholz M, Lingner J. Regulation of human telomerase activity: repression by normal chromosome 3 abolishes nuclear telomerase reverse transcriptase transcripts but does not affect c-Myc activity. Cancer Research 2001;7594-602.

225. Tanaka H, Horikawa I, Barrett JC, Oshimura M. Evidence for inactivation of distinct telomerase repressor genes in different types of human cancers. International Journal of Cancer 2005;653-7.

226. Yokoyama Y, Takahashi Y, Morishita S, Hasimoto M, Niwa K, Tamaya T. Telomerase activity in the human endometrium throughout the menstrual cycle. Molecular Human Reproduction 1998;173-7.

227. Tanaka M, Kyo S, Takakura M, Kanaya T, Sagawa T, Yamashita K, Okada Y,

Hiyama E, Inoue M. Expression of telomerase activity in human endometrium is localized to epithelial glandular cells and regulated in a menstual phase-dependent manner correlated with cell proliferation. American Journal of Pathology 1998;1985-91.

228. Kyo S, Takakura M, Kanaya T, Zhuo W, Fujimoto K, Nishio Y, Orimo A, Inoue M. Estrogen activates telomerase. Cancer Research 1999;5917-21.

229. Misiti S, Nanni S, Fontemaggi G, Cong Y-S, Wen J, Hirte HW, Piaggio G, Sacchi A, Pontecorvi A, Bacchetti S, Farsetti A. Induction of hTERT expression and telomerase activity by estrogens in human ovary epithelium cells. Mol Cell Biol 2000;3764-71.

230. Wang Z, Kyo S, Maida Y, Takakura M, Tanaka M, Yatabe N, Kanaya T, Nakamura M, Koike K, Hisamoto K, Ohmichi M, Inoue M. Tamoxifen regulates human telomerase reverse transcriptase (hTERT) gene expression differently in breast and endometrial cancer cells. Oncogene 2002;3517-24.

231. Williams CD, Boggess JF, LaMarque LR, Meyer WR, Murray MJ, Fritz MA, Lessey BA. A prospective, randomized study of endometrial telomerase during the menstrual cycle. The Journal of Clinical Endocrinology & Metabolism 2001;3912-7.

232. Cong Y-S, Bacchetti S. Histone deacetylation is involved in the transcriptional repression of *hTERT* in normal human cells. JBC 2000;35665-8.

233. Hou M, Wang X, Popov N, Zhang A, Zhao X, Zhou R, Zetterberg A, Bjorkholm M, Henriksson M, Gruber A, Xu D. The histone deactylase inhibitor trichostatin A derepressed the telomerase reverse transcriptase (*hTERT*) gene in human cells. Experimental Cell Research 2002;25-34.

234. Wang S, Zhu J. Evidence for a Relief of Repression Mechanism for Activation of the Human Telomerase Reverse Transcriptase Promoter. JBC 2003;18842-50.

235. Wang S, Zhu J. The *hTERT* gene in embedded in a nuclease-resistant chromatin domain. JBC 2004;55401-10.

236. Atkinson SP, Hoare SF, Glasspool RM, Keith WN. Lack of telomerase gene expression in alternative lengthening of telomere cells is associated with chromatin remodeling of the *hTR* and *hTERT* gene promoters. Cancer Research 2005;7585-90.

237. Ge Z, Liu C, Bjorkholm M, Gruber A, Xu D. Mitogen-activated protein kinase cascade-mediated histone H3 phosphorylation is critical for telomerase reverse transcriptase expression/telomerase activation induced by proliferation. Mol Cell Biol 2006;230-7.

238. Liu X, Tesfai J, Evrard YA, Dent SYR, Martinez E. c-Myc transformation

domain recruits the human STAGA complex and requires TRRAP and GCN5 acetylase activity for transcription activation. J.Biol.Chem. 2003;20405-12.

239. Szutoriz H, Lingner J, Cuthbert AP, Trott DA, Newbold RF, Nabholz M. A chromosome 3-encoded repressor of the *human telomerase reverse transcriptase* (*hTERT*) gene controls the state of hTERT chromatin. Cancer Research 2003;689-95.

240. Knight JS, II MAC, Robertson ES. The latency-associated nuclear antigen of Kaposi's sarcoma-associated herpesvirus transactivates the telomerase reverse transcriptase promoter. J.Biol.Chem. 2001;22971-8.

241. Kilian A, Bowtell DDL, Abud HE, Hime GR, Venter DJ, Keese PK, Duncan EL, Reddel RR, Jefferson RA. Isolation of a candidate human telomerase catalytic subunit gene, which reveals complex splicing patterns in different cell types. Human Molecular Genetics 1997;2011-9.

242. Colgin LM, Wilkinson C, Englezou A, Kilian A, Robinson MO, Reddel RR. The hTERTα splice variant is a dominant negative inhibitor of telomerase activity. Neoplasia 2000;426-32.

243. Yi X, White DM, Aisner DL, Baur JA, Wright WE, Shay JW. An alternate splicing variant of the human telomerase catalytic subunit inhibits telomerase activity. Neoplasia 2000;433-40.

244. Yi X, Shay JW, Wright WE. Quantitation of telomerase components and hTERT mRNA splicing patterns in immortal human cells. Nucleic Acids Res. 2001;4818-25.

245. Brenner CA, Wolny YM, Adler RR, Cohen J. Alternative splicing of the telomerase catalytic subunit in human oocytes and embryos. Molecular Human Reproduction 1999;845-50.

246. Ulaner GA, Hu J-F, Vu TH, Giudice LC, Hoffman AR. Tissue-specific alternate splicing of human telomerase reverse transcriptase (hTERT) influences telomere lengths during human development. International Journal of Cancer 2001;644-9.

247. Wenz C, Enenkel B, Amacker M, Kelleher C, Damm K, Lingner J. Human telomerase contains two cooperating telomerase RNA molecules. EMBO J. 2001;3526-34.

248. Beattie TL, Zhou W, Robinson MO, Harrington L. Functional multimerization of the human telomerase reverse transcriptase. Mol Cell Biol 2001;6151-60.

249. Moriarty TJ, Huard S, Dupuis S, Autexier C. Functional multimerization of human telomerase requires an RNA interaction domain in the N-terminus of the catalytic subunit. Mol Cell Biol 2002;1253-65.

250. Ly H, Xu L, Rivera MA, Parslow TG, Blackburn EH. A role for a novel 'trans-pseudoknot' RNA-RNA interaction in the functional dimerization of human telomerase. Genes and Development 2003;1078-83.

251. Moriarty TJ, Marie-Egyptienne DT, Autexier C. Functional organization of repeat addition processivity and DNA synthesis determinant in the human telomerase multimer. Mol Cell Biol 2004;3720-33.

252. Li H, Zhao L-L, Funder JW, Liu J-P. Protein phosphatase 2A inhibits nuclear telomerase activity in human breast cancer cells. J.Biol.Chem. 1997;16729-32.

253. Liu W-J, Jiang J-F, Xiao D, Ding J. Down-regulation of telomerase activity via protein phosphatase 2A activation in salvicine-induced human leukemia HL-60 cell apoptosis. Biochemical Pharmacology 2002;1677-87.

254. Li H, Zhao L, Yang Z, Funder JW, Liu J-P. Telomerase is controlled by Protein Kinase Cα in human breast cancer cells. J.Biol.Chem. 1998;33436-42.

255. Chang JT, Lu Y-C, Chen Y-J, Tseng C-P, Chen Y-L, Fang C-W, Cheng A-J. hTERT phosphorylation by PKC is essential for telomerase holoprotein integrity and enzyme activity in head neck cancer cells. British Journal of Cancer 2006;870-8.

256. Kang SS, Kwon T, Kwon DY, Do SI. Akt protein kinase enhances human telomerase activity through phosphorylation of telomerase reverse trnascriptase subunit. J.Biol.Chem. 1999;13085-90.

257. Breitschopf K, Zeiher AM, Dimmeler S. Pro-atherogenic factors induce telomerase inactivation in endothelial cells through an Akt-dependent mechanism. FEBS Letters 2001;421-5.

258. Haendeler J, Hoffman J, Rahman S, Zeiher AM, Dimmeler S. Regulation of telomerase activity and anti-apoptotic function by protein-protein interaction and phosphorylation. FEBS Letters 2003;180-6.

259. Liu K, Hodes RJ, Weng N. Telomerase activation in human T lymphocytes deos not require increase in telomerase reverse transcriptase (hTERT) protein but is associated with hTERT phosphorylation and nuclear translocation. The Journal of Immunology 2001;4826-30.

260. Kimura A, Ohmichi M, Kawagoe J, Kyo S, Mabuchi S, Takahashi T, Ohshima C, Arimoto-Ishida E, Nishio Y, Inoue M, Kurachi H, Tasaka K, Murata Y. Induction of hTERT expression and phosphorylation by estrogen via Akt cascase in human ovarian cancer cell lines. Oncogene 2004;4505-15.

261. Kharbanda S, Kumar V, Dhar S, Pandey P, Chen C, Majumder P, Yuan Z-M, Whang Y, Strauss W, Pandita TK, Weaver D, Kufe D. Regulation of the hTERT telomerase catalytic subunit by the c-Abl tyrosine kinase. Current Biology

2000;568-75.

262. Collins J, Hohn B. Cosmids: a type of plasmid gene-cloning vector that is packageable in vitro in Bacteriophage λ heads. PNAS 1978;4242-6.

263. Giraldo P, Montoliu L. Size matters: use of YACs, BACs and PACs in transgenic animals. Transgenic Research 2001;83-103.

264. Burke DT, Carle GF, Olson MV. Cloning of large segments of exogenous DNA into yeast by means of artificial chromosome vectors. Science 1987;806-12.

265. Dausset J, Ougen P, Abderrahim H, Billault A, Sambucy JL, Cohen D, Paslier DL. The CEPH YAC library. Behring Inst Mitt. 1992;13-20.

266. Green ED, Riethman HC, Dutchik JE, Olson MV. Detection and characterization of chimeric yeast artificial-chromosome clones. Genomics 1991;658-69.

267. Nagaraja R, Kere J, MacMillan S, Masisi MWj, Johnson D, Molini BJ, Halley GR, Wein K, Trusgnich M, Eble B, Railey B, Bernard H B, Schlessinger D. Characterization of four human YAC libraries for clone size, chimerism and X chromosome sequence representation. Nucleic Acids Res. 1994;3406-11.

268. Wada M, Little RD, Abidi F, Porta G, Labella T, Cooper T, Valle GD, D'Urso M, Schlessinger D. Human Xq24-Xq28: approaches to mapping with yeast artificial chromosomes. American Journal of Human Genetics 1990;95-106.

269. Bellis M, Gerard A, Charlieu JP, Marcais B, Brun ME, Viegas-Pequignot E, Carter DA, Roizes G. Construction and characterization of a partial library of yeast artificial chromosomes from human chromosome 21. DNA and Cell Biology 1991;301-10.

270. Shizuya H, Birren B, Kim U-J, Mancino V, Slepak T, Tachiiri Y, Simon M. Cloning and stable maintenance of 300-kilobase pair fragments of human DNA in *Escherichia coli* using an F-factor-based vector. PNAS 1992;8794-7.

271. Frengen E, Weichenhan D, Zhao B, Osoegawa K, Geel Mv, Jong PJd. A Modular, Positive Selection Bacterial Artificial Chromosome Vector with Multiple Cloning Sites. Genomics 1999;250-3.

272. Zeng C, Kouprina N, Zhu B, Cairo A, Hoek M, Cross G, Osoegawa K, Larionov V, Jong Pd. Large-insert BAC/YAC libraries for selective re-isolation of genomic regions by homologous recombination in yeast. Genomics 2001;27-34.

273. Ioannou PA, Amemiya CT, Garnes J, Kroisel PM, Shizuya H, Chen C, Batzer MA, Jong PJd. A new bacteriophage P1-derived vector for the propagation of large human DNA fragments. Nature Genetics 1994;84-9.

274. Sternberg N. Bacteriophage P1 cloning system for the isolation, amplification,

and recovery of DNA fragments as large as 100 kilobase pairs. PNAS 1990;103-7.

275. Strauss WM, Dausman J, Beard C, Johnson C, Lawrence JB, Jaenisch R. Germ line transmission of a yeast artificial chromosome spanning the murine α_1(I) collagen locus. Science 1993;1904-7.

276. Jakobovits A, Moore AL, Green LL, Vergara GJ, Maynard-Currie CE, Austin HA, Klapholz S. Germ-line transmission of a human-derived yeast artificial chromosome. Nature 1993;255-8.

277. Schedl A, Montoliu L, Kelsey G, Schutz G. A yeast artificial chromosome covering the tyrosinase gene confers copy number-dependent expression in transgenic mice. Nature 1993;258-61.

278. Tanaka S, Yamamoto H, Takeuchi S, Takeuchi T. Melanization in albino mice transformed by introducing cloned mouse *tyronsinase* gene. Development 1990;223-7.

279. Yokoyama T, Silversides DW, Waymire KG, Kwon BS, Takeuchi T, Overbrook PA. Conserved cysteine to serine mutation in tyrosinase is responsible for the classical albino mutation in laboratory mice. Nucleic Acids Res. 1990;7293-8.

280. Lamb BT, Call LM, Slunt HH, Bardel KA, Lawler AM, Eckman CB, Younkin SG, Holtz G, Wagner SL, Price DL, Sisodia SS, Gearhart JD. Altered metabolism of familial Alzheimer's disease-linked amyloid precurosr protein variants in yeast artificial chromosome transgenic mice. Human Molecular Genetics 1997;1535-41.

281. Lehman EJH, Kulnane LS, Gao Y, Petriello MC, Pimpis KM, Younkin L, Dolios G, Wang R, Younkin GG, Lamb BT. Genetic background regulates β-amyloid precurosr protein processing and β-amyloid deposition in the mouse. Human Molecular Genetics 2003;2942-56.

282. Smith DJ, Zhu Y, Zhang J, Cheng J-F, Rubin EM. Construction of a panel of transgenic mice containing a contiguous 2-Mb set of YAC/P1 clones from human chromosome 21q22.2. Genomics 1995;425-234.

283. Ahn K-J, Jeong HK, Choi H-S, Ryoo S-R, Kim YJ, Goo J-S, Choi S-Y, Han J-S, Ha I, Song W-J. DYRK1A BAC transgenic mice show altered synaptic plasticity with learning and memory defects. Neurobiology of Disease 2006;463-72.

284. Manson AL, Trezise AEO, MacVinish LJ, Kasschau KD, Birchall N, Episkopou V, Vassaux G, Evans MJ, Colledge WH, Cuthbert AW, Huxley C. Complementation of null CF mice with a human *CFTR* YAC transgene. EMBO J. 1997;4238-49.

285. Manson A, Huxley C. Skipping of exon 9 of human *CFTR* in YAC-transgenic

mice. Genomics 2001;127-34.

286. Hodgson JG, Smith DJ, McCutcheon K, Koide HB, Nishiyama K, Dinulos MB, Stevens ME, Bissada N, Nasi J, Kanazawa I, Disteche CM, Rubin EM, Hayden MR. Human huntingtin derived from YAC transgenes compensates for loss of murine huntingtin by rescue of the embryonic lethal phenotype. Human Molecular Genetics 1993;1875-85.

287. Shehadeh J, Fernandes HB, Mullins MMZ, Graham RK, Leavitt BR, Hayden MR, Raymond LA. Striatal neuronal apoptosis is preferentially enhanced by NMDA receptor activation in YAC transgenic mouse model of Huntington disease. Neurobiology of Disease 2006;392-403.

288. Heard E, Kress C, Mongelard F, Courtier B, Rougeulle C, Ashworth A, Vourc'h C, Babinet C, Avner P. Transgenic mice carrying an *Xist*-containing YAC. Human Molecular Genetics 1996;441-50.

289. Al-Hasani K, Vadolas J, Voullaire L, Williamson R, Ioannou PA. Complementation of α-thalassaemia in α-globin knockout mice with a 191 kb transgene containing the human α-globin locus. Transgenic Research 2004;235-43.

290. Zweigerdt R, Braun T, Arnold H-H. Faithful expression of the Myf-5 gene during mouse myogenesis requires distant control regions: a transgene approach using yeast artificial chromosomes. Developmental Biology 1997;172-80.

291. Brem G, Besenfelder U, Aigner B, Muller M, Liebl I, Schutz G, Motoliu L. YAC transgenesis in farm animals: rescue of albinism in rabbits. Mol Reprod Dev 1996;56-62.

292. Michalkiewicz M, Michalkiewicz T, Ettinger RA, Rutledge EA, Fuller JM, Moralejo DH, Yserloo BV, MacMurray AJ, Kwitek AE, Jacob HJ, Lander ES, Lernmark A. Transgenic rescue demonstrates involvement of the Ian5 gene in T cell development in the rat. Physiological Genomics 2004;228-32.

293. Shin J, Park H-C, Topczewska JM, Mawdsley DJ, Appel B. Neural cell fate analysis in zebrafish using *olg2* BAC transgenics. Methods in Cell Science 2003;7-14.

294. Orford M, Nefedov M, Vadolas J, Zaibak F, Williamson R, Ioannou PA. Engineering EGFP reporter constructs into a 200 kb human β-globin BAC clone using *GET recombination*. Nucleic Acids Res. 2000;e84.

295. Sarsero JP, Li L, Wardan H, Sitte K, RW, Ioannou PA. Upregulation of expression from the FRDA genomic locus for the therapy of Friedreich ataxia. Journal of Gene Medicine 2002;72-81.

296. Chi X, Zhang S, Yu W, DeMayo FJ, Rosenberg S, Schwartz RJ. Expression of

Nkx2-5-GFP bacterial artificial chromosome transgenic mice closely resembles endogenous *Nkx2-5* gene activity. Genesis 2003;220-6.

297. Mortlock DP, Guenther C, Kingsley DM. A general approach for identifying distant regulatory elements applied to the *Gdf6* gene. Genome Res 2003;2069-81.

298. Rowan S, Cepko C. Genetic analysis of the homeodomain transcription factor Chx10 in the retina using a novel multifunctional BAC transgenic mouse reporter. Developmental Biology 2004;388-402.

299. Jeong Y, El-Jaick K, Roessler E, Muenke M, Epstein DJ. A functional screen for sonic hedgehog regulatory elements across a 1 MB interval identifies long-range ventral forebrain enhancers. Development 2006;761-72.

300. Barton K, Muthusamy N, Fischer C, Ting C-N, Walunas TL, Lanier LL, Leiden JM. The Ets-1 transcription factor is required for the development of natural killer cells in mice. Immunity 1998;555-63.

301. Bhat NK, Komschlies KL, Fujiwara S, Fisher RJ, Mathieson BJ, Greggorio TA, Young HA, Kasik JW, Ozato K, Paps TS. Expression of *ets* genes in mouse thymocyte subsets and T cells. Journal of Immunology 1989;672-8.

302. Cesari F, Brecht S, Vintersten K, Vuong LG, Hofmann M, Klingel K, Schnorr J-J, Arsenian S, Schild H, Herdegen T, Wiebel FF, Nordheim A. Mice deficient for the Ets transcription factor Elk-1 show normal immune responses and mildly impaired neuronal gene activation. Molecular and Cellular Biology 2004;294-305.

303. Costello PS, Nicolas RH, Watanabe Y, Rosewell I, Treisman R. Ternary complex factor SAP-1 is required for Erk-mediated thymocyte positive selection. Nature Immunology 2004;289-98.

304. Favier B, Dolle P. Developmental functions of mammalian *Hox* genes. Molecular Human Reproduction 1997;115-31.

305. Li S, III EBC, Rawson EJ, Simmons DM, Swanson LW, Rosenfeld MG. Dwarf locus mutants lacking three pituitary cell types result from mutations in the POU-domain gene *pit-1*. Nature 1990;528-33.

306. Nichols J, Zevnik B, Anastassiadis K, Niwa H, Klew-Nebenius D, Chambers I, Scholer H, Smith A. Formation of pluripotent stem cells in the mammalian embryo depends on the POU transcription factor Oct4. Cell 1998;379-91.

307. Rudnicki MA, Scnegelsberg PNJ, Stead RH, Braun T, Arnold H-H, Jaenisch R. MyoD or Myf-5 is required for the formation of skeletal muscle. Cell 1993;1351-9.

308. Amati B, Littlewood TD, Evan GI, Land H. The c-Myc protein induces cell cycle progression and apoptosis through dimerization with Max. EMBO J. 1993;5083-

7.

309. Foley KP, McArthur GA, Queva C, Hurlin PJ, Soriano P, Eisenman RN. Targeted disruption of the MYC antagonist MAD1 inhibits cell cycle exit during granulocyte differentiation. EMBO J. 1998;774-85.

310. Wang N, Finegold MJ, Bradley A, Ou CN, Abdelsayed SV, Wilde MD, Wilson DR, Darlington GJ. Impaired energy homeostasis in C/EBPα knockout mice. Science 1995;1108-12.

311. Zhang D-E, Zhang P, Wang N, Hetherington CJ, Darlington GJ, Tenen DG. Absence of granulocyte colony-stimulating factor signaling and neutrophil development in CCAAT enhancer binding protein α-deficient mice. PNAS 1997;569-74.

312. Karin M, Liu Z, Zandi E. AP-1 function and regulation. Current Opinion in Cell Biology 1997;240-6.

313. Couse JF, Korach KS. Estrogen receptor null mice: what have we learned and where will they lead us? Endocrine Reviews 1999;358-417.

314. Mark M, Ghyselinck NB, Chambon P. Function of retinoid nuclear receptors: lessons from genetic and pharmacological dissections of the retinoic acid signaling pathway during mouse embryogenesis. Annual Reviews in Pharmacology and Toxicology 2006;451-80.

315. Koopman P, Gubbay J, Vivian N, Goodfellow P, Lovell-Badge R. Male development of chromosomally female mice transgenic for *Sry*. Nature 1991;117-21.

316. Taranova OV, Magness ST, Fagan BM, Wu Y, Surzenko N, Hutton SR, Penvy LH. SOX2 is a dose-dependent regulator of retinal neural progenitor ceompetence. Genes and Development 2006;1187-202.

317. Bouwman P, Gollner H, Elsasser H-P, Eckhoff G, Karis A, Grosveld F, Philipsen S, Suske G. Transcription factor Sp3 is essential for post-natal survival and late tooth development. EMBO J. 2000;655-61.

318. Loo PFv, Bouwman P, Ling K-W, Middendorp S, Suske G, Grosveld F, Dzierzak E, Philipsen S, Hendriks RW. Impaired hematopoiesis in mice lacking the transcription factor Sp3. Blood 2003;858-66.

319. Gollner H, Bouwman P, Mangold M, Karis A, Braun H, Rohner I, Rey AD, Besedovsky H-O, Meinhardt A, Broek Mvd, Cutforth T, Grosveld F, Philipsen S, Suske G. Complex phenotype of mice homozygous for a null mutation in the *Sp4* transcription factor gene. Genes to Cells 2001;689-97.

320. Klobutcher LA, Swanton MT, Donini P, Prescott DM. All gene-sized DNA

molecules in four species of hypotrichs have the same terminal sequence and an unusual 3' terminus. PNAS 1981;3015-9.

321. Dahlen M, Olsson T, Kanter-Smoler G, Ramme A, Sunnerhagen P. Regulation of telomere length by checkpoint genes in *Schizosaccharomyces pombe*. Molecular Biology of the Cell 1998;611-21.

322. Meyne J, Ratliff RL, Moyzis RK. Conservation of the human telomere sequence $(TTAGGG)_n$ among vertebrates. PNAS 1989;7049-53.

323. Kipling D, Cooke HJ. Hypervariable ultra-long telomeres in mice. Nature 1990;400-2.

324. Muller HJ. Types of invisible variations induced by X-rays in Drosophila. Genetics 1930;299-334.

325. Schotta G, Ebert A, Dorn R, Reuter G. Position-effect variegation and the genetic dissection of chromatin regulation in *Drosophila*. Seminars in Cell & Developmental Biology 2003;67-75.

326. Katsuki M, Sato M, Kimura M, Yokoyama M, Kobayashi K, Nomura T. Conversion of normal behavior to shiverer by myelin basic protein antisense cDNA in transgenic mice. Science 1988;593-5.

327. Mintz B, Bradl M. Mosaic expression of a tyrosinase fusion gene in albino mice yields a heritable striped coat color pattern in transgenic homozygotes. PNAS 1991;9643-7.

328. Kimura S, Mullins JJ, Bunnemann B, Metzger R, Hilgenfeldt U, Zimmerman F, Jacob H, Fuxe K, Ganten D, Kaling M. High blood pressure in transgenic mice carrying the rat angiotensinogen gene. EMBO J. 1992;821-7.

329. Pravtcheva DD, Wise TL, Ensor NJ, Ruddle FH. Mosaic expression of an Hprt transgene integrated in a region of Y heterochromatin. The Journal of Experimental Zoology 1994;452-68.

330. Robertson G, Garrick D, Wu W, Kearns M, Martin D, Whitelaw E. Position-dependent variegation of globin transgene expression in mice. PNAS 1995;5371-5.

331. Boyer O, Zhao JC, Cohen JL, Depetris D, Yagello M, Lejeune L, Bruel S, Mattei M-G, Klatzmann D. Position-dependent variegation of a CD4 minigene with targeted expression to mature $CD4^+$ T cells. The Journal of Immunology 1997;3383-90.

332. Engler P, Doglio LT, Bozek G, Storb U. A cis-acting element that directs the activity of the murine methylation modifier locus *Ssm1*. PNAS 1998;10763-8.

333. Pikaart MJ, Recillas-Targa F, Felsenfeld G. Loss of transcriptional activity of a transgene is accompanied by DNA methylation and histone deacetylation and is prevented by insulators. Genes and Development 1998;2852-62.

334. Zhuma T, Tyrrell R, Sekkali B, Skavdis G, Saveliev A, Tolaini M, Roderick K, Norton T, Smerdon S, Sedgwick S, Festenstein R, Kioussis D. Human HMG box transcription factor HBP1: a role in hCD2 LCR function. EMBO J. 1999;6396-406.

335. Sekkali B, Szabat E, Ktistaki E, Tolaini M, Roderick K, Harker N, Patel A, WIlliams K, Norton T, Kioussis D. Human high mobility group box transcription factor 1 affects thymocyte development and transgene variegation. The Journal of Immunology 2005;5203-12.

336. Ayyanathan K, Lechner MS, Bell P, Maul GG, Schultz DC, Yamada Y, Tanaka K, Torigoe K, Frank J.Rauscher I. Regulated recruitment of HP1 to a euchromatic gene induces mitotically heritable, epigenetic gene silencing: a mammalian cell culture model of gene variegation. Genes and Development 2003;1855-69.

337. Li Q, Peterson KR, Fang X, Stamatoyannopoulos G. Locus control regions. Blood 2002;3077-86.

338. Grosveld F, Assendelft GBv, Greaves DR, Kollias G. Position-independent, high-level expression of the human β-globin gene in transgenic mice. Cell 1987;975-85.

339. Tewari R, Gillemans N, Harper A, Wijgerde M, Zafarana G, Drabek D, Grosveld F, Philipsen S. The human β-globin locus control region confers an early embryonic erythroid-specific expression pattern to a basic promoter driving the bacteria *lacZ* gene. Development 1996;2991-3999.

340. Heydemann A, Warming S, Clendenin C, Sigrist K, Hjorth JP, Simon MC. A minimal *c-fes* cassette directs myeloid-specific expression in transgenic mice. Blood 2000;3040-8.

341. Kowolik CM, Hu J, Yee J-K. Locus control region of the human *CD2* gene in a lentivirus vector confers position-independent transgene expression. Journal of Virology 2001;4641-8.

342. Lee GR, Fields PE, IV TJG, Flavell RA. Regulation of the Th2 cytokine locus by a locus control region. Immunity 2003;145-53.

343. Chung JH, Bell AC, Felsenfeld G. Characterization of the chicken β-globin insulator. PNAS 1997;575-80.

344. Litt MD, Simpson M, Gaszner M, Allis CD, Felsenfeld G. Correlation between histone lysine methylation and developmental changes at the chicken β-globin locus. Science 2001;2453-5.

345. Yao S, Osborne CS, Bharadwaj RR, Pasceri P, Sukonnik T, Pannell D, Recillas-Targa F, West AG, Ellis J. Retrovirus silencer blocking by the cHS4 insulator is CTCF independent. Nucleic Acids Res. 2003;5317-23.

346. Emery DW, Yannaki E, Tubb J, Stamatoyannopoulos G. A chromatin insulator protects retrovirus vectors from chromosomal position effects. PNAS 2000;9150-5.

347. Rivella S, Callegari JA, May C, Tan CW, Sadelain M. The cHS4 insulator increases the probability of retroviral expression at random chromosomal integration sites. Journal of Virology 2000;4679-87.

348. Jakobsson J, Rosenqvist N, Thompson L, Barraud P, Lundberg C. Dynamics of trangene expression in a neural stem cell line transduced with lentiviral vectors incorporating the cHS4 insulator. Experimental Cell Research 2004;611-23.

349. Goetze S, Baer A, Winkelmann S, Nehlsen K, Seibler J, Maass K, Bode J. Performance of genomic bordering elements at predefined genomic loci. Mol Cell Biol 2005;2260-72.

350. Bronson SK, Plaehn EG, Kluckman KD, Hagaman JR, Maeda N, Smithies O. Single-copy transgenic mice with chosen-site integration. PNAS 1996;9067-72.

351. Cvetkovic B, Yang B, Williamson RA, Sigmund CD. Appropriate tissue- and cell-specific expression of a single copy human angiotensinogen transgene specifically targeted upstream of the HPRT locus by homologous recombination. J.Biol.Chem. 2000;1073-8.

352. Guillot PV, Liu L, Kuivenhoven JA, Guan J, Rosenberg RD, Aird WC. Targeting of human eNOS promoter to the *Hprt* locus of mice leads to tissue-restricted transgene expression. Physiological Genomics 2000;77-83.

353. Heaney JD, Rettew AN, Bronson SK. Tissue-specific expression of a BAC transgene targeted to the *Hprt* locus in mouse embryonic stem cells. Genomics 2004;1072-82.

354. Thomas KR, Capecchi MR. Site-directed mutagenesis by gene targeting in mouse embryo-derived stem cells. Cell 1987;503-12.

355. Tsuzuki T, Rancourt DE. Embryonic stem cell gene targeting using bacteriophage λ vectors generated by phage-plasmid recombination. Nucleic Acids Res. 1998;988-93.

356. Thomas KR, Capecchi MR. Targeted disruption of the murine *int-1* proto-oncogene resulting in severe abnormalities in midbrain and cerebellar development. Nature 1990;847-50.

357. Sekine S, Shibata T, Sakamoto M, Hirohashi S. Targeted disruption of the mutant

β-catenin gene in colon cancer cell line HCT116: preservation of its malignant phenotype. Oncogene 2002;5906-11.

358. Seo KW, Wang Y, Kokubo H, Kettlewell JR, Zarkower DA, Johnson RL. Targeted disruption of the DM domain containing transcription factor *Dmrt2* reveals an essential role in somite patterning. Developmental Biology 2006;200-10.

359. Testa G, Zhang Y, Vintersten K, Benes V, Pijnappel WWMP, Chambers I, Smith AJH, Smith AG, Stewart AF. Engineering the mouse genome with bacterial artificial chromosomes to create multipurpose alleles. Nature Biotechnology 2003;443-7.

360. Yang Y, Seed B. Site-specific gene targeting in mouse embryonic stem cells with intact bacterial artificial chromosomes. Nature Biotechnology 2003;447-51.

361. Abremski K, Hoess R, Sternmberg N. Studies on the properties of P1 site-specific recombination: evidence for topologically unlinked products following recombination. Cell 1983;1301-11.

362. Andrews BJ, Proteau GA, Beatty LG, Sadowski PD. The FLP recombinase of the 2μ circle DNA of yeast: interaction with its target sequences. Cell 1985;795-803.

363. Sauer B, Henderson N. Site-specific DNA recombination in mammalian cells by the Cre recombinase of bacteriophage P1. PNAS 1988;5166-70.

364. Sauer B, Henderson N. Cre-stimulated recombination at *loxP*-containing DNA sequences placed into the mammalian genome. Nucleic Acids Res. 1989;147-61.

365. O'Gorman S, Fox DT, Wahl GM. Recombinase-mediated gene activation and site-specific integration in mammalian cells. Science 1991;1351-5.

366. Mills AA, Bradley A. From mouse to man: generating megabase chromosome rearrangements. Trends in Genetics 2001;331-8.

367. Yu Y, Bradley A. Engineering chromosomal rearrangements in mice. Nature Reviews in Genetics 2001;780-90.

368. Fukushige S, Sauer B. Genomic targeting with a positive-selection *lox* integration vector allows highly reproducible gene expression in mammalian cells. PNAS 1992;7905-9.

369. Call LM, Moore CS, Stetten G, Gearhart JD. A Cre-*lox* recombination system for the targeted integration of circular yeast artificial chromosomes into embryonic stem cells. Human Molecular Genetics 2000;1745-51.

370. Choi S, Begum D, Koshinsky H, Ow DW, Wing RA. A new approach for the identifictaion and cloning of genes: the pBACwich system using Cre/*lox* site-

specific recombination. Nucleic Acids Res. 2000;e19.

371. Weyden Lvd, Adams DJ, Bradley A. Tools for targeted manipulation of the mouse genome. Physiological Genomics 2002;133-64.

372. Nagy A, Mar L. Creation and use of a Cre recombinase transgenic database. In: Tymms MJ, Kola I, eds. Methods in Molecular Biology: Gene Knockout Protocols. Totowa, NJ: Humana Press Inc., 2001;95-106.

373. Bouhassira EE, Westerman K, Leboulch P. Transcriptional behaviour of LCR enhancer elements integrated at the same chromosomal locus by recombinase-mediated cassette exchange. Blood 1997;3332-44.

374. Seibler J, Bode J. Double-reciprocal crossover mediated by FLP-recombinase: a concept and an assay. Biochemistry 1997;1740-7.

375. Hoess RH, Wierzbicki A, Abremski K. The role of th *loxP* spacer region in P1 site-specific recombination. Nucleic Acids Res. 1986;2287-300.

376. Schlake T, Bode J. Use of mutated FLP recognition target (FRT) sites for the exchange of expression cassettes at defined chromosomal loci. Biochemistry 1994;12746-51.

377. Langer SJ, Ghafoori AP, Byrd M, Leinwand L. A genetic screen identifies novel non-compatible *loxP* sites. Nucleic Acids Res. 2002;3067-77.

378. Soukharev S, Miller JL, Sauer B. Segmental genomic replacement in embryonic stem cells by double *lox* targeting. Nucleic Acids Res. 1999;e21.

379. Cheng EY, Collins C, Berru M, Shulman MJ. A system for precise analysis of transcription-regulating elements of immunoglobulin genes. BMC Biotechnology 2005;27.

380. Wong ET, Kolman JL, Li Y-C, Mesner LD, Hillen W, Berens C, Wahl GM. Reproducible doxycycline-inducible transgene expression at specific loci generated by Cre-recombinase mediated cassette exchange. Nucleic Acids Res. 2005;e147.

381. Roebroek AJM, Reekmans S, Lauwers A, Feyaerts N, Smeijers L, Hartman D. Mutant *Lrp1* knock-in mice generated by recombinase-mediated cassette exchange reveal differential importance of the NPXY motifs in the intracellular domain of LRP1 for normal fetal development. Mol Cell Biol 2006;605-16.

382. Toledo F, Liu C-W, Lee CJ, Wahl GM. RMCE-ASAP: a gene targeting method for ES and somatic cells to accelerate phenotype analyses. Nucleic Acids Res. 2006;e92.

383. Markowitz AJ, Wu GD, Birkenmeier EH, Traber PG. The human sucrase-

isomaltase gene directs complex patterns of gene expression in transgenic mice. American Journal of Physiology.Gastrointestinal and Liver Physiology 1993;526-39.

384. Mulder LCF, Rossini M, Mora M. Human *CD46* aberrant splicing in transgenic mice. Gene 1997;83-6.

385. Szalai G, Xie D, Wassenich M, Veres M, Ceci JD, Dewey MJ, Molotkov A, Duester G, Felder MR. Distal and proximal *cis*-linked sequences are needed for the total expression phenotype of the mouse alcohol dehydrogenase 1 (*Adh1*) gene. Gene 2002;259-70.

386. Lakshmanan G, Lieuw KH, Grosveld F, Engel JD. Partial rescue of GATA-3 by yeast artificial chromosomes transgenes. Developmental Biology 1998;451-63.

387. Alami R, Greally JM, Tanimoto K, Hwang S, Feng Y-Q, Engel JD, Fiering S, Bouhassira EE. *β-globin* YAC transgenes exhibit uniform expression levels but position effect variegation in mice. Human Molecular Genetics 2000;631-6.

388. Wunderle VM, Critcher R, Hastie N, Goodfellow PN, Schedl A. Deletion of long-range regulatory elements upstream of *SOX9* causes campomelic dysplasia. PNAS 1998;10649-54.

389. Pfeifer D, Kist R, Dewar K, Devon K, Lander ES, Birren B, Korniszewski L, Back E, Scherer G. Campomelic dysplasia translocation breakpoints are scattered over 1 Mb proximal to *SOX9*: evidence for an extended control region. American Journal of Human Genetics 1999;111-24.

390. Bagheri-Fam S, Barrionuevo F, Dohrman U, Gunther T, Schule R, Kemler R, Mallo M, Kanzler B, Scherer G. Long-range upstream and downstream enhancer control distinct subsets of the complex spatiotemporal *Sox9* expression pattern. Developmental Biology 2006;382-97.

391. Hallauer PL, Hastings KEM, Peterson AC. Fast skeletal muscle-specific expression of a quail troponin I gene in transgenic mice. Mol Cell Biol 1988;5072-9.

392. Gilfillan S, Aiso S, Michie SA, McDevitt HO. Immune deficiency due to high numbers of an A^k_β transgene. PNAS 1990;7319-23.

393. Garrick D, Fiering S, Martin DIK, Whitelaw E. Repeat-induced gene silencing in mammals. Nature Genetics 1998;56-9.

394. McBurney MW, Mai T, Yang X, Jardine K. Evidence for repeat-induced gene silencing in cultured mammalian cells: inactivation of tandem repeats of transfected genes. Experimental Cell Research 2002;1-8.

395. Dorer DR, Henikoff S. Expansions of transgene repeats cause heterochromatin

formation and gene silencing in Drosophila. Cell 1994;993-1002.

396. Mutskov V, Felsenfeld G. Silencing of transgene transcription precedes methylation of promoter DNA and histone H3 lysine 9. EMBO J. 2004;138-49.

397. Stoker AW. Retroviral Vectors. In: Davison AJ, Elliot RM, eds. Molecular virology: a practical approach. Oxford: IRL Press, 1993;171-197.

398. Kurian KM, Watson CJ, Wyllie AH. Retroviral vectors. Journal of Clinical Pathology: Molecular Pathology 2000;173-6.

399. Young LS, Searle PF, Onion D, Mautner V. Viral gene therapy strategies: from basic science to clinical application. The Journal of Pathology 2006;299-318.

400. Goncalves MAFV, Vries AAFd. Adenovirus: from foe to friend. Reviews in Medical Virology 2006;167-86.

401. Vasileva A, Jessberger R. Precise hit: adeno-associated virus in gene targeting. Nature Reviews in Microbiology 2005;837-47.

402. Lachmann RH. Herpes simplex virus-based vectors. International Journal of Experimental Pathology 2004;177-90.

403. Griffiths RA, Boyne JR, Whitehouse A. Herpesvirus saimiri-based gene delivery vectors. Current Gene Therapy 2006;1-15.

404. Guo ZS, Bartlett DL. Vaccinia as a vector for gene delivery. Expert Opinion on Biological Therapy 2004;901-17.

405. Palu G, Parolin C, Takeuchi Y, Pizzato M. Progress with retroviral gene vectors. Reviews in Medical Virology 2000;185-202.

406. Baum C, Schambach A, Bohne J, Galla M. Retrovirus vectors: toward the plentivirus? Molecular Therapy 2006;1050-63.

407. Cone RD, Mulligan RC. High-efficiency gene transfer into mammalian cells: generation of helper-free recombinant retrovirus with broad mammalian host range. PNAS 1984.

408. Danos O, Mulligan RC. Safe and efficient generation of recombinant retroviruses with amphotropic and ecotropic host ranges. PNAS 1988;6460-4.

409. Cosset F-L, Takeuchi Y, Battini J-L, Weiss RA, Collins MKL. High-titer packaging cells producing recombinant retroviruses resistant to human serum. Journal of Virology 1995;7430-6.

410. Soneoka Y, Cannon PM, Ramsdale EE, Griffiths JC, Romano G, Kingsman SM, Kingsman AJ. A transient three-plasmid expression system for the production of

high titer retroviral vectors. Nucleic Acids Res. 1995;628-33.

411. Rigg RJ, Chen J, Dando JS, Forestell SP, Plavec I, Bohnlein E. A novel human amphotropic packaging cell line: high titer, complement resistance, and improved safety. Virology 1996;290-5.

412. Reitman M, Felsenfeld G. Developmental Regulation of Topoisomerase II Sites and DNas I-Hypersensitive Sites in the Chicken β-Globin Locus. Molecular and Cellular Biology 1990;2774-86.

413. Schwartz F, Maeda N, Smithies O, Hickey R, Edelmann W, Skoultchi A, Kucherlapati R. A Dominant Positive and Negative Selectable Gene For Use in Mammalian Cells. PNAS 1991;10416-20.

414. Shimshek DR, Kim J, Hubner MR, Spergel DJ, Buchholz F, Cassanova E, Stewart AF, Seeburg PH, Sprengel R. Codon-Improved Cre Recombinase (iCre) Expression in the Mouse. Genesis 2002;19-26.

415. Lee E-C, Yu D, Velasco JMd, Tessarollo L, Swing DA, Court DL, Jenkins NA, Copeland NG. A Highly Efficient *Eschericia coli*-Based Chromosome Engineering System Adapted for Recombinogenic Targeting and Subcloning of BAC DNA. Genomics 2001;56-65.

416. Nolan, Garry. Phoenix helper-free retrovirus producer lines. http://www.stanford.edu/group/nolan/retroviral_systems/phx.html.

417. Richmond JY, McKinney RW. Biosafety in Microbiological and Biomedical Laboratories. CDC-NIH, 1999.

418. Lobe CG, Koop KE, Kreppner W, Lomeli H, Gertsenstein M, Nagy A. Z/AP, a Double Reporter for Cre-Mediated Recombination. Developmental Biology 1999;281-92.

419. Jang SK, Krausslich H-G, Nicklin MJH, Duke GM, Pamenberg AC, Wimmer E. A segment of the 5' nontranslated region of encephalomyocarditis virus RNA directs internal entry of ribosomes during in vitro translation. Journal of Virology 1988;2636-43.

420. Pelletier J, Sonenberg N. Internal initiation of translation of eukaryotic mRNA directed by a sequence derived from poliovirus RNA. Nature 1988;320-5.

421. Adam MA, Ramesh N, Miller AD, Osborne WRA. Internal initiation of translation in retroviral vectors carrying picornavirus 5' nontranslated regions. Journal of Virology 1991;4985-90.

422. Ghattas IR, Sanes JR, Majors JE. The encephalmyocarditis virus internal ribosome entry site allows efficient coexpression of two genes from a recombinant provirus in cultured cells and in embryos. Mol Cell Biol 1991;5848-

59.

423. Yu S-F, Ruden Tv, Kantoff PW, Garber C, Seiberg M, Ruther U, Anderson WF, Wgner EF, Gilboa E. Self-inactivating retroviral vectors designed for transfer of whole genes into mammalian cells. PNAS 1986;3194-8.

424. Wilson TJ, Kola I. The *loxP/Cre* system and genome modification. In: Tymms MJ, Kola I, eds. Methods in Molecular Biology: Gene Knockout Protocols. Totowa, NJ: Humana Press Inc., 2001;83-94.

425. Zheng B, Sage M, Sheppeard EA, Jurecic V, Bradley A. Engineering mouse chromosomes with Cre-*loxP*: range, efficiency, and somatic applications. Mol Cell Biol 2000;648-55.

426. Feng Y-Q, Seibler J, Alami R, Eisen A, Westerman KA, Leboulch P, Fiering S, Bouhassira EE. Site-specific chromosomal integration in mammalian cells: highly efficient Cre recombinase-mediated cassette exchange. J.Mol.Biol. 1999;779-85.

427. Kolb AF. Selection-marker-free modification of the murine β-casein gene using a *lox2722* site. Analytical Biochemistry 2001;260-71.

428. Kolb AF. Erratum. Analytical Biochemistry 2001;127.

429. Loonstra A, Vooijs M, Beverloo HB, Allak BA, Druene Ev, Kanaar R, Berns A, Jonkers J. Growth inhibition and DNA damage induced by Cre recombinase in mammalian cells. PNAS 2001;9209-14.

430. Silver DP, Livingston DM. Self-excising retroviral vectors encoding the Cre recombinase overcome Cre-mediated cellular toxicity. Molecular Cell 2001;233-43.

431. Berthois Y, Katzenellenbogen JA, Katzenellenbogen BS. Phenol red in tissue culture media is a weak estrogen: implication concerning the study of estrogen-responsive cells in culture. PNAS 1986;2496-500.

432. Cheng Y, Grill SP, Dutschman GE, Nakayama K, Bastow KF. Metabolism of 9-(1,3-dihydroxy-2-propoxymethyl)guanine, a new anti-herpes virus compound, in herpes simplex virus-infected cells. J.Biol.Chem. 1983;12460-4.

433. Freeman SM, Abboud CN, Whartenby KA, Packman CH, Koeplin DS, Moolten FL, Abraham GN. The Bystander Effect - Tumor-Regression When A Fraction of the Tumor Mass Is Genetically-Modified. Cancer Research 1993;5274-83.

434. Fillat C, Carrio M, Cascante A, Sangro B. Suicide gene therapy mediated by the herpes simplex virus thymidine kinase gene/ganciclovir system: fifteen years of application. Current Gene Therapy 2003;13-26.

435. Thomas JW, LaMantia C, Magnuson T. X-ray-induced mutations in mouse

embryonic stem cells. PNAS 1998;1114-9.

436. Baubonis W, Sauer B. Genomic targeting with purified Cre recombinase. Nucleic Acids Res. 1993;2025-9.

437. McGowan R, Campbell R, Peterson A, Sapienza C. Cellular mosaicism in the methylation and expression of hemizygous loci in the mouse. Genes and Development 1989;1669-76.

438. Elliott JI, Festenstein R, Tolaini M, Kioussis D. Random activation of a transgene under the control of a hybrid hCD2 locus control region/Ig enhancer regulatory element. EMBO J. 1995;575-84.

439. Schweizer J, Valenza-Schaerly P, Goret F, Pourcel C. Control of expression and methylation of a hepatitis B virus transgene by strain-specific modifiers. DNA and Cell Biology 1998;427-35.

440. Opsahl ML, McClenaghan M, Springbett A, Reid S, Lathe R, Colman A, Whitelaw CBA. Multiple effects of genetic background on variegated transgene expression in mice. Genetics 2002;1107-12.

441. Mizuhara H, Kuno M, Seki N, Yu W-G, Yamaoka M, Yamashita M, Ogawa T, Kaneda K, Fujii T, Senoh H, Fujiwara H. Strain difference in the induction of T-cell activation-associated interferon gamma-dependent hepatic injury in mice. Hepatology 1998;513-9.

442. Ge Y, Jippo T, Lee Y-M, Adachi S, Kitamura Y. Independent influence of strain difference and *mi* transcription factor on the expression of mouse mast cell chymases. American Journal of Pathology 2001;281-92.

443. Ohmura K, Johnsen A, Ortiz-Lopez A, Desany P, Roy M, Besse W, Rogus J, Bogue M, Puech A, Lathrop M, Mathis D, Benoist C. Variation in IL-1b gene expression is a major determinant of genetic differences in arthritis aggressivity in mice. PNAS 2005;12489-94.

444. Casley WL, Menzies JA, Girard M, Larocque L, Mousseau M, Whitehouse LW, Moon TW. Differences in caffeine 3-demethylation activity among inbred mouse strains: a comparison of hepatic *Cyp1a2* gene expression between two inbred strains. Fundamental and Applied Toxicology 1997;228-37.

445. Smith AG, Clothier B, Robinson S, Scullion MJ, Carthew P, Edwards R, Luo J, lim CK, Toledano M. Interaction between iron metabolism and 2,3,7,8-tetrachlorodibenzo-*p*-dioxin in mice with variants of the *Ahr* gene: a hepatic oxidative mechanism. Molecular Pharmacology 1998;52-61.

446. Zhang Q-Y, Dunbar D, Kaminsky LS. Characterization of mouse small intestinal cytochrome P450 expression. Drug Metabolism and Disposition 2003;1346-51.

447. Pettaway CA. Racial differences in the androgen/androgen receptor pathway in prostate cancer. Journal of the National Medical Association 1999;653-60.

448. Barnes KC. Genetic determinants and ethnic disparities in sepsis-associated acute lung injury. The Proceedings of the American Thoracic Society 2005;195-201.

449. Miwa K, Fujita M, Sasayama S. Recent insights into the mechanisms, predisposing factors, and racial differences of coronary vasospasm. Heart and Vessels 2005;1-7.

450. Mizuno N, Niwa T, Yotsumoto Y, Sugiyama Y. Impact of drug transporter studies on drug discovery and development. Pharmacological Reviews 2003;425-61.

451. Bock KW, Kohle C. UDP-glucuronsyltransferase 1A6: structural, functional, and regulatory aspects. Methods in Enzymology 2005;57-75.

452. Daly AK. Significance of the minor cytochrome P450 3A isoforms. Clinical Pharmacokinetics 2006;13-31.

453. Finger F, Schorle C, Zien A, Gebhard P, Goldring MB, Aigner T. Molecular phenotyping of human chondrocyte cell lines T/C-28a2, T/C-28a4, and C-28/I2. Arthritis & Rheumatism 2003;3395-403.

454. Ami Y, Shimazui T, Akaza H, Uematsu N, Yano Y, Tsujimoto G, Uchida K. Gene expression profiles correlate with the morphology and metastasis characteristics of renal cell carcinoma cells. Oncology Reports 2005;75-80.

455. Stewart SA. Telomere maintenance and tumorigenesis: an "alt"ernative road. Current Molecular Medicine 2005;253-7.

456. Coffin J, Hughes SH, Varmus HE. Historical Introduction to the General Properties of Retroviruses. In Retroviruses. Plainview, NY: Cold Spring Harbor Laboratory Press, 1997.

457. Meyers BC, Scalabrini S, Morgante M. Mapping and sequencing complex genomes: let's get physical! Nature Reviews in Genetics 2004;578-88.

458. Copeland NG, Jenkins NA, Court DL. Recombineering: a powerful new tool for mouse functional genomics. Nature Reviews in Genetics 2001;769-79.

459. Muyrers JPP, Zhang Y, Stewart AF. Techniques: recombinogenic engineering-new options for cloning and manipulating DNA. Trends in Biochemical Sciences 2001;325-31.

460. Court DL, Sawitzke JA, Thomason LC. Genetic engineering using homologous recombination. Annual Reviews in Genetics 2002;361-88.

461. Amundsen SK, Smith GR. Interchangeable parts of the *Escherichia coli* recombination machinery. Cell 2003;741-4.

462. Hamilton CM, Aldea M, Washburn BK, Babitzke P, Kushner SR. New method for generating deletions and gene replacements in *Escherichia coli*. Journal of Bacteriology 1989;4617-22.

463. Yang XW, Model P, Heintz N. Homologous recombination based modification in *Escherichia coli* and germline transmission in transgenic mice of a bacteria artificial chromosome. Nature Biotechnology 1997;859-65.

464. Imam AMA, Patrinos GP, Krom Md, Bottardi S, Janssens RJ, Katsantoni E, Wai AWK, Sherratt DJ, Grosveld FG. Modification of human β-globin locus PAC clones by homologous recombination in *Escherichia coli*. Nucleic Acids Res. 2000;e65.

465. Gong S, Yang XW, Li C, Heintz N. Highly efficient modification of bacterial artificial chromosomes (BACs) using novel shuttle vectors containing the R6Kγ origin of replication. Genome Res 2002;1992-8.

466. Jessen JR, Meng A, McFarlane RJ, Paw BH, Zon LI, Smith GR, Lin S. Modification of bacterial artificial chromosomes through Chi-stimulated homologous recombination and its application in zebrafish transgenesis. PNAS 1998;5212-126.

467. Nistala R, Sigmund CD. A reliable and efficient method for deleting operational sequences in PACs and BACs. Nucleic Acids Res. 2002;e41.

468. Zhang Y, Buchholz F, Muyrers JPP, Stewart AF. A new logic for DNA engineering using recombination in *Escherichia coli*. Nature Genetics 1998;123-8.

469. Kolodner R, Hall SD, Luisi-DeLuca C. Homologous pairing proteins encoded by the *Escherichia coli* recE and recT genes. Molecular Microbiology 1994;23-30.

470. Murphy KC. λ gam protein inhibits the helicase and χ-stimulated recombination activities of *Escherichia coli* RecBCD enzyme. Journal of Bacteriology 1991;5808-21.

471. Muyrers JPP, Zhang Y, Testa G, Stewart AF. Rapid modification of bacterial artificial chromosomes by ET-recombination. Nucleic Acids Res. 1999;1555-7.

472. Muyrers JPP, Zhang Y, Benes V, Testa G, Ansorge W, Stewart AF. Point mutation of bacterial artificial chromosomes by ET recombination. EMBO Rep. 2000;239-43.

473. Wang J, Sarov M, Rientjes J, Fu J, Hollak H, Kranz H, Xie W, Stewart AF, Zhang Y. An improved recombineering approach by adding RecA to λ Red

recombination. Molecular Biotechnology 2006;43-54.

474. Narayanan K, Williamson R, Zhang Y, Stewart AF, Ioannou PA. Efficient and precise engineering of a 200 kb β-globin human/bacterial artificial chromosome in *E.coli* DH10B using an inducible homologous recombination system. Gene Therapy 1999;442-7.

475. Yu D, Ellis HM, Lee E-C, Jenkins NA, Copeland NG, Court DL. An Efficient Recombination System for Chromosome Engineering in *Eschericia coli*. PNAS 2000;5978-83.

476. Swaminathan S, Ellis HM, Waters LS, Yu D, Lee E-C, Court DL, Sharan SK. Rapid engineering of bacterial artificial chromosomes using oligonucleotides. Genesis 2001;14-21.

477. Warming S, Costantino N, Court DL, Jenkins NA, Copeland NG. Simple and highly efficient BAC recombineering using *galK* selection. Nucleic Acids Res. 2005;e36.

478. Khandekar M, Suzuki N, Lewton J, Yamamoto M, Engel JD. Multiple, distant *Gata2* enhancers specify temporally and tissue-specific patterning in the developing urogenital system. Mol Cell Biol 2004;10263-76.

479. Netterwald J, Yang S, Wang W, Ghanny S, Cody M, Soteropooulos P, Tian B, Dunn W, Liu F, Zhu H. Two gamma interferon-activated site-like elements in the human cytomegalovirus major immediate-early promoter/enhancer are important for viral replication. Journal of Virology 2005;5035-46.

480. Schumacher D, Tishcer BK, Trapp S, Osterrider N. The protein encoded by the Us3 orthologue of Marek's disease virus is required for efficient de-envelopment of perinuclear virions and involved in actin stress fiber breakdown. Journal of Virology 2005;3987-97.

481. Yu D, Silva MC, Shenk T. Functional map of human cytomegalovirus AD169 defined by global mutational analysis. PNAS 2003;12396-401.

482. Han SJ, Jeong J, DeMayo FJ, Xu J, Tsai SY, Tsai M-J, O'Malley BW. Dynamic cell type specificity of SRC-1 coactivator in modulating uterine progesterone receptor function in mice. Mol Cell Biol 2005;8150-65.

483. Yang Y, Sharan SK. A simple two-step, 'hit and fix' method to generate subtle mutations in BACs using short denatured PCR fragments. Nucleic Acids Res. 2003;e80.

484. Britt WJ, Jarvis M, Seo J-Y, Drummond D, Nelson J. Rapid genetic engineering of human cytomegalovirus by using a lambda phage linear recombination system: demonstration that pp28 (UL99) is essential for production of infectious virus. Journal of Virology 2004;539-43.

485. Oppenheim AB, Rattray AJ, Bubunenko M, Thomason LC, Court DL. In vivo recombineering of bacteriophage λ by PCR fragments and single-strand oligonucleotides. Virology 2004;185-9.

486. Court DL, Swaminathan S, Yu D, Wilson H, Baker T, Bubunenko M, Sawitzke J, Sharan SK. Mini-λ: a tractable system for chromosome and BAC engineering. Gene 2003;63-9.

487. Shuman S. Novel approach to molecular cloning and polynucleotide synthesis using vaccinia DNA topoisomerase. J.Biol.Chem. 1994;32678-84.

488. Morgenstern J, Land H. Advanced mammalian gene transfer: high titre retroviral vectors with multiple drug selection markers and a complementary helper-free packaging cell line. Nucleic Acids Res. 1990;3587-96.

489. Osoegawa K, Mammoser AG, Wu C, Frengen E, Zeng C, Catanese JJ, Jong PJd. A bacterial artificial chromosome library for sequencing the complete human genome. Genome Res 2001;483-96.

490. UCSC. UCSC Genome Bioinformatics. http://www.genome.ucsc.edu/index.html?org=Human.

491. Hoglund PJ, Adzic D, Scicluna SJ, Lindblom J, Fredriksson R. The repertoire of solute carriers of family 6: Identification of new human and rodent genes. Biocehmical and Biophysical Research Communications 2005;175-89.

492. Broer S. The SLC6 orphans are forming a family of amino acid transporters. Neurochemistry International 2006;559-67.

493. Yamamoto K, Okamoto A, Isonishi S, Ochiai K, Ohtake Y. A novel gene, CRR9, which was up-regulated in CDDP-resistant ovarian tumor cell line, was associated with apoptosis. Biocehmical and Biophysical Research Communications 2001;1148-54.

494. Asakura T, Imai A, Ohkubo-Uraoka N, Kuroda M, Iidaka Y, Shibasaki T, Ohkawa K. Relationship between expression of drug-resistance factors and drug sensitivity in normal human renal proximal tubular epithelial cells in comparison with renal cell carcinoma. Oncology Reports 2005;601-7.

495. Shmueli O, Horn-Saban S, Chalifa-Caspi V, Shmoish M, Ophir R, Benjamin-Rodrig H, Safran M, Domany E, Lancet D. GeneNote: whole genome expression profiles in normal human tissues. C.R.Biologies 2003;1067-72.

496. Wang S, Robertson GP, Zhu J. A novel human homologue of *Drosophila* polycomblike gene is up-regulated in multiple cancers. Gene 2004;69-78.

497. Vergnaud G, Denoeud F. Minisatellites: mutability and genome architecture. Genome Res 2000;899-907.

498. Bois PRJ. Hypermutable minisatellites, a human affair? Genomics 2003;349-55.

499. Anjos S, Polychronakos C. Mechanisms of genetic susceptibility to type I diabetes: beyond HLA. Molecular Genetics and Metabolism 2004;187-95.

500. Raeder H, Johansson S, Holm PI, Haldorsen IS, Mas E, Sbarra V, Nermoen I, Eide SA, Grevle L, Bjorkhaug L, Sagen JV, Aksnes L, Sovik O, Lombardo D, Molven A, Njolstad PR. Mutations in the CEL VNTR cause a syndrome of diabetes and pancreatic exocrine dysfunction. Nature Genetics 2006;54-62.

501. Szutorisz H, Palmqvist R, Roos G, Stenling R, Scorderet DF, Reddel R, Lingner J, Nabholz M. Rearrangements of minisatellites in the human telomerase reverse transcriptase gene are not correlated with its expression in colon carcinomas. Oncogene 2001;2600-5.

502. Leem S-H, Londono-Vallejo JA, Kim J-H, Bui H, Tubacher E, Solomon G, Park J-E, Horikawa I, Kouprina N, Barrett JC, Larionov V. The human telomerase gene: complete genomic sequence and analysis of tandem repeat polymorphisms in intronic regions. Oncogene 2002;769-77.

503. Wang L, Soria J-C, Chang Y-S, Lee H-Y, Wei Q, Mao L. Association of a functional tandem repeats in the downstream of human telomerase gene and lung cancer. Oncogene 2003;7123-9.

504. Toba-Minowa M, Hashimoto-Gotoh T. Characterization of the spontaneous elimination of streptomycin sensitivity (Sm^S) on high-copy number plasmids: Sm^S-enforcement cloning vectors with a synthetic *rpsL* gene. Gene 1992;25-33.

505. Gondo Y, Shioyama Y, Nakao K, Katsuki M. A novel positive detection system of in vivo mutations in *rpsL* (*strA*) transgenic mice. Mutations Research 1996;1-14.

506. Stavropoulos TA, Strathdee CA. Synergy between *tetA* and *rpsL* provides high-stringency positive and negative selection in bacterial artificial chromosome vectors. Genomics 2001;99-104.

507. Doi S, Campbell C, Kucherlapati R. Directed modification of genes by homologous recombination in mammalian cells. In: Grosveld F, Kollias G, eds. Transgenic Animals. San Diego: Academic Press Inc., 1992;27-46.

508. Sedivy JM, Joyner AL. Gene Targeting. New York, New York: W. H. Freeman and Company, 1992.

509. Sedivy JM, Dutriaux A. Gene targeting and somatic cell genetics: a rebirth or a coming of age? Trends in Genetics 1999;88-90.

510. Araki K, Araki M, Miyazaki J, Vassalli P. Site-specific recombination of a transgene in fertilized eggs by transient expression of Cre recombinase. PNAS

1995;160-4.

511. Sauer B, Henderson N. Targeted insertion of exogenous DNA into the eukaryotic genome by the Cre recombinase. New Biologist 1990;441-9.

512. Bi WL, Parysek LM, Warnick R, Stambrook PJ. *In vitro* evidence that metabolic cooperation is responsible for the bystander effect observed with HSV *tk* retroviral gene therapy. Human Gene Therapy 1993;725-31.

513. Touraine RL, Ishii-Morita H, Ramsey WJ, Blaese RM. The bystander effect in the HSVtk/gancicolvir system and its relationship to gap junctional communication. Gene Therapy 1998;1705-11.

514. Burrows FJ, Gore M, Smiley WR, Kanemitsu MY, Jolly DJ, Read SB, Nicholas T, Kruse CA. Purified herpes simplex virus thymidine kinase retroviral particles: III. Characterization of bystander killling mechanisms in transfected tumor cells. Cancer Gene Therapy 2002;87-95.

515. Long Q, Shelton KD, Lindner J, Jones JR, Magnuson MA. Efficient DNA cassette exchange in mouse embryonic stem cells by staggered positive-negative selection. Genesis 2004;256-62.

516. Ahuja D, Saenz-Robles MT, Pipas JM. SV40 large T antigen targets multiple cellular pathways to elicit cellular transformation. Oncogene 2005;7729-45.

517. Colbere-Garapin F, Ryhiner M-L, Stephany I, Kourilsky P, Garapin A-C. Patterns of integration of exogenous DNA sequences transfected into mammalian cells of primate and rodent origin. Gene 1986;279-88.

518. Palombo F, Monciotti A, Recchia A, Cortese R, Ciliberto G, La Monica N. Site-specific integration in mammalian cells mediated by a new hybrid baculovirus adeno-associated virus vector. Journal of Virology 1998;5025-34.

519. Philpott NJ, Gomos J, Falck-Pedersen E. Transgene expression after Rep-mediated site-specific integration into chromosome 19. Human Gene Therapy 2004;47-61.

520. Wake CT, Gudewicz T, Porter T, White A, Wilson JH. How damaged is the biologicaly active subpopulation of transfected DNA? Mol Cell Biol 1984;387-98.

521. Murnane JP, Yezzi MJ, Young BR. Recombination events during integration of transfected DNA into normal human cells. Nucleic Acids Res. 1990;2733-8.

522. Phillips JW, Morgan WF. Illegitimate recombination induced by DNA double-strand breaks in a mammalian chromosome. Mol Cell Biol 1994;5794-803.

523. Merrihew RV, Marburger K, Pennington SL, Roth DB, Wilson JH. High-

frequency illegitimate integration of transfected DNA at preintegated target sites in a mammalian genome. Mol Cell Biol 1996;10-8.

524. White RE, Wade-Martins R, Hart SL, Frampton J, Huey B, Desai-Mehta A, Cerosaletti KM, Concannon P, James MR. Functional delivery of large genomic DNA to human cells with a peptide-lipid vector. The Journal of Gene Medicine 2003;883-92.

525. Kaur GP, Reddy DE, Zimonjic DB, Riel JKd. Functional identification of a BAC clone from 16q24 carrying a senescence gene SEN16 for breast cancer cells. Oncogene 2005;47-54.

526. Igoucheva O, Alexeev V, Yoon K. Differential cellular responses to exogenous DNA in mammalian cells and its effect on oligonucleotide-directed gene modification. Gene Therapy 2006;266-75.

527. Montigny WJ, Phelps SF, Illenye S, Heintz NH. Parameters influencing high-efficiency transfection of bacterial artificial chromosomes into cultured mammalian cells. Biotechniques 2003;796-807.

528. Siegel RW, Jain R, Bradbury A. Using an in vivo phagemid system to identify non-compatible *loxP* sequences. FEBS Letters 2001;147-53.

529. Shmerling D, Danzer C-P, Mao X, Boisclair J, Haffner M, Lemaistre M, Schuler V, Kaeslin E, Korn R, Burki K, Ledermann B, Kinzel B, Muller M. Strong and ubiquitous expression of transgenes targeted into the β-actin locus by Cre/lox cassette replacement. Genesis 2005;229-35.

530. Brown TC, Jiricny J. Different base/base mispairs are corrected with different efficiencies and specificities in monkey kidney cells. Cell 1988;705-11.

531. Chen C, Okayama H. High-Efficiency Transformation of Mammalian-Cells by Plasmid Dna. Molecular and Cellular Biology 1987;2745-52.

532. Brinster RL, Chen HY, Trumbauer ME, Yagle MK, Palmiter RD. Factors Affecting the Efficiency of Introducing Foreign Dna Into Mice by Microinjecting Eggs. Proceedings of the National Academy of Sciences of the United States of America 1985;4438-42.

533. Hogan B, Beddington R, Costantini F, Lacy E. Production of Transgenic. In Manipulating the Mouse Embryo. Cold Spring Harbor University Press, 1994;217-252.

534. Masutomi K, Yu EY, Khurts S, Ben Porath I, Currier JL, Metz GB, Brooks MW, Kaneko S, Murakami S, DeCaprio JA, Weinberg RA, Stewart SA, Hahn WC. Telomerase maintains telomere structure in normal human cells. Cell 2003;241-53.

535. Masutomi K, Possemato R, Wong JMY, Currier JL, Tothova Z, Manola JB, Ganesan S, Lansdorp PM, Collins K, Hahn WC. The telomerase reverse transcriptase regulates chromatin state and DNA damage responses. Proceedings of the National Academy of Sciences of the United States of America 2005;8222-7.

536. Won J, Chang S, Oh S, Kim TK. Small-molecule-based identification of dynamic assembly of E2F-pocket protein-histone deacetylase complex for telomerase regulation in human cells. Proceedings of the National Academy of Sciences of the United States of America 2004;11328-33.

537. Tomlinson RL, Ziegler TD, Supakorndej T, Terns RM, Terns MP. Cell cycle-regulated trafficking of human telomerase to telomeres. Molecular Biology of the Cell 2006;955-65.

538. Wang S, Hu C, Zhu J. Transcriptional Silencing of a Novel hTERT Reporter Locus during In Vitro Differentiation of Mouse Embryonic Stem Cells. Molecular Biology of the Cell 2006;In Press.

539. Baker A, Cotten M. Delivery of bacterial artificial chromosomes into mammalian cells with psoralen-inactivated adenovirus carrier. Nucleic Acids Research 1997;1950-6.

540. Illenye S, Heintz NH. Functional analysis of bacterial artificial chromosomes in mammalian cells: Mouse Cdc6 is associated with the mitotic spindle apparatus. Genomics 2004;66-75.

541. Wade-Martins R, Smith ER, Tyminski E, Chiocca EA, Saeki Y. An infectious transfer and expression system for genomic DNA loci in human and mouse cells. Nature Biotechnology 2001;1067-70.

542. Shay JW, Wright WE. Telomerase therapeutics for cancer: challenges and new directions. Nature Reviews Drug Discovery 2006;577-84.

543. Shin JS, Hong A, Solomon MJ, Lee CS. The role of telomeres and telomerase in the pathology of human cancer and aging. Pathology 2006;103-13.

Curriculum Vitae

Melanie Ann Leiby

Born:

March 6, 1978 in Reading, Pennsylvania

Education:

2000-2007
The Pennsylvania State University
College of Medicine
Department of Cellular and Molecular Physiology
Ph.D. in Cell and Molecular Biology expected May 2007

1996-2000
Elizabethtown College, Elizabethtown, Pennsylvania
Department of Chemistry and Biochemistry
B.S. in Biochemistry, May 2000

Awards and Scholarships:

2000-2001	The Pennsylvania State University Graduate Fellow
1998-2000	College Scholar, Elizabethtown College
1996-2000	Presidential Scholar, Elizabethtown College